

Structural and Functional Characterization of Bacterial LOV Domain-containing Blue-Light Photoreceptors

Cao, Zhen
aus Shandong, V.R. China



Dissertation
Zur
Erlangung des akademischen Grades eines Doktors der
Mathematisch-Naturwissenschaftlichen Fakultät
der Heinrich-Heine Universität Düsseldorf

Mülheim an der Ruhr, April 2010

Referent: Prof. Dr. W. Gärtner
Koreferent: Prof. Dr. K.-E. Jäger

Zusammenfassung

Ende des 19. Jahrhunderts berichteten Charles Darwin und sein Sohn über ein interessantes Phänomen, das in verschiedenen Pflanzenarten beobachtet worden war: „Phototropismus“, ein lichtabhängiges Richtungswachstum in Richtung der Lichtquelle. Allerdings wurde das zugehörige Photorezeptorprotein, Phototropin, mit einer hochkonservierten LOV- (light, oxygen, voltage) Domäne erst gegen Ende des 20. Jahrhunderts identifiziert. In Folge konnte nachgewiesen werden, dass die Existenz dieses konservierten Signal-gebenden Moduls nicht auf Pflanzen beschränkt war, sondern im Gegenteil weit verbreitet in allen drei Reichen des Lebens mit Ausnahme der Tiere vorhanden ist.

YtvA aus *Bacillus subtilis*, ein Protein mit 261 Aminosäuren, war das erste bakterielle LOV-Domänen enthaltende Protein, für das nachgewiesen wurde, dass es einen Phototropin vergleichbaren Photozyklus durchläuft. Seither wächst die Kenntnis über prokaryotische LOV-Domänen Proteine extrem, und viele andere bakterielle LOV-Proteine mit erstaunlich unterschiedlichen Effektordomänen wurden charakterisiert.

Mit der vorgelegten Dissertation soll unsere Kenntnis über die molekularen Grundlagen der Signaltransduktion innerhalb verschiedener LOV-Domänen Proteine erweitert werden. Das Erstellen einer Verbindung zwischen der Struktur dieser Proteine und ihrer (physiologischen) Funktion ist ebenfalls Teil dieser Arbeit.

Die funktionelle Charakterisierung von YtvA aus *B. subtilis* wird hier fortgesetzt unter Einbeziehung der kürzlich entdeckten NTP-Bindungsfunktion, der Interdomänen-Interaktion und des Kommunikations-„Weges“, der ausführlich untersucht wurde. Die dreidimensionale Struktur einer weiteren LOV-Domäne

aus *B. amyloliquefaciens* ergab weitere Informationen über die Dimerisierung von LOV-Domänen und zeigte einen neuen Typus einer Dimerenanordnung.

Weitere bakterielle LOV-enthaltende Proteine mit unterschiedlichen Effektor-domänen wurden hier zum ersten Mal charakterisiert. Hierzu gehört ein Blaublicht-reguliertes Zweikomponenten-Protein aus *Pseudomonas syringae* und ein LOV-Domänen enthaltendes GGDEF/EAL-Protein aus *Synechococcus*. In beiden Proteinen sind Blaublicht-sensitive LOV-Domänen mit gut charakterisierten Signal-gebenden Modulen verknüpft, die in vielen bakteriellen Spezies weit verbreitet sind.

Summary

In the late 19th century, Charles Darwin and his son had noticed in several plant species an interesting feature: phototropism, a light dependent directional growth towards the light source. However, the responsible photoreceptor protein, phototropin with a conserved light, oxygen and voltage (LOV) domain, could only be identified until the end of 20th century. Later, it has been discovered that this conserved LOV signaling module is not restricted to plants; it is actually widely distributed in all three kingdoms of life with the only exception of animals.

YtvA from *Bacillus subtilis* was the first bacterial LOV-domain containing protein that has been proven to undergo a phototropin-like blue light induced photocycle. Since then, the knowledge about prokaryotic LOV domain-containing proteins was rapidly growing and many other bacterial LOV proteins with quite diversified downstream effector domains have been characterized.

This present thesis broadens significantly our knowledge about the molecular basis of signal transmission within several bacterial LOV domain-containing proteins. The connections between the structure of these proteins and their functions will also be part of this work.

The study of YtvA from *Bacillus subtilis* has been continued in this present work. Besides its recently discovered NTP-binding function, the inter-domain interaction of YtvA and the detailed communicating pathway have been extensively investigated. A possible common connecting interface for the signal transmission in this protein was examined. The structure of another LOV domain from *Bacillus amyloliquefaciens* that has been solved during this thesis, also adds further information on LOV domain dimerization and presents a novel type of dimer formation.

Some other bacterial LOV-containing proteins with different effector domains have been characterized for the first time, including a blue light regulated two-component signaling protein from *Pseudomonas syringae* and a LOV-containing GGDEF/EAL protein from *Synechococcus*. Both these two proteins have combined the blue light sensing LOV domain to some well-established signaling modules that are found widely distributed in many bacterial species.

Publications and Poster Presentation

Buttani V, Losi A, Eggert T, Krauss U, Jaeger KE, **Cao Z.**, Gärtner W.

Conformational analysis of the blue-light sensing protein YtvA reveals a competitive interface for LOV-LOV dimerization and interdomain interactions.
Photochem Photobiol Sci. 6:41-9 (2007).

Cao Z., Krauss U, Buttani V, Jaeger KE, Eggert T, Losi A, Gärtner W.

Blue light inducible functions of bacterial LOV proteins.
The 12th European Society for Photobiology Congress,
University of Bath, UK, September 1-6, (2007).

Cao Z., Buttani V, Losi A, Gärtner W.

A blue light inducible two-component signal transduction system in the plant pathogen *Pseudomonas syringae* pv. *tomato*.
Biophys J. 94:897-905 (2008).

Ogata H., **Cao Z.**, Losi A, Gärtner W.

Crystallization and X-ray analysis of LOV domain of blue-light receptor YtvA from *Bacillus amyloliquefaciens* FZB42
Acta Crystallogr Sect F Struct Biol Cryst Commun. 65:853-5 (2009).

Tang, Y, **Cao Z.**, Livoti, E, Krauss U, Gärtner W, Losi A.

Mapping the pathway of signal transmission within a blue-light photoreceptor.
Photochem Photobiol Sci. 9:47-56 (2010).

Cao Z., Livoti, E, Losi A, Gärtner W.

A blue-light inducible cyclic diguanylate phosphodiesterase in cyanobacteria.
Photochem Photobiol. 86:606-11(2010).

Acknowledgements

Writing this thesis would not have been possible without the help of a number of people.

First of all, my sincere thanks go to Prof. Dr. Wolfgang Gärtner and Dr. Aba Losi, my thesis supervisors, who initiated this exciting research project and supported me by providing fantastic working conditions and excellent scientific guidance. Prof. Wolfgang Gärtner also gave me great help in revising and organizing this thesis.

I also would like to thank Prof. Dr. Karl-Erich Jäger, the co-evaluator of this thesis.

Special thanks go to Dr. Ulrich Krauss for helping me a lot throughout my Ph.D. research. I am also grateful to all the colleagues in my group for many, many essential discussions and good advices, Dr. Amrit Kaur, Björn Zorn, Gopal Pathak, Rashmi Shah, Shivani Sharda, and Yifen Tang. I also appreciate Mrs. Helene Steffen for her great help during the past few years in laboratory.

Very special thanks go to my parents, Xue-jian Cao and Li-juan Yang who fully supported me throughout my long studies.

Last but not least, I would like to share this work with my wife, Qunzi Zhang.

Abbreviation List

Some unusual abbreviations have been repeatedly used in this thesis, below is a summarized list of all these abbreviations.

aa	Amino acid
Asphot	<i>Avena sativa</i> phototropin
ATP	Adenosine 5'-triphosphate
Atphot	<i>Arabidopsis thaliana</i> phototropin
BLUF	Blue-Light sensors Using FAD domain
CD	Circular dichroism
C-di-GMP	bis-(3',5')-cyclic dimeric guanosine monophosphate
Crphot	<i>Chlamydomonas reinhardtii</i> phototropin
CRY	Cryptochrome
C-terminal	Carboxy-terminal
DNA	Deoxyribonucleic acid
FAD	Flavin Adenine Dinucleotide (Riboflavin 5'-adenosine diphosphate)
FKF1	Flavin-Binding Kelch Repeat F-Box Protein
FMN	Flavin Mononucleotide (Riboflavin 5'-monophosphate)
GMP	Guanosine monophosphate
GTP	Guanosine 5'-triphosphate
HK	Histidine Kinase domain
HPLC	High Performance Liquid Chromatography
HTH	Helix-Turn-Helix DNA binding domain
LOV	Light, Oxygen, Voltage domain
LOV390	LOV light state
LOV447	LOV dark state
LOV660	LOV excited triplet-state
LOV-HK	LOV Histidine Kinase
LOV-HK-RR	Hybrid LOV Histidine Kinase
N-cap	Amino-terminal cap
NMR	Nuclear Magnetic Resonance
N-terminal	Amino-terminal
PAS	Per, Arndt, Sim domain
Phot	Phototropin
PYP	Photoactive Yellow Protein
RF	Riboflavin
RR	Response Regulator
STAS	Sulfate Transporter Anti-Sigma factor antagonist domain
UV	Ultra-Violet
WC-1	White-Collar-1
ZTL	ZEITLUPE

Content Index

Zusammenfassung-----	1
Summary-----	3
Publications and Poster Presentation-----	5
Acknowledgements-----	6
Abbreviation List-----	7
I. Introduction-----	9
1.1 Light in photo-processes-----	10
1.2 The molecules that respond to photo-absorption-----	12
1.3 The classification and distribution of photoreceptors-----	15
1.3.1 Photoreceptors using light as an energy source-----	16
1.3.2 Photo-sensors using light as an environmental signal-----	21
1.3.2.1 Rhodopsins-----	22
1.3.2.2 Phytochromes-----	23
1.3.2.3 Xanthopsins-----	24
1.4 Flavin based photoreceptors-----	25
1.4.1 Cryptochromes and photolyases-----	27
1.4.2 The LOV proteins: phototropin and ZTL/ADO/FKF1 families-----	28
1.4.3 BLUFs (blue light sensing using FAD)-----	31
1.5 The phototropin-like LOV proteins-----	32
1.5.1 The structure and photochemistry of the LOV paradigm-----	33
1.5.2 The signal transduction from LOV to effector domains-----	35
1.6 Aim of this work and outline of this thesis-----	40
1.7 References for chapter 1-----	42
II. Domain-domain interactions in YtvA-LOV and YtvA full-length proteins-----	48
2.1 The competitive interface for LOV-LOV dimerization and interdomain interactions-----	48
2.2 The LOV-domain crystal structure of YtvA from <i>Bacillus amyloliquefaciens</i> FZB42-----	58
2.3 The signal transmission pathway between YtvA-LOV domain and YtvA-STAS domain-----	63
III. A blue light inducible two component signal transduction system in bacterial LOV proteins-----	74
IV. Light-regulated GGDEF-EAL proteins-----	84
V. General Discussion-----	91
5.1 Domain-domain interactions in YtvA-LOV and YtvA full-length proteins-----	93
5.1.1 The competitive interface for LOV-LOV dimerization and interdomain interactions-----	97
5.1.2 The LOV-domain crystal structure of YtvA from <i>Bacillus amyloliquefaciens</i> FZB42-----	100
5.1.3 The signal transmission pathway between YtvA-LOV domain and YtvA-STAS domain-----	103
5.1.3.1 The H β -sheet in the LOV core-----	103
5.1.3.2 The J α -Linker region-----	106
5.1.3.3 The NTP binding site in the STAS domain-----	107
5.2 A blue light inducible two component signal transduction system in bacterial LOV proteins-----	110
5.2.1 Two-component signal transduction systems-----	110
5.2.2 The plant pathogen <i>Pseudomonas syringae</i> pv. <i>tomato</i> DC3000-----	114
5.2.3 The two-component systems in bacterial pathogenicity-----	114
5.3 Light-regulated GGDEF-EAL proteins-----	118
5.3.1 The regulation of the bacterial second messenger c-di-GMP-----	118
5.3.2 The photosynthetic cyanobacterium <i>Synechococcus elongatus</i> -----	121
5.3.3 The two LOV-containing GGDEF-EAL proteins from <i>Synechococcus elongatus</i> PCC 7942-----	122
5.4 References for chapter 5-----	129

I. Introduction

Talking from “The Origin of Species”

Light from the sun has been associated with life since the very origin of life itself. Although the exact process that led to the first living organism is far from being resolved, it is unquestionable that solar radiation played a key role even in abiogenesis on our planet. Solar UV light was identified as the most abundant energy source for the production of prebiotic organic molecules on early earth¹. The origin and evolution of photosynthesis is also considered to be essential to the spontaneous generation of RNA world and Protein world².

As the most important energy source for life on earth, it is therefore not surprising that solar radiation has also been a crucial factor in evolution. In 1858, Charles Darwin^{3,4} and Alfred Russel Wallace^{3,5} independently provided the key to the theory of evolution; they proposed natural selection as the driving force for the origin of new species. The natural selection served as an evolutionary force to favor an organism's features that could bring it into a more efficient relationship with its environment, and this accounted for every living creature's adaption to its specific environment⁶. Darwin and his son⁷ also noticed and experimented the photosensitivity of plants and animals, e.g. phototropism, but due to the lack of more detailed, molecular based knowledge in plant physiology, they did not explore the question of the impact of solar radiation as an important evolutionary force.

Photo-processes are so essential that all organisms, from bacterial to human, exhibit some form of photosensitivity to solar radiation. In order to understand how life can utilize solar energies, it is necessary to examine the solar radiation that reaches the earth and to find out what kinds of molecules are absorbing

these energies and how they are organized within the cell to function as a photosensitive system.

1.1 Light in photo-processes

When interacting with matter, light can exhibit properties of both waves and particles; the particles would then be called photons or quanta and contain a certain amount of energy in the form of oscillating electric and magnetic fields, which is proportional to the frequency of this particular radiation. The response of a photosensitive system to light is generally an interaction between one photon and one molecule. In this process the molecule can be promoted from its electronic ground state to an excited state by absorbing the energy from the photon⁶. Because the energy gap between the two states must be equal to the incoming photon energy, a molecule can only absorb energy from a particular electromagnetic radiation with a proper frequency that matches the vibration frequency of the electrons in this system⁸. Therefore, the intensity of the solar radiation at earth's surface should be a crucial condition for the selectivity of specific molecules that could effectively utilize the energy to make life on earth possible.

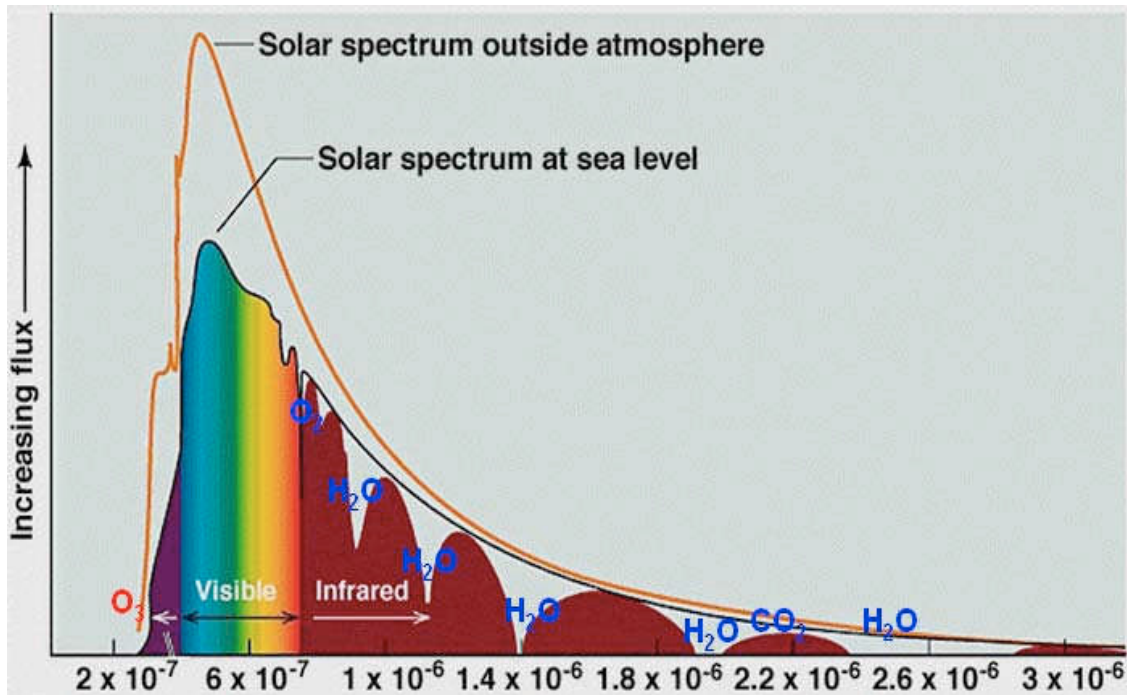


Figure 1-1: Solar radiation spectrum¹⁰, modified picture from the American Society for Testing and Materials (ASTM)⁹.

As living organisms evolved, they adapted themselves to a very narrow band of solar radiation spectrum. With “the invention of oxygen”, the ozone layer did screen out most of the biological harmful UV radiation (entire UV-C, most UV-B and little UV-A), allowing life to emerge from water onto land. On the other end of the solar spectrum, infrared radiation is mostly absorbed by water vapor and CO_2 in atmosphere⁹. Therefore, only a relatively small part of the overall radiation emitted by sun, i.e., the so-called “visible light” between 380 nm and 780 nm produces most of the energy that reaches the surface of earth and thus is central to the development of different photosensory systems in living organisms (Figure 1-1).

1.2 The molecules that respond to photo-absorption

In most cases, photosensory systems in living organisms are composed of different photoreceptor proteins that are sensitive to light. But normally, a protein itself can not capture a photon directly. Therefore the ability for a certain photoreceptor to absorb light usually depends on the type of its co-factors that then directly respond to light radiation. These co-factors are called chromophores. A chromophore (from Greek word *chromos*=color) in a photoreceptor protein is the moiety responsible for the color of this photoreceptor by absorbing certain wavelengths of visible light and transmitting or reflecting others.

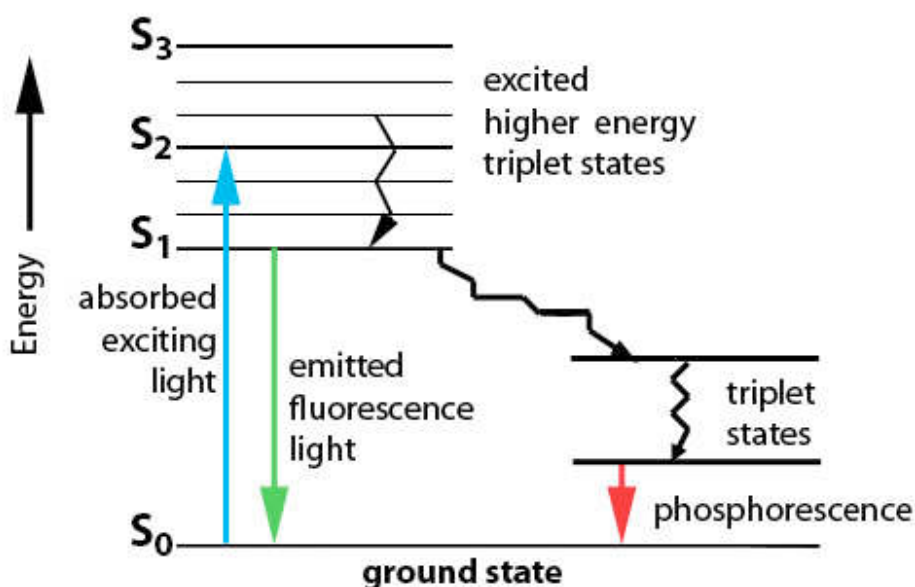


Figure 1-2: Jablonski Diagram^{11,12}. Different states are arranged vertically according to energy levels and horizontally according to spin multiplicity. Radiative transitions (absorption and emission) are indicated by straight arrows and non-radiative transitions (relaxation, internal conversion and intersystem crossing) by squiggly arrows. Different excited states are indicated with thick lines, the higher vibrational states of each excited state are indicated with thinner lines.

According to the electronic configuration, a molecule can have many electronic states with different energy levels. A Jablonski diagram (Figure 1-2), named after the Polish physicist Aleksander Jabłoński¹², is a diagram that illustrates the

electronic states of a molecule and the transitions between them. The state with lowest energy is called ground state (S_0) and electrons in ground state can be promoted to an excited state (S_n) by absorbing energy. The energy difference between a chromophore's ground state and a certain excited state falls within the range of the radiation spectrum that the respective photoreceptor protein can absorb. The dissipation of energy to its surrounding environment can cause relaxation of the excited state to a lower vibrational level, while the internal conversion can also cause the transition between two excited states by releasing heat. The electrons finally will return to the ground state by emission of photons (fluorescence). Another possible transition pathway is intersystem crossing with the change of spin multiplicity from a singlet state to a triplet state (T_n), this type of transition can finally come back to the ground state by producing phosphorescence. The intensity of light absorption by a chromophore depends on the transition probability of its electron system, which is a substance-specific molecular property described as the absorption coefficient.

According to their molecular configuration, most of the chromophores (with some exceptions) can be divided into two forms, either as conjugated π -systems or as metal complexes.

A conjugated system is an organic compound with alternating single and multiple bonds (e.g., $C=C-C=C-C$). This system results in a general delocalization of the electrons across all of the adjacent parallel aligned p-orbitals of the atoms, which increases stability and thereby lowers the overall energy of the molecule. In a chromophore with a conjugated π -system, the energy levels between which the electrons can jump, are extended π -orbitals created by the conjugated system, often in aromatic rings with bonds such as $C=O$, $N=N$ and $C=N$ in addition to conjugated $C-C$ bonds. Such chromophores include retinal (Figure 1-3), lycopene, β -carotene, anthocyanins etc.

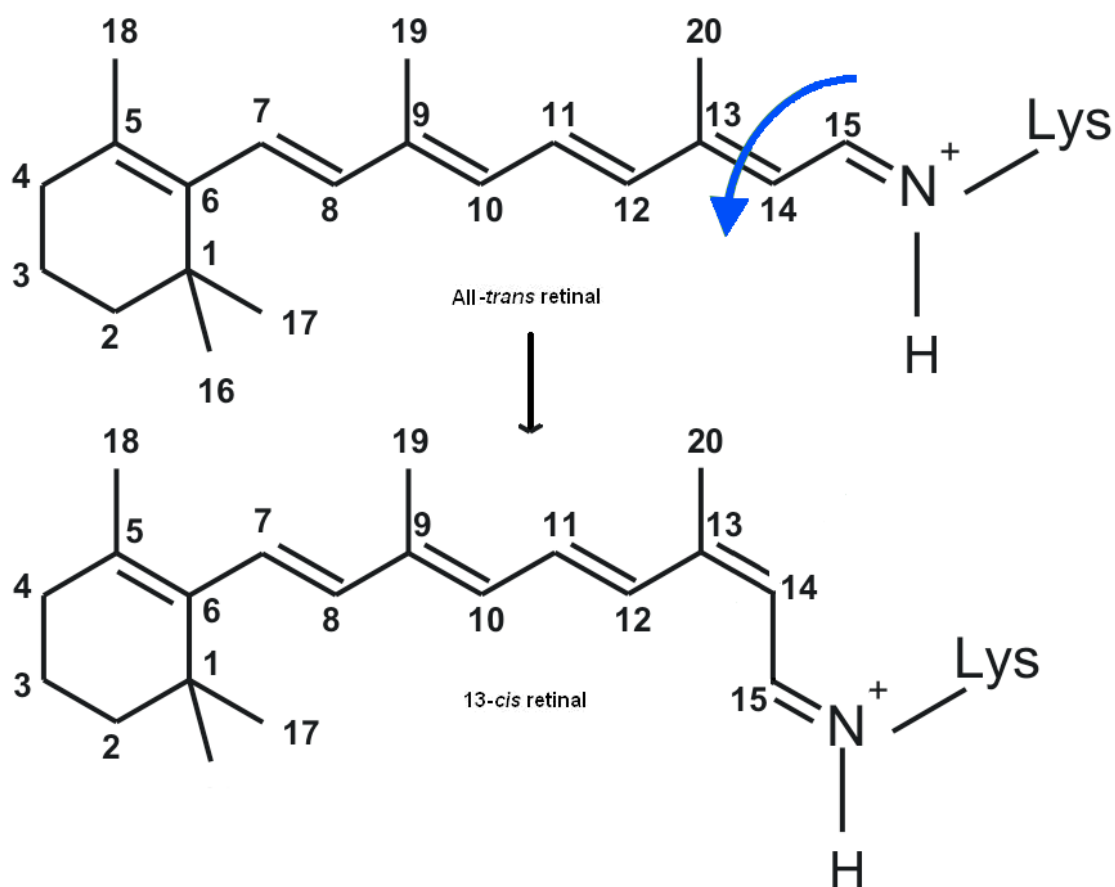


Figure 1-3: Photoisomerization in retinal¹³ (a photoreaction found in bacterial rhodopsins, e.g., bacteriorhodopsin)

The metal complex chromophores arise from a coordinate covalent bond between a transition metal and the molecules surrounding the metal called ligands. In most metal complexes, the electronic transitions upon the absorption of light are caused either by a d-d transitions or charge transfer bands. In a d-d transition, an electron in a d-orbital of the metal atom can be excited by a photon to another d-orbital of higher energy. A charge transfer band promotes an electron from a metal-based orbital into an empty ligand-based orbital (Metal-to-Ligand Charge Transfer or MLCT) or vice versa (Ligand to Metal Charge Transfer or LMCT)¹⁴. Examples of such chromophores can be found in hemoglobin and hemocyanin etc.

1.3 The classification and distribution of photoreceptors

Besides the primary photochemical event taking place in the chromophore that triggers different photo-processes, another practical criterion for the classification of photoreceptor proteins is to divide them according to the modes of action by which light is used. Biological photo-processes can then be categorized into two types: light as a source of energy or as a signal for photomorphogenesis in the most general sense.

In biological photoreceptors that serve to capture or detect light energy, most of the corresponding biological response is thus triggered by the photon-capture in a given chromophore, which then leads to the primary photochemical event such as photoisomerization of a certain double bond¹⁵ (Figure 1-3), electron or energy transfer and sometimes even photo-adduct formation through a triplet state intermediate¹⁶.

Different with photoreceptors, photo-sensors detect light as stimuli; the primary photochemical events in their chromophores can result in conformational changes in photoreceptor proteins, which in turn start to transmit the signal caused by photon absorption to a downstream signal transduction partner that could be either fused protein modules or separate proteins or sometimes even nucleotides or nucleic acids. Eventually a relevant biological event can be triggered, such as direct energy capture, photomorphogenesis, phototaxis, protein degradation, gene regulation, circadian rhythm regulation, etc (Figure 1-4).

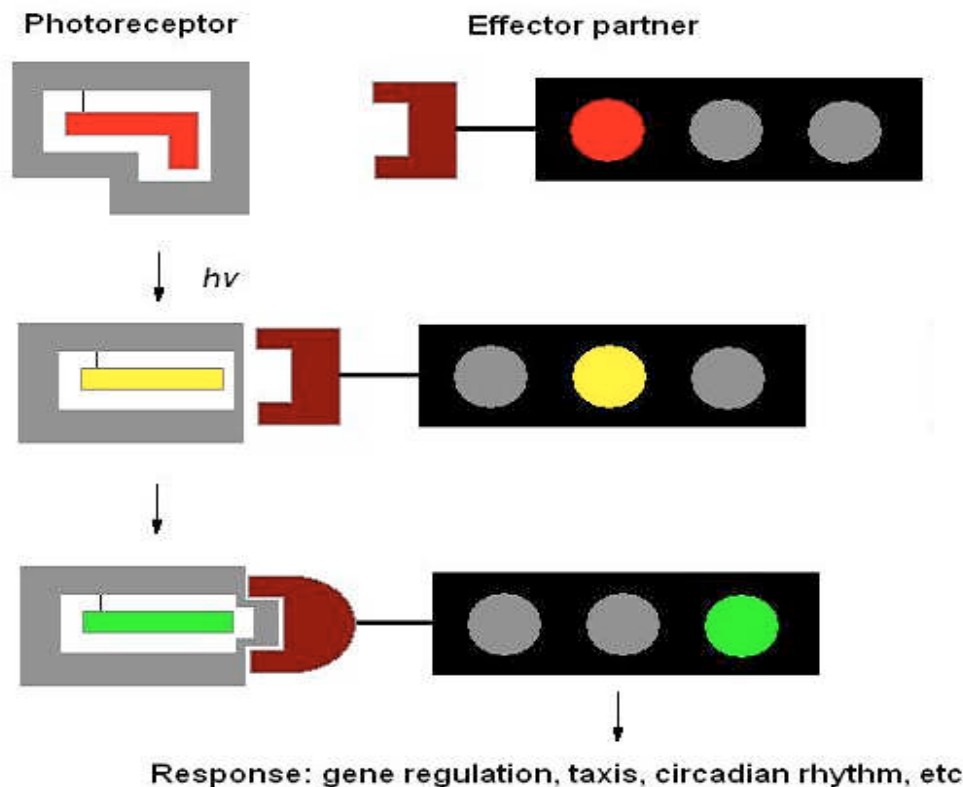


Figure 1-4: Conformational changes of the chromophore induce changes of the photoreceptor proteins.

1.3.1 Photoreceptors using light as an energy source

Photosynthesis is the most important process to convert light energy into chemical energy for cellular metabolism in plants, algae, and many species of Bacteria. It consumes carbon dioxide and water and releases oxygen as a waste product (in the case of oxygenic photosynthesis). Thus photosynthesis is crucially important for life on Earth, since on the one hand it maintains the normal level of oxygen in the atmosphere, and on the other hand nearly all life either directly depends on it as an energy source, or indirectly as the ultimate energy source in their food^{17,18}.

Photosynthesis in different species can occur in very similar ways. The process normally begins with the absorption of light energy by proteins called

photosynthetic reaction centers that use chlorophyll (Figure 1-5) as chromophore. In plants, most of these proteins are held inside organelles called chloroplasts. In some exceptional cases structures like “phycobilisomes” are anchored to thylakoid membranes. In bacteria these proteins are normally embedded in the plasma membrane. Photosynthesis occurs in two stages. In the first stage, light-dependent reactions capture the energy of light and store it in the form of ATP and NADPH. During the second stage, the light-“independent” reactions use this energy to convert carbon dioxide into sugars in a process called carbon fixation, according to the following equation:



The reaction center is a complex of many proteins that bind functional chromophores or pigments such as chlorophyll and pheophytin. These molecules can be found in all green plants and many bacteria and algae. A reaction center can capture the energy of photons either directly by its pigments or with the help from surrounding light-harvesting complexes called antenna complexes, which are usually composed of one or more polypeptide chains containing photosynthetic pigments wrapped around the reaction centre. The antenna complex uses additional pigments like chlorophyll b, lycopene and β -carotene to pass the absorbed energy into the reaction center via resonance energy transfer; this can only occur when an energy acceptor is present with an equal or lower energy state than the donor. The reaction centers in plants and bacteria contain a chlorophyll dimer, called the special pair. The excited state of this special pair is lower in energy than that of a single chlorophyll molecule; therefore resonance energy can be transferred from single chlorophyll molecules present in antenna complexes to the special pairs that are present directly in the reaction centre¹⁹.

There are several different kinds of photosynthetic pigments found in either chloroplasts or photosynthetic bacteria; each of them absorbs light of a different

spectral range. This is a reasonable finding since the light energy capturing can be much more efficient with pigments sensitive to a broader light source.

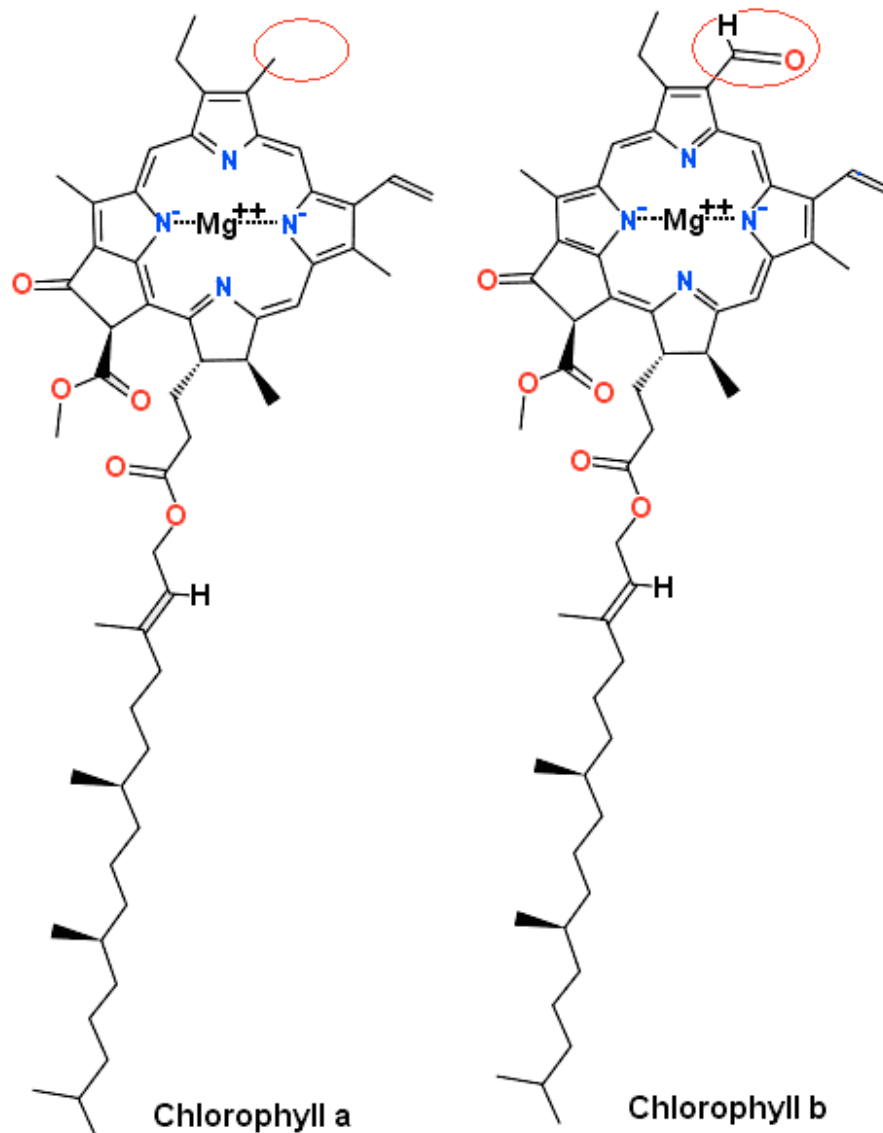


Figure 1-5: Structure of chlorophyll a and chlorophyll b (The difference has been highlighted by the red circle, methyl vs. formyl substituent).

The most common pigment in green plants is chlorophyll a (Figure 1-5), which is present in every plant that performs photosynthesis. Chlorophyll a absorbs well at a wavelength of about 400-450 nm and 650-700 nm; chlorophyll b (Figure 1-5) absorbs at 450-500 nm and 600-650 nm. Additional light absorbance is

accomplished by the “Xanthophylls”, structurally these are carotenoids (Figure 1-6) that absorb well at 400-530 nm. However, the green-yellow region of light is reflected by most of the pigments giving us the abundant green appearance in nature¹⁹.

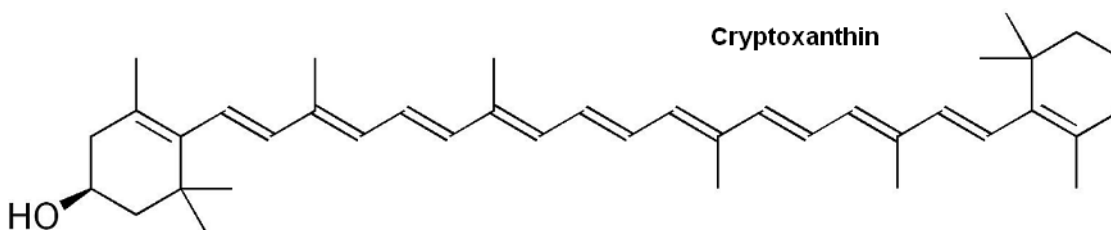


Figure 1-6: Structure of cryptoxanthin, an example of xanthophylls. Xanthophylls are yellow pigments from the carotenoid group carrying keto- or hydroxyl substituents at one or both cyclohexene rings.

Like plants, the photosynthesis in cyanobacteria uses water as electron donor and releases oxygen; it also contains chlorophyll as pigment. In addition, most cyanobacteria use phycobiliproteins to capture light energy and pass it on to the chlorophylls of the reaction center. Some cyanobacteria use chlorophyll b instead of phycobilins. Also, several other bacteria use the bacteriochlorophyll pigments for photosynthesis. Unlike the cyanobacteria, these bacteria do not produce oxygen; they absorb different region of light than plants and typically use hydrogen sulfide rather than water as the electron donor²⁰.

An entirely different principle of photosynthesis has been developed in some Archaea. Photosynthetic archaea use the pigment bacteriorhodopsin (BR) to capture light energy and to use this energy to transport protons across the membrane out of the cell. The resulting proton gradient is subsequently converted into chemical energy via ATP synthesis in a light-independent reaction.

Bacteriorhodopsin is an integral membrane protein usually found in two-dimensional crystalline patches known as "purple membrane", which has a

repeating element of the hexagonal crystalline structure made of trimer molecules (Figure 1-7). Each molecule consists of seven transmembrane α -helices arranged in a bundle around a retinal molecule that is bound to a lysine residue via a Schiff base²¹. It is the photoisomerization of the retinal chromophore that results in a conformational change of the surrounding protein and triggers the proton pumping action.



Figure 1-7: Hexagonal structure of bacteriorhodopsin trimer; several closely located lipid molecules are also displayed²²

Recently, a pigment with similar photosynthetic process like BR has been found in some marine γ -proteobacteria, which has been called proteorhodopsin²³. Unlike all other photosynthetic systems in bacteria, proteorhodopsin produces a proton gradient very similar as BR, and as for BR, its photoprocess is not coupled with carbon fixation like in chlorophyll-based photosynthesis. Thus it is likely that photosynthesis independently evolved at least twice, once in chlorophyll-based systems and once in BR-based systems.

1.3.2 Photo-sensors using light as an environmental signal

Since light is the most important energy source for all the photosynthetic organisms, it is not surprising that these organisms have developed signaling systems to sense their only energy source. Such photo-sensors will enable them to optimally obtain that spectral part of the sunlight that they can utilize for photosynthesis and to avoid that part that might be harmful. Thus, these photo-sensors should sense not only the direction of light, but also the intensities, durations and spectral properties of light as an environmental signal.

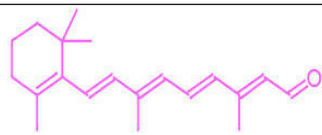
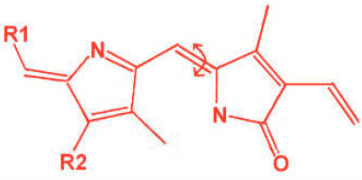
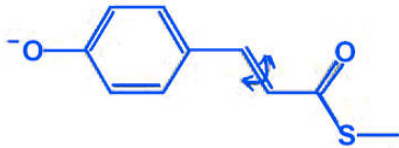

Photo-sensor Families	Photochemistry	Chromophore (with some examples)
Rhodopsins	<i>trans</i> ↔ <i>cis</i>	retinals 
Phytochromes	<i>trans</i> ↔ <i>cis</i>	tetrapyrroles 
Xanthopsins	<i>trans</i> ↔ <i>cis</i>	<i>trans</i> -p-coumaric acid 
Cryptochromes	E+e ⁻ transfer	flavin derivatives 
BLUF proteins	e ⁻ transfer(?)	
Phototropins	adduct formation [3FMN-cys(C4a)]	
ZTL/ADO/FKF1		

Table 1-1: Well-Characterized Classes of Chromophores and Photosensor Families

According to the chemical structure of the light-absorbing chromophores involved in photo-sensing, the many different well characterized photoreceptor proteins

can be classified into a limited number of families, among which there are several different types of photoreceptor proteins that bind flavin derivatives as chromophore. Up to now, the most important photoreceptors with a wide distribution in the three domains of life (bacteria, archaea and eukaryotes) can be divided into seven families (Table 1-1): rhodopsins²⁴, phytochromes²⁵, xanthopsins²⁶, phototropins²⁷, cryptochromes²⁸, BLUFs²⁹ and ADAGIO(ADO)/FKF1³⁰. For the first three families, the primary photochemical event of their different chromophores is a *cis-trans* photoisomerization of a certain double bond. The other four families are photoreceptors using flavin derivatives as chromophore, but they undergo different photochemical reactions.

1.3.2.1 Rhodopsins

Rhodopsins are a family of proteins that use a photo-isomerizable retinal as chromophore for light reception. Thus this group of proteins is also called retinal-binding proteins or retinylidene proteins. They are the molecular basis for a variety of light-sensing systems from phototaxis in algae to visual perception and circadian clock in animals³¹.

All rhodopsins consist of a bundle of seven transmembrane helices that form an internal pocket to bind the photoactive retinal (retinaldehyde)³², which can be activated by light via photoisomerization and thus induces a conformational change in the protein. This change acts as a molecular switch to activate a downstream signalling pathway within the cell. Depending on the type of rhodopsin, it either opens an ion channel (for example in alga), activates an associated G protein and triggers a second messenger cascade (for example in animal retina), or interacts with a “signal transducer” protein (in archaea).

Rhodopsins are present in many species from bacteria to algae and animals, but no rhodopsin-like protein has been found in higher plants to date. Rhodopsins can be divided into two distinct groups based on their sequence as well as on the

retinal isomer they contain at the ground state and their signal transduction mechanisms. The retinal molecule can adapt several different *cis-trans* isomeric forms, such as all-*trans*, 11-*cis* and 13-*cis*.

Rhodopsins found in prokaryotes and algae commonly contain an all-*trans* retinal isomer at the ground state that isomerizes to 13-*cis* upon light activation. They act as light-regulated ion pumps and can be further divided by the type of ion that is transported. Whereas bacteriorhodopsin functions as a proton pump, halorhodopsin act as a chloride pump³³. On the other hand, rhodopsins of the animal kingdom belong to the class of G protein-coupled receptors and bind an 11-*cis* isomer of retinal at the ground state that photoisomerizes to the all-*trans* isomer upon light activation. They are commonly found in the light-sensing organs, for example in the photoreceptor cells of the vertebrate retina where they enable eyesight²¹.

1.3.2.2 Phytochromes

The phytochrome family was first discovered as the photoreceptors responsible for red/far-red light regulated plant responses (summarized as photomorphogenesis), such as flowering (photoperiodism) and circadian rhythms in plants. They are also believed to be involved in other responses like the chloroplast movement, cytoplasmic motility, gravitropism, germination of seeds, elongation of seedlings and the synthesis of chlorophyll³⁴.

The light sensitive chromophore in phytochromes is an open-chain tetrapyrrole that is bound to a conserved cysteine residue via a thioether linkage. Red light triggers a *cis-trans* change in one of the double bonds in the “all-*cis*” Pr form of this bilin chromophore, converting it into the far-red light-absorbing Pfr form, which slowly reverts back to the Pr form in the dark, but is readily re-converted to Pr by far-red irradiation. Phytochromes are widely distributed throughout the bacterial and eukaryotic domains of life, but have not been found up to now in

archaea. In plants and cyanobacteria, they use phytochromobilin and phycocyanobilin respectively, as chromophores. The structure of phytochromes from plants and cyanobacteria also presents a conserved GAF (cGMP phosphodiesterase/ adenylate cyclase/ FhlA) motif. The more recently identified proteobacterial and fungal phytochromes bind biliverdin as chromophore in a PAS(Per/ Arndt/ Sim) motif³⁵. In most cases the prokaryotic phytochromes have been linked to red/far red light dependent responses *in vitro*. Identified were the regulation of the phosphorylation in the typical two component system (histidine kinase and response regulator)³⁶, and the synthesis and degradation of second messenger c-di-GMP³⁷. However, unlike the well characterized physiological function of phytochromes in plants, the physiological response has been demonstrated only in few cases, such as the control of photosynthesis in *Rhodopseudomonas palustris*³⁸.

1.3.2.3 Xanthopsins

The family of the xanthopsins is the photoreceptor family that carries *trans*-p-coumaric acid as its light-sensitive chromophore, covalently bound through a thioester linkage. This family is less distributed than other photoreceptor families, as they are only found in proteobacteria. Photoactive Yellow Protein (PYP) from *Ectothiorhodospira halophila* is by far the best studied xanthopsin^{39,40}. Although this protein has been well characterized in structure and photochemistry, its physiological function is still far from being resolved. It is proposed that PYP regulates a blue light induced avoidance response from harmful UV light, but this regulatory role of PYP has not been proven to date^{39,40}. The PYP-phytochrome fusion protein Ppr from *Rs. centenum* is of particular interest because it is the first xanthopsin of which the biological function has been genetically demonstrated. It was shown that this protein regulates chalcone synthase gene expression in response to blue light⁴¹.

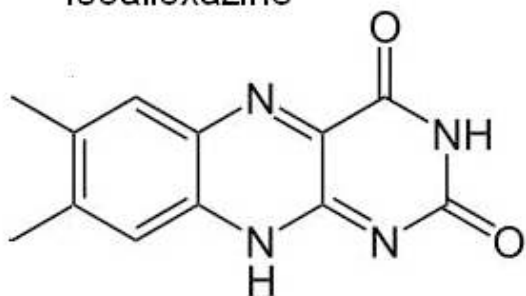
The four photoreceptor families that use flavin derivatives as chromophore are discussed in greater detail in chapter 1.4.

1.4 Flavin based photoreceptors

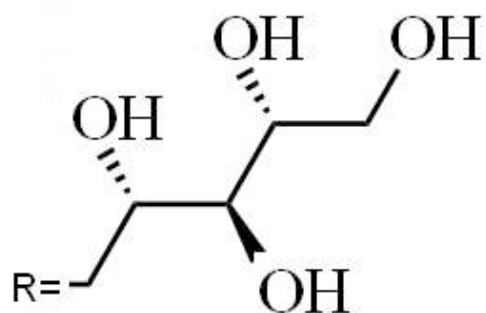
The region between (420-480 nm) of the visible light has the highest inherent energy. On the one hand a higher energy content can facilitate energy utilization in photosynthetic process, but on the other hand it can also represent a caution signal for the avoidance of energy-rich blue/UV light, which may cause severe damage in living organisms. Therefore it is not surprising that life on earth has developed many different photoreceptors that are sensitive to blue light; most of these proteins belong to the flavin-binding photoreceptor protein families.

Flavin (from Latin flavus, "yellow") is the common name for a group of organic compounds derived from the tricyclic heteronuclear organic compound isoalloxazine (Figure 1-8a). They have important functions in many biochemical reactions as coenzymes or photoactive chromophores. Riboflavin (Figure 1-8b), also known as vitamin B₂, is the precursor of the two commonly distributed derivatives, flavin adenine dinucleotide (FAD figure 1-8c) and flavin mononucleotide (FMN figure 1-8d). The flavins are capable of redox reactions and can accept either one or two electrons, sometimes with the addition of protons, which makes flavins good electrophiles in electron transfer reactions. Besides, oxidized flavin molecules are also susceptible to a nucleophilic attack at their N-5 and C4 α position. Both free and protein-bound flavins are photoreducible, light excitation in flavins can introduce alternations of the charge distribution and redox potential, enabling flavins for a variety of photochemical reactions like electron or energy transfer⁴².

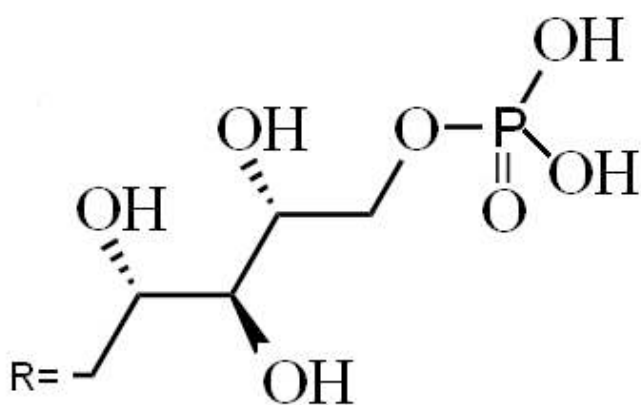
A Parent compound
isoalloxazine



B Riboflavin



C FMN



D FAD

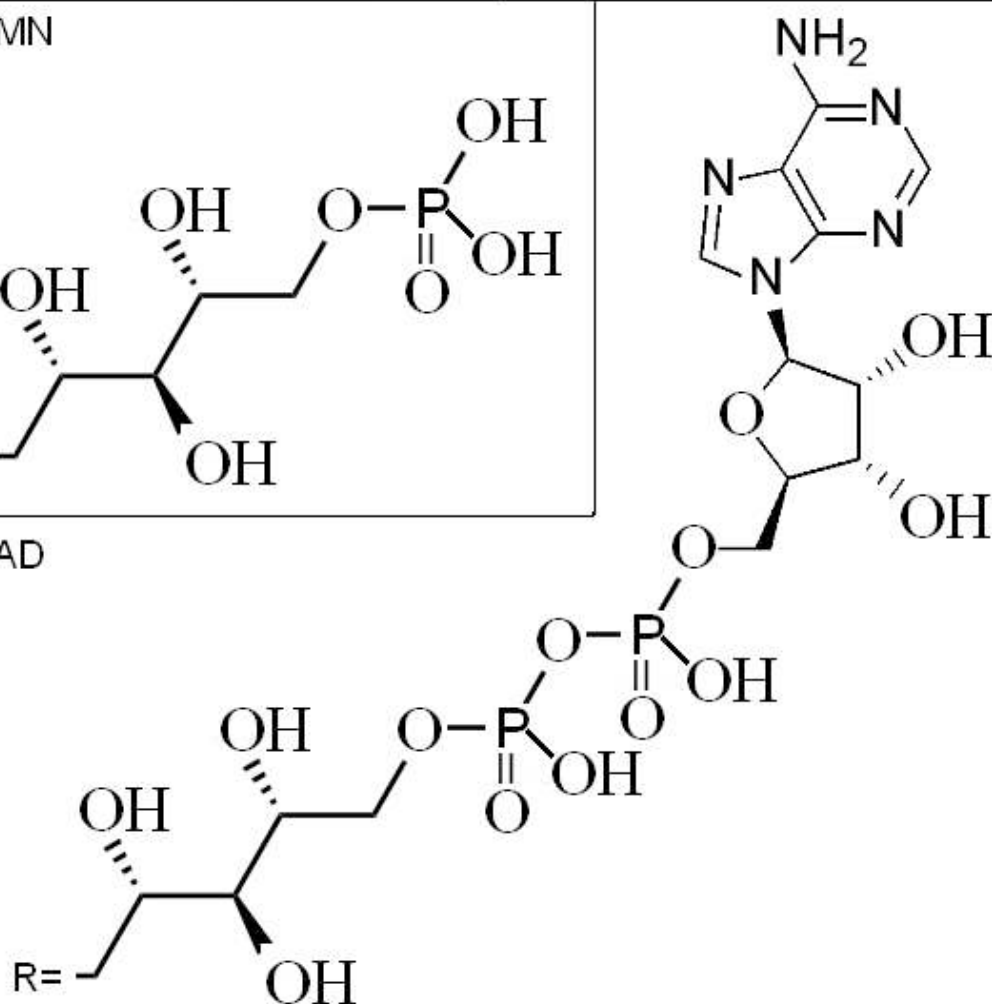


Figure 1-8: Structure of different flavin derivatives, (A) the parent compound isoalloxazine; (B) Riboflavin; (C) FMN, flavin mononucleotide; and (D) FAD, flavin adenine dinucleotide.

1.4.1 Cryptochromes and photolyases

Cryptochrome (Cry) is the first identified family of flavin-containing photoreceptors. It is named according to the long-hidden nature of its chromophore (cryptochrome derives from the Greek *krypto chroma*, means hidden color). These blue-light photosensors are present in lower and higher eukaryotes, including algae, plants, insects and animals. Cryptochromes play a pivotal role in the generation and maintenance of circadian rhythms. In higher plants they are involved in processes that regulate germination, elongation, photoperiodism, and other responses^{28,43}. It has also been proven that cryptochromes are important in magnetic orientation of birds during migration and essential for fruit flies to sense magnetic fields^{44,45}.

The cryptochrome family added an exciting dimension to the primary photochemistry of photosensing; they are photoactive proteins that possess two chromophores (derivatives from either flavin or pterin), but none of these chromophores is feasible in *cis-trans* isomerization. This had led to many proposals on its primary photochemistry, such as light-induced transfer of either energy or an electron, either intra- or inter-molecular. Recently, evidences were provided that the activation of cryptochromes is based on reversible electron transfer^{46,47}.

Cryptochromes were identified because of their high sequential and structural similarity with photolyases (PHR), enzymes that bind complementary DNA strands and break certain types of pyrimidine dimers caused by exposure to ultraviolet light. Photolyases are also flavin-binding proteins that were initially identified in bacteria, but undergo a light-induced enzymatic function. They contain two photoactive cofactors including the fully reduced FADH^- as one ubiquitous chromophore, which is required for the catalytic activity of DNA repair. FADH^- acts as an electron donor in an electron transfer reaction that leads to a fission of a pyrimidine dimer. The second cofactor functions as an antenna

pigment to harvest photon energy and transfer this energy to FADH^- , which thus increases the yield due to higher photon capture in low-light condition⁴⁸. Currently, the known light-harvesting cofactors include 5,10-methenyltetrahydrofolate (MTHF), 8-hydroxy-5-deaza-riboflavin (8-HDF), FMN and FAD⁴⁹.

The shared characteristic feature between cryptochromes and photolyases is the joint involvement of two chromophores in photosensing. In addition, the overall fold and primary sequence show high similarity. Also, some of the amino acids involved in DNA binding are conserved between Crys and PHRs, and also a Trp triad that allows external electron transport. Recently a new class of putative cryptochromes referred as CRY-DASH (*Drosophila*, *Arabidopsis*, *Synechocystis* and *Homo*) was found in both photosynthetic and non-photosynthetic prokaryotes, but so far no blue light-dependent sensor activity could be demonstrated in CRY-DASH. In recent experiments, some members of this sub-family have been proven to possess DNA-photolyase activity towards cyclobutane pyrimidine dimers in single strand, but not in double strand DNA⁵⁰.

Cry plus PHR as one big family is by far the most widely distributed flavin binding photoreceptors group that can be found in many different domains of life, from bacteria to plants and to animals⁵¹.

1.4.2 The LOV proteins: phototropin and ZTL/ADO/FKF1 families

Already in the late 19th century, Charles Darwin and his son had noticed in several plant species an interesting feature: phototropism, a light dependent directional growth towards the light source⁷. The responsible photoreceptor protein, however, could only be identified until 1997, even a few years later than Cry. This protein is called phototropin, which was the product of a gene named *nph1* and was proven to play a key role in the early stage of phototropism in *Arabidopsis thaliana*²⁷. There are two phototropins (phot1 and phot2) in

Arabidopsis thaliana. Later they were also characterized as part of the sensory system that causes various blue-light regulated responses in plants, like chloroplast movement, leaf expansion and stomatal opening⁵².

The conserved module in phototropin that functions as a blue light sensor is the LOV domain, which was named according to its homology to a subset of PAS domain proteins that could be regulated by external signals such as light, oxygen, or voltage. The LOV domain binds an oxidized FMN as chromophore. Blue-light illumination causes the formation of a covalent bond between the C4 α position of flavin and the SH-group of a conserved cysteine (Figure 1-9)⁵³, and this photo-adduct can slowly reconvert to the unbound state in a time scale from minutes to hours.

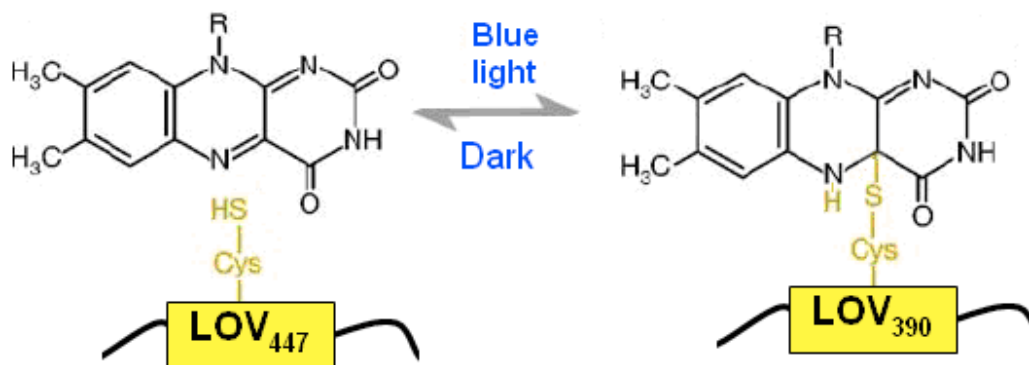


Figure 1-9: Primary photoreaction of the LOV domain.

The phototropins possess two LOV domains (LOV1 and LOV2) in a tandem array that are coupled with a downstream serine/threonine kinase (Figure 1-10). Accordingly phototropin is a member of AGC kinase family (cAMP-dependent protein kinase, cGMP-dependent protein kinase G and phospholipid-dependent protein kinase C)⁵⁴. The covalent binding of FMN upon blue-light absorption leads to a conformational change in the protein and results in enhanced kinase activity, and this activation is dark reversible⁵⁴. LOV1 and LOV2 have distinct properties and functions. The LOV2 domain is believed to play a predominant

role in the light activation, whereas the function of LOV1 is still not as clearly determined although it has been proposed as a possible dimerization domain⁵⁵.



Figure 1-10: Domains organization in phototropin

Besides plants, the LOV paradigm is also widely distributed in fungi, bacteria and archaea, but it has never been found in animals. Unlike phototropin, all other LOV proteins contain only one LOV domain, which is associated with a variety of effector domains like kinases, transcription factors, phosphodiesterases, etc. Some bacterial LOV proteins even consist of only a single LOV core without any fused effector domains^{51,56}. These LOV proteins are presumable modular systems for blue-light signal transduction, and will be further discussed in chapter 1.5.2.

The ZTL/ADO/FKF1 family is another class of LOV domain containing photoreceptors that has recently been identified mainly in higher plants, which comprises three members: Zeitlupe (ZTL, also referred to as Adagio, ADO); Flavin-binding, Kelch Repeat, F-box 1 (FKF1); and LOV Kelch, Protein 2 (LKP2)⁵⁴. These proteins are believed to play a key role in circadian rhythm control of higher plants³⁰. They possess an N-terminal LOV domain followed by an F-box and six Kelch repeats (Figure 1-11). The F-box is a typical motif in E3 ubiquitin ligases that degrade proteins, and the Kelch repeats are normally involved in mediating protein-protein interactions. This may suggest ZTL/ADO/FKF1 proteins to be involved in light regulated proteolysis⁵⁴.



Figure 1-11: Domains organization in ZTL/ADO/FKF1

The LOV domain of this novel family also binds an FMN as chromophore, and displays analogous photochemical properties, but unlike the phototropin LOV domains, ZTL, FKF1, and LKP2 either can not recover to the ground state in the dark⁵⁴ or the decay may occur but in a quite slow mode that will take several days⁵⁷. This distinct photochemical property might correlate with the relatively slow responses triggered by FKF1, ZTL, and LKP2 (e.g. induction of flowering) in comparison to the rapid responses controlled by the phototropins (e.g. chloroplast movements)⁵⁵.

1.4.3 BLUFs (blue light sensing using FAD)

Besides cryptochromes and phototropins, BLUF (blue light sensing using FAD) is the third photoreceptor family that uses flavin derivatives as their chromophore. Most BLUF proteins are from prokaryotic genera. Members of this family are involved in photophobic responses and transcriptional regulation^{58,59}. Many BLUF domains are part of multidomain proteins involved in catalytic conversion of regulatory cyclic nucleotides, such as cAMP and c-di-GMP. The BLUF domains bind FAD noncovalently. AppA from *Rhodobacter sphaeroides* exhibits a typical UV/Vis spectrum for an oxidized flavin and undergoes a redshift of several nanometers upon blue-light absorption⁶⁰. The initial characterization of the primary photochemistry for Slr1694 from *Synechocystis* sp. PCC 6803 showed a photo-induced electron transfer followed by a reversible proton transfer from the flavin to protein⁶¹.

1.5 The phototropin-like LOV proteins

The LOV signaling module is widely distributed in all three kingdoms of life with the only exception of animals. After the discovery of this photo-sensory paradigm in plant phototropins, efforts in genome mining have revealed the presence of LOV modules not only in photosynthetic plants and prokaryotes, but also in non-photosynthetic fungi and proteobacteria. As an example given, LOV domains have been found in a variety of plant and animal pathogens such as *Pseudomonas syringae*, *Brucella abortus*, in some plant root colonizing species like *Pseudomonas putida*, and also in common soil bacteria like *Bacillus subtilis*⁶². Although the photochemical activities have been proven in some of the LOV proteins from non-photosynthetic species, their physiological function is still an open question. Does the presence of a photo-active LOV domain in a protein necessarily mean that this protein functions as a photoreceptor? Thus, more detailed insights into the structural and biochemical information of the LOV-domain involving signal pathways will be necessary for us to have a better functional and physiological understanding of these proteins.

1.5.1 The structure and photochemistry of the LOV paradigm

LOV domains in proteins are members of the PAS superfamily, as the LOV domain exhibits a conserved α/β PAS fold with an anti-parallel central β -scaffold surrounded by four α -helices. In the dark state, the FMN is non-covalently held in a pocket formed by two parts ($A\beta B\beta$ and $G\beta H\beta I\beta$) of the five β -sheets. The conserved sequence motif GXNCRFLQ contains the covalently binding cysteine and resides in and around one of the helical connectors ($E\alpha$) and is responsible for binding and stabilization of the chromophore FMN (Figure 1-12).

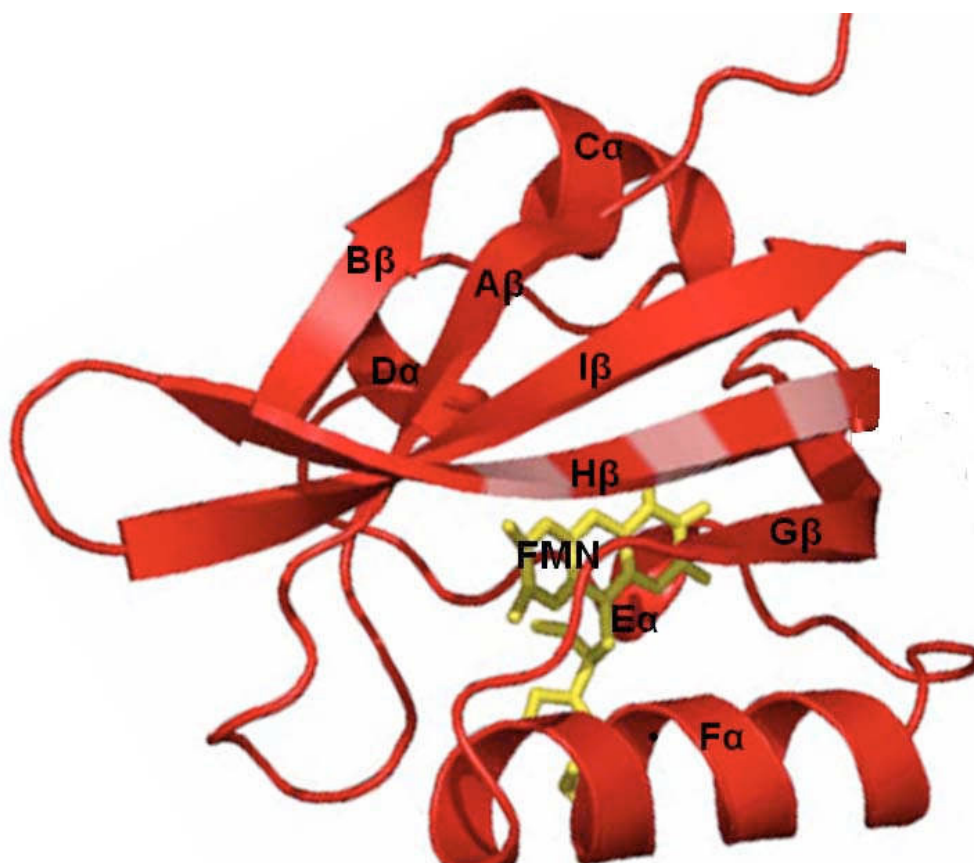


Figure 1-12: 3D-Ribbon structure of the dark state of *Bacillus subtilis* YtvA-LOV domain (pdb entry: 2PR5)⁷³. Protein is represented in red and FMN is in yellow.

The LOV mediated photochemistry is similar in all the characterized LOV proteins. The non-covalently bound FMN in the dark state has a maximum absorption around 447 nm, and the absorption of light by the FMN molecule

results in the promotion of FMN molecule to its excited triplet state via intersystem crossing in pico-second time scale. The excited triplet state has a maximum absorption at 660 nm, and decays in about 2 μ s. During this process, a covalent bond is formed between the C4a of FMN and the SH-group of the cysteine in the conserved motif. This photo-adduct represents the light state and has a typical absorption at 390 nm. In the dark it slowly reconverts to the initial parent (dark) state in a time scale from seconds to hours (Figure 1-13)⁶².

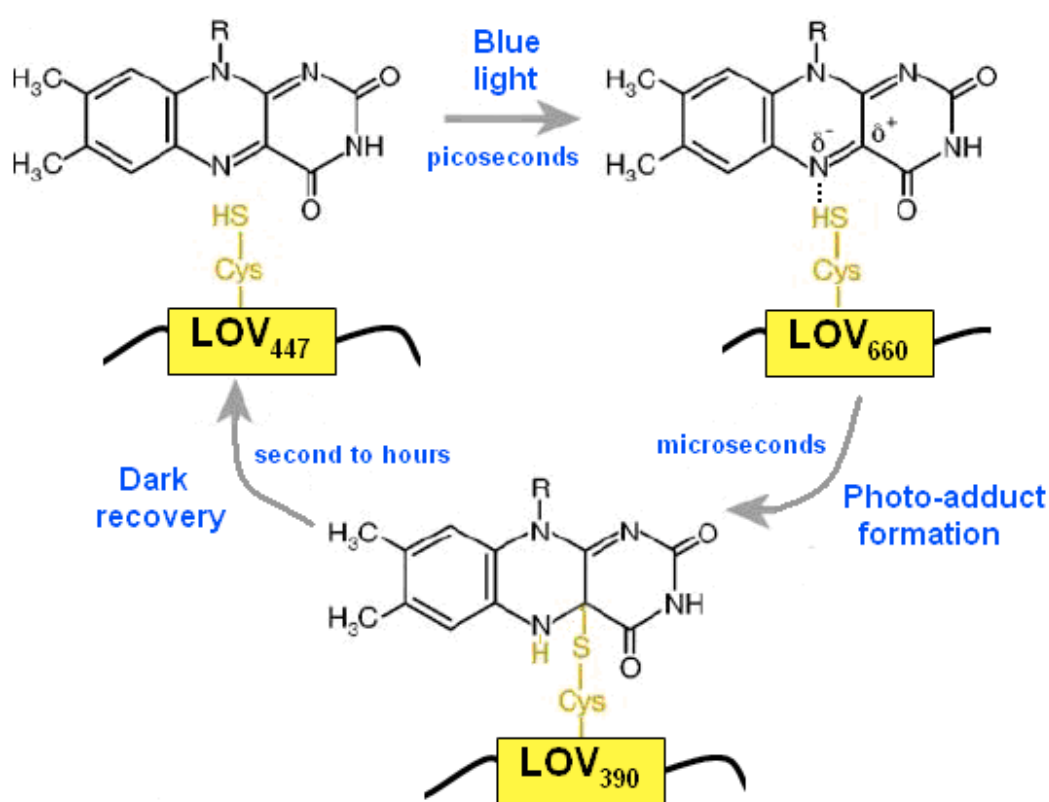


Figure 1-13: Typical photocycle of a LOV protein

Because of the very fast conversion of the triplet state, the detailed molecular mechanism for the formation of the photo-adduct is still under debate, with four possible ways having been proposed (Figure 1-14)⁶³.

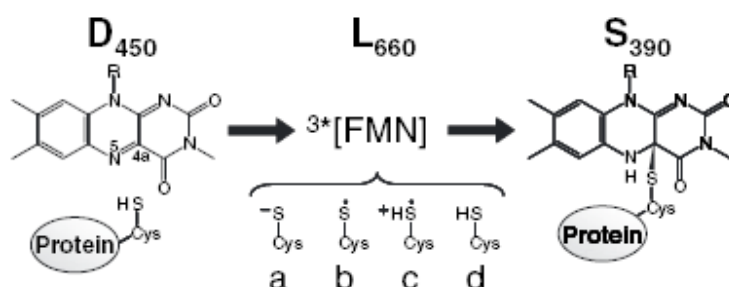


Figure 1-14: Four possible molecular mechanism of the photo-adduct formation from the triplet excited state⁶³. a) A proton transfer from Cys to the N(5) of the FMN isoalloxazine ring converting the S–H to an S[•] form in L660; b) The sulfur of the S–H becomes a neutral radical in L660 due to an electron and a proton transfer from the S–H to the FMN; c) An electron is transferred from the cysteine to the FMN, the S–H remains as a cationic radical, then the adduct is formed between the pair radicals; d) Direct formation of photo-adduct through a concerted reaction.

1.5.2 The signal transduction from LOV to effector domains

Being one of the most extensively studied area in LOV photo-sensing, much is known about the early events in the LOV photo-cycle. But due to the lack of any structure from full length LOV proteins, there remain also many aspects unclarified, such as by which mechanism could the signal generated in the FMN-binding pocket regulate the effector domains and finally trigger many different biological outputs.

The structural comparison between the dark and light state of single LOV domains showed minor differences in the overall structure with conformational changes centered in close proximity of the FMN. As an example given, the conserved glutamine on Iβ can form a H-bond with the oxygen from the C4 carbonyl group in dark state, while the formation of photo-adduct can cause a rotation of this glutamine and diminish the strength of this H-bond⁵¹. The FMN binding pocket is quite conserved among LOV domain proteins and thus the geometry of active sites surrounding the FMN is also remarkably similar in these

proteins, giving the reason of the practically identical primary photoreaction in different LOV proteins. Yet differences at some crucial positions in these LOV domains can introduce dissimilar structural properties, which play an important role in governing the response to the conformational stress caused by photo-adduct formation. Considering the *Avena sativa* LOV2 domain it is found that conformational changes initiated by blue light are mainly propagated to the central β -sheets, which in turn cause an unfolding of the J α helix^{51,64}. In the *Adiantum capillus-veneris* LOV domain, minor changes are also introduced to the C α -D α loop and E α -F α loop^{51,63,64}. In the short LOV protein VIVID from *Neurospora crassa*, the photo-adduct formation seems to regulate the unfolding or restructuring of the helix in the N-terminal cap that initially shows extensive contact to the central β -sheet^{51,64}. Another mechanism has been proposed for *Chlamydomonas reinhardtii* phot-LOV1, where light activation can strengthen a salt bridge on the surface of LOV core between E51 (D α) and K92 (G β -H β loop)⁴⁸.

In phototropin, light enhances auto-phosphorylation in several positions between LOV1 and LOV2, and also in the N-terminal region in front of the LOV1 domain; phototropin has also shown kinase activity on casein⁶⁵. LOV2 is believed to play a predominant role in regulating the phosphorylation by direct binding to the kinase domain. Thereby, this binding inhibits phosphorylation, but can be cancelled by light illumination (Figure 1-15). LOV1 was found to act as an “enhancer” of light sensitivity and a dimerization site for the function of LOV2⁶³.

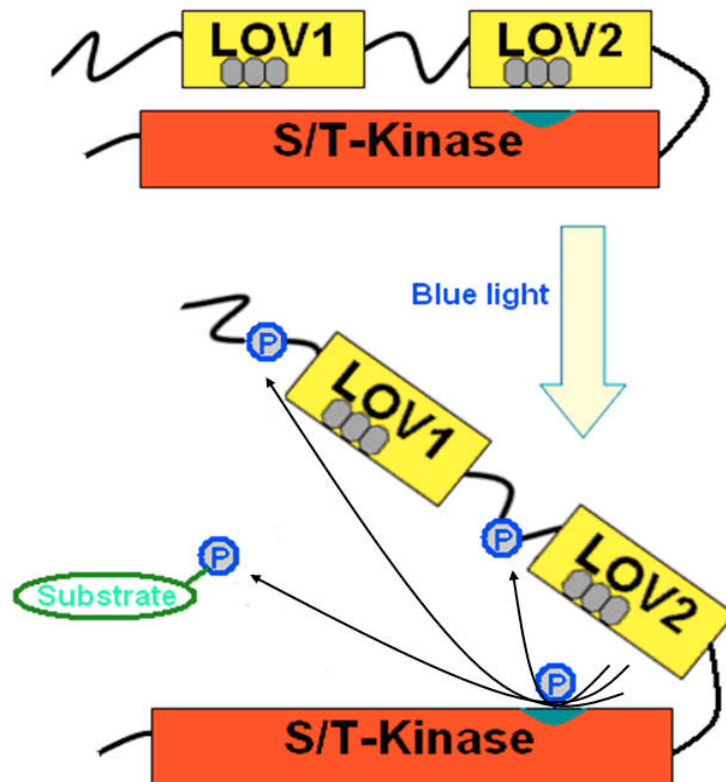


Figure 1-15: Blue light regulation of the kinase activity in phototropin. LOV2 inhibits the phosphorylation by binding to the kinase in dark state; in the light state this inhibition is cancelled and kinase can catalyze phosphorylation at several different possible positions as well as an exogenous substrate.

Some of the prokaryotic LOV domain-containing proteins are also coupled with kinases (although bacteria favor histidine kinases rather than S/T-kinases), which is a typical construct for signal transduction in all kinds of organisms, a sensory domain being organized together with a downstream effector domain like kinases. This construct makes it possible to couple a few common signal pathways to many different stimuli for cells, as for instance spectrally different light qualities. It has been reported that light absorption can increase the phosphorylation level of several kinases⁶⁶. Besides kinases, the bacterial LOV-domain containing proteins are coupled with many different effector domains (Figure 1-16) rather than the invariably fused S/T-kinase in plants.

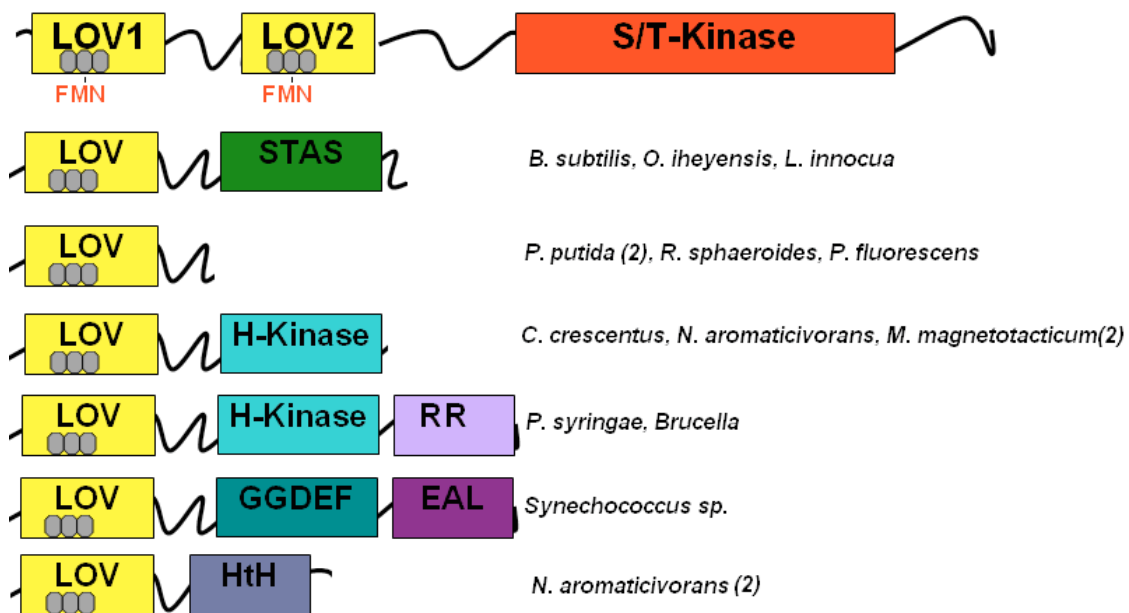


Figure 1-16: LOV-domain containing domain organizations⁶² (for abbreviations see text) . The plant phototropin structure (first entry) is shown for comparison. All other LOV domain proteins are of prokaryotic origin.

YtvA from *Bacillus subtilis*, a 261 a.a. protein was the first bacterial LOV protein that has been proven to bind FMN and to undergo a phot-like blue light induced photocycle. It is composed of the LOV domain and a C-terminal STAS (sulfate transporter anti-sigma factor antagonist) domain⁶⁰, which has been shown to have blue-light regulated NTP-binding activity⁶⁷. More than half (50.5%)⁶⁸ of the bacterial LOV-domain containing proteins possess a histidine kinase (H-Kinase) and in some cases a fused response regulator (RR) domain, as the LOV proteins from *Pseudomonas syringae*. In some cases, e.g., the LOV protein from *Caulobacter crescentus*, one finds only an H-Kinase, however, a response regulator encoding gene is arranged together in an operon. This protein can undergo a phototropin-like photocycle⁶², and visible light can increase its ATPase and auto-phosphorylation activities. It was also demonstrated to possess a light dependent regulatory function for cell attachments⁶⁹. Another large group of bacterial LOV proteins are fused with conserved diguanylate cyclases (GGDEF) and phosphodiesterase (EAL) functions, both of these two domains have been

reported to regulate the cellular level of a new second messenger, cyclic-di-GMP⁷⁰. Some other LOV proteins are comprised of a transcriptional regulator helix-turn-helix (HtH), and in some cases, LOV domains do not possess any effector domains such as the two LOV proteins from *P. putida*⁷¹.

Giving the fact that the LOV-domain- containing proteins are coupled with so many different domains, some interesting questions arise immediately: 1) how can the signal generated by photon absorption in the photo-sensing LOV core be transmitted to this variety of effector domains? 2) does the signal transduction between domains and also between proteins always follow the same or a similar pathway? 3) how do these putative effector domains really function after being activated by the LOV domains? These questions are the subject of this thesis and more details will be discussed in the following chapters.

1.6 Aim of this work and outline of this thesis

As discussed in the previous chapter, LOV domain-containing proteins were first characterized in plants as the molecular basis of several physiological responses associated with blue light irradiation. Whereas the knowledge about prokaryotic phototropin-like proteins is also growing, many of them have been demonstrated to undergo the typical LOV photo-cycle and some of them have even been connected with physiological functions^{66,69,71}. But how the LOV proteins function on the molecular basis is still an open question. Most of the research at the molecular level done so far has concentrated on the mechanisms of the photo-cycle as well as the light induced conformational changes within the LOV domain, while only little information regarding the inter-domain connections has been collected.

This present thesis will try to broaden our understanding about the molecular basis of signal transmission within bacterial LOV domain-containing proteins. The connections between the structure of these proteins and their functions will also be part of this work. Based on published and unpublished results, this thesis is organized in five parts; Following the introduction (chapter 1),

- Chapter 2 will describe experiments that continue the already extensive studies on YtvA from *Bacillus subtilis*, including its recently discovered NTP-binding function, the inter-domain interaction and detailed communicating pathway. A possible common connecting interface for the signal transmission in this protein will be examined. A recently determined crystal structure of a LOV domain from *Bacillus amyloliquefaciens* adds further information on LOV domain dimerization and presents a novel type dimer formation.
- Chapter 3 focuses on the two-component signaling system in a blue light photoreceptor. This work combines blue light sensing to a well-established signaling module that is found widely distributed in many bacteria.

- Chapter 4 will present work on another popular effector domain in bacterial LOV proteins, the conserved GGDEF and EAL motifs that can adjust the cellular level of cyclic-di-GMP, and by that mechanism can regulate community formation of microbes in biofilms. Cyclic-di-GMP has recently been identified as a typical quorum sensing molecule.
- As the final chapter, an overall discussion and conclusions part will summarize the knowledge that was gathered by this work.

1.7 References for chapter 1

1. Miller, S. L. & H.C.Urey Organic compound synthesis on the primitive earth: several questions about the origin of life have been answered, but much remains to be studied. *Science* **130**, 245-251 (1959).
2. Hartman, H. Photosynthesis and the origin of life. *Orig. Life Evol. Biosph.* **28**, 515-521 (1998).
3. Darwin, C. R. & A.R.Wallace On the tendency of species to form varieties; and on the perpetuation of varieties and species by natural means of selection. *J. Proc. Linn. Soc. Lond* **3**, 45-63 (1858).
4. Darwin, C. R. *On the origin of species by means of natural selection, or the preservation of favoured races in the struggle of life*. John Murray, London (1859).
5. Wallace, A. R. *Darwinism. An exposition of the theory of natural selection with some of its applications*. MacMillan, London (1889).
6. Wolken, J. J. *Photoprocesses, photoreceptors and evolution*. Academic Press, INC., New York (1975).
7. Darwin, C. R. & F.Darwin *The power of movement in plants*. John Murray, London (1880).
8. Balzani, V. & F.Scandola *Supramolecular Photochemistry*. Ellis Horwood Limited, West Sussex, UK (1991).
9. *Book of standard: standard tables for reference solar spectral irradiances: direct normal and hemispherical on 37°tilted surface* . ASTM International, West Conshohocken, PA, USA (2006).
10. Solar spectrum. <http://ess.geology.ufl.edu/ess/Notes/040-Sun/spectrum.GIF> . 2002.
Ref Type: Electronic Citation
11. Advanced Imaging Laboratory, University of Victoria, Canada . 9-21-2005.
Ref Type: Electronic Citation
12. Jablonski, A. Über den Mechanismus der Photolumineszenz von Farbstoffphosphoren. *Z. Phys.* **94**, 38-46 (1935).

13. The structure of 13-*cis* and all-*trans* retinal.
http://www.biochem.mpg.de/oesterhelt/web_page_list/Topic_retinal_proteins_Hasal/absatz_04_bild.gif . 2009.
 Ref Type: Electronic Citation
14. Gray, H. B. & A.W.Maverick Solar Chemistry of Metal Complexes. *Science* **214**, 1201-1205 (1981).
15. Wald, G. The molecular basis of visual excitation. *Nature* **219**, 800-807 (1968).
16. Kennis, J. T. *et al.* Primary reactions of the LOV2 domain of phototropin, a plant blue-light photoreceptor. *Biochemistry* **42**, 3385-3392 (2003).
17. Nealson, K. H. & P.G.Conrad Life: past, present and future. *Philos. Trans. R. Soc. Lond B: Biol. Sci.* **354**, 1923-1939 (1999).
18. Bryant, D. A. & N.U.Frigaard Prokaryotic photosynthesis and phototrophy illuminated. *Trends Microbiol.* **14**, 488-496 (2006).
19. Berg, J. M., J.L.Tymoczko & L.Stryer *Biochemistry*. W. H. Freeman, (2002).
20. Bryant, D. A. *et al.* *Candidatus* Chloracidobacterium thermophilum: an aerobic phototrophic Acidobacterium. *Science* **317**, 523-526 (2007).
21. Engel, A. & H.E.Gaub Structure and mechanics of membrane proteins. *Annu. Rev. Biochem.* **77**, 127-148 (2008).
22. Cao, Z. Molecular dynamic simulation of bacteriorhodopsin. 2004.
 Ref Type: Thesis/Dissertation
23. B  j  , O. *et al.* Bacterial rhodopsin: evidence for a new type of phototrophy in the sea. *Science* **289**, 1902-1906 (2000).
24. Spudich, J. L., C.S.Yang, K.H.Jung & E.N.Spudich Retinylidene proteins:structures and functions from archaea to humans. *Annu. Rev. Cell Dev. Biol.* **16**, 365-392 (2000).
25. Quail, P. H. The phytochrome family: dissection of functional roles and signalling pathways among family members. *Philos. Trans. R. Soc. Lond B: Biol. Sci.* **353**, 1399-1403 (1998).

26. Kort, R. *et al.* The xanthopsins: a new family of eubacterial blue-light photoreceptors. *EMBO J.* **15**, 3209-3218 (1996).
27. Huala, E. *et al.* *Arabidopsis* NPH1: a protein kinase with a putative redox-sensing domain. *Science* **278**, 2120-2123 (1997).
28. Ahmad, M. & A.R.Cashmore. HY4 gene of *A. thaliana* encodes a protein with characteristics of a blue-light photoreceptor. *Nature* **366**, 162-166 (1993).
29. Gomelsky, M. & G.Klug BLUF: a novel FAD-binding domain involved in sensory transduction in microorganisms. *Trends Biochem. Sci.* **27**, 497-500 (2002).
30. Somers, D. E., T.F.Schultz, M.Milnamow & S.A.Kay ZEITLUPE encodes a novel clock-associated PAS protein from *Arabidopsis*. *Cell* **101**, 319-329 (2000).
31. Yoshizawa, T. Photophysiological functions of visual pigments. *Adv. Biophys.* **17**, 5-67 (1984).
32. Sakmar, T. P. Structure of rhodopsin and the superfamily of seven-helical receptors: the same and not the same. *Curr. Opin. Cell Biol.* **14**, 189-195 (2002).
33. Nagel, G. *et al.* Channelrhodopsins: directly light-gated cation channels. *Biochem. Soc. Trans.* **33**, 863-866 (2005).
34. Mathews, S. Phytochrome-mediated development in land plants: red light sensing evolves to meet the challenges of changing light environments. *Mol. Ecol.* **15**, 3483-3503 (2006).
35. Rockwell, N. C. & J.C.Lagarias The structure of phytochrome: a picture is worth a thousand spectra. *Plant Cell* **18**, 4-14 (2006).
36. Hübschmann, T., Jorissen, H. J. M. M., Börner, T., Gärtner, W. & deMarsac, N. T. Phosphorylation of proteins in the light-dependent signalling pathway of a filamentous cyanobacterium. *European Journal of Biochemistry* **268**, 3383-3389 (2001).
37. Tarutina, M., Ryjenkov, D. A. & Gomelsky, M. An unorthodox bacteriophytochrome from *Rhodobacter sphaeroides* involved in turnover of the second messenger c-di-GMP. *J. Biol. Chem.* **281**, 34751-34758 (2006).
38. Evans, K., T.Georgiou, T.Hillon, A.Fordham-Skelton & M.Papiz *The Purple Phototrophic Bacteria.*, pp. 799-809 (Springer Netherlands,2008).

39. Van Der Horst, M. A. & K.J.Hellingwerf Photoreceptor proteins, "star actors of modern times": a review of the functional dynamics in the structure of representative members of six different photoreceptor families. *Acc. Chem. Res.* **37**, 13-20 (2004).
40. Imamoto, Y. & M.Kataoka Structure and photoreaction of photoactive yellow protein, a structural prototype of the PAS domain superfamily. *Photochem. Photobiol.* **83**, 40-49 (2007).
41. Jiang, Z. *et al.* Bacterial photoreceptor with similarity to photoactive yellow protein and plant phytochromes. *Science* **285**, 406-409 (1999).
42. Edwards, A. M. & *Et al.* *Flavins: photochemistry and photobiology*. The Royal Society of Chemistry, Cambridge, UK (2006).
43. Lin, C. & T.Todo The cryptochromes. *Genome Biol.* **6**, 220-220.9 (2005).
44. Gegear, R. J., A.Casselmann, S.Waddell & S.M.Reppert Cryptochrome mediates light-dependent magnetosensitivity in *Drosophila*. *Nature* **454**, 1014-1018 (2008).
45. Heyers, D., M.Manns, H.Luksch, O.Güntürkün & H.Mouritsen A visual pathway links brain structures active during magnetic compass orientation in migratory birds. *PLoS ONE* **2**, e937 (2007).
46. Galland, P. & N.Toelle Light-induced fluorescence changes in *Phycomyces*: evidence for blue light-receptor associated flavosemiquinones. *Planta* **217**, 971-982 (2003).
47. Lin C. Blue light receptors and signal transduction. *Plant Cell* **14**, S207-S225 (2002).
48. Sancar, A. Structure and function of DNA photolyase and cryptochrome blue-light photoreceptors. *Chem. Rev.* **103**, 2203-2237 (2003).
49. Fujihashi, M. *et al.* Crystal structure of archaeal photolyase from *Sulfolobus tokodaii* with two FAD molecules: implication of a novel light-harvesting cofactor. *J. Mol. Biol.* **365**, 903-910 (2007).
50. Selby, C. P. & A.Sancar A cryptochrome/photolyase class of enzymes with single-stranded DNA-specific photolyase activity. *Proc. Natl. Acad. Sci. USA* **103**, 17696-17700 (2006).
51. Losi, A. Flavin-based blue-light photosensors: a photobiophysics update. *Photochem. Photobiol.* **83**, 1283-1300 (2007).

52. Ohgishi, M., K.Saji, K.Okada & T.Sakai Functional analysis of each blue light receptor, cry1, cry2, phot1, and phot2, by using combinatorial multiple mutants in Arabidopsis. *Proc. Natl. Acad. Sci. USA* **101**, 2223-2228 (2004).
53. Richter, G. *et al.* Photochemically Induced Dynamic Nuclear Polarization in a C450A Mutant of the LOV2 Domain of the Avena sativa Blue-Light Receptor Phototropin. *J. Am. Chem. Soc.* **127**, 17252 (2005).
54. Christie, J. M. Phototropin blue-light receptors. *Annu. Rev. Plant Biol.* **58**, 21-45 (2007).
55. Demarsy, E. & C.Fankhauser Higher plants use LOV to perceive blue light. *Curr. Opin. Plant Biol.* **12**, 69-74 (2008).
56. Crosson, S., S.Rajagopal & K.Moffat The LOV domain family: photoresponsive signaling modules coupled to diverse output domains. *Biochemistry* **42**, 2-10 (2003).
57. Zikihara, K. *et al.* Photoreaction cycle of the light, oxygen, and voltage domain in FKF1 determined by low temperature absorption spectroscopy. *Biochemistry* **45**, 10828-10837 (2006).
58. Masuda, S. & C.E.Bauer AppA is a blue light photoreceptor that antirepresses photosynthesis gene expression in *Rhodobacter sphaeroides*. *Cell* **110**, 613-623 (2002).
59. Iseki, M. *et al.* A blue-light-activated adenylyl cyclase mediates photoavoidance in *Euglena gracilis*. *Nature* **415**, 1047-1051 (2002).
60. Laan, W., M.A.van der Horst, I.H.van Stokkum & K.J.Hellingwerf Initial characterization of the primary photochemistry of AppA, a blue-light-using flavin adenine dinucleotide-domain containing transcriptional antirepressor protein from *Rhodobacter sphaeroides*: a key role for reversible intramolecular proton transfer from the flavin adenine dinucleotide chromophore to a conserved tyrosine? *Photochem. Photobiol.* **78**, 290-297 (2003).
61. Gauden, M. *et al.* Hydrogen-bond switching through a radical pair mechanism in a flavin-binding photoreceptor. *Proc. Natl Acad. Sci. USA* **103**, 10895-10900 (2006).
62. Losi, A. The bacterial counterparts of plant phototropins. *Photochem. Photobiol. Sci.* **3**, 566-574 (2004).
63. Matsuoka, D., T.Iwata, K.Zikihara, H.Kandori & S.Tokutomi Primary processes during the light-signal transduction of phototropin. *Photochem. Photobiol.* **83**, 122-130 (2007).

64. Möglich, A. & K.Moffat Structural basis for light-dependent signaling in the dimeric LOV domain of the photosensor YtvA. *J. Mol. Biol.* **373**, 112-126 (2007).
65. Matsuoka, D. & S.Tokutomi Blue light-regulated molecular switch of Ser/Thr kinase in phototropin. *Proc. Natl. Acad. Sci. USA* **102**, 13337-13342 (2005).
66. Briggs, W. R. The LOV domain: a chromophore module servicing multiple photoreceptors. *J. Biomed. Sci.* **14**, 499-504 (2007).
67. Buttani, V., A.Losi, E.Polverini & W.Gärtner Blue news: NTP binding properties of the blue-light sensitive YtvA protein from *Bacillus subtilis*. *FEBS Lett.* **580**, 3818-3822 (2006).
68. Losi, A. & W.Gärtner Bacterial bilin- and flavin-binding photoreceptors. *Photochem. Photobiol. Sci.* **7**, 1168-1178 (2008).
69. Purcell, E. B., D.Siegal-Gaskins, D.C.Rawling, A.Fiebig & S.Crosson A photosensory two-component system regulates bacterial cell attachment. *Proc. Natl. Acad. Sci. USA* **104**, 18241-18246 (2007).
70. Galperin, M. Y., A.N.Nikolskaya & E.V.Koonin Novel domains of the prokaryotic two-component signal transduction systems. *FEMS. Microbiol. Lett.* **203**, 11-21 (2001).
71. Krauss, U., A.Losi, W.Gärtner, K.E.Jaeger & T.Eggert Initial characterization of a blue-light sensing, phototropin-related protein from *Pseudomonas putida*: a paradigm for an extended LOV construct. *Phys. Chem. Chem. Phys.* **7**, 2804-2811 (2005).
72. Swartz, T. E. *et al.* Blue-light-activated histidine kinases: two-component sensors in bacteria. *Science* **317**, 1090-1093 (2007).
73. Avila-Pérez, M. *et al.* *In vivo* mutational analysis of the *Bacillus subtilis* LOV-domain containing protein YtvA: mechanism of light-activation of the general stress response. *J. Biol. Chem.* **284**, 24958-24964 (2010).

II. Domain-domain interactions in YtvA-LOV and YtvA full-length proteins

2.1 The competitive interface for LOV-LOV dimerization and interdomain interactions



Conformational analysis of the blue-light sensing protein YtvA reveals a competitive interface for LOV–LOV dimerization and interdomain interactions†

Valentina Buttani,^a Aba Losi,^{*a,b} Thorsten Eggert,^c Ulrich Krauss,^c Karl-Erich Jaeger,^c Zhen Cao^d and Wolfgang Gärtner^d

Received 20th July 2006, Accepted 6th October 2006

First published as an Advance Article on the web 27th October 2006

DOI: 10.1039/b610375h

The *Bacillus subtilis* protein YtvA is related to plant phototropins in that it senses UVA–blue-light by means of the flavin binding LOV domain, linked to a nucleotide-binding STAS domain. The structural basis for interdomain interactions and functional regulation are not known. Here we report the conformational analysis of three YtvA constructs, by means of size exclusion chromatography, circular dichroism (CD) and molecular docking simulations. The isolated YtvA-LOV domain (YLOV, aa 25–126) has a strong tendency to dimerize, prevented in full-length YtvA, but still observed in YLOV carrying the N-terminal extension (N-YLOV, aa 1–126). The analysis of CD data shows that both the N-terminal cap and the linker region (aa 127–147) between the LOV and the STAS domain are helical and that the central β -scaffold is distorted in the LOV domains dimers. The involvement of the central β -scaffold in dimerization is supported by docking simulation of the YLOV dimer and the importance of this region is highlighted by light-induced conformational changes, emerging from the CD data analysis. In YtvA, the β -strand fraction is notably less distorted and distinct light-driven changes in the loops/turn fraction are detected. The data uncover a common surface for LOV–LOV and intraprotein interaction, involving the central β -scaffold, and offer hints to investigate the molecular basis of light-activation and regulation in LOV proteins.

Introduction

B. subtilis YtvA is a blue-light responsive protein (261 aa), carrying a flavin-binding LOV (light, oxygen, voltage) domain, with LOV belonging to the PAS (PerArntSim) superfamily.¹ The photochemical LOV paradigm has emerged during the last years, thanks to the discovery and molecular characterization of phototropins (phot), blue-light receptors for a variety of responses in plants.^{2–4} Phot are organized in two N-terminal LOV domains (LOV1 and LOV2, *ca.* 110 amino acids) and a C-terminally located ser/thr kinase domain. A self-phosphorylation reaction^{5,6} is activated by UVA–blue light illumination of phot, thanks to the activation the LOV domains that carry a flavin-monomonucleotide (FMN) as chromophore.⁷ Light activation of LOV domains triggers a photocycle that involves the reversible formation of a covalent adduct between a conserved cysteine residue and position C(4a) of FMN,^{7–11} formed upon decay of the FMN triplet state.^{12–14} Despite the similarities in the light-triggered reactions, the two phot-LOV

domains have not the same functional significance, with the self-phosphorylation reaction being mostly mediated by LOV2,^{15,16} that also presents a larger quantum yield for the formation of the covalent adduct.⁹ The LOV paradigm is configuring as one of the most conserved among distant phyla, and LOV proteins are now well documented in eukaryotes and prokaryotes.^{17,18} In bacteria they are present in about 15–17% of the sequenced genomes, and light-induced, phot-like reactions have been demonstrated for some of them.^{18–20}

Although the mechanistic details of the photochemical FMN–Cys adduct formation are still under debate (see ref. 19 and references therein, and ref. 21) the photocycle of LOV domains is by far the best characterized part of the light-to-signal transduction chain, thanks to the fact that isolated LOV domains are readily expressed and have been functionally and structurally analyzed.^{9,10,22,23} A structure of full-length phot is not yet available and little is known about the mechanism leading to kinase activation and on the protein surfaces involved in domain–domain interactions. Light-driven unfolding of the helical linker connecting LOV2 and the kinase domain (Ja-linker) has been recently proposed to trigger the self-phosphorylation reaction, based on NMR spectroscopy and mutagenesis experiments.^{24,25} This idea has recently been challenged by the observation that the Ja-linker is not needed either for LOV2-kinase interaction or for light-driven phosphorylation of a heterologous substrate.¹⁵

In prokaryotes the LOV light-sensing module is coupled to diverse effector domains, such as kinases (similar to phot), phosphodiesterases, response regulators, DNA-binding transcription

^aDept. of Physics, University of Parma, via G.P. Usberti 7/A, 43100-Parma, Italy. E-mail: losia@fis.unipr.it

^bCNR-INFM, Parma, Italy

^cInstitut für Molekulare Enzymtechnologie, Heinrich-Heine Universität Düsseldorf, Forschungszentrum Jülich, D-52426 Jülich, Germany

^dMax-Planck-Institut für Bioanorganische Chemie, Stiftstr. 34-36, 45470 Mülheim, Germany

† Electronic supplementary information (ESI) available: Calculation of accessible and buried surface areas using the VADAR tool. See DOI: 10.1039/b610375h

factors, regulators of stress sigma factors.^{17,18,26} Therefore, besides the intrinsic interest regarding their structure, function and physiological role, they also represent a powerful tool to understand fundamental and still open questions in the field of LOV-based photoperception. (i) Are the light-induced reactions, centered on the LOV domain, transmitted to effector partners by means of the same molecular mechanisms, and do LOV domains interact with partner domains by means of the same protein surface? In phot1-LOV2 the central β -scaffold has been demonstrated to participate in interdomain communication, making contact with the $J\alpha$ -linker.^{24,25} A similar process has been observed with phot2-LOV2.²⁷ (ii) Why only one LOV domain is present in bacterial LOV proteins, whereas phot possess two of such units organized in tandem?^{17,18} The LOV2 domain has a higher photocycle quantum yield than LOV1,⁹ and acts as the principal light-sensing domain triggering phot1 and phot2 kinase activity, whereas LOV1 might have a regulative role.¹⁶ The amino acid sequence of bacterial LOV domains has in general intermediate characteristics between LOV1 and LOV2.¹⁸ (iii) Which factors govern LOV–LOV dimerization, considered a key feature in PAS-mediated sensing/regulation,^{28,29} and which is the relevance of it during light sensing? It was shown by gel filtration chromatography that phot1-LOV1 has a tendency to dimerize, whereas LOV2 is monomeric.³⁰ This has led to the suggestion that LOV1 is responsible for phot dimerization, providing a possible functional role for the tandem organization of LOV domains in phot.³⁰ By means of pulsed thermal grating Terazima and coworkers, detected a transient volume increase (about 1.8 times, with time constant of 300 μ s) during light activation of an extended phot1-LOV2 construct (including an N-terminal cap and the $J\alpha$ -linker), and interpreted this phenomenon as a transient dimerization,³¹ whose functional significance is not known. Dimeric states have been detected by means of small-angle X-ray scattering (SAXS) for the LOV domain of FKF1³² and phot LOV1 domains.³³ The SAXS experiments showed that phot1-LOV2 is a dimer (in contrast with ref. 30 and 31) whereas phot2-LOV2 is monomeric.³³ The LOV domain of WC-1 from *Neurospora* has also been shown to homodimerize *in vitro*.³⁴

In this work we have investigated three different constructs of YtvA, in order to partially address these problems. In YtvA the LOV domain is linked to a C-terminal STAS domain (sulfate transporters antisigma-factor antagonists).³⁵ This architecture is conserved in LOV proteins from other Firmicutes, e.g. in *Listeria* and *Oceanobacillus* genera.¹⁸ Recent work has shown that YtvA is a positive regulator in the environmental signaling pathway that activates the general stress factor $\sigma^{B36,37}$ and, most importantly, that the cysteine involved in the photoadduct formation is needed for its *in vivo* function,³⁷ in turn regulated by blue-light activation.³⁸ These last two recent studies allow to regard YtvA as a real flavin-based blue-light photoreceptor in *B. subtilis*, not only a blue-light sensitive protein. The STAS is thought to be the effector domain of YtvA, although little is known of its molecular functionality, with the exception that it confers to YtvA the ability to bind GTP and ATP,³⁹ in analogy with another STAS protein.⁴⁰ The constructs that we used are the LOV core (YLOV, aa 25–126), the N-YLOV comprising also the first 24 aa (aa 1–126) and the full-length protein YtvA. We applied gel filtration chromatography to detect possible dimers and circular dichroism spectroscopy for secondary structure determination, improving the data analysis with respect to previous work.⁴¹ The data uncover a common surface for YLOV

homodimerization and interdomain interactions, and corroborate a molecular model of the YLOV dimer obtained by docking simulations. Similarities and differences with phot-LOV domains are discussed.

Experimental

Protein samples and chemicals

For the N-YLOV protein, the DNA sequence encoding LOV core + N-terminal cap (aa 1–126 of the full protein) was amplified by PCR (Polymerase Chain Reaction). The recombinant plasmid of full-length YtvA in (pET28a) was used as template, the primers were:

5'-CAGCCATATGGCTAGTTTTCAATCATT (forward)

5'-TATTACTCGAGTTAGGTGATATCATTCTGAATC (reverse)

Platinum® Taq DNA Polymerase (Invitrogen, Karlsruhe, Germany) was used for the PCR. PCR product, digested with NdeI/XhoI (NEB, Ipswich, UK), was ligated into the expression vector pET28a (Novagen-Merck, Darmstadt, Germany), which was digested with the same restriction enzymes. An N-terminal extension, including the 6 \times His-tag (sequence: MGSSHHHH-HHSSGLVPRGSH) was furnished, in the same way as for YtvA and YLOV. For the details of full-length His-tagged YtvA and its isolated LOV core (YLOV) generation, see previous reports.^{19,42} The His-tagged proteins were expressed in *E. coli* BL21 DE3 (Stratagene, Amsterdam, The Netherlands) using IPTG (BioMol, Hamburg, Germany) induction. The proteins were then purified by affinity chromatography on Talon (Qiagen, Hilden, Germany) and finally concentrated in Na-phosphate buffer 10 mM, NaCl 10 mM, pH = 8.

Chromatography

Gel filtration chromatography experiments were performed on a Pharmacia FPLC apparatus, using a Superdex 75 HR 10/30 column (Amersham Biosciences), equilibrated with Na-phosphate 10 mM, pH = 8, NaCl = 0.15 M. A calibration curve was made using bovine serum albumin (69 kDa), ovalbumin (42.7 kDa), α -chymotrypsin (25 kDa), myoglobin (16.9 kDa) and ribonuclease (13.7 kDa) (low M_w calibration kit, Amersham Biosciences). YtvA, YLOV and N-YLOV were loaded on the column at a concentration between 1 and 50 μ M, to give a final concentration ranging from 0.05 to 2.5 μ M at the detection peak, due to dilution through the column.

Circular dichroism spectroscopy and data analysis

Circular dichroism (CD) experiments were carried out using a Jasco J715 spectropolarimeter, calibrated with ammonium d-10-camporsulfonic acid. The measurements were carried out in the far-UV spectral region (195–240 nm) at a temperature of 20 °C and the buffer background was always subtracted. The optical pathlength was 0.2 cm. Protein concentration was estimated from the absorption coefficient at 220 nm, $\epsilon_{220}^{YTV A} = 492800 \text{ M}^{-1} \text{ cm}^{-1}$, $\epsilon_{220}^{YLOV} = 223900 \text{ M}^{-1} \text{ cm}^{-1}$ and $\epsilon_{220}^{N-YLOV} = 267900 \text{ M}^{-1} \text{ cm}^{-1}$, calculated by comparison with $\epsilon_{447}^{FMN} = 12500 \text{ M}^{-1} \text{ cm}^{-1}$, in a 1 : 1 protein to chromophore ratio (*vide infra*). The corresponding value for FMN is $\epsilon_{220}^{FMN} = 34500 \text{ M}^{-1} \text{ cm}^{-1}$, thus introducing a negligible error also in case that some apoprotein is present. The mean

residue ellipticity Θ_{MRW} was calculated from the concentration of residues, c , (281 aa for YtvA, 122 aa for YLOV and 146 aa for N-YLOV, including the tag, according to the formula $\Theta_{\text{MRW}} = \Theta_{\text{obs}} / (10 \times c l)$, where c is in mol liter⁻¹, $l = 0.2$ cm and Θ_{obs} is in mdeg and Θ_{MRW} in deg cm² dmol⁻¹. Typically, the protein concentration was in the μM range and $c = 10^{-6} \times 281 = 2.8 \times 10^{-4}$ mol liter⁻¹ for YtvA, $c = 10^{-6} \times 122 = 1.2 \times 10^{-4}$ mol liter⁻¹ for YLOV and $c = 10^{-6} \times 146 = 1.4 \times 10^{-4}$ mol liter⁻¹ for N-YLOV. Prediction of secondary structure composition was performed using the convex constraint analysis (CCA) algorithm,^{43,44} and an extended curves dataset comprising 46 protein spectra.⁴⁵ In CCA, the sum of the fractional weights of each component spectrum is constrained to be 1. In addition, a constraint-called volume minimization is defined which allows a finite number of component curves to be extracted from a set of spectra without relying on spectral nodes. CCA does not use X-ray crystallographic data in the deconvolution procedure. Once the basis curves are obtained, they must be assigned to specific secondary structures. The secondary structure was also predicted from the amino acid sequence by means of bioinformatic tools, using the consensus secondary structure prediction method at the Pôle Bioinformatique Lyonnais.⁴⁶

Docking simulation, evaluation of complexes and model validation

Docking simulations of the YLOV dimer were carried out at the ClusPro Server,⁴⁷ using the DOT 1.0⁴⁸ and ZDOCK v. 2.3⁴⁹ programmes, employing the previously published YLOV structural model (PDB databank accession code 1IUM).¹⁹ The ClusPro docking algorithm evaluates billions of putative complexes, retaining a preset number with favourable surface complementarities. A filtering method is then applied to this set of structures, selecting those with good electrostatic and desolvation free energies for further clustering. Evaluation of the ClusPro predicted complexes was carried out using the VADAR tool,⁵⁰ which calculates multi-chain parameters such as the accessible surface area and the percentage of accessible hydrophobic side chains. The quality of the ClusPro predicted YLOV dimer model was verified by using the protein structure analysis and validation server (SAVS) of the NIH MBI Laboratory for Structural Genomics and Proteomics at the University of California, Los Angeles (UCLA) (<http://nihserver.mbi.ucla.edu/SAVS/>) that implements the programs PROCHECK,⁵¹ WHAT_CHECK,⁵² ERRAT,⁵³ VERIFY_3D,⁵⁴ and PROVE.⁵⁵ Additionally, PPI-Pred⁵⁶ and the computational interface alanine scanning tool at the Robetta server⁵⁷ were used to predict the dimerization interface of the YLOV-monomer and of the YLOV dimers respectively.

Results and discussion

Gel filtration chromatography

The elution profile of YLOV (Fig. 1) reveals that the majority of the protein is present in a state having $M_w = 36.44$ kDa, namely 2.63 times larger than the theoretical M_w (13.81 kDa, considering also the 20 aa at the N-terminal His-tag). This suggests a dimeric state that deviates from a spherical shape, as previously reported for other LOV domains.^{30,32,33} Traces of a globular monomer are observable in some preparations, as well as a small fraction of a

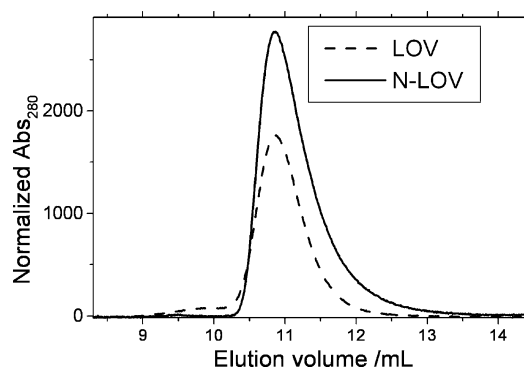


Fig. 1 Elution profiles of the YLOV (dashed line) and N-YLOV (full line) domains of YtvA. The main peaks correspond to $M_w = 2.6 \times M_{w\text{YLOV}}$ and $M_w = 2.1 \times M_{w\text{N-YLOV}}$, respectively.

larger aggregate, most probably a trimer, with $M_w = 51.97$ kDa. Light activation does not appreciably affect the elution profile of YLOV. N-YLOV is also mostly present in a dimeric state, with apparent $M_w = 34.00$ kDa, 2.06 times larger than the theoretical M_w (16.54 kDa, again including the His-tag). For N-YLOV the shape of the dimer is therefore approximately spherical.

The full-length protein YtvA presents a larger heterogeneity and the elution profile is different among different preparations (Fig. 2). Up to three peaks can be identified, with peak 1 resulting in $M_w = 72.85$ kDa, peak 2 with $M_w = 48.39$ kDa and peak 3 with $M_w = 35.07$ kDa. The theoretical M_w of YtvA is 31.36 kDa, therefore we can assign the three peaks to a dimeric state (peak 1), an elongated monomer (peak 2, $M_w = 1.56 \times M_{w\text{YtvA}}$) and a spherical monomer (peak 3, $M_w = 1.12 \times M_{w\text{YtvA}}$). Peak 2 (elongated monomer) represents in all YtvA preparations observed

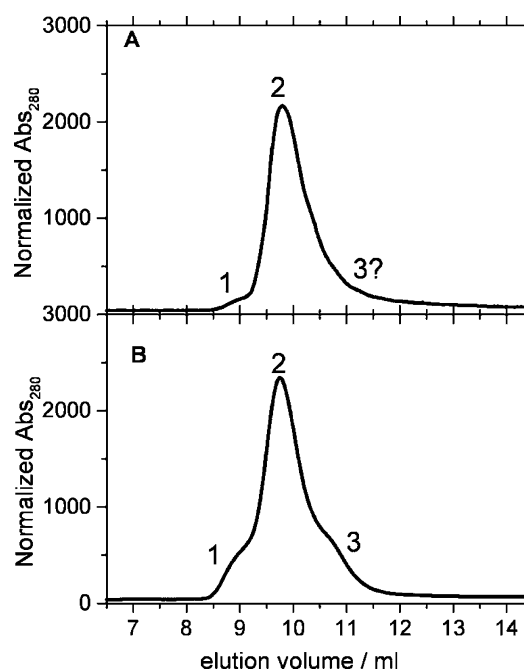


Fig. 2 Elution profile of 2 different YtvA preparations. Peak 1 corresponds to $M_w = 2.32 \times M_{w\text{YtvA}}$ ($M_{w\text{YtvA}} = 31.36$ kDa); peak 2 corresponds to $M_w = 1.56 \times M_{w\text{YtvA}}$; peak 3 corresponds to $M_w = 1.12 \times M_{w\text{YtvA}}$. A. YtvA : FMN = 1 : 1 (no apoprotein). B. YtvA : FMN \approx 2 : 1 (apoprotein is present).

(nine in total) the predominant protein fraction. Peaks 1 and 3 are more evident in preparations that contain considerable amount of apoprotein (without the flavin chromophore). Nevertheless, even in these cases, the flavin chromophore is present in all three fractions, as proven by detection at 390 nm (data not shown). Again light activation does not result in appreciable changes in the elution profile. For the three protein constructs, the elution profile is not affected by concentration, in the low range employed here (0.05–2.5 μ M).

As a whole, the gel filtration experiments show that the LOV domain of YtvA has a strong tendency to dimerize in solution that is not hindered by the N-terminal cap. Dimerization is instead prevented by the presence of the C-terminal domain of the protein, pointing to the fact that the LOV core employs the same surface (partially or totally) for homodimerization and for interdomain interactions.

Circular dichroism spectroscopy

The UV-CD spectra for the three analyzed constructs of YtvA, in the dark adapted state, are shown in Fig. 3. The mean residue ellipticity, Θ_{MRW} , was calculated as explained in the experimental section. The spectra shown are an average of all measurements (5 sets of measurements with 2 different preparations for YLOV; 4 sets of measurements with 2 different preparations for N-YLOV; 11 sets of measurements, 9 different preparations for YtvA), but each single spectral output was analyzed separately using the CCA algorithm.

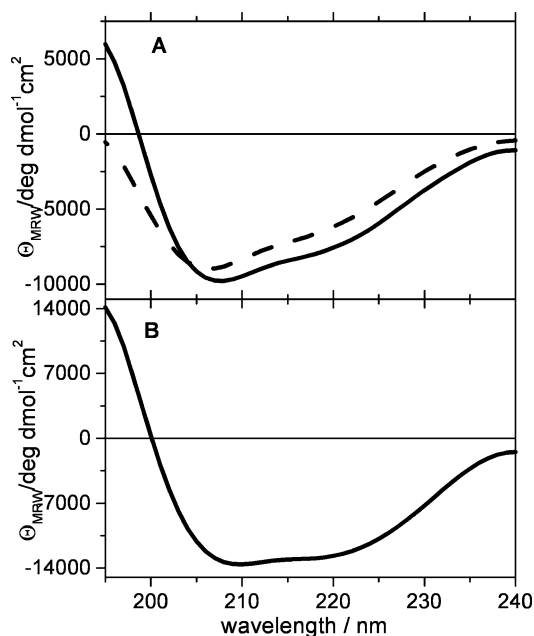


Fig. 3 CD spectra in the UV region for (A) the YLOV (dashed line) and N-YLOV (full line) domains and (B) full-length YtvA, in the dark adapted state.

A critical step during CCA analysis of CD data, is the assignment of the component curves (Fig. 4) to specific secondary structures. In the literature there is a large agreement about the CD spectrum of regular α -helices and unordered polypeptides

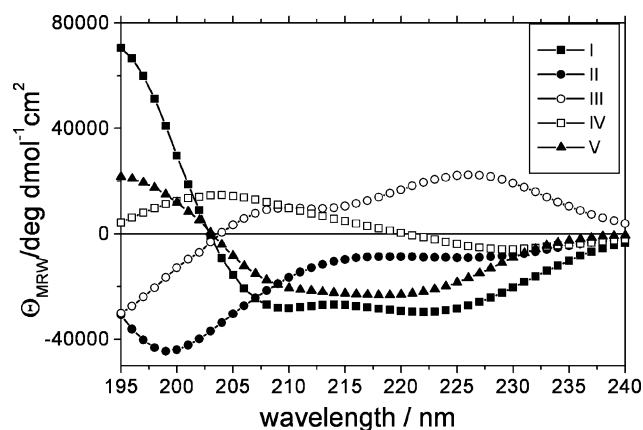


Fig. 4 The 5 component curves as extracted from the CCA analysis. The assignment is as follows: I, α -helix, II, unordered structures, III, turns and other structures, IV, distorted/twisted β -strands/parallel β -sheet, V, antiparallel β -sheet (see text for details).

(random coil, RC) that can be assigned to curve I and II respectively (ref. 58 and 59 and references therein).

Curve V was assigned to the turn fraction⁶⁰ and the β -structures were assigned to curve IV + V, whose sum is similar to the curve corresponding to β -strands in Matsuo *et al.*⁶⁰ Based on the fact that distorted/twisted β -sheets present a strong positive band in the 190–220 region,⁶¹ curve IV is assumed to include this fraction. Furthermore, the antiparallel β -sheet has three allowed transitions (the $\pi\pi^*$ transition is splitted),^{62,63} whereas the parallel β -sheet has two; therefore, we assigned curve V to the regular antiparallel β -sheet and curve IV to twisted + parallel β -sheet. Curve IV may also receive contributions from turn structures, in that different type of turns have very different CD spectra.^{44,64,65} The results of the CCA analysis, with the curve assignment as discussed above, are reported in Table 1, both for the dark and light-adapted state.

To test the quality/reliability of our component assignment, we made a prediction of secondary structure composition based on the three dimensional models of the LOV and STAS domains^{19,39} and on the consensus method for the remaining parts of the protein.⁴⁶ The N-cap and the linker region are predicted to be largely helical, whereas the His-tag (20 aa in length) is, as expected, predicted to be unordered (Table 2).

The comparison with CD data is very good in the case of the helical fraction, although for YtvA the statistical error associated with this component is quite large. This may be due to the variability in the preparations, and/or to the fact that component I and V are in some cases difficult to separate (see Fig. 4 and Table 1). The results confirm that the N-cap and the linker region are mostly helical. For full-length YtvA also the turn/loops and β -strands predicted fractions match the sum of component II + III and IV + V, respectively, within the experimental error, (Table 2), supporting our curve assignment. In the case of LOV and, particularly, N-LOV, the fraction of β -strands is smaller than expected, to the advantage of the RC/turns/others component. Furthermore, LOV domains do not contain parallel β -sheets^{19,22,23} and the large percentage associated to component IV has to be assigned to the distortion/twisting of the central, antiparallel β -scaffold. This is in contrast with YtvA, for which the number of aa associated to component IV, can be readily explained with the presence of four parallel β -strands localized on the STAS

Table 1 Results of the CCA analysis on CD spectra

Secondary structure	LOV ^a (122 aa) ^b (%)		N-LOV ^a (147 aa) ^b (%)		YtvA ^a (281 aa) ^b (%)	
	Dark	Light	Dark	Light	Dark	Light
I, α -Helix	16.9 \pm 2.7 (21 \pm 3)	19.5 \pm 5.8 (24 \pm 7)	24.9 \pm 2.4 (37 \pm 4)	27.3 \pm 0.9 (40 \pm 1)	30.9 \pm 4.7 (87 \pm 13)	32.0 \pm 6.5 (90 \pm 18)
II, RC	23.9 \pm 4.1 (29 \pm 5)	22.8 \pm 3.9 (28 \pm 5)	24.9 \pm 0.9 (37 \pm 1)	23.6 \pm 0.9 (35 \pm 1)	22.4 \pm 1.0 (63 \pm 3)	21.7 \pm 3.5 (61 \pm 10)
III, β -Turns/others	27.9 \pm 1.1 (34 \pm 1)	28.8 \pm 2.3 (35 \pm 3)	27.5 \pm 1.0 (40 \pm 1)	28.3 \pm 1.5 (42 \pm 2)	16.8 \pm 3.6 (47 \pm 10)	18.7 \pm 3.5 (52 \pm 10)
IV, β -Twisted/ β -parallel	14.7 \pm 1.6 (18 \pm 2)	18.6 \pm 1.0 (23 \pm 1)	12.1 \pm 1.6 (18 \pm 2)	15.9 \pm 0.9 (23 \pm 1)	9.9 \pm 4.1 (28 \pm 11)	11.0 \pm 3.7 (31 \pm 10)
V, β -Antiparallel	16.2 \pm 4.1 (20 \pm 5)	10.2 \pm 4.7 (12 \pm 6)	10.6 \pm 3.4 (15 \pm 5)	4.9 \pm 2.1 (7 \pm 3)	19.9 \pm 5.6 (56 \pm 16)	16.6 \pm 5.8 (47 \pm 16)
$\left\langle \sum_{i=1}^n [y_i - f(\lambda)]^2 \right\rangle^c$	1.9 \pm 0.4	3.6 \pm 2.9	2.2 \pm 1.8	2.1 \pm 0.7	6.2 \pm 2.8	5.2 \pm 2.3

^a The statistical error is the standard deviation and comes from 5 sets of measurements on 2 different preparations for LOV, 4 sets of measurements on 2 different preparations for N-LOV, 11 sets of measurements, and 9 different preparations for YtvA. ^b The number of aa is given in parentheses, below the percentage, together with the statistical error. ^c Average squared error, where y_i = experimental curve, $f(\lambda)$ = fitting curve.

Table 2 Comparison between expected and CD-derived secondary structure composition

YtvA segments	Helices Number of aa	Turns/loops Number of aa	β -Strands Number of aa
His-Tag ^a	—	20	—
N-Cap ₁₋₂₄ ^a	10	13	1
LOV ₂₅₋₁₂₆ ^b	24	36	42
Linker ₁₂₇₋₁₄₆ ^a	18	2	—
STAS ₁₄₇₋₂₅₄ ^b	36	41	31
C-End ₂₅₅₋₂₆₁ ^a	2	4	1
YtvA ^c	90	116	75
N-LOV ^c	34	69	43
LOV ^c	24	56	42
CCA analysis—dark state	α-Helix	RC/turns/others	β-Strands
YtvA	87 \pm 13	110 \pm 9	84 \pm 17
N-LOV	37 \pm 4	77 \pm 1	33 \pm 5
LOV	21 \pm 3	63 \pm 4	38 \pm 5

^a Consensus secondary structure prediction at the Pôle Bioinformatique Lyonnais server.⁴⁶ ^b Structural homology models of the LOV core¹⁹ and of the STAS domain.³⁹ ^c Predicted number of aa for each of the constructs analyzed.

domain and a modest distortion of the overall β -fraction.³⁹ These observations suggest that dimerization in YLOV and N-YLOV markedly affects the central β -sheet of the LOV core (see the docking section).

Inspection of Table 1 and of the light – dark difference spectra (Fig. 5) shows that light activation of the three analyzed constructs does not result in large secondary structure conformational changes, as previously noticed for full-length YtvA.⁴¹ A further distortion of the central β -sheet is induced in YLOV and N-YLOV, and the difference spectra are very similar for the two proteins.

Light-induced changes of the central β -sheet have been recently demonstrated with low temperature Fourier transformed infrared spectroscopy (FTIR) also for phy3-LOV2.⁶⁶ The CD light-difference spectrum of phot1-LOV2 was interpreted as a loss of helical structure, but without the support of a detailed data analysis.⁶⁷

In full-length YtvA there is still a perturbation of the β -fraction, but a distinct change in the turn fraction (positive shoulder at *ca.* 230 nm in Fig. 5), missing in YLOV and N-YLOV. The determinations are affected by a large error, but confirmed by previous data as obtained with FTIR, that show a distinct

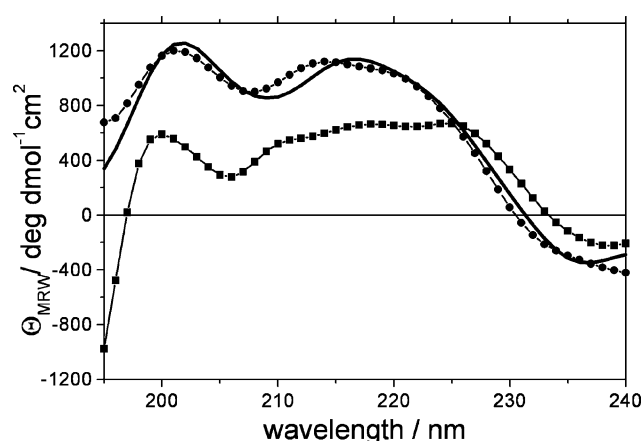


Fig. 5 Light – dark plots of the mean residue ellipticity Θ_{MRW} for YtvA (squares + line), LOV (circles + line) and N-LOV (full line), calculated from the average CD spectra (see Fig. 1 and Table 1).

difference between YtvA and YLOV in the light-induced changes of the turns fraction (around 1700 cm^{-1}).⁶⁸ These results could be

interpreted as a conformational change transmitted from the LOV core to the STAS domain, but actually we have no hint to localize precisely the position of the altered turn fraction, that could even be on the LOV domain itself and its changes being not detectable in the LOV dimers. Temperature-dependent FTIR experiments show indeed that changes in the turn fraction occur before the conformational alterations of the β -sheet in phy3-LOV2, the latter changes only detectable at room temperature.⁶⁶ In this view, the light-induced conformational changes could reach the β -scaffold only in the YLOV and N-YLOV dimers and be limited by the presence of the second domain, so that the changes on the turn fraction can persist during the lifetime of the adduct in YtvA.

The YLOV–YLOV dimer

The ClusPro best ranked model (ZDOCK generated) is shown in Fig. 6. A very similar model is ranked at the first position by using the DOT docking software (not shown).

The evaluation of the complexes performed with the VADAR tool,⁵⁰ reveals that this model has a quite large buried surface area as well as a high percentage of buried hydrophobic side-chains (33.76%) (see electronic supplementary information, ESI†). This feature would favour dimerization in an aqueous environment, and agrees with the fact that YLOV is a stable dimer in solution, even at very low concentrations. The quality of the model, evaluated at the SAVS server (<http://nihserver.mbi.ucla.edu/SAVS/>) was as an overall good, with 84.1% of residues in most favoured regions, 12.5% of residues in additionally allowed region, 2.3% of residues in generously allowed regions and only 1.1% of residues in disallowed regions of the Ramachandran plot. The Verify-3D⁵⁴ score (96.1) and the Errat-quality factor⁵³ (98.9) were very high, both indicative of a reasonable and good resolved model-structure. Finally, the dimerization surface predicted with PPI-Pred⁵⁶ and Robetta,⁵⁷ identified high scoring regions for YLOV–YLOV interactions within A β , B β , H β and I β strands and the H β –I β loop (Fig. 6).

In the dimer models of Fig. 6, the two YLOV domains face each other with the central β -sheet, presenting an antiparallel mirror symmetry. The interface is mostly stabilized by hydrophobic interactions. This feature is not in common with phy3-LOV2, where a bunch of charged/polar amino acids forms an extended HB (hydrogen bonds) network with the corresponding residues on the second monomer, centered around His1011, Gln1013 (H β) and Asp1017 (H β –I β loop). Interestingly, His1011 and Gln1013 of LOV2 domains (Thr and A/T respectively on LOV1 domains), and this feature may account for the fact that LOV1 has a stronger tendency to dimerize than LOV2 in an aqueous environment.³⁰ Although the dimerization of phy3-LOV2 and the specific orientation of the two monomers may be an artifact of crystallization, a complex very similar to the phy3-LOV dimer is readily obtained by the docking algorithm (not shown) and the residues at the interface are part of the hot spots predicted by PPI-Pred and Robetta (Fig. 6). We note that for YLOV, complexes with similar orientation as phy3-LOV are also detected by the ClusPro docking algorithm (cluster 2 and 8 in the DOT output and cluster 10 in the ZDOCK output, see ESI†). Our choice of the model in Fig. 6 (cluster 1 for both DOT and ZDOCK outputs) is based on the ClusPro ranking, on the high surface complementarity and interactions symmetry, and on the presence of a cluster of hydrophobic amino acids at the interface, that nicely accounts for the stability of the dimer in solution.

The antiparallel mirror symmetry and the interface observed in our YLOV–YLOV model and in the phy3-LOV dimer is very similar to the one reported for homo and heterodimers of the ARNT PAS-B domain in solution⁶⁹ and in dimers of the heme-binding PAS domain of *E. coli* Dos (EcDos)⁷⁰ and *R. meliloti* FIXL (RmFIXL).⁷¹ An antiparallel mirror symmetry has also been suggested for the LOV–LOV dimer of the FKF1 protein and for phot-LOV1 on the basis of small-angle X-ray scattering experiments, although in that case the authors favoured a different model for the complex, where the two LOV domains do not face each other *via* the central β -sheet.^{32,33}

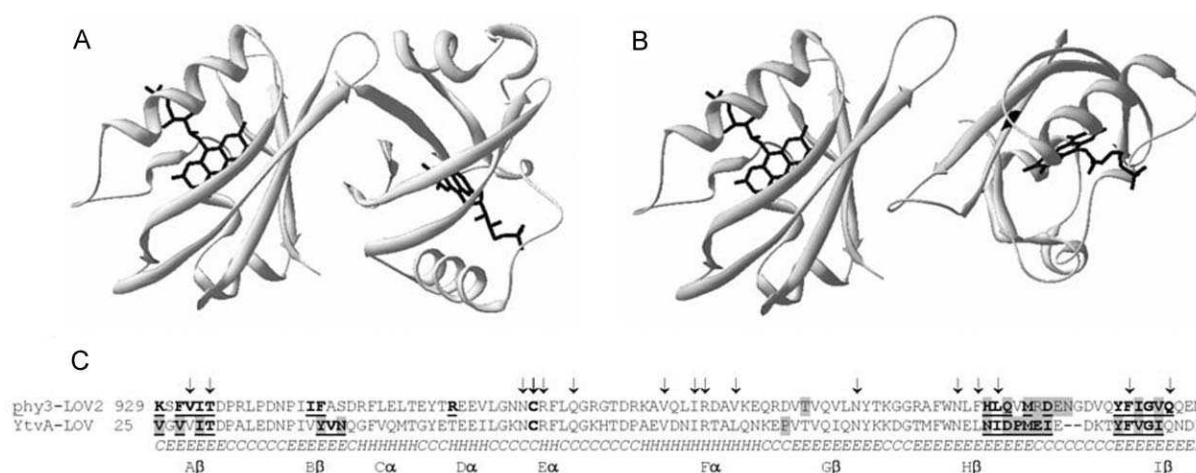


Fig. 6 (A) The YLOV dimer model (see text for details). (B) The phy3-LOV2 dimer in the crystal unit cell (PDB accession code 1G28, chains a,c).²² (C) Residues at the dimer interface (within 4 Å, shadowed), mapped on the sequence of YLOV and phy3-LOV2. For comparison the interaction hot-spots predicted by PPI-Pred⁵⁶ (in bold) and by Robetta⁵⁷ are also shown (in bold and underlined). Arrows indicate the residues interacting with FMN in phy3-LOV2. Secondary structure elements are shown below the phy3-LOV2/YLOV alignment and indicated with conventional letters. E = strands, H = helices, C = unordered. The nomenclature of the secondary structure elements is after Harper *et al.*²⁴

The model as in Fig. 6 not only corresponds to the best quality/validation parameters, but also agrees with the observations that in YLOV the β -scaffold is distorted/twisted within the dimer, as indicated by the CD data. With this respect we have to remind that the docking simulation requires that the partners within the complex are kept rigid, a feature that may not be verified in the real complex, as again suggested by the distortion of the β -scaffold. Therefore, the model structure reported in Fig. 6 has to be taken with care and, albeit probably qualitatively correct, may not match the solution dimer-structure as far as the details are concerned.

In the structure of EcDos and RmFIXL PAS domains, the dimers are further stabilized by the helical N-cap and the dimers retain an elongated shape.^{70,71} In the case of N-YLOV, although the N-cap is helical (from CD data), the dimer is instead approximately spherical (gel filtration). This observation, together with low similarity to the corresponding sequences in EcDos and RmFIXL, does not allow to build a reliable model of the N-cap in YLOV and of its orientation with respect to LOV core.

Similar considerations apply to a structural model of the full-length protein. The LOV-STAS linker region is predicted to be helical and CD data confirm the prediction (see above), nevertheless we cannot safely state that it assumes an orientation similar to that in phot1-LOV2, namely underneath the central β -scaffold of the LOV core,²⁴ because of low sequence similarity. The amino acid sequence of YtvA α -linker is much more similar to the C-terminal extension of the heme binding PAS domain of FIXL from *B. japonicum*, actually protruding outside the PAS core.⁷² Although this might be, in the latter case, an artifact of crystallization (in the absence of the associated kinase domain), such orientation of the α -linker cannot be excluded. This would imply a direct interaction of the STAS domain with the LOV core, competing with the dimerization surface, different to the structural features proposed for phot as a basis for the self-phosphorylation reaction.²⁴ We must also consider that alternative complex conformations may exist: the linker is not needed for the activation of the kinase activity in phot2 towards a substrate, a reaction carried out *via* direct interaction between the separately expressed LOV2 and kinase domains.¹⁵ As a whole we still have too little structural and functional information about the N-cap and α -linker to build a reliable model of full-length YtvA. In order to gain further structural information, *e.g.*, orientation of the helical linker with respect to the LOV core and its relevance in the LOV-STAS interaction, we are designing separated constructs for the STAS domain and the LOV core furnished with the linker region.

We wish to point out that with CD experiments we can only see modifications in the secondary structure elements, but protein movements could occur without large conformational changes of the secondary structure. Furthermore our experiments are not time resolved, therefore we cannot detect transient structural changes occurring within the time-scale for the formation of the adduct (*ca.* 2 μ s).¹⁹ Another problem is represented by the fact that we are working with a system that only partially resembles physiological conditions. In fact, from a very recent paper we know that YtvA functions within a large macromolecular complex, about which we presently do not have any structural information.³⁷ Some hints about the way the STAS domain is activated may come from our recent experiments showing that YtvA binds Nucleotide Triphosphate (NTP = GTP, ATP)³⁹ and that light-

induced conformational changes are transmitted from the LOV-core to the NTP binding cavity on the STAS domain.³⁹ These changes are very small and certainly do not imply large structural changes in YtvA, but may have a larger significance within the macromolecular complex mentioned above.

Conclusions

In this work we have investigated the conformation of YtvA in solution. The analysis of CD spectra by means of the CCA algorithm and curve assignment has been improved with respect to previous work and can be now reliably employed to determine the secondary structural composition of LOV proteins. The LOV domain of YtvA has been proven to be an elongated dimer, stabilized by interactions that involve the β -scaffold, for which we have modelled a structure that agrees with experimental data and bioinformatic analysis. In the N-YLOV construct, the helical N-terminal cap is expected to participate in dimerization, although we could not model the complex due to lack of information about the orientation of this segment. In the full-length protein YtvA, dimerization appears only in case that apoprotein is present, most probably with the formation of heterodimers (apoprotein/FMN-bound YtvA). The data strongly suggest that the β -scaffold is involved both in YLOV dimerization and intraprotein interactions with the linker and/or STAS domain, confirming that this region is a good candidate as a surface responsible for signal transmission to the effector domains in LOV proteins. This latter aspect highlights a sharp similarity with phot-LOV2,²⁴ but the missing light-driven unfolding of the α -linker also points to a distinct difference between phot and YtvA, in the way the effector domain is activated. Furthermore, the data presented here suggest that dimerization of LOV domains might play an important regulative role by competing with domain-domain interactions and should be thoroughly investigated.

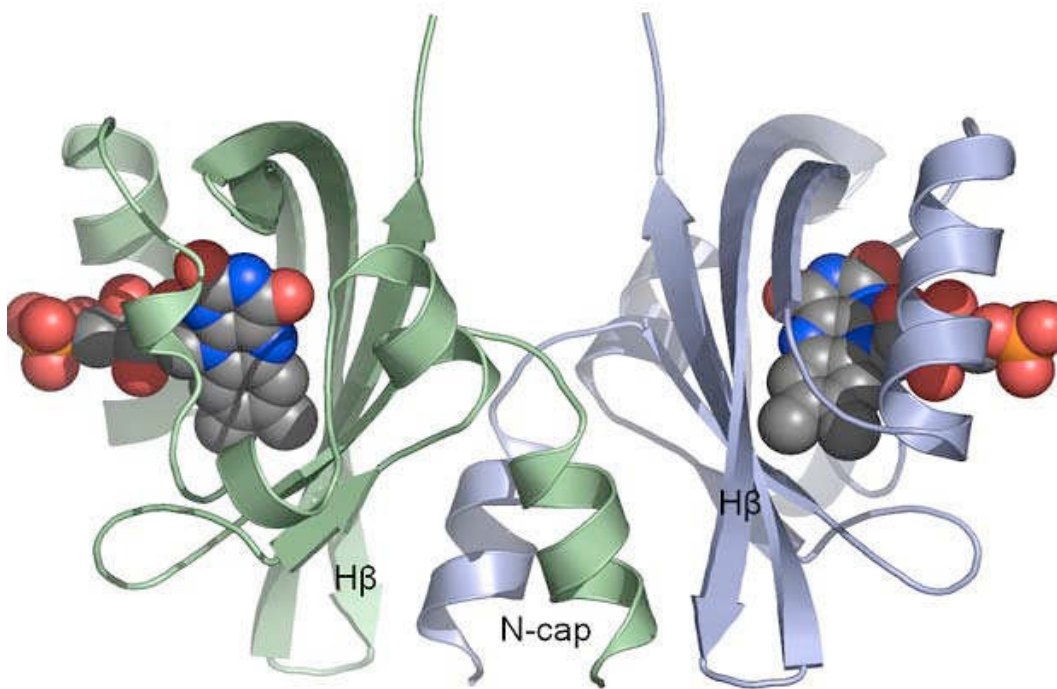
References

- 1 M. H. Hefti, K. J. Francoijs, S. C. de Vries, R. Dixon and J. Vervoort, The PAS fold: A redefinition of the PAS domain based upon structural prediction, *FEBS J.*, 2004, **271**, 1198–1208.
- 2 W. R. Briggs, C. F. Beck, A. R. Cashmore, J. M. Christie, J. Hughes, J. A. Jarillo, T. Kagawa, H. Kanegae, E. Liscum, A. Nagatani, K. Okada, M. Salomon, W. Rüdiger, T. Sakai, M. Takano, M. Wada and J. C. Watson, The phototropin family of photoreceptors, *Plant Cell*, 2001, **13**, 993–997.
- 3 W. R. Briggs and J. M. Christie, Phototropins 1 and 2: versatile plant blue-light receptors, *Trends Plant Sci.*, 2002, **7**, 204–210.
- 4 R. Banerjee and A. Batschauer, Plant blue-light receptors, *Planta*, 2005, **220**, 498–502.
- 5 E. Huala, P. W. Oeller, E. Liscum, I. S. Han, E. Larsen and W. R. Briggs, *Arabidopsis* NPH1: A Protein Kinase with a Putative Redox-Sensing Domain, *Science*, 1997, **278**, 2120–2123.
- 6 E. Knieb, M. Salomon and W. Rüdiger, Autophosphorylation, electrophoretic mobility and immunoreaction of oat Phototropin 1 Under UV and Blue Light, *Photochem. Photobiol.*, 2005, **81**, 177–182.
- 7 M. Salomon, J. M. Christie, E. Knieb, U. Lempert and W. R. Briggs, Photochemical and mutational analysis of the FMN-binding domains of the plant blue light receptor phototropin, *Biochemistry*, 2000, **39**, 9401–9410.
- 8 M. Salomon, W. Eisenreich, H. Dürr, E. Schleicher, E. Knieb, V. Massey, W. Rüdiger, F. Müller, A. Bacher and G. Richter, An optomechanical transducer in the blue light receptor phototropin from *Avena sativa*, *Proc. Natl. Acad. Sci. U. S. A.*, 2001, **98**, 12357–12361.
- 9 M. Kasahara, T. E. Swartz, M. A. Olney, A. Onodera, N. Mochizuki, H. Fukuzawa, E. Asamizu, S. Tabata, H. Kanegae, M. Takano, J. M.

- Christie, A. Nagatani and W. R. Briggs, Photochemical properties of the flavin mononucleotide-binding domains of the phototropins from *Arabidopsis*, rice, and *Chlamydomonas reinhardtii*, *Plant Physiol.*, 2002, **129**, 762–773.
- 10 S. Crosson and K. Moffat, Photoexcited structure of a plant photoreceptor domain reveals a light-driven molecular switch, *Plant Cell*, 2002, **14**, 1067–1075.
 - 11 C. W. M. Kay, E. Schleicher, A. Kuppig, H. Hofner, W. Rüdiger, M. Schleicher, M. Fischer, A. Bacher, S. Weber and G. Richter, Blue light perception in plants. Detection and characterization of a light-induced neutral flavin radical in a C450A mutant of phototropin, *J. Biol. Chem.*, 2003, **278**, 10973–10982.
 - 12 J. T. M. Kennis, S. Crosson, M. Gauden, I. H. M. van Stokkum, K. Moffat and R. van Grondelle, Primary Reactions of the LOV2 Domain of Phototropin, a Plant Blue-Light Photoreceptor, *Biochemistry*, 2003, **42**, 3385–3392.
 - 13 T. E. Swartz, S. B. Corchnoy, J. M. Christie, J. W. Lewis, I. Szundi, W. R. Briggs and R. A. Bogomolni, The photocycle of a flavin-binding domain of the blue light photoreceptor phototropin, *J. Biol. Chem.*, 2001, **276**, 36493–36500.
 - 14 T. Kottke, J. Heberle Dominic Hehn and P. Hegemann, Phot-LOV1: Photocycle of a Blue-Light Receptor Domain from the Green Alga *Chlamydomonas reinhardtii*, *Biophys. J.*, 2003, **84**, 1192–1201.
 - 15 D. Matsuoka and S. Tokutomi, Blue light-regulated molecular switch of Ser/Thr kinase in phototropin, *Proc. Natl. Acad. Sci. U. S. A.*, 2005, **102**, 13337–13342.
 - 16 J. M. Christie, T. E. Swartz, R. A. Bogomolni and W. R. Briggs, Phototropin LOV domains exhibit distinct roles in regulating photoreceptor function, *Plant J.*, 2002, **32**, 205–219.
 - 17 S. Crosson, S. Rajagopal and K. Moffat, The LOV domain family: photoresponsive signaling modules coupled to diverse output domains, *Biochemistry*, 2003, **42**, 2–10.
 - 18 A. Losi, The bacterial counterparts of plants phototropins, *Photochem. Photobiol. Sci.*, 2004, **3**, 566–574.
 - 19 A. Losi, E. Polverini, B. Quest and W. Gärtner, First evidence for phototropin-related blue-light receptors in prokaryotes, *Biophys. J.*, 2002, **82**, 2627–2634.
 - 20 U. Krauss, A. Losi, W. Gärtner, K.-E. Jaeger and T. Eggert, Initial characterization of a blue-light sensing, phototropin-related protein from *Pseudomonas putida*: a paradigm for an extended LOV construct, *Phys. Chem. Chem. Phys.*, 2005, **7**, 2229–2236.
 - 21 E. Schleicher, R. M. Kowalczyk, C. W. M. Kay, P. Hegemann, A. Bacher, M. Fischer, R. Bittl, G. Richter and S. Weber, On the reaction mechanism of adduct formation in LOV domains of the plant blue-light receptor phototropin, *J. Am. Chem. Soc.*, 2004, **126**, 11067–11076.
 - 22 S. Crosson and K. Moffat, Structure of a flavin-binding plant photoreceptor domain: insights into light-mediated signal transduction, *Proc. Natl. Acad. Sci. U. S. A.*, 2001, **98**, 2995–3000.
 - 23 R. Fedorov, I. Schlichting, E. Hartmann, T. Domratcheva, M. Fuhrmann and P. Hegemann, Crystal structures and molecular mechanism of a light-induced signaling switch: the Phot-LOV1 domain from *Chlamydomonas reinhardtii*, *Biophys. J.*, 2003, **84**, 2492–2501.
 - 24 S. M. Harper, L. C. Neil and K. H. Gardner, Structural basis of a phototropin light switch, *Science*, 2003, **301**, 1541–1544.
 - 25 S. M. Harper, J. M. Christie and K. H. Gardner, Disruption of the LOV-Jalpha helix interaction activates phototropin kinase activity, *Biochemistry*, 2004, **43**, 16184–16192.
 - 26 A. Losi, in *Flavin photochemistry and photobiology*, ed. D.-P. Häder and G. Jori, Elsevier, Amsterdam, 4th edn, 2006, ch. 10, pp. 223–276.
 - 27 T. Eitoku, Y. Nakasone, D. Matsuoka, S. Tokutomi and M. Terazima, Conformational dynamics of phototropin 2 LOV2 domain with the linker upon photoexcitation, *J. Am. Chem. Soc.*, 2005, **127**, 13238–13244.
 - 28 B. L. Taylor and I. B. Zhulin, PAS domains: internal sensors of oxygen, redox potential and light, *Microbiol. Mol. Biol. Rev.*, 1999, **63**, 479–506.
 - 29 M. A. Gilles-Gonzalez and G. Gonzalez, Heme-based sensors: defining characteristics, recent developments, and regulatory hypotheses, *J. Inorg. Biochem.*, 2005, **99**, 1–22.
 - 30 M. Salomon, U. Lempert and W. Rüdiger, Dimerization of the plant photoreceptor phototropin is probably mediated by the LOV1 domain, *FEBS Lett.*, 2004, **572**, 8–10.
 - 31 Y. Nakasone, T. Eitoku, D. Matsuoka, S. Tokutomi and M. Terazima, Kinetic Measurement of Transient Dimerization and Dissociation Reactions of Arabidopsis Phototropin 1 LOV2 Domain, *Biophys. J.*, 2006, **91**, 645–653.
 - 32 M. Nakasako, D. Matsuoka, K. Zikihara and S. Tokutomi, Quaternary structure of LOV-domain containing polypeptide of *Arabidopsis* FKF1 protein, *FEBS Lett.*, 2005, **579**, 1067–1071.
 - 33 M. Nakasako, T. Iwata, D. Matsuoka and S. Tokutomi, Light-Induced Structural Changes of LOV Domain-Containing Polypeptides from *Arabidopsis* Phototropin 1 and 2 Studied by Small-Angle X-ray Scattering, *Biochemistry*, 2004, **43**, 14881–1489.
 - 34 P. Ballario, C. Talora, D. Galli, H. Linden and G. Macino, Roles in dimerization and blue light photoresponse of the PAS and LOV domains of *Neurospora crassa* white collar proteins, *Mol. Microbiol.*, 1998, **29**, 719–729.
 - 35 L. Aravind and E. V. Koonin, The STAS domain a link between anion transporters and antisigma-factor antagonists, *Curr. Biol.*, 2000, **10**, R53–R55.
 - 36 S. Akbar, T. A. Gaidenko, K. Min, M. O'Reilly, K. M. Devine and C. W. Price, New family of regulators in the environmental signaling pathway which activates the general stress transcription factor of *Bacillus subtilis*, *J. Bacteriol.*, 2001, **183**, 1329–1338.
 - 37 T. A. Gaidenko, T. J. Kim, A. L. Weigel, M. S. Brody and C. W. Price, The blue-light receptor YtvA acts in the environmental stress signaling pathway of *Bacillus subtilis*, *J. Bacteriol.*, 2006, **188**, 6387–6395.
 - 38 M. Avila-Perez, K. J. Hellingwerf and R. Kort, Blue light activates the sigmaB-dependent stress response of *Bacillus subtilis* via YtvA, *J. Bacteriol.*, 2006, **188**, 6411–6414.
 - 39 V. Buttani, A. Losi, E. Polverini and W. Gärtner, Blue news: NTP binding properties of the blue-light sensitive YtvA protein from *Bacillus subtilis*, *FEBS Lett.*, 2006, **580**, 3818–3822.
 - 40 S. M. Najafi, D. A. Harris and M. D. Yudkin, The SpoIIAA protein of *Bacillus subtilis* has GTP-binding properties, *J. Bacteriol.*, 1996, **178**, 6632–6634.
 - 41 A. Losi, E. Ghiraldelli, S. Jansen and W. Gärtner, Mutational effects on protein structural changes and interdomain interactions in the blue-light sensing LOV protein YtvA, *Photochem. Photobiol. Sci.*, 2005, **81**, 1145–1152.
 - 42 A. Losi, B. Quest and W. Gärtner, Listening to the blue: the time-resolved thermodynamics of the bacterial blue-light receptor YtvA and its isolated LOV domain, *Photochem. Photobiol. Sci.*, 2003, **2**, 759–766.
 - 43 A. Perczel, M. Hollosi, G. Tusnady and G. D. Fasman, Convex constraint analysis: a natural deconvolution of circular dichroism curves of proteins, *Protein Eng.*, 1991, **4**, 669–679.
 - 44 A. Perczel, K. Park and G. D. Fasman, Analysis of the circular dichroism spectrum of proteins using the convex constraint algorithm: A practical guide, *Anal. Biochem.*, 1992, **203**, 83–93.
 - 45 I. R. Bates, P. Matharu, N. Ishiyama, D. Rochon, D. D. Wood, E. Polverini, M. A. Moscarello, N. J. Viner and G. Harauz, Characterization of a Recombinant Murine 18.5-kDa Myelin Basic Protein, *Protein Expression Purif.*, 2000, **20**, 285–299.
 - 46 C. Combet, C. Blanchet, C. Geourjon and G. Deleage, NPS@: Network Protein Sequence Analysis, *Trends Biochem. Sci.*, 2000, **25**, 147–150.
 - 47 S. R. Comeau, D. W. Gatchell, S. Vajda and C. J. Camacho, ClusPro: An automated docking and discrimination method for the prediction of protein complexes, *Bioinformatics*, 2004, **20**, 45–50.
 - 48 J. G. Mandell, V. A. Roberts, M. E. Pique, V. Kotlovsky, J. C. Mitchell, E. Nelson, I. Tsigelny and L. F. Ten Eyck, Protein docking using continuum electrostatics and geometric fit, *Protein Eng.*, 2001, **14**, 105–113.
 - 49 R. Chen, L. Li and Z. Weng, ZDOCK: an initial-stage protein-docking algorithm, *Proteins*, 2003, **52**, 80–87.
 - 50 L. Willard, A. Ranjan, H. Zhang, H. Monzavi, R. F. Boyko, B. D. Sykes and D. S. Wishart, VADAR: a web server for quantitative evaluation of protein structure quality, *Nucleic Acids Res.*, 2003, **31**, 3316–3319.
 - 51 R. A. Laskowski, M. W. MacArthur, D. S. Moss and J. M. Thornton, PROCHECK-A program to check the stereochemical quality of protein structures, *J. Appl. Crystallogr.*, 1993, **26**, 283–291.
 - 52 R. W. Hooft, G. Vriend, C. Sander and E. E. Abola, Errors in protein structures, *Nature*, 1996, **381**, 272–272.
 - 53 C. Colovos and T. O. Yeates, Verification of protein structures: patterns of nonbonded atomic interactions, *Protein Sci.*, 1993, **2**, 1511–1519.
 - 54 R. Luthy, J. U. Bowie and D. Eisenberg, Assessment of protein models with three-dimensional profiles, *Nature*, 1992, **356**, 83–85.
 - 55 J. Pontius, J. Richelle and S. J. Wodak, Deviations from standard atomic volumes as a quality measure for protein crystal structures, *J. Mol. Biol.*, 1996, **264**, 121–136.

- 56 J. R. Bradford and D. R. Westhead, Improved prediction of protein-protein binding sites using a support vector machines approach, *Bioinformatics*, 2005, **21**, 1487–1494.
- 57 T. Kortemme, D. E. Kim and D. Baker, Computational alanine scanning of protein–protein interfaces, *Sci. STKE*, 2004, **2004**(219), p12.
- 58 N. Sreerama, S. Y. Venyaminov and R. W. Woody, Estimation of protein secondary structure from circular dichroism spectra: inclusion of denatured proteins with native proteins in the analysis, *Anal. Biochem.*, 2000, **287**, 243–251.
- 59 N. Sreerama, S. Y. Venyaminov and R. W. Woody, Estimation of the number of alpha-helical and beta-strand segments in proteins using circular dichroism spectroscopy, *Protein Sci.*, 1999, **8**, 370–380.
- 60 K. Matsuo, R. Yonehara and K. Gekko, Improved Estimation of the Secondary Structures of Proteins by Vacuum-Ultraviolet Circular Dichroism Spectroscopy, *J. Biochem.*, 2005, **138**, 79–88.
- 61 N. Sreerama and R. W. Woody, Structural composition of betaI- and betaII-proteins, *Protein Sci.*, 2003, **12**, 384–388.
- 62 N. J. Greenfield, Analysis of circular dichroism data, *Methods Enzymol.*, 2004, **383**, 282–317.
- 63 R. W. Woody and A. Koslowski, Recent developments in the electronic spectroscopy of amides and alpha-helical polypeptides, *Biophys. Chem.*, 2002, **101–102**, 535–551.
- 64 N. J. Greenfield, Methods to estimate the conformation of proteins and polypeptides from circular dichroism data, *Anal. Biochem.*, 1996, **235**, 1–10.
- 65 C. T. Chang, C. S. Wu and J. T. Yang, Circular dichroic analysis of protein conformation: inclusion of the beta-turns, *Anal. Biochem.*, 1978, **91**, 13–31.
- 66 T. Iwata, D. Nozaki, S. Tokutomi and H. Kandori, Comparative investigation of the LOV1 and LOV2 domains in *Adiantum* Phytochrome3, *Biochemistry*, 2005, **44**, 7427–7434.
- 67 S. B. Corchnoy, T. E. Swartz, J. W. Lewis, I. Szundi, W. R. Briggs and R. A. Bogomolni, Intramolecular proton transfers and structural changes during the photocycle of the LOV2 domain of phototropin 1, *J. Biol. Chem.*, 2003, **278**, 724–731.
- 68 T. Bednarz, A. Losi, W. Gärtner, P. Hegemann and J. Heberle, Functional variations among LOV domains as revealed by FT-IR difference spectroscopy, *Photochem. Photobiol. Sci.*, 2004, **3**, 575–579.
- 69 P. B. Card, P. J. A. Erbel and K. H. Gardner, Structural Basis of ARNT PAS-B dimerization: use of a common beta-sheet interface for hetero- and homodimerization, *J. Mol. Biol.*, 2005, **353**, 664–677.
- 70 H. J. Park, C. Suquet, J. D. Satterlee and C. Kang, Insights into signal transduction involving PAS domain oxygen-sensing heme proteins from the X-ray crystal structure of *Escherichia Coli* Dos Heme Domain (EcDosH), *Biochemistry*, 2004, **43**, 2738–2746.
- 71 H. Miyatake, M. Mukai, S. Y. Park, S. Adachi, K. Tamura, H. Nakamura, K. Nakamura, T. Tsuchiya, T. Iizuka and Y. Shiro, Sensory mechanism of oxygen sensor FixL from *Rhizobium meliloti*: crystallographic, mutagenesis and resonance Raman spectroscopic studies, *J. Mol. Biol.*, 2000, **301**, 415–431.
- 72 W. Gong, B. Hao, S. S. Mansy, G. Gonzalez, M. A. Gilles-Gonzalez and M. K. Chan, Structure of a biological oxygen sensor: a new mechanism for heme-driven signal transduction, *Proc. Natl. Acad. Sci. U. S. A.*, 1998, **95**, 15177–15182.

2.2 The LOV-domain crystal structure of YtvA from *Bacillus amyloliquefaciens* FZB42



Crystallization and preliminary X-ray analysis of the LOV domain of the blue-light receptor YtvA from *Bacillus amyloliquefaciens* FZB42

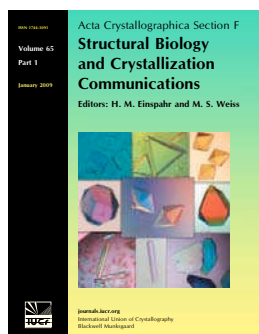
Hideaki Ogata, Zhen Cao, Aba Losi and Wolfgang Gärtner

Acta Cryst. (2009). **F65**, 853–855

Copyright © International Union of Crystallography

Author(s) of this paper may load this reprint on their own web site or institutional repository provided that this cover page is retained. Republication of this article or its storage in electronic databases other than as specified above is not permitted without prior permission in writing from the IUCr.

For further information see <http://journals.iucr.org/services/authorrights.html>



Acta Crystallographica Section F: Structural Biology and Crystallization Communications is a rapid all-electronic journal, which provides a home for short communications on the crystallization and structure of biological macromolecules. It includes four categories of publication: protein structure communications; nucleic acid structure communications; structural genomics communications; and crystallization communications. Structures determined through structural genomics initiatives or from iterative studies such as those used in the pharmaceutical industry are particularly welcomed. *Section F* is essential for all those interested in structural biology including molecular biologists, biochemists, crystallization specialists, structural biologists, biophysicists, pharmacologists and other life scientists.

Crystallography Journals **Online** is available from journals.iucr.org

Hideaki Ogata,^a Zhen Cao,^a Aba Losi^b and Wolfgang Gärtner^{a*}^aMax-Planck-Institut für Bioorganische Chemie, Stiftstrasse 34-36, D-45470 Mülheim an der Ruhr, Germany, and ^bDepartment of Physics, University of Parma and Istituto Nazionale per la Fisica della Materia, Parco Area delle Scienze 7/A, 43100 Parma, ItalyCorrespondence e-mail:
gaertner@mpi-muelheim.mpg.de

Received 18 May 2009

Accepted 8 July 2009

Crystallization and preliminary X-ray analysis of the LOV domain of the blue-light receptor YtvA from *Bacillus amyloliquefaciens* FZB42

Light–oxygen–voltage (LOV) proteins play an important role in blue-light-dependent physiological processes in many organisms. The LOV domain of the blue-light receptor YtvA from *Bacillus amyloliquefaciens* FZB42 has been purified and crystallized at 277 K using the sitting-drop vapour-diffusion method with 2-ethoxyethanol as a precipitant. A data set was collected to 1.60 Å resolution from a single crystal at 100 K using synchrotron radiation. The LOV domain of YtvA crystallized in space group $C222_1$, with unit-cell parameters $a = 64.95$, $b = 83.76$, $c = 55.81$ Å. The crystal structure of the LOV domain of YtvA was determined by the molecular-replacement method. The crystal contained one molecule per asymmetric unit, with a Matthews coefficient (V_M) of $3.04 \text{ Å}^3 \text{ Da}^{-1}$; the solvent content was estimated to be 59.5%.

1. Introduction

A large number of light-regulated physiological functions in plants (e.g. phototropism and stomata opening) are controlled by the blue-light receptors phototropins (phot; for a review, see Wada *et al.*, 2005). Phot contain two light–oxygen–voltage (LOV) domains (LOV1 and LOV2) in a tandem array, each consisting of ~110 amino acids and each binding a flavin mononucleotide (FMN) as a chromophore. LOV domains, which belong to the PAS (Per–Arnt–Sim) superfamily (Losi & Gärtner, 2008), have a similar α/β structural motif in various proteins, e.g. in blue-light receptors, oxygen-sensor proteins and voltage-gated potassium-channel proteins.

In the dark, LOV domains absorb blue light at around 450 nm (LOV₄₄₇). Photoexcitation of LOV domains causes a cysteine residue located near to the FMN molecule to form an adduct with the 4a position of FMN. This reaction takes place during the microsecond decay of the FMN triplet state. The photoadduct form (LOV₃₉₀) is considered to be the signalling state of LOV domains and has been shown to be essential for YtvA to exert its positive regulation on σ^B during environmental stress (Gaidenko *et al.*, 2006; Avila-Pérez *et al.*, 2006). In a thermally driven process, the LOV₃₉₀ state converts back to the LOV₄₄₇ state within minutes.

YtvA from *Bacillus subtilis* was the first prokaryotic counterpart of plant phot to be identified (Losi *et al.*, 2002) and carries a single LOV domain connected to a C-terminal sulfate transporter and anti- σ -factor antagonist (STAS) domain (Aravind & Koonin, 2000). The LOV and STAS domains are connected by a linker region J α (amino acids 127–146, *B. subtilis* numbering). The STAS domain has recently been shown to bind ATP and GTP (Buttani *et al.*, 2006, 2007), a functionality that is probably linked to the role of YtvA as a positive regulator of the general stress transcription factor σ^B (Akbar *et al.*, 2001). In recent years, LOV-domain proteins have been found in about 13% of all sequenced prokaryotic genomes, making this light-sensing motif the most abundant light-sensing motif among blue-light receptors (Losi, 2006; Losi & Gärtner, 2008).

YtvA from *B. amyloliquefaciens* FZB42 is closely related to YtvA from *B. subtilis*, showing a similar two-domain architecture consisting of a LOV domain and a STAS domain. Isolated LOV domains (amino acids 25–126 in *B. subtilis* YtvA) have a strong tendency to dimerize, which is prevented in the full-length protein but was still observed in a LOV domain carrying the N-terminal extension (amino

acids 1–24; N-terminal cap). Analysis of circular-dichroism measurements showed that both the N-terminal cap and the linker region (amino acids 127–146) between the LOV and the STAS domain from *B. subtilis* are helical and that the central β -scaffold is distorted in the LOV-domain dimers (Buttani *et al.*, 2007). To date, several crystal structures of LOV domains have been determined (Crosson & Moffat, 2001; Fedorov *et al.*, 2003; Nakasako *et al.*, 2008). In order to understand the interaction between the reactive cysteine and FMN during the photocycle, we purified the LOV domain of YtvA from *B. amyloliquefaciens* FZB42 and crystallized it. The protein was overexpressed in *Escherichia coli* with a 6 \times His tag. In this paper, we report the crystallization and preliminary X-ray analysis of the LOV domain of the photosensor YtvA from *B. amyloliquefaciens* FZB42.

2. Materials and methods

2.1. Protein expression and purification

The genomic DNA of *B. amyloliquefaciens* FZB42 was provided by Professor Rainer Borriss of Humboldt-University, Berlin. The ORF RBAM_027270 was amplified by PCR using the primers 5'-CAG GGA CCC GGT **CAT ATG** GCT GAC TCA AAT GTA TTC GG (forward) and 5'-GGC ACC AGA GCG TTA **AGC TTA** TAC GAC CGG AAG CAC GT (reverse), containing an *Nde*I and a *Hind*III restriction site (shown in bold), respectively. Platinum Taq DNA polymerase (Invitrogen, Karlsruhe, Germany) was used for PCR. The PCR product was then digested with *Nde*I/*Hind*III (NEB, Ipswich, England) and ligated into the digested expression vector pET28a (Novagen–Merck, Darmstadt, Germany). The recombinant proteins carried an N-terminal extension sequence (derived from the cloning vector) including a 6 \times His tag (MGSSHHHHHSSGLVPRGSH).

The His-tagged protein was expressed in *E. coli* BL21 (DE3) (Stratagene, Amsterdam, Netherlands) via induction with IPTG (final concentration of 0.25 mM). The protein was then purified by affinity chromatography and concentrated in 10 mM sodium phosphate buffer pH 8.0. The identity of the LOV domain was confirmed by SDS–PAGE and MALDI–TOF. The molecular weight of the purified protein was determined to be 20 480 Da, corresponding to the protein sequence up to position 160 (leucine) and the N-terminal His tag.

2.2. Crystallization

The purified protein was concentrated to 10 mg ml^{−1} in 10 mM sodium phosphate buffer pH 8.0 and 10 mM NaCl by centrifugation using a Millipore Ultrafree 0.5 centrifugal filter device (10 kDa molecular-weight cutoff, Millipore). Crystallization screening was carried out at 277 K using the sitting-drop vapour-diffusion method. Crystal Screen (Hampton Research, USA) and Cryo 1 (Emerald BioSystems Inc., USA) were used for initial screening. The protein droplets were prepared by mixing 1 μ l purified protein solution and 1 μ l reservoir buffer solution and were set up in a 96-well plate (Corning, USA) with 100 μ l reservoir solution. Crystals suitable for diffraction experiments were obtained using conditions consisting of 35%(v/v) 2-ethoxyethanol and 0.1 M cacodylate pH 6.5. The crystal dimensions were typically 0.1 \times 0.1 \times 0.1 mm.

2.3. Data collection and analysis

A complete native data set was collected at 100 K on beamline BL14.2 at BESSY II (Berlin, Germany). The detector was a Rayonix 225. 225 frames of 4 s exposure time and 0.8 $^\circ$ oscillation were

Table 1

X-ray data-collection statistics.

Values in parentheses are for the highest resolution shell (1.64–1.60 Å).

Wavelength (Å)	0.91841
Space group	C222 ₁
Unit-cell parameters (Å)	
<i>a</i>	64.95
<i>b</i>	83.76
<i>c</i>	55.81
Resolution range (Å)	33.50–1.60 (1.64–1.60)
Observed reflections	136343
Unique reflections	19550
<i>R</i> _{merge} [†]	0.040 (0.467)
Completeness (%)	95.6 (86.6)
$\langle I/\sigma(I) \rangle$	28.2 (3.7)
<i>V</i> _M (Å ³ Da ^{−1})	3.04

[†] $R_{\text{merge}} = \sum_{hkl} \sum_i |I_i(hkl) - \langle I(hkl) \rangle| / \sum_{hkl} \sum_i I_i(hkl)$, where $I_i(hkl)$ is the intensity of the *i*th observation and $\langle I(hkl) \rangle$ is the mean intensity of the reflections.

collected. The X-ray wavelength was chosen to be 0.91841 Å. The distance between the crystal and the detector was maintained at 180 mm. In order to collect the data at cryogenic temperature, the crystal was frozen directly in liquid nitrogen and mounted on the goniostat in a nitrogen-gas stream at 100 K. Data collection was carried out in room light. The data set was indexed and integrated using the program *XDS* (Kabsch, 1993). The scaling was carried out with *XSCALE* (Kabsch, 1993). The conditions of the data collection and the results obtained are summarized in Table 1.

3. Results and discussion

The LOV domain of YtvA from *B. amyloliquefaciens* FZB42 was successfully purified, characterized and crystallized. It showed all the salient features of flavin-containing LOV domains such as an absorption maximum at 450 nm, light-induced formation of the photoproduct and a thermally driven dark recovery of the parent state ($\tau_{\text{rec}} = 25\,700 \pm 30$ s at 293 K). Crystals suitable for diffraction

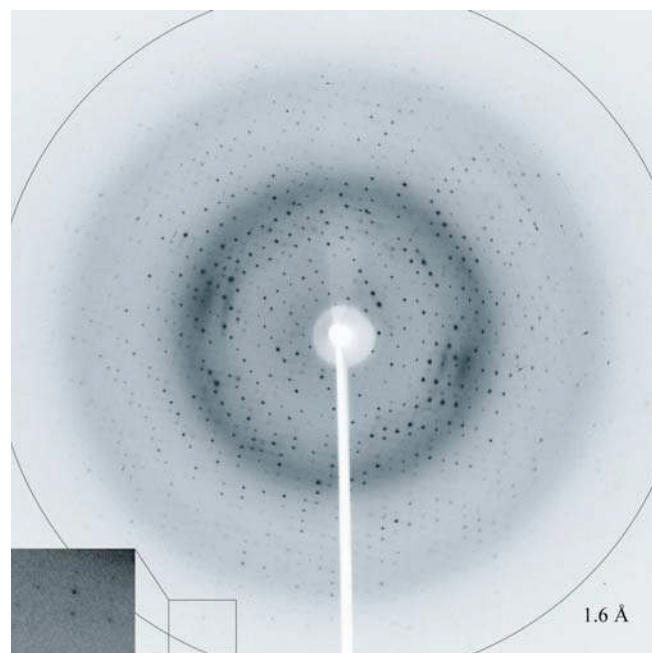


Figure 1

Diffraction pattern of the LOV domain of YtvA from *B. amyloliquefaciens* FZB42.

experiments were obtained using conditions consisting of 35%(v/v) 2-ethoxyethanol and 0.1 M cacodylate pH 6.5. The crystal dimensions were typically $0.1 \times 0.1 \times 0.1$ mm. The crystals diffracted to 1.60 Å resolution (Fig. 1) and belonged to space group $C222_1$, with unit-cell parameters $a = 64.95$, $b = 83.76$, $c = 55.81$ Å. The calculated Matthews coefficient (V_M) of $3.04 \text{ Å}^3 \text{ Da}^{-1}$ with a solvent content of 59.4% indicated the presence of one molecule in the asymmetric unit. The crystal structure of the LOV domain of YtvA from *B. amyloliquefaciens* FZB42 was solved by the molecular-replacement method using the program *MOLREP* (Vagin & Isupov, 2001) from the *CCP4* package (Collaborative Computational Project, Number 4, 1994). Data for the LOV domain of YtvA from *B. subtilis* (PDB code 2pr6), which has 72% amino-acid sequence identity to the LOV domain of YtvA from *B. amyloliquefaciens* FZB42, were used as coordinates for the search model.

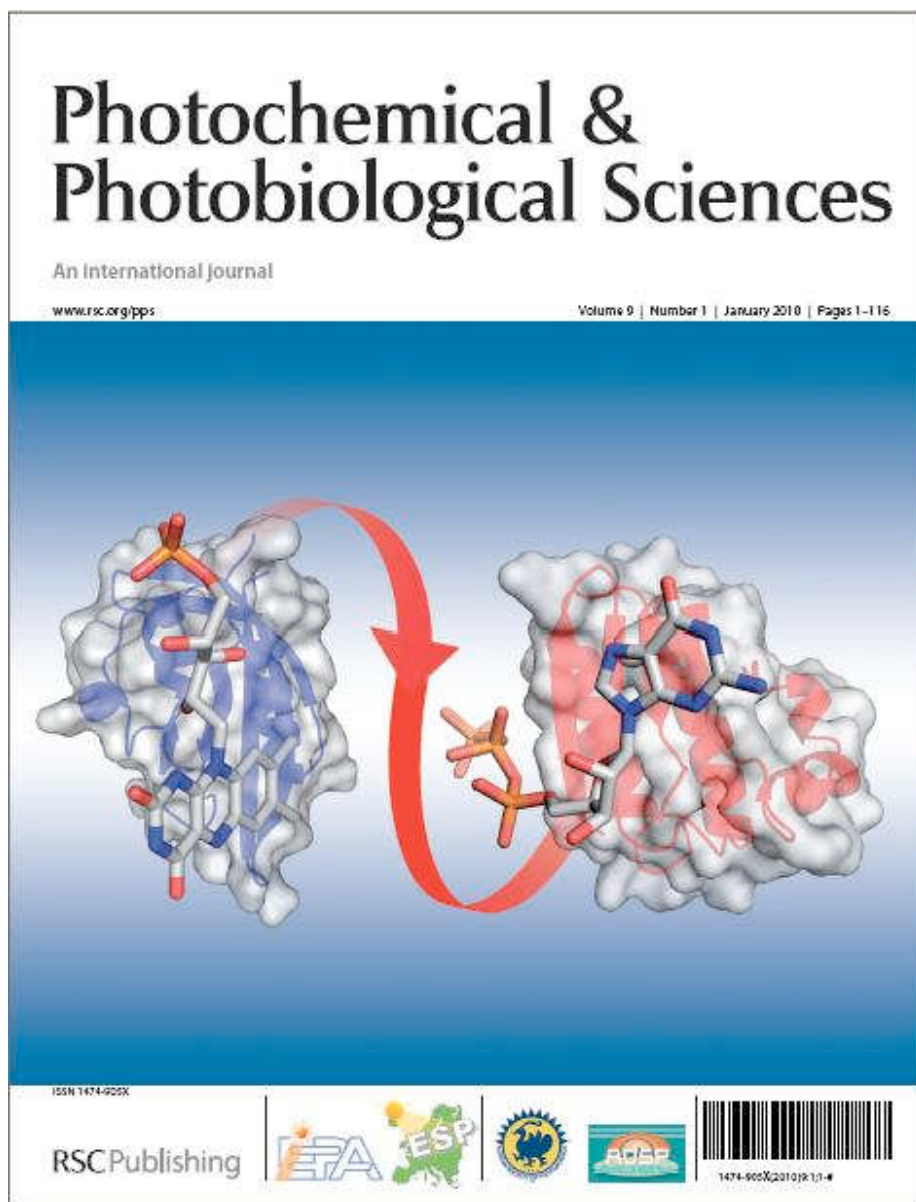
After calculation of the electron-density map using the molecular-replacement solution and initial refinement with the program *REFMAC5* (Vagin *et al.*, 2004), the electron-density map of FMN was determined. The side chain of the reactive cysteine showed a multiple conformation without binding to FMN, suggesting that the crystal contained the dark state of the LOV domain. Data analysis revealed that two molecules assemble to give a dimer by crystallographic twofold symmetry. The dimer was formed by an interaction between the N-terminal α -helices of each molecule. This is in contrast to the LOV domain of YtvA from *B. subtilis*, in which a dimeric form was observed that was formed by an interaction between the α -helices at the C-terminal end of the LOV domain (Möglich & Moffat, 2007). Dimerization similar to that found in this work for the LOV domain of YtvA from *B. amyloliquefaciens* has also been reported for the redox-sensor domain of Nifl (PDB code 2gj3; Key *et al.*, 2007). A total of 115 amino-acid residues (Leu13–Glu128) were traced in the electron-density map. Model building and refinement using the program *SHELX-97* (Sheldrick, 2008) are now in progress.

We thank the staff of beamline BL14.2 at BESSY II (Berlin, Germany) for their assistance during data collection. This work was supported by the Max-Planck Society and the DFG (FOR526).

References

- Akbar, S., Gaidenko, T. A., Min, K., O'Reilly, M., Devine, K. M. & Price, C. W. (2001). *J. Bacteriol.* **183**, 1329–1338.
- Aravind, L. & Koonin, E. V. (2000). *Curr. Biol.* **10**, R53–R55.
- Avila-Pérez, M., Hellingwerf, K. J. & Kort, R. (2006). *J. Bacteriol.* **188**, 6411–6414.
- Buttani, V., Losi, A., Eggert, T., Krauss, U., Jaeger, K. E., Cao, Z. & Gärtner, W. (2007). *Photochem. Photobiol. Sci.* **6**, 41–49.
- Buttani, V., Losi, A., Polverini, E. & Gärtner, W. (2006). *FEBS Lett.* **580**, 3818–3822.
- Collaborative Computational Project, Number 4 (1994). *Acta Cryst.* **D50**, 760–763.
- Crosson, S. & Moffat, K. (2001). *Proc. Natl Acad. Sci. USA*, **98**, 2995–3000.
- Fedorov, R., Schlichting, I., Hartmann, E., Domratcheva, T., Fuhrmann, M. & Hegemann, P. (2003). *Biophys. J.* **84**, 2474–2482.
- Gaidenko, T. A., Kim, T. J., Weigel, A. L., Brody, M. S. & Price, C. W. (2006). *J. Bacteriol.* **188**, 6387–6395.
- Key, J., Hefti, M., Purcell, E. B. & Moffat, K. (2007). *Biochemistry*, **46**, 3614–3623.
- Kabsch, W. (1993). *J. Appl. Cryst.* **26**, 795–800.
- Losi, A. (2006). *Flavin Photochemistry and Photobiology*, edited by E. Silva & A. E. Edwards, pp. 223–276. Cambridge: RSC Publishing.
- Losi, A. & Gärtner, W. (2008). *Photochem. Photobiol. Sci.* **7**, 1168–1178.
- Losi, A., Polverini, E., Quest, B. & Gärtner, W. (2002). *Biophys. J.* **82**, 2627–2634.
- Möglich, A. & Moffat, K. (2007). *J. Mol. Biol.* **373**, 112–126.
- Nakasako, M., Zikihara, K., Matsuoka, D., Katsura, H. & Tokutomi, S. (2008). *J. Mol. Biol.* **381**, 718–733.
- Sheldrick, G. M. (2008). *Acta Cryst.* **A64**, 112–122.
- Vagin, A. A. & Isupov, M. N. (2001). *Acta Cryst.* **D57**, 1451–1456.
- Vagin, A. A., Steiner, R. S., Lebedev, A. A., Potterton, L., McNicholas, S., Long, F. & Murshudov, G. N. (2004). *Acta Cryst.* **D60**, 2184–2195.
- Wada, M., Shimazaki, K. & Iino, M. (2005). *Light Sensing in Plants*. Tokyo: Springer.

2.3 The signal transmission pathway between YtvA-LOV domain and YtvA-STAS domain



Interdomain signalling in the blue-light sensing and GTP-binding protein YtvA: A mutagenesis study uncovering the importance of specific protein sites

Yifen Tang,^a Zhen Cao,^a Elsa Livoti,^b Ulrich Krauss,^c Karl-Erich Jaeger,^c Wolfgang Gärtner^a and Aba Losi^{*b}

Received 5th August 2009, Accepted 28th October 2009

First published as an Advance Article on the web 30th November 2009

DOI: 10.1039/b9pp00075e

YtvA from *Bacillus subtilis* is a blue-light responsive, flavin-binding photoreceptor, built of a light-sensing LOV domain (aa 25-126) and an NTP (nucleoside triphosphate)-binding STAS domain (aa 147-261). The STAS domain is supposed to be the effector part of the protein or a secondary switch. Both domains are connected by a linker polypeptide. The active form of YtvA is generated upon light excitation, causing the formation of a covalent bond between a cysteine residue (Cys62) in the LOV domain and the position 4a of the flavin chromophore. This photoadduct formation within the LOV domain results in a conformational change of the NTP-binding cavity, evidencing intra-protein signal transmission. We have previously shown that Glu105, localized on the beta-scaffold of the LOV-core, is involved in this process. Here, we extend this work by the identification of further residues that upon mutation suppress or strongly impair signal transmission by interfering with the communication between the two domains. These comprise L106 and D109 on the LOV domain; K130 and K134 on the linker region; D193, L194 and G196 within the DLSG GTP-binding motif (switch region) and N201 on the STAS domain. Furthermore in the mutated L195A and D193A proteins, GTP affinity is diminished. Other mutations investigated have little or no effect on signal transmission and GTP-binding affinity: R63K that was found to accelerate the thermal recovery of the parent state *ca.* ten-fold; K128A, Q129A and Y132A within the linker region, and S183A and S212A on the STAS domain. The results show a key role of the LOV domain beta-scaffold and of positively charged residues within the linker for intra-protein signal transmission. Furthermore they evidence the conformational switch function of a structurally conserved strand-loop-helix region (bearing the DLSG GTP-binding motif and N201) within the STAS domain that constitutes a novel GTP-binding fold.

Introduction

The YtvA protein from *Bacillus subtilis* acts as a positive regulator for the general stress transcription factor σ^B , specifically in the environmental signalling pathway.¹ Like other regulators of the stress responsive network in *B. subtilis*, YtvA bears a STAS (Sulfate Transporters and Anti-Sigma factor antagonist) domain. Among the σ^B regulators YtvA has the unique ability to sense and respond to blue light (BL) *via* its N-terminally located LOV (Light, Oxygen and Voltage) domain, a feature shared with a growing family of BL-sensing proteins.² This light-sensitivity has recently been shown to up-regulate the σ^B factor.³⁻⁶ A photoactive LOV domain binds a flavin mononucleotide (FMN) as chromophore.⁷ Photoactivation is achieved by the transient formation of a covalent bond between carbon atom 4a of FMN and a conserved cysteine (Cys62 in YtvA-LOV).⁸ Structurally, a LOV domain shows a PAS (PerArntSims) fold with an extended, five-stranded (A β , B β , G β , H β , I β) antiparallel β -scaffold and helical connectors

(C α , D α , E α , F α), such that the N-terminus of the LOV-core (beginning of strand A β) is in close vicinity to its C-terminus (end of strand I β , Fig. 1) (reviewed in Ref. 9).

The LOV-based photochemistry has first been discovered in the plant blue-light receptors phototropins (phot), built of two LOV domains in tandem, LOV1 and LOV2, and a C-terminally located S/T-kinase domain.^{10,11} In phot, the activity of the effector S/T-kinase domain is enhanced after LOV photoactivation with blue-light, resulting in phot auto-phosphorylation,¹²⁻¹⁴ a key event in signaling.¹⁵ LOV proteins other than phot, including the steadily growing bacterial family, bear solely one LOV domain, and the effector module can be represented by several functional motifs, *e.g.*, a histidine kinase, gene-expression regulators, phosphodiesterases, phosphatases).^{2,16,17} This poses the question whether LOV domains communicate with effector partners through the same or partially overlapping surfaces, such that the structural basis for light-to-signal transduction is basically the same in the different LOV proteins, with only few residues acting as specific signal transmitters within the different systems. There is increasing experimental evidence that this surface largely involves the β -scaffold of the LOV-core (Fig. 1) which on one side hosts residues directly interacting with the isoalloxazine ring of FMN^{18,19} and on the other side communicates with helical regions flanking the LOV-core.^{20,21} As an example, a conserved glutamine on strand I β (Gln513 in *Avena sativa* phot1-LOV2) participates in

^aMax-Planck-Institute for Bioinorganic Chemistry, Stifstrasse 34-36, 45470, Mülheim, Germany

^bDepartment of Physics, University of Parma, viale G.P. Usberti 7/A, 43100, Parma, Italy. E-mail: aba.losi@fis.unipr.it

^cInstitute of Molecular Enzyme Technology, Heinrich-Heine-University Düsseldorf, Research Center Jülich, Stettener Forst, 52426, Jülich, Germany

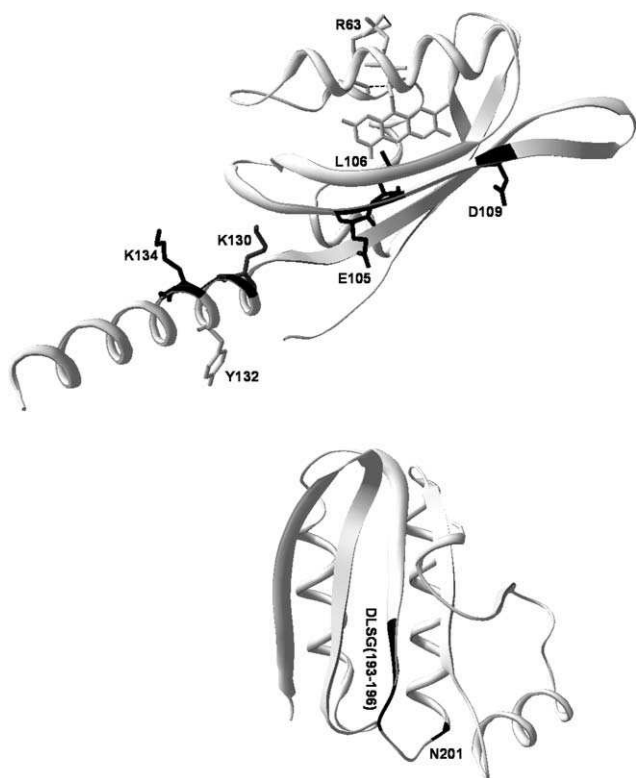


Fig. 1 (top) Structure of YtvA-LOV + linker (PDB entry 2pr5, chain A; (bottom) model of YtvA-STAS. Mutated residues causing a negative effect on signal transmission or GTP_{TR}-binding are shown in black. For the effects of Y132A and R63A see text.

light-driven conformational changes of LOV2,^{22–26} and of the LOV protein VIVID²¹ and in the light-activation of phot self-phosphorylation.²⁷ The latter process is triggered by the light-induced unfolding of the so called J α -linker helix, that interacts in the dark with the β -scaffold of LOV2 and connects LOV2 to the kinase domain.^{28,29,30} Moreover, the β -scaffold is involved in LOV-LOV dimerization, with or without the assistance/competition of the helical flanking regions.^{31–33} In VIVID, light-activation induces dimerization through the helical N-cap, but cross-linking data suggest that dissociation or removal of the N-cap induces dimerization *via* a β -sheet– β -sheet contact.³⁴ In YtvA, the β -scaffold of the LOV-core has been identified as a competitive interface for LOV-LOV dimerization and intraprotein domain interactions,³¹ and a recently crystallized structure confirms the β -sheet mediated contact within the YtvA-LOV dimer.³²

Due to its prokaryotic origin and the relatively small size (261 aa), YtvA is readily expressed as a full length protein and thus offers the possibility to study light induced changes also in the effector/signalling STAS domain. However, no three-dimensional structure of full-length YtvA is yet available, leaving a discussion on residues that potentially enable communication between the LOV- and the STAS domain at a speculative level. A preliminary investigation revealed that glutamic acid 105, localized on strand H β , is involved in signal transmission from LOV- into STAS domain (STAS, Sulfate Transporter and Anti-sigma factor antagonist).³⁵ Although its exact function is not yet known, the STAS domain is thought to be the effector module of the protein or a secondary switch. It has been shown to bind ATP (adenosine

triphosphate) and GTP (guanosine triphosphate),³⁶ in agreement with a proposed general role of STAS domains as NTP (Nucleotide triphosphate) binding folds.³⁷ E105 should therefore be located at that surface of the LOV domain interacting with the linker region or/and the STAS domain.

Communication between the two domains of YtvA is readily monitored by the blue light-induced conformational changes of the NTP-binding cavity of the STAS domain, *i.e.* by recording the spectroscopical changes in case a fluorescent, red light absorbing GTP derivative is employed.³⁶ Specifically, a BODIPY® TR GTP (GTP_{TR}) compound was chosen whose absorption and fluorescence maxima (*ca.* 590 and 620 nm, respectively) do not interfere with those of FMN (*ca.* 450 and 500 nm).³⁸ Upon binding to YtvA (dissociation constant K_D *ca.* 40 μ M in the light-activated state), the fluorescence of GTP_{TR} increases with a concomitant, few nanometers red-shift of the absorption maximum.³⁶ The thermally driven recovery reaction results in a further increment of fluorescence and of the absorption red-shift, indicative of conformational changes in the GTP_{TR} binding cavity.³⁶ These light-dark differences are fully reversible in the wild-type protein, but are completely suppressed in the mutated YtvA-E105L protein, although binding of GTP_{TR} is not impaired.³⁵ E105 is conserved in all YtvA-like proteins in the Firmicutes, while in phot-LOV domains this position is invariably occupied by a hydrophobic amino acid (generally leucine).¹⁷ In phot1-LOV2 this residue, Leu493, makes van der Waals contact to Ile532 on the J α -linker,²⁰ and the Ile532E mutation disrupts the LOV2-J α interaction, rendering the kinase domain constitutively active.²⁹ For YtvA, there is no evidence that light activation implies unfolding of the J-linker,³¹ neither does the presence of the J-linker prevent YtvA-LOV dimerization.^{32,39} Dimerization *via* the LOV-domain is only impaired in the full-length protein, at least in diluted solution.³¹ It is therefore conceivable that the LOV-core directly interacts with the STAS domain through the β -scaffold, possibly with the participation of the J-linker and by employing specific residues devoted to signal transmission.

We here present an extended investigation on the signalling pathway in YtvA, employing a set of selectively designed mutations, and using the GTP_{TR}-binding assay and the GTP_{TR}-based LOV-STAS signal transmission detection. A similar set of mutations has been recently investigated to study their role in the physiological function of YtvA in *B. subtilis*, making use of a reporter-protein mediated assay.⁶

By means of a fast cycling mutated protein, YtvA-R63K, suitable for spectroscopical studies and here fully characterized, we demonstrate the tight coupling between the LOV domain and the GTP_{TR}-binding cavity on the STAS domain, even for the case of a strongly accelerated thermal recovery reaction. We also highlight the functional role of a second acidic amino acid, D109, typical of the YtvA-family and of L106, both localized on strand H β . In addition, our data reveal the functional role of charged amino acids (K130 and K134) within the J-linker, and of the DLSG_{193–196} Walker B- (Switch II) motif⁴⁰ on the STAS domain. As a whole, the results stress the importance of the LOV-core strand H β and of specific residues within the J-linker in inter-domain signal transmission and confirm that YtvA-STAS is a novel NTP-binding fold, showing a conformational change switched by light within its NTP-binding cavity, through its coupling to the LOV domain.

Materials and methods

Site directed mutagenesis of YtvA and generation of recombinant proteins

A total of 16 new mutations had been generated: R63K, L106F, D109L, K128A, Q129A, K130A, Y132A, K134A, S183A, D193A, L194A, S195A, G196A, N201A, S212A. Mutagenesis was performed in two different ways, either by the Quick Change method (QuikChange® II XL, Stratagene) or by the megaprimer approach. The mutated sites in all primers are underlined.

Primers used for the Quick Change method were:

R63K. Forward: 5'-GAAATTTTAGGAAAGAACTGT-AAGTTCTTACAGGGGAAACACAC-3'

Reverse: 5'-GTGTGTTTCCCCTGTAAGAACTTACAGTTCTTTCCTAAAATTTC-3'

L106F. Forward: 5'-GGAACGATGTTCTGGAATGAATT-CAATATTGATCCAATGGAAATAGAG-3'

Reverse: 5'-CTCTATTTCCATTGGATCAATATTGAAATTCATTCCAGAACATCGTTCC-3'

D109L. Forward: 5'-TGGAATGAATTAATATTCTTCC-AATGGAAATAGAGGATAAAACG-3'

Reverse: 5'-CGTTTTATCCTCTATTTCATTGGAGAATATTTAATTCATTCCA-3'

K128A. Forward: 5'TGATATCACCGCACAAAAAGAAT-ATGAAAAGCTTCTCGAGGATTCCCTCACG-3'

Reverse: 5'-CGTGAGGGAATCCTCGAGAAGCTTTTCAT-ATTCTTTTGTGCGGTGATATCA-3'

Q129A. Forward: 5'-CAGAAATGATATCACCAAGGCAAA-AGAATATGAAAAGC-3'

Reverse: 5'-GCTTTTCATATTCTTTTGCCTTGGTGATAT-CATTCTG-3'

K130A. Forward: 5'- GAATGATATCACCAAGCAAGCCG-AATATGAAAAGCTTCTCG-3'

Reverse: 5'-CGAGAAGCTTTTCATATTCCGGCTTGCTTGGTGATATCATTC-3'

Y132A. Forward: 5'- CCAAGCAAAAAGAAGCAGAAAA-GCTTCTCGAGGATTCCCTCACG-3'

Reverse: 5'-CGTGAGGGAATCCTCGAGAAGCTTTTCT-GCTTCTTTTGCTTGG-3'

The remaining mutations had been performed by a two step protocol following the megaprimer approach by using a plasmid-specific universal reverse primer and a mutagenic forward primer in a first run and then continuing with the thus generated DNA duplex in a second PCR reaction.

Universal reverse primer: 5'-TTTTGGATCCTTACATAA-TCGGAAGCACTTTAAC-3',

Mutagenic forward primers

K134A 5'-CAAAAAGAATATGAAGCACTTCTCGAGGA-TTC-3'

S183A 5'-TTGACGAATATCTTAGCAACATCCAAAGATG-3'

D193A 5'-GATTATTTGATCATTGCATTATCCGGATTGG-3'

L194A 5'-TATTTGATCATTGATGCATCCGGATTGGCCC-3'

S195A 5'-TTGATCATTGATTTAGCAGGATTGGCCCAA-G-3'

G196A 5'-ATCATTGATTTATCCGCATTGGCCCAAGTG-AAC-3'

N201A 5'-GATTGGCCCAAGTGGCAGAAACAAACGGCC-3'

S212A 5'-CAAATTTTCAAGCTGGCACATTTGCTGAAA-TTG-3'

For all mutagenesis experiments, the obtained PCR products were treated with the restriction enzyme *DpnI* (New England BioLabs). *DpnI* is specific for methylated and hemimethylated DNA (targeting sequence: 5'-Gm⁶ATC-3') and is used to digest the parental DNA template in the PCR products. 0.5 µl *DpnI* (20000 U/ml) was added to each PCR product and the digestion reaction was carried out at 37 °C for 30 minutes. In all cases, mutations were confirmed by sequencing.

His-tagged, mutated proteins were obtained from expression in *E. coli* (BL21) (Stratagene, Amsterdam, The Netherlands) using IPTG- (BioMol, Hamburg, Germany) induction and employing the pET28a plasmid (Novagen-Merck, Darmstadt, Germany), as described.⁸ The proteins were purified by affinity chromatography on a Talon resin (Qiagen, Hilden, Germany) according to the standard given protocol and adding in each step 200 mM PEFABLOC and 0.8 mM mercaptoethanol; the Talon resin loaded with the cell extract, was washed 5 times with the protocol given washing buffer plus 10 mM imidazole. The protein was then eluted in one step with 130 mM imidazole. The protein was concentrated by centrifugation at 10 °C employing centrifuge tubes with 10,000 Da cutoff and a final, storage buffer composed of Na-phosphate 10 mM, NaCl 10 mM, pH = 8. Care was taken not to concentrate the protein above 170 µM during centrifugation, because this leads, in our experience, to irreversible aggregation and inhomogeneous oligomeric composition.

GTP-binding assays and spectroscopy

Guanosine 5'-triphosphate, BODIPY® TR 2'-(or-3')-O-(N-(2-aminoethyl) urethane), trisodium salt (GTP_{TR}) was purchased from Molecular Probes (Eugene, OR, USA). Absorbance spectra were recorded with a Jasco 7850 UV/Vis spectrophotometer. Steady-state fluorescence measurements were carried out at 20 °C on a Perkin-Elmer LS50 luminescence spectrometer. GTP_{TR} was excited at 590 nm. The output signal was divided by the fraction of absorbed energy (1-10^{-A}, where A = absorbance at the excitation wavelength) in order to obtain a signal, referred to as normalized fluorescence, that is proportional to the fluorescence quantum yield.

With the exception of YtvA-R63K, binding experiments for the determination of the dissociation constant, *K_D*, were carried out with YtvA proteins in their blue-light activated state (*i.e.* FMN covalently bound to Cys 62), achieved by illuminating the sample with a blue-light emitting Led-Lenser® V8 lamp (470 nm, Zweibrüder Optoelectronics, Solingen, Germany) as previously described.³⁶ The blue-light was switched-off just prior recording of the absorption and fluorescence spectra, ensuring that at least 95% of the sample is present as FMN-Cys adduct, given the long lifetime for the recovery to the dark state (denoted as YtvA₄₅₀ from the absorption maximum of the bound flavin), $\tau_{\text{rec}} > 3500$ s at 20 °C.^{8,41,42} The fluorescence spectra were always recorded upon

Table 1 GTP_{TR} affinity and light-induced spectral changes of bound nucleotide

	prot/FMN	$K_D^{a,b}/\mu\text{M}$ (ΔFluo)	$K_D^{a,b}/\mu\text{M}$ (ΔAbs)	Dark-Light GTP _{TR} Spectral Changes
YtvA-WT	1	38 ± 5	26 ± 5	Yes
YtvA-WT	4	15 ± 7	8.5 ± 2	Yes
LOV domain mutations				
R63K	1	28 ± 11	16 ± 2	Yes
E105L	1	43 ± 6	43 ± 10	No
L106F	1	60 ± 13	81 ± 23	Minor
D109L	2	13 ± 3	11 ± 2	No
Linker				
K128A	1	26 ± 2	36 ± 4	Yes
Q129A	1	20 ± 5	42 ± 11	Yes
K130A	1	54 ± 9	92 ± 23	Minor
Y132A	1	62 ± 7	79 ± 18	Yes, > ΔF than WT
K134A	1	76 ± 20	19 ± 5	No
S139A	1	19 ± 2	11 ± 2	Yes
STAS domain				
D193A	4	67 ± 23	61 ± 6	No
L194A	1	84 ± 25	34 ± 5	Minor
S195A	1	300 ± 70	120 ± 50	Yes
G196A	2	10 ± 3	2 ± 1	No
N201A	1	23 ± 5	52 ± 27	Minor
S183A	1	76 ± 40	65 ± 19	Yes
S212A	1	87 ± 10	84 ± 15	Yes

^a K_D = dissociation constants. ^b Errors derive from at least 2 sets of measurements for each sample and from errors reported by the fitting algorithm.

excitation at 590 nm (where solely GTP_{TR} absorbs) and no energy transfer can occur from or to other fluorophores (e.g. FMN or aromatic amino acids).

The calculation of K_D was carried out as previously described.³⁶ We define $\alpha = \Delta F / \Delta F_{\max}$ as the fraction of bound ligand, where ΔF is the variation of the normalized fluorescence of GTP_{TR} in the presence of the protein with respect to free GTP_{TR}; ΔF_{\max} is the maximum fluorescence enhancement corresponding to α_{\max} , i.e. $\alpha = 1$. The value of ΔF_{\max} was determined by the non-linear fitting for one-site binding (eqn 1):

$$[\text{P}]_{\text{tot}} = \frac{\Delta F_{\max} \Delta F}{K'_D + \Delta F} \quad (1)$$

Where $[\text{P}]_{\text{tot}}$ = total concentration of protein added (bound + free), in our cases ranging between ca. 8 and 80 μM . Assuming a 1:1 complex and with $\alpha = \Delta F / \Delta F_{\max}$ we can fit α vs. the concentration of free protein, as detailed in (eqn 2), where α_{\max} must extrapolate to 1 if the assumption is correct:

$$[\text{P}]_{\text{free}} = \frac{\alpha_{\max} \alpha}{K_D + \alpha} \quad (2)$$

In principle, K_D in eqn 2 is different from K'_D in eqn 1, but in our case the two values are very similar given that the association is weak and $[\text{P}]_{\text{tot}} \cong [\text{P}]_{\text{free}}$ total. Given that binding of GTP_{TR} to YtvA induces a red-shift in the absorption spectrum, we also evaluate K_D by employing ΔAbs in place of ΔF in eqn 1.

Results

The residues mutated in this work are shown in Fig. 1, evidenced on a published structure of YtvA-LOV + linker³² and on the modelled structure of the STAS domain.³⁶ Most of the mutated proteins could be expressed as holoproteins (ratio between protein and FMN ca. 1:1), except for D109L, D193A and G196A

mutations, for which protein/FMN ratios were 2, 4, and 2, respectively (Table 1). This determination has been carried out as previously described,⁴³ knowing that a 1:1 ratio of protein to chromophore results in a UV/VIS (272/447 nm) absorbance ratio of ca. 4. The presence of chromophore-free apoprotein can cause an overestimation of the affinity for GTP_{TR},³⁵ possibly by competition with the FMN-binding site on the LOV domain or by conformational modifications occurring when FMN is not bound. To show this “contaminating” effect of the apoprotein, data from an only partially chromophore-loaded YtvA wild type preparation were also included in Table 1. Further, mutated proteins did not show changes in their oligomeric state, i.e. they are present in solution chiefly as monomers as indicated by gel filtration experiments.³⁹

The effects of mutations were monitored by recording two distinct phenomena: 1) the protein binding capacity for GTP_{TR} (dissociation constant K_D , see eqn 1 and 2), determined by the change in its (normalized) fluorescence intensity and by the red-shift in the absorption maximum upon binding; 2) effects on LOV-STAS signal transmission, monitored by following the spectral changes of bound GTP_{TR} after formation of the FMN-cysteine photoadduct. This effect had been described in YtvA-WT as a slight absorption blue-shift and fluorescence decrease that reverses in the dark.³⁵ Throughout the text, α is defined as the fraction of bound ligand, as detailed in the material and methods section.

All the proteins investigated exhibited a photocycle similar to YtvA-WT, with a slow recovery (ca. 4000 ± 1000 s at 20 °C) to the parent state. The sole exception was YtvA- R63K (*vide infra*).

Ribityl-phosphate binding region

YtvA has a remarkably long photocycle with a recovery lifetime $\tau_{\text{rec}} = \text{ca. } 3900 \text{ s}$ at 20 °C⁴¹ showing some variation in dependence of the preparation. This long photocycle may hinder functional and spectroscopical studies, because monitoring light-to-dark

state conversion requires lengthy measurements, during which the protein, the fluorescent probe and/or instrumental parameters might change and introduce artefacts, particularly when the observed changes are small as in the case of GTP_{TR} bound to YtvA.^{35,36} The R63K mutation strongly accelerates the photocycle and the recovery lifetime for FMN, $\tau_{\text{rec,F}}$, becomes *ca.* 480 s at 20 °C (Fig. 2), although the photoadduct is formed with the same kinetics as the WT protein (Livoti, E., unpublished data), namely with a lifetime of *ca.* 2 μs .⁸

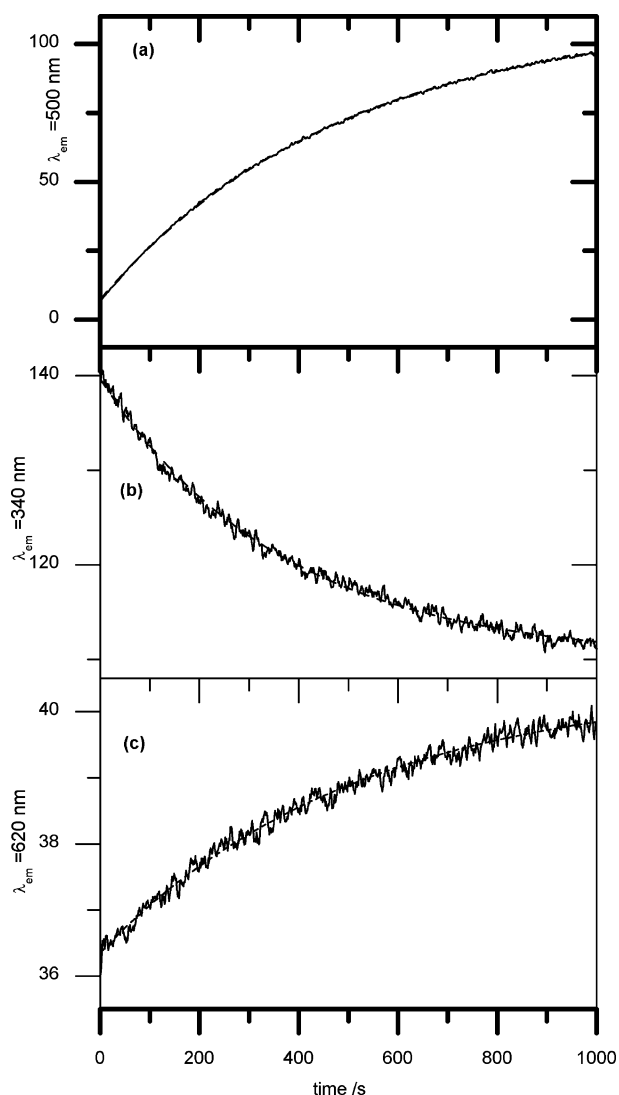


Fig. 2 Dark recovery of (a) FMN, (b): W103 (LOV core), and (c) GTP_{TR} (STAS domain) fluorescence for YtvA-R63K. The excitation wavelengths were 305, 280 and 590 nm, respectively. Kinetics traces were recorded at 20 °C. The values of τ_{rec} obtained from a mono-exponential fitting were: (a) 485 s; (b) 365 s; (c) 511 s.

The kinetic effects of this mutation are similar to those observed in the LOV1 from *Chlamydomonas reinhardtii* phot, where the corresponding mutation (R58K) accelerates the recovery time from 204 to 73 s at 20 °C.⁴⁴ As for the GTP-binding capacity and signal transmission, YtvA-R63K behaves very similar to the WT protein, showing the previously characterized absorption blue-

shift and fluorescence decrease of bound GTP_{TR} upon formation of the photoadduct (Table 1).

YtvA-R63K is thus suitable for spectroscopic and functional studies, given its accelerated photocycle and the fact that the dark recovery of three different regions of the protein can be easily followed by monitoring the fluorescence of FMN (LOV core), GTP_{TR} (STAS domain) and of W103 (H β strand of the LOV core). Observation of changes of W103 is very supportive, since it was previously demonstrated to be an independent marker for interdomain interactions.⁴⁵ The resulting recovery lifetimes are $\tau_{\text{rec,F}} = 480$ s, $\tau_{\text{rec,TR}} = 511$ s and $\tau_{\text{rec,W}} = 365$ s, respectively (20 °C), clearly demonstrating the tight coupling of the three protein regions (Fig. 2).

For monitoring the kinetics traces, excitation (λ_{ex}) and emission (λ_{em}) wavelengths were selected as follows: for FMN $\lambda_{\text{ex}} = 305$ nm and $\lambda_{\text{em}} = 500$ nm, for GTP_{TR} $\lambda_{\text{ex}} = 590$ nm and $\lambda_{\text{em}} = 620$ nm, for W103 $\lambda_{\text{ex}} = 280$ nm and $\lambda_{\text{em}} = 340$ nm. FMN was excited in a “valley” of the absorption spectrum, in the UVB region and not with blue-light, in order to minimize secondary photochemistry leading to formation of the photoproduct during recording of the traces. We have in fact verified that this methodology gives identical results as tracing the recovery of absorption, whereas flavin excitation at 450 nm triggers photolysis during emission spectroscopy, leading to artifacts in the kinetics traces.³⁹

Amino acids in the LOV-core β -scaffold

The light-induced absorption and fluorescence changes of bound GTP_{TR} reflecting LOV-STAS signal transmission, are not observed for YtvA-E105L as recently reported³⁵ and the same occurs with YtvA-D109L. The somehow higher affinity of YtvA-D109L for GTP_{TR} (see Table 1) is most probably due to the presence of some apoprotein that could not be avoided with this mutation. These data stress the functional importance of these two negatively charged amino acids, uniquely conserved within the YtvA-like proteins and localized on strand H β , on the external side with respect to the FMN cavity (Fig. 1a).

Another strategically positioned amino acid of this region is L106. Its side chain points towards the chromophore cavity and comes into close contact with the isoalloxazine ring.³² The L106F mutation diminishes but not completely abolishes the light-induced changes of GTP_{TR} (see Table 1). The affinity for GTP appears to be slightly lower than for YtvA-WT, but remains definitely within the same range; this latter effect might result from a perturbation of the overall protein tertiary structure due to the introduced change and is observed also for other mutations (Table 1). We note nevertheless that these three mutations do not affect either the oligomeric state of the protein, that remains mainly monomeric as shown by gel filtration experiments, or the secondary structure composition, as indicated by circular dichroism data.^{39,43}

Amino acids within the linker region

Other mutations that suppress partially or completely the LOV-STAS signal transmission include K130A and K134A, both located within the linker region (Table 1, Fig. 3). On the other hand, K128, Q129 or S139 do not affect appreciably either affinity for GTP or signal-transmission, but behave similar to YtvA-WT.

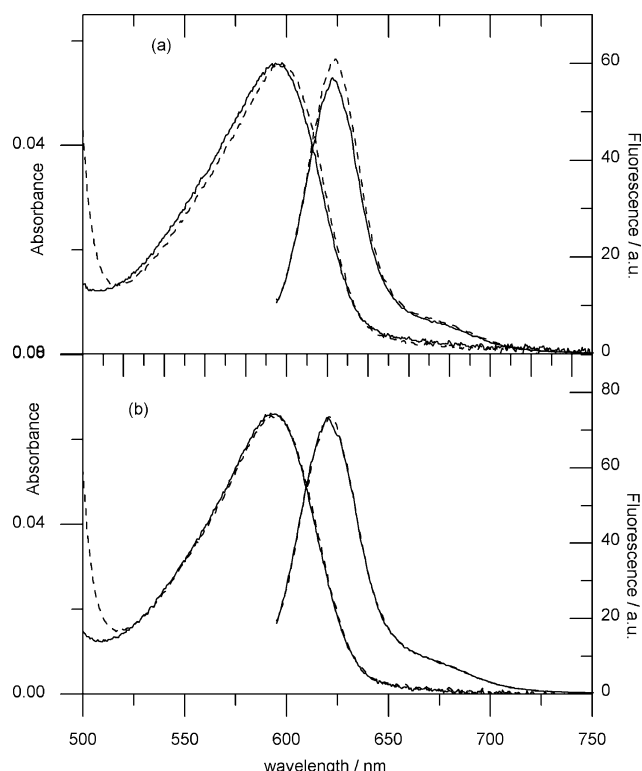


Fig. 3 Absorption and fluorescence spectra of GTP_{TR} partially bound to (a) YtvA-K128A and (b) YtvA-K130A, in the dark (dashed lines) and light (solid lines) state. The value of α is *ca.* 0.5 for both proteins. The two proteins are examples for signal-transmission “innocent” (K128A) and “guilty” (K130A) mutations.

The uncoupling between LOV domain and GTP-binding site on the STAS domain is best appreciated by observing the kinetics traces for the dark-recovery fluorescence of FMN and of GTP_{TR} . For a signal-transmission “guilty” mutation (*e.g.* K130) the latter fluorescence does not change, whereas the recovery of FMN fluorescence follows the usual pattern (Fig. 4). For a signal-transmission “innocent” change (*e.g.* K128) the two traces follow instead a similar time-course.

In the case of mutation Y132A, light induced absorption changes are similar to YtvA-WT (showing a shift of *ca.* 2.5 nm with $\alpha = 0.5$), but the light-induced decrease of GTP_{TR} fluorescence is larger (*ca.* 10% with $\alpha = 0.5$, compared to 5% in YtvA-WT) (Table 1, Fig. 5), suggesting a larger conformational change in the nucleotide-binding cavity.

STAS-domain residues

Within the STAS domain all four residues of the supposed GTP-binding/switch DLSG motif (positions 193-196) have been changed and show some effect on the binding of GTP or light-induced changes of bound GTP_{TR} . L194A and G196A impair this signal transmission, whereas S195A strongly diminishes the affinity for GTP_{TR} . The situation is less clear for D193A due to the presence of a large percentage of apoprotein that could not be avoided for this sample, even by changing induction times and expression temperature during three different preparations. It is possible that this mutation, as well as others for which we could not

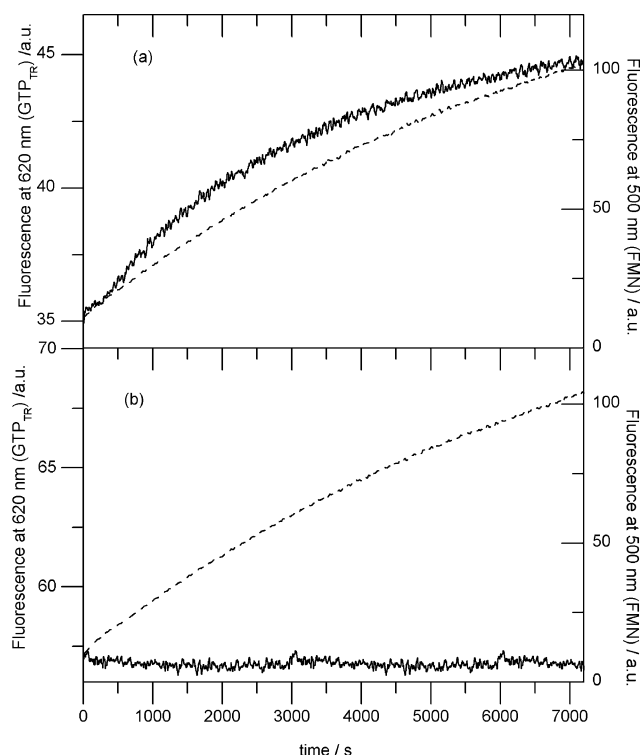


Fig. 4 Time course for the dark-recovery of fluorescence for (a) YtvA-K128A and (b) YtvA-K130A at 20 °C. The GTP_{TR} fluorescence (full lines) has been recorded at 620 nm after 590 nm excitation. FMN (dashed lines) was excited at 305 nm and fluorescence was recorded at 500 nm. Conditions as in Fig. 3.

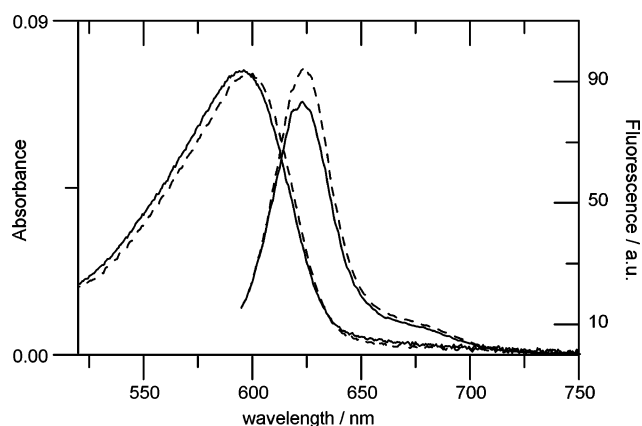


Fig. 5 Absorption and fluorescence spectra of GTP_{TR} partially bound to YtvA-Y132A, in the dark (dashed lines) and light (solid lines) state. The value of α is *ca.* 0.5. The light-induced spectral changes in this protein are larger than in YtvA-WT.

obtain a fully chromophore-loaded protein, somehow interferes with the expression system, given that the chromophore is picked up from the flavins pool of *E. coli* cells. The fraction of GTP_{TR} bound to apoprotein does not undergo light-induced changes, but obviously interferes with fluorescence of GTP_{TR} bound to the holoprotein. This mutation thus seems to impair GTP_{TR} binding and also the light-switched changes. Among the other STAS

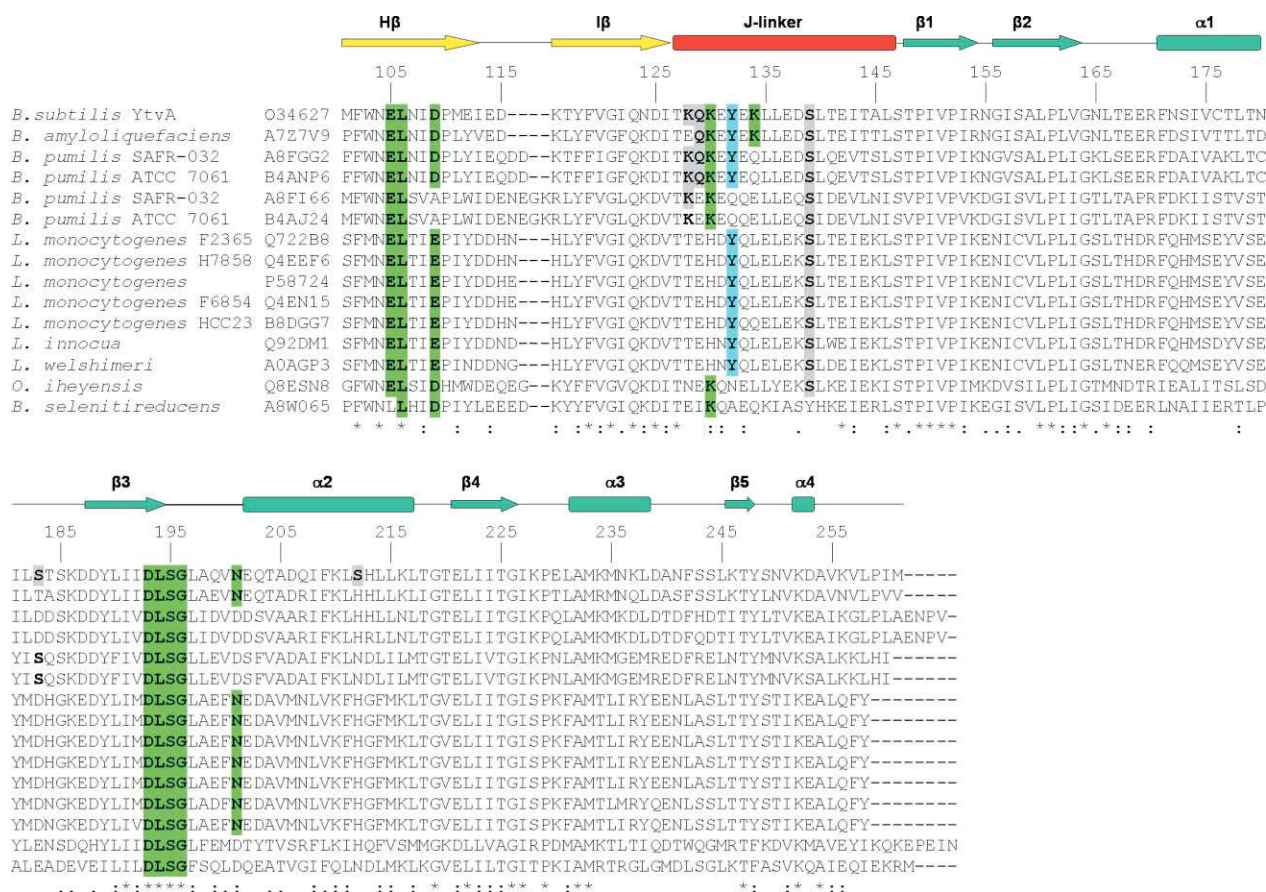


Fig. 6 Partial alignment of LOV proteins forming the YtvA-family in Firmicutes, highlighting the mutations studied in this work (with the exception of R63K, that solely accelerates the photocycle) and their conservation throughout the family (Glu in place of Asp109 has been held as conservative substitution). Accession numbers for the proteins are taken from the UniProt Knowledgebase (Swiss-Prot + TrEMBL) databank.⁵⁰ Abbreviations: *B.* = *Bacillus*, *O.* = *Oceanobacillus*, *L.* = *Listeria*. Residues whose mutation impairs light triggered conformational changes transmission from LOV domain to the GTP-binding cavity on STAS domain and/or GTP affinity, are highlighted in green. Y132, whose mutation in alanine increases the light triggered conformational changes is highlighted in light-blue. Residues whose mutations have negligible effects are in grey. Numbering is from YtvA. Published secondary structures for the LOV domain are shown on top (arrows = strand, cylinders = helices, lines = turns/coils),³² with the nomenclature used in this work. Our modelled secondary structure elements for the STAS domain are shown,³⁶ with nomenclature as in Aravind and Koonin.³⁷

domain mutations tested, only N201A has an impairing effect on signal transmission (Table 1), whereas the serine-to-alanine changes at positions 183 and 212 behaved similarly to the WT protein.

Discussion

The Hβ strand of the LOV-core β-scaffold

The extended β-scaffold of the LOV-core has previously been discussed as a potential surface that conveys the signal to effector domains (see introduction). Here we have focused on residues within the Hβ strand because this element of secondary structure bears amino acids that characterize a certain class of LOV proteins (see Fig. 6).

An acidic amino acid corresponding to E105 is present solely in bacteria and a second acidic residue (aspartate or glutamate) at position 109 is exclusive for YtvA-like proteins in the Firmicutes.¹⁷ Both E105 and D109 are oriented towards the exterior of the FMN binding cavity and at the interface of the YtvA-LOV

dimer.^{31,32} Here we have shown that both amino acids are key elements for LOV-to-STAS signal transmission, as detected by the light-induced conformational changes of the GTP-binding cavity. A careful inspection of the GTP_{TR} absorption spectra when bound to YtvA-E105L suggests that this mutated protein is locked in a light-activated conformation,³⁵ whereas the presence of apoprotein in the YtvA-D109L preparation does not allow a similarly strict conclusion. If the NTP-binding properties are linked to a physiological response, the E105L mutation should thus result in constitutive activity of YtvA, *e.g.* activation of σ^B, and in any case there should be no light influence for both E105L and D109L. We have now evidence, from comparative *in vivo* data, that this is indeed the case: in particular, the mutated YtvA-E105L protein constitutively up-regulates σ^B, whereas the contrary holds for YtvA-D109L.⁶

It is striking that E105 seems to have a similar role as the corresponding Leu493 in plant phot that makes contact to Ile532 on the Jα-linker.²⁰ The disruption of this contact by the I532E mutation disrupts the LOV2-Jα interaction and renders the kinase domain constitutively active.²⁹ In case of YtvA, nevertheless, we

cannot extrapolate with certainty that E105 makes contact with the linker, given that in the dimeric YtvA-LOV this is definitely not the case (*vide infra*).³²

Our results confirm a previous conformational analysis that proposed the β -scaffold as a competitive interface for LOV-LOV dimerization and intraprotein interactions. They further identify the two conserved negatively charged amino acids as essential for the LOV-to-STAS signal transfer.

A leucine or another small apolar amino acid in the position corresponding to L106, is typical for phot-LOV1 and is changed for phenylalanine in LOV2, where it has been suggested to be a key element during phototropin activation.⁴⁶ In known LOV domain structures, FMN is sandwiched between this residue and the reactive cysteine.^{18–20,32} In neochrome1-LOV2 (neo1-LOV2),¹⁸ a substitution of the corresponding Phe1010 by a leucine renders LOV2 similar to LOV1 in terms of light-induced structural changes, *i.e.* they become smaller and temperature independent.⁴⁶ The reported larger light-induced structural changes of LOV2 with respect to LOV1 are in part ascribed to this residue (F1010) due to its larger capacity to activate the kinase domain *via* perturbations that propagate from FMN to F1010 *via* π - π stacking interaction, and further to the α -helix facilitating its unfolding.⁴⁶ On the contrary, the opposite substitution, L106F in YtvA-LOV impairs signal transmission to the STAS domain, instead of facilitating it (this work). We cannot compare this result with similar data for phot-LOV1 because, to our knowledge, a similar mutation has not been reported so far. It might be that in YtvA-LOV a phenylalanine in this position cannot assume the same conformation as in LOV2 (being stacked with the isoalloxazine ring of FMN), due to other and still undetermined factors. However, our data stress the importance of the amino acid that faces the flavin ring, opposite to the reactive cysteine, in conveying the signal to the partner domain.

We are aware that the oligomeric state of YtvA is subject of controversy. The crystal structure of the extended YtvA-LOV+J-linker domain is dimeric,³² and it was suggested that the J-linker forms a coiled-coil dimer that works as light-activated rotary switch during regulation of a fused kinase domain.⁴⁷ Nevertheless we showed that the full-length protein is mostly monomeric, at least at μ M concentrations (see also Materials and methods) and that the oligomeric state and secondary structure pattern of the protein is not altered by the present mutations of the H β -strand.³⁹ This, together with the *in vivo* data, allows us to conclude that the said mutations are truly affecting light-to-signal-transmission and not the overall conformation of the protein.

The J-linker region

The linker region of YtvA is rich in polar and charged amino acids, of which at least K130 and K134 are involved in signal transmission. Contrary to the LOV2 extended construct^{28,30} we do not have any indication for a helix unfolding upon light activation of YtvA.³¹ In the dimeric crystal structure of YtvA-LOV (lacking the STAS domain and the N-cap), the helical linker is not organized underneath the β -scaffold, but points away from the LOV domain, as a clear evidence that it cannot compete with the strong LOV-LOV interaction, largely mediated by this surface (Fig. 3).³² This might not be the case for the full-length protein, for which dimerization is prevented (at least in diluted solution),

but solely if the STAS domain is present, *i.e.* only in the full-length protein.³¹ We have in fact evidences that both the N-cap³¹ and the J-linker^{32,39} are not able to prevent dimerization of YtvA-LOV, although we cannot exclude a different way of dimerization when the flanking regions are present. Unfortunately it is currently not possible to draw with safety the configuration of the linker within the full-length protein, also due to low sequence homology with phot1-LOV2 J-linker. If the protein is functioning as a monomer, it is highly improbable that the J-linker adopts a conformation as in the crystallized YtvA-LOV dimer, because it would be impossible for E105 and D109 to perform their role of “transmitter” to the STAS domain. With the present scenario, we can only state that also in YtvA, as in LOV2, the linker region has a role in signal transmission, involving two positively charged amino acids, K130 and K134. Contrary to E105 and D109, conserved as negatively charged amino acids within the majority of YtvA-like proteins in the Firmicutes,¹⁷ K130 is only conserved within the *Bacillus* species and is substituted for a histidine among *Listeria*. Position 134, instead, is very variable, being substituted sometimes even with a leucine.

The switch region of the STAS domain

It was previously outlined that within STAS domains the loop between strand 3 and helix 2 (Fig. 1) is structurally conserved and does not tolerate inserts.³⁷ In those STAS proteins that are regulated by phosphorylation (*e.g.* SPOIIAA and RsBr), this loop bears, adjacent to helix 2, the serine or threonine that become phosphorylated,³⁷ corresponding to E202 in YtvA, *i.e.* directly adjacent to N201. Furthermore, the NTPase activity of SPOIIAA is abolished by phosphorylation or by mutation of Ser58.⁴⁸ YtvA-STAS lacks a phosphate-binding Ser or Thr residue in the same position as SPOIIAA (Ser58) or Thr205 in RsBr,^{1,37} and the corresponding E202A mutation in YtvA does have an effect *in vivo*.⁶ Still, the conserved loop seems to bear a functional role. In fact the DLSG (193–196) sequence is part of this loop, being localized at the C-terminal end of strand 3 and the beginning of the loop. A DXXG motif is usually referred to as Walker B or Switch II sequence in small GTP-binding proteins,⁴⁰ and we previously noticed a partial topological and sequence similarity between this protein family and YtvA-STAS.³⁶ Accordingly, from our data it is clear that the DLSG sequence not only is important for GTP-binding to YtvA-STAS (D193A and S195A), but also has a conformational switch activity (D193A, G196A). Quite importantly, and in agreement with our data *in vitro*, mutation of D193 and S195 abolishes light activation of σ^B *in vivo*.⁶

Notwithstanding the similarity, it is quite improbable that YtvA-STAS binds NTPs with the same configuration as GTP-binding proteins, because the required P-loop structure (Walker A)⁴⁰ is missing. An alternative way of NTP-binding to STAS domains has been suggested, resembling lipid association by Sec14 domains, which have a very similar folding as SPOIIAA but show a poor sequence similarity.³⁷ The conserved loop would thus be involved in binding of the γ -phosphate group, resembling the role of DXXG in small GTP-binding proteins, whereas the β -scaffold and helix 1 and 2 might accommodate the rest of the nucleotide. Structures of Sec14 domains are available in the PDB databank (*e.g.* 3B74),⁴⁹ but their similarity with STAS domains, as for ligand binding, remains to be demonstrated.

This hypothesis is nevertheless supported by the observation that in YtvA the N201A mutation impairs the light-switched conformational changes within the GTP-binding cavity, given that N201 is localized within the conserved loop at the N-terminal end of helix 2. The DXXG sequence is in the vicinity of the phospholipid end I in Sec14, in the same position as YtvA-STAS and GTP-binding proteins, although it is not directly involved in binding.⁴⁹

Conclusion

In this work we have definitely established the role of two charged amino acids (E105 and D109), localized on the β -scaffold of the LOV core and typical of the bacterial YtvA-like family, in delivering the light-triggered signal to the GTP-binding cavity on the STAS domain. As discussed above, this nicely fit with *in vivo* novel results.⁶ Furthermore, it is now clear that also in YtvA the J-linker participates in intraprotein signal-transmission, although not *via* a light-triggered unfolding as in phot1. Structural features for the full length protein are still needed in order to fully elucidate the pathway of signal-transmission.

Finally we have shown that an up-to-now putative GTP-binding/switch motif is indeed strongly involved both in binding and in switching the conformational changes of the nucleotide cavity on the STAS module upon light activation of the LOV domain. Only a few data are available to support a general NTP-binding role for the wide-spread STAS domains, but this functionality is likely to be relevant, as evidenced by the above discussed link with *in vivo* data.

Abbreviations used:

ATP	adenosine triphosphate
FMN	flavin mononucleotide
GTP	guanosine triphosphate
GTP _{TR}	Guanosine 5'-triphosphate, BODIPY® TR 2'-(or-3')-O-(N-(2-aminoethyl) urethane)
LOV	Light, Oxygen and Voltage
NTP	nucleotide triphosphate
phot	phototropin
STAS	domain found in Sulfate Transporters and Anti-Sigma factor antagonist

Acknowledgements

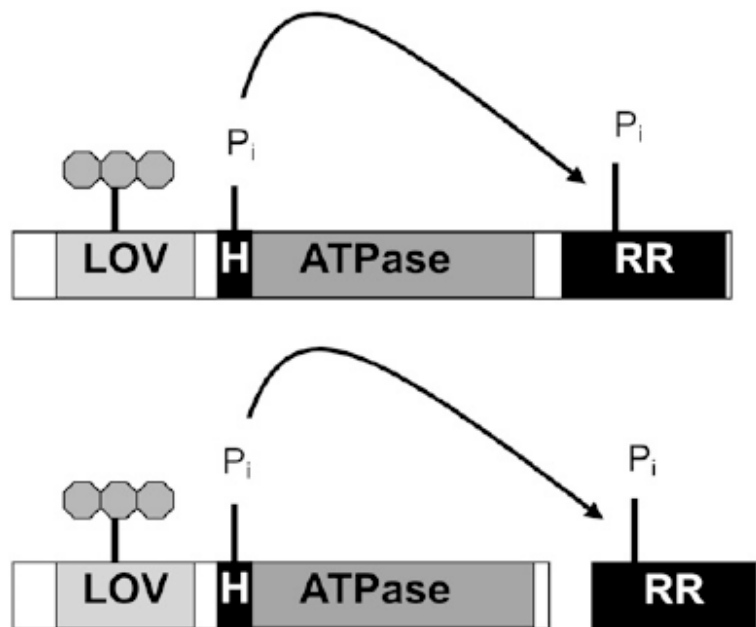
This work has been supported by the Deutsche Forschungsgemeinschaft (FOR526, Z.C., Y.T., A.L.), and by a study-exchange grant of the Socrates-Erasmus program of the European Community (E.L.). Sven Jansen contributed in part of the mutagenesis work during his Diploma Thesis.

References

- 1 S. Akbar, T. A. Gaidenko, K. Min, M. O'Reilly, K. M. Devine and C. W. Price, New family of regulators in the environmental signaling pathway which activates the general stress transcription factor of *Bacillus subtilis*, *J. Bacteriol.*, 2001, **183**, 1329–1338.
- 2 A. Losi and W. Gaertner, Bacterial bilin- and flavin-binding photoreceptors, *Photochem. Photobiol. Sci.*, 2008, **7**, 1168–1178.
- 3 T. A. Gaidenko, T. J. Kim, A. L. Weigel, M. S. Brody and C. W. Price, The blue-light receptor YtvA acts in the environmental stress signaling pathway of *Bacillus subtilis*, *J. Bacteriol.*, 2006, **188**, 6387–6395.
- 4 M. Avila-Perez, K. J. Hellingwerf and R. Kort, Blue light activates the sigmaB-dependent stress response of *Bacillus subtilis* via YtvA, *J. Bacteriol.*, 2006, **188**, 6411–6414.
- 5 N. Suzuki, N. Takaya, T. Hoshino and A. Nakamura, Enhancement of a σ^B -dependent stress response in *Bacillus subtilis* by light via YtvA photoreceptor, *J. Gen. Appl. Microbiol.*, 2007, **53**, 81–88.
- 6 M. Avila-Perez, J. Vreede, Y. Tang, O. Bende, A. Losi and W. Gaertner, *In vivo* mutational analysis of YTV A from *Bacillus subtilis*: Mechanism of light-activation of the general stress response, *J. Biol. Chem.*, 2009, **284**, 24958–24964.
- 7 W. R. Briggs, The LOV domain: a chromophore module servicing multiple photoreceptors, *J. Biomed. Sci.*, 2007, **14**, 499–504.
- 8 A. Losi, E. Polverini, B. Quest and W. Gärtner, First evidence for phototropin-related blue-light receptors in prokaryotes, *Biophys. J.*, 2002, **82**, 2627–2634.
- 9 A. Losi and Flavin-based, Blue-light Photosensors: a Photobiophysics Update, *Photochem. Photobiol.*, 2007, **83**, 1283–1300.
- 10 W. R. Briggs, T. S. Tseng, H. Y. Cho, T. E. Swartz, S. Sullivan, R. A. Bogomolni, E. Kaiserli and J. M. Christie, Phototropins and their LOV domains: Versatile plant blue-light receptors, *J. Integr. Plant Biol.*, 2007, **49**, 4–10.
- 11 J. M. Christie, Phototropin Blue-Light Receptors, *Annu. Rev. Plant Biol.*, 2007, **58**, 21–45.
- 12 E. Huala, P. W. Oeller, E. Liscum, I. S. Han, E. Larsen and W. R. Briggs, *Arabidopsis* NPH1: A Protein Kinase with a Putative Redox-Sensing Domain, *Science*, 1997, **278**, 2120–2123.
- 13 M. Salomon, E. Knieb, T. von Zeppelin and W. Rüdiger, Mapping of Low- and High-Fluence Autophosphorylation Sites in Phototropin 1, *Biochemistry*, 2003, **42**, 4217–4225.
- 14 S. Tokutomi, D. Matsuoka and K. Zikihara, Molecular structure and regulation of phototropin kinase by blue light, *Biochim. Biophys. Acta, Proteins Proteomics*, 2008, **1784**, 133–142.
- 15 S. Inoue, T. Kinoshita, M. Matsumoto, K. I. Nakayama, M. Doi and K. Shimazaki, Blue light-induced autophosphorylation of phototropin is a primary step for signaling, *Proc. Natl. Acad. Sci. U. S. A.*, 2008, **105**, 5626–5631.
- 16 S. Crosson, S. Rajagopal and K. Moffat, The LOV domain family: photoresponsive signaling modules coupled to diverse output domains, *Biochemistry*, 2003, **42**, 2–10.
- 17 A. Losi, The bacterial counterparts of plants phototropins, *Photochem. Photobiol. Sci.*, 2004, **3**, 566–574.
- 18 S. Crosson and K. Moffat, Structure of a flavin-binding plant photoreceptor domain: insights into light-mediated signal transduction, *Proc. Natl. Acad. Sci. U. S. A.*, 2001, **98**, 2995–3000.
- 19 R. Fedorov, I. Schlichting, E. Hartmann, T. Domratcheva, M. Fuhrmann and P. Hegemann, Crystal structures and molecular mechanism of a light-induced signaling switch: the Phot-LOV1 domain from *Chlamydomonas reinhardtii*, *Biophys. J.*, 2003, **84**, 2474–2501.
- 20 A. S. Halavaty and K. Moffat, N- and C-Terminal Flanking Regions Modulate Light-Induced Signal Transduction in the LOV2 Domain of the Blue Light Sensor Phototropin 1 from *Avena sativa*, *Biochemistry*, 2007, **46**, 14001–14009.
- 21 B. D. Zoltowski, C. Schwerdtfeger, J. Widom, J. J. Loros, A. M. Bilwes, J. C. Dunlap and B. R. Crane, Conformational switching in the fungal light sensor Vivid, *Science*, 2007, **316**, 1054–1057.
- 22 D. Nozaki, T. Iwata, T. Ishikawa, T. Todo, S. Tokutomi and H. Kandori, Role of Gln1029 in the photoactivation processes of the LOV2 domain in *Adiantum* phytochrome3, *Biochemistry*, 2004, **43**, 8373–8379.
- 23 A. I. Nash, W. H. Ko, S. M. Harper and K. H. Gardner, A Conserved Glutamine Plays a Central Role in LOV Domain Signal Transmission and Its Duration GČá, *Biochemistry*, 2008, **47**, 13842–13849.
- 24 A. Pfeifer, T. Majerus, K. Zikihara, D. Matsuoka, S. Tokutomi, J. Heberle and T. Kottke, Time-Resolved Fourier Transform Infrared Study on Photoadduct Formation and Secondary Structural Changes within the Phototropin LOV Domain, *Biophys. J.*, 2009, **96**, 1462–1470.
- 25 M. T. A. Alexandre, R. van Grondelle, K. J. Hellingwerf and J. T. M. Kennis, Conformational Heterogeneity and Propagation of Structural Changes in the LOV2/J alpha Domain from *Avena sativa* Phototropin 1 as Recorded by Temperature-Dependent FTIR Spectroscopy, *Biophys. J.*, 2009, **97**, 238–247.

- 26 T. Koyama, T. Iwata, A. Yamamoto, Y. Sato, D. Matsuoka, S. Tokutomi and H. Kandori, Different Role of the J alpha Helix in the Light-Induced Activation of the LOV2 Domains in Various Phototropins, *Biochemistry*, 2009, **48**, 7621–7628.
- 27 M. A. Jones, K. A. Feeney, S. M. Kelly and J. M. Christie, Mutational analysis of phototropin 1 provides insights into the mechanism underlying LOV2 signal transmission, *J. Biol. Chem.*, 2006, **282**, 6405–6414.
- 28 S. M. Harper, L. C. Neil and K. H. Gardner, Structural basis of a phototropin light switch, *Science*, 2003, **301**, 1541–1544.
- 29 S. M. Harper, J. M. Christie and K. H. Gardner, Disruption of the LOV-Jalpha helix interaction activates phototropin kinase activity, *Biochemistry*, 2004, **43**, 16184–16192.
- 30 X. Yao, M. K. Rosen and K. H. Gardner, Estimation of the available free energy in a LOV2-Ja photoswitch, *Nat. Chem. Biol.*, 2008, **4**, 491–497.
- 31 V. Buttani, A. Losi, T. Eggert, U. Krauss, K.-E. Jaeger, Z. Cao and W. Gärtner, Conformational analysis of the blue-light sensing protein YtvA reveals a competitive interface for LOV-LOV dimerization and interdomain interactions, *Photochem. Photobiol. Sci.*, 2007, **6**, 41–49.
- 32 A. Möglich and K. Moffat, Structural Basis for Light-dependent Signaling in the Dimeric LOV Domain of the Photosensor YtvA, *J. Mol. Biol.*, 2007, **373**, 112–126.
- 33 M. Nakasako, K. Zikihara, D. Matsuoka, H. Katsura and S. Tokutomi, Structural basis of the LOV1 dimerization of Arabidopsis phototropins 1 and 2, *J. Mol. Biol.*, 2008, **381**, 718–733.
- 34 B. D. Zoltowski and B. R. Crane, Light activation of the LOV protein Vivid generates a rapidly exchanging dimer, *Biochemistry*, 2008, **47**, 7012–7019.
- 35 V. Buttani, W. Gärtner and A. Losi, NTP-binding properties of the blue-light receptor YtvA and effects of the E105L mutation, *Eur. Biophys. J.*, 2007, **36**, 831–839.
- 36 V. Buttani, A. Losi, E. Polverini and W. Gärtner, Blue news: NTP binding properties of the blue-light sensitive YtvA protein from *Bacillus subtilis*, *FEBS Lett.*, 2006, **580**, 3818–3822.
- 37 L. Aravind and E. V. Koonin, The STAS domain a link between anion transporters and antisigma-factor antagonists, *Curr. Biol.*, 2000, **10**, R53–R55.
- 38 D. P. McEwen, K. R. Gee, H. C. Kang and R. R. Neubig, Fluorescent BODIPY-GTP Analogs: Real-Time Measurement of Nucleotide Binding to G Proteins, *Anal. Biochem.*, 2001, **291**, 109–117.
- 39 V. Buttani, Struttura e funzione di recettori batterici di luce blu contenenti i domini proteici LOV (Light, Oxygen and Voltage), Ph.D. Thesis, University of Parma, 2009.
- 40 D. D. Leipe, Y. I. Wolf, E. V. Koonin and L. Aravind, Classification and evolution of P-loop GTPases and related ATPases, *J. Mol. Biol.*, 2002, **317**, 41–72.
- 41 A. Losi, B. Quest and W. Gärtner, Listening to the blue: the time-resolved thermodynamics of the bacterial blue-light receptor YtvA and its isolated LOV domain, *Photochem. Photobiol. Sci.*, 2003, **2**, 759–766.
- 42 T. Bednarz, A. Losi, W. Gärtner, P. Hegemann and J. Heberle, Functional variations among LOV domains as revealed by FT-IR difference spectroscopy, *Photochem. Photobiol. Sci.*, 2004, **3**, 575–579.
- 43 A. Losi, E. Ghiraldelli, S. Jansen and W. Gärtner, Mutational effects on protein structural changes and interdomain interactions in the blue-light sensing LOV protein YtvA, *Photochem. Photobiol.*, 2005, **81**, 1145–1152.
- 44 A. Losi, T. Kottke and P. Hegemann, Recording of Blue Light-Induced Energy and Volume Changes within the Wild-Type and Mutated Phot-LOV1 Domain from *Chlamydomonas reinhardtii*, *Biophys. J.*, 2004, **86**, 1051–1060.
- 45 A. Losi, E. Ternelli and W. Gärtner, Tryptophan Fluorescence in the *Bacillus subtilis* Phototropin-related Protein YtvA as a Marker of Interdomain Interaction, *Photochem. Photobiol.*, 2004, **80**, 150–153.
- 46 A. Yamamoto, T. Iwata, S. Tokutomi and H. Kandori, Role of Phe1010 in Light-Induced Structural Changes of the neo1-LOV2 Domain of *Adiantum*, *Biochemistry*, 2008, **47**, 922–928.
- 47 A. Möglich, R. A. Ayers and K. Moffat, Design and Signaling Mechanism of Light-Regulated Histidine Kinases, *J. Mol. Biol.*, 2009, **385**, 1433–1444.
- 48 S. M. Najafi, D. A. Harris and M. D. Yudkin, The SpoIIAA protein of *Bacillus subtilis* has GTP-binding properties, *J. Bacteriol.*, 1996, **178**, 6632–6634.
- 49 G. Schaaf, E. A. Ortlund, K. R. Tyeryar, C. J. Mousley, K. E. Ile, T. A. Garrett, J. Ren, M. J. Woolls, C. R. H. Raetz, M. R. Redinbo and V. A. Bankaitis, Functional anatomy of phospholipid binding and regulation of phosphoinositide homeostasis by proteins of the sec14 superfamily, *Mol. Cell*, 2008, **29**, 191–206.
- 50 C. O'Donovan, M. J. Martin, A. Gattiker, E. Gasteiger, A. Bairoch and R. Apweiler, High-quality protein knowledge resource: SWISS-PROT and TrEMBL, *Brief. Bioinform.*, 2002, **3**, 275–284.

III. A blue light inducible two component signal transduction system in bacterial LOV proteins



A Blue Light Inducible Two-Component Signal Transduction System in the Plant Pathogen *Pseudomonas syringae* pv. *tomato*

Z. Cao,* V. Buttani,[†] A. Losi,[†] and W. Gärtner*

*Max-Planck-Institut für Bioanorganische Chemie, D-45470 Mülheim, Germany; and [†]Department of Physics, University of Parma, Italy

ABSTRACT The open reading frame *PSPTO2896* from the plant pathogen *Pseudomonas syringae* pv. *tomato* encodes a protein of 534 amino acids showing all salient features of a blue light-driven two-component system. The N-terminal LOV (light, oxygen, voltage) domain, potentially binding a flavin chromophore, is followed by a histidine kinase (HK) motif and a response regulator (RR). The full-length protein (PST-LOV) and, separately, the RR and the LOV+HK part (PST-LOV_{ΔRR}) were heterologously expressed and functionally characterized. The two LOV proteins showed typical LOV-like spectra and photochemical reactions, with the blue light-driven, reversible formation of a covalent flavin-cysteine bond. The fluorescence changes in the lit state of full-length PST-LOV, but not in PST-LOV_{ΔRR}, indicating a direct interaction between the LOV core and the RR module. Experiments performed with radioactive ATP uncover the light-driven kinase activity. For both PST-LOV and PST-LOV_{ΔRR}, much more radioactivity is incorporated when the protein is in the lit state. Furthermore, addition of the RR domain to the fully phosphorylated PST-LOV_{ΔRR} leads to a very fast transfer of radioactivity, indicating a highly efficient HK activity and a tight interaction between PST-LOV_{ΔRR} and RR, possibly facilitated by the LOV core itself.

INTRODUCTION

Light is an energy source and an ever present stimulus on earth. The short wavelength region, i.e., the ultraviolet (UV) and blue light range, however, can be harmful to organisms because of the deleterious effects on DNA (UV range) (1) or the capability to excite, with high yield, ubiquitously present photosensitizing compounds, e.g., porphyrins and flavins (blue light effects) (2). Photoexcitation converts such compounds with high efficiency into the triplet state, which in the presence of oxygen generates the highly oxidative oxygen singlet state and other reactive oxygen containing species (3). Blue light detecting photosensors are thus of the utmost importance for any organism, allowing the development of repair systems (4), the formation of protective (shielding) substances, or—for motile organisms—the escape from regions with high UV/blue light intensity (5). At least three systems have been identified recently that fulfill this function. All are based on flavin derivatives that serve as chromophores in these photoreceptors. They were named cryptochromes; light, oxygen, voltage (LOV) proteins; and blue-light-sensing using flavins (BLUF) proteins (6). The most widely spread of these flavin-based photoreceptors are the LOV domain-containing proteins (LOV) (7). They are assumed to be present in all plants, and prokaryotic genome analysis revealed the presence of LOV proteins in ~15% of all sequenced genomes (6). In prokaryotes the light-sensing LOV module is coupled to diverse effectors domains, such as kinases (similar to the plant phototropins), phosphodiesterases, response regulators (RRs), DNA-binding transcription factors, and regulators of stress σ factors (7,8). The majority

of LOV domains is found together with histidine kinase (HK) motifs or with transcription factors in the same open reading frame (ORF) or arranged in a single operon, allowing an efficient physiological response of the cell to a light pulse. This relatively simple, stereotypical structure of photoreceptors, together with their instantaneous (=light triggered) activation or deactivation makes these sensory proteins excellent candidates to study signal transduction mechanisms.

A considerably large percentage of the bacterial LOV proteins are members of the histidine protein kinase (HPK) kinase superfamily (6,8). In bacteria, signal transducing HPKs, together with phosphoaspartyl RRs, are the key elements of two-component signal transduction systems (9). The HPKs generally contain an N-terminal sensing domain (e.g., LOV) and a C-terminal kinase core, but additional domains may be present. The kinase core of HPK features the phosphoaccepting histidine box (H-box) within the homodimerization domain and, downstream to it, the highly conserved homology boxes of the nucleotide-binding, catalytic domain (N-, D-, F-, and G-boxes) (10). In response to a signal, HPKs autophosphorylate the H-box histidine residue from which the phosphoryl group is transferred to a conserved aspartic acid residue in the receiver domain of an RR (9). HPKs can be further divided into subfamilies according to their sequence similarity (10). The hybrid HPK-RR LOV proteins from Pseudomonadales and Xanthomonadales (γ -proteobacteria) are highly homologous and form a distinct family (6,8). The kinase domain is characteristic of the HPK4 class: besides a typical H-box, these proteins exhibit the PF-TTK signature in the so-called F-box. Furthermore, their LOV domains are among those that are most homologous to (plant) phot-LOVs. Given these features, namely, the association of an “ideal” phot-like LOV domain with prototyp-

Submitted March 21, 2007, and accepted for publication August 23, 2007.
Address reprint requests to W. Gärtner, E-mail: gaertner@mpi-muelheim.mpg.de.

Editor: Janos K. Lanyi.

© 2008 by the Biophysical Society
0006-3495/08/02/897/09 \$2.00

ical kinase and RR motifs, they are good candidates to test the molecular properties of this novel, putatively a blue light-driven two-component signaling system in bacteria. Additionally, although there is no report on light-elicited responses in these organisms, a few links have been established among plant defense systems, plant photosensors, and bacterial pathogens belonging to *Pseudomonales* (11–13), prompting an investigation of bacterial photosensors in view of their potential role during the infectivity process.

We present studies on the molecular and spectroscopic properties of the LOV-HPK-RR hybrid protein (gene name *PSPTO2896*) from *P. syringae* pv. *tomato* DC3000 (*Pst* DC3000), an important plant pathogen whose genome was recently sequenced (14). The recombinant protein from ORF *PSPTO2896* will be named PST-LOV. To this purpose three protein constructs were built: i), the full protein PST-LOV2896 encompassing the LOV, HPK, and RR domains; ii), the truncated PST-LOV2896_{ΔRR} (comprising the LOV and HPK domain); and iii), the separated RR.

Pseudomonas syringae has gained remarkable interest due to its capability to infect a wide variety of plants, exhibiting strain-to-host specificity with ~50 known pathovars (pv.) (15). Three strains, *P. syringae* pv. *syringae* B728a, *P. syringae* pv. *tomato* DC3000, and *P. syringae* pv. *phaseolicola* 1448A have been genome sequenced (14,16,17). An inspection revealed ORFs with strong homology to LOV domains. The ORF *PSPTO2896* from the genome of *P. syringae* pv. *tomato* DC3000 encodes a LOV protein of 534 amino acids (PST-LOV), corresponding to a molecular mass of 58.9 kDa. Sequence alignment reveals a domain architecture with a typical LOV domain (aa 33–136) containing all salient amino acids required for flavin-mononucleotide (FMN) binding, followed by a HK motif and an ATP-binding domain (aa 154–389). The final part of PST-LOV is built as an RR domain (aa 409–534), making this protein a typical two-component system, in this case the HPK activity being fused to the RR domain (Fig. 1). The HK domain is characteristic of the HPK4 class (8,10). Although generally RRs contain one or more output domains downstream of the receiver domain, in some cases, as in the here investigated protein, only the receiver domain is present, often fused with the cognate HPK (hybrid HPK-RR) (10). In this case, no RR-output domain was identified in the vicinity of this encoding gene.

Analysis of this protein and the demonstration of light-induced signal transduction between the two domains would add blue light as a stimulus to the two-component system, which is present in many prokaryotic microorganisms.

MATERIALS AND METHODS

Cloning and biochemistry

Pst DC3000 was grown in Luria-Bertani medium overnight at 37°C. Genomic DNA was isolated with Qiagen DNeasy Tissue kit (Qiagen,

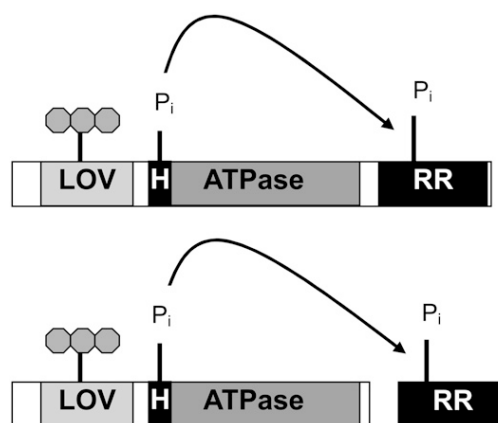


FIGURE 1 Principal architecture of two-component systems. Both arrangements that have been used in this study, i.e., the HK and RR as a fusion protein and as two separate proteins, are shown.

Duesseldorf, Germany). i) Full-length protein: The ORF *PSPTO2896* was amplified by polymerase chain reaction (PCR) from genomic *P. syringae* DNA, using the primers 5'-TCCAGTACATATGTCGGAAAACAAGAC-CCGTGTCG (forward) and 5'-TACAATCTCGAGTCAGGCAATGCCG-TTGGGAC (reverse); PCR conditions: 95°C 2 min, 25 times (95°C 30 s, 58°C 45 s, 72°C 2 min), 72°C 10 min, 4°C hold. Both primers contained restriction sites (shown in bold) for insertion of the PCR product into the plasmid pET28a (Novagen-Merck, Darmstadt, Germany), which is furnished at its 5'-end with an octadecanucleotide encoding for a His₆ tag. Heterologous expression in *Escherichia coli* BL21 DE3 (Stratagene, Amsterdam, The Netherlands) was induced by IPTG (30°C, 1 mM, for 6 h). PST-LOV was isolated from the lysed *E. coli* cells (lysis was by an Ultraturax, IKA, Staufen, Germany, in liquid nitrogen) by passage of the crude lysate (separated from the cell debris by ultracentrifugation, 368,000 × g, 1 h, 4°C) over a Ni²⁺-resin affinity chromatography column (Prochem, Englewood, CO). Such obtained protein was practically pure and was used for further studies without additional purifications. Matrix-assisted laser desorption ionization (MALDI) spectra were measured with an ABI Voyager DE Pro MALDI-time-of-flight (TOF), using Sina and 2,5-dihydroxybenzoic acid as matrix. ii) Truncated proteins: For generation of protein fragments holding the LOV domain and the HPK motif (aa 1–402), and separately the RR (aa 403–534), the two parts of PST-LOV were amplified by PCR from the full-length encoding DNA, using the primers 5'-TCCAGTACATATGTCGGAAAACAAGACCCGTGTCG (LOV and HPK forward), 5'-CTCGAGTCACGATCCCTGAGGTGA (LOV and HPK reverse), and 5'-CCATGGATAGACGCTGGGCAGCA (RR forward), 5'-TACAATCTCGAGGCAATGCCGT (RR reverse); again, the restriction site motifs used from cloning into pET28a are shown in bold. The front part of PST-LOV was furnished with an N-terminal His₆ tag, whereas the RR domain was followed by a C-terminal His₆ tag. Further procedures, i.e., cell growth, IPTG-induction, harvest, and purification were performed as for the full-length protein (see above).

Chromophore composition

The protein-bound chromophore was released by heat denaturation. The sample was kept at 100°C for 10 min, after which time the sample was centrifuged to remove denatured protein (14,000 rpm, 20 min). The supernatant was passed through a Microcon YM3 centrifugal concentrator (13,000 rpm, 1 h, Millipore, Billerica, MA, molecular weight cutoff 3'000) and directly used for high performance liquid chromatography (HPLC) analysis. Each injection was repeated two times to follow statistical errors. HPLC: A HPLC system from Shimadzu (LC10Ai; Shimadzu Deutschland,

Duisburg, Germany) was used, employing a 250/4 C18-RP column (Macherey and Nagel, Düren, Germany). The column was equipped with a precolumn of the same material, and 50 mM ammonium acetate, pH 6 (eluent B) and 70% acetonitrile in B (eluent A) were used as solvents. Authentic FMN, flavin-adenine dinucleotide (FAD), and riboflavin (purchased from Sigma-Aldrich, St. Louis, MO) were used as reference compounds. Besides that, spectra of the eluted samples were recorded during the separation by a diode array detection system. A solvent gradient ($t = 0$, 5:95 A:B, $t = 20$ min, 40:60 A:B, $t = 22$ min, 40:60 A:B, $t = 29$ min, 5:95 A:B) was applied.

Spectroscopy

All measurements were carried out in phosphate buffer 10 mM, pH = 8, NaCl 10 mM. Absorption spectra and kinetic traces were recorded at 20°C with a temperature-controlled Shimadzu UV-2401PC spectrophotometer. Origin 7.5 (OriginLab, Northampton, MA) was employed for data treatment and kinetic fitting. Photoequilibrium conditions, with accumulation of the photoactivated state, were achieved illuminating the sample with a blue light emitting Led-LenserV8 lamp (Zweibrüder Optoelectronics, Solingen, Germany). Steady-state fluorescence spectra have been recorded with a temperature-controlled Perkin-Elmer LS-50 luminescence spectrometer (Perkin-Elmer, Beaconsfield, England). To measure the fluorescence quantum yield (Φ_F) of the bound flavin chromophore, FMN (Fluka, Neu-Ulm, Germany) was used as a standard ($\Phi_F = 0.26$) (18), and measurements were carried out at 10°C with 450 nm excitation to achieve conditions similar to the laser-induced optoacoustic spectroscopy (LIOAS) experiments (vide infra). Other fluorescence measurements (excitation at 295 and 280 nm) were carried out at 20°C.

Laser-induced optoacoustic spectroscopy

For the LIOAS experiments, excitation at 450 nm was achieved by pumping the frequency-tripled pulse of a neodymium-doped yttrium aluminum garnet laser (SL 456G, 6-ns pulse duration, 355 nm, Spectron Laser System, Rugby, Great Britain) into a β -barium borate optical parametric oscillator (OPO-C-355, bandwidth 420–515 nm, Laser Technik Vertriebs, Ertestadt-Friesheim, Germany) as previously described (19). The cuvette holder FLASH 100 (Quantum Northwest, Spokane, WA) was temperature controlled to $\pm 0.02^\circ\text{C}$. The signal was detected by a V103-RM ultrasonic transducer and fed into a 5662 preamplifier (Panametrics, Waltham, MA). The pulse fluence was varied with a neutral density filter and measured with a pyroelectric energy meter (RJP735 head connected to a meter RJ7620 from Laser Precision, Libertyville, IL). The beam was shaped by a 1×12 mm slit, allowing a time resolution of ~ 60 ns by employing deconvolution techniques (20). The experiments were performed in the linear regime of amplitude versus laser fluence, and the total incident energy normally used was $\sim 20 \mu\text{J/pulse}$ (this corresponds to 7.5×10^{-11} einstein for 450 nm excitation, photon energy 265.82 kJ/mol). The sample concentration was $\sim 7.5 \mu\text{M}$, corresponding to 0.9×10^{-9} mol in the excitation volume $V_0 = 0.12$ mL. These conditions correspond to 0.08 photon per protein molecule. New coccine (Fluka) was used as calorimetric reference (21). The time evolution of the pressure wave was assumed to be a sum of monoexponential functions. The deconvolution analysis yielded the fractional amplitudes (ϕ_i) and the lifetimes (τ_i) of the transients (Sound Analysis 3000, Quantum Northwest). The time window was between 20 ns and 5 μs . At a given temperature and for each resolved i th step, the fractional amplitude ϕ_i is the sum of the fraction of absorbed energy released as heat (α_i) and the structural volume change per absorbed einstein (ΔV_i), according to Eq. 1 (22,23)

$$\phi_i = \alpha + \frac{\Delta V_i}{E_\lambda} \frac{c_p \rho}{\beta}. \quad (1)$$

E_λ is the molar excitation energy, $\beta = (\partial V / \partial T)_P / V$ is the volume expansion coefficient, c_p is the heat capacity at constant pressure, and ρ is the

mass density of the solvent. In this work we used the so-called “two temperature” (TT) method to separate α_i from ΔV_i (24). The sample waveform was acquired at a temperature for which heat transport is zero, $T_{\beta=0} = 3.7^\circ\text{C}$ and at a slightly higher temperature $T_{\beta>0} = 10^\circ\text{C}$. At $T_{\beta=0}$ the LIOAS signal is only due to ΔV_i . The reference for deconvolution was recorded at $T_{\beta>0}$, and Eqs. 2a and 2b were then used to derive α_i and ΔV_i :

$$\Delta V_i = \phi_i|_{T_{\beta=0}} \times E_\lambda \frac{\beta}{c_p \rho}|_{T_{\beta>0}} \quad (2a)$$

$$\alpha_i = \phi_i|_{T_{\beta>0}} - \phi_i|_{T_{\beta=0}}. \quad (2b)$$

To minimize the photoconversion of the dark state and to avoid experimental artifacts related to the long recovery kinetics of the adduct, we used low repetition rates for the excitation (1/25 Hz). Under the conditions employed the absorption decrease at 450 nm was $< 5\%$ at the end of each experiment. Two sets of experiments were carried out for each protein, and a total of eight deconvolution fittings at each temperature.

Size exclusion chromatography

Gel filtration chromatography experiments were performed on a Pharmacia (Piscataway, NJ) fast protein liquid chromatography apparatus, using a Superdex 75 HR 10/30 column (Amersham Biosciences, Buckinghamshire, UK), equilibrated with a Na-phosphate buffer, 10 mM, pH = 8, NaCl = 0.15 M, as previously described (25). Bovine serum albumin (69 kDa), ovalbumin (42.7 kDa), α -chymotrypsin (25 kDa), myoglobin (16.9 kDa), and ribonuclease (13.7 kDa) (low Mw calibration kit, Amersham Biosciences) were used for calibration of the column. The proteins were loaded on the column at a concentration between 1 and 50 μM to give a final concentration ranging from 0.05 to 2.5 μM at the detection peak, due to dilution through the column.

Radioactivity experiments

Auto- and transphosphorylation experiments were performed using ^{32}P - γ -ATP (37 mBq 100 μl , Hartmann Analytik, Braunschweig, Germany). A 100 μl reaction buffer (26) contains 20 μg PST-LOV or LOV-HK fragment. The reactions were performed at room temperature in dark and light separately. At given time points, 10 μl of the reaction mixture was extracted and quenched with 10 μl sodium dodecylsulfate (SDS) stop buffer (26). For transphosphorylation experiments, a 10 \times excess (m/m) of the RR domain was added into the reaction tube. Again, 10 μl of the new mixture was withdrawn at different time points and quenched with 10 μl SDS stop buffer. After heating at 55°C for 5 min, radioactive proteins were separated on SDS-polyacrylamide-gel electrophoresis (PAGE) gels, which were kept in a BAS cassette 2025 (Fujifilm, Tokyo, Japan) for detection of radioactivity. Autoradiograms were obtained from a fluorescence image analyzer FLA-3000 (Fujifilm). Spot intensity is read as PSL mm^{-2} (PSL, photostimulated luminescence). Pixel size was $50 \times 50 \mu\text{m}^2$.

RESULTS AND DISCUSSION

Steady-state absorption measurements and kinetics of the dark recovery reaction

Heterologous expression of *PSPTO2896* and *PSPTO2896*_{ARR} in *E. coli* BL21 DE3, followed by His tag mediated affinity purification yielded recombinant proteins of expected size (MALDI- mass spectrometry: 61,049.2 and 46,299.3, expected mass: 61,098.4 and 46,367.4, respectively, including the 20 aa long His tag) with an absorbance spectrum typical

for an oxidized flavin species ($\lambda_{\text{max}} = 447$ nm, Fig. 2) under dark conditions. Blue light irradiation produced bleaching in the visible region, with concomitant loss of flavin fluorescence and appearance of a species absorbing maximally at ~ 390 nm, all features characterizing the formation of the covalent adduct in LOV proteins (27,28). The absorption spectra of purified PST-LOV $_{\Delta\text{RR}}$ in the dark- and light-adapted state are shown in Fig. 2, together with the light-dark difference spectrum. Similar spectra are obtained for PST-LOV, albeit with a slightly larger scattering (not shown).

The high UV/Visible ratio in the dark state ($\text{Abs}_{280}/\text{Abs}_{447} = 8.6$) indicates that a certain amount of apoprotein is present (29). The calculated absorption coefficient of apo-PST-LOV $_{\Delta\text{RR}}$ at 280 nm is $22,015 \text{ M}^{-1}\text{cm}^{-1}$ (ProtParam tool at the ExPASy Proteomics Server <http://expasy.org>), whereas for bound FMN it is $\sim 26,250 \text{ M}^{-1}\text{cm}^{-1}$ (29). From these data we can estimate that $\text{Abs}_{280}/\text{Abs}_{447} = \sim 4$ for a 1:1 protein/FMN ratio (no apoprotein present). Therefore, in the sample shown in Fig. 2 we may estimate that the protein/FMN ratio is ~ 3.5 . The full-length PST-LOV protein shows an even larger amount of apoprotein, as the protein/FMN ratio is ~ 4.5 for the measured $\text{Abs}_{280}/\text{Abs}_{447} = 12.5$ (ideal ratio $\text{Abs}_{280}/\text{Abs}_{447} = 4.5$ for a 1:1 complex). The full-length protein was subjected to a chromophore extraction to determine the chromophore composition (which could influence the spectroscopic properties). HPLC analysis showed preferentially FMN as chromophore (86%), accompanied by some FAD (13.3%), and a small amount of riboflavin (0.7%). It should be mentioned that especially older samples show a change of the latter two flavin derivatives due to decomposition of FAD: a

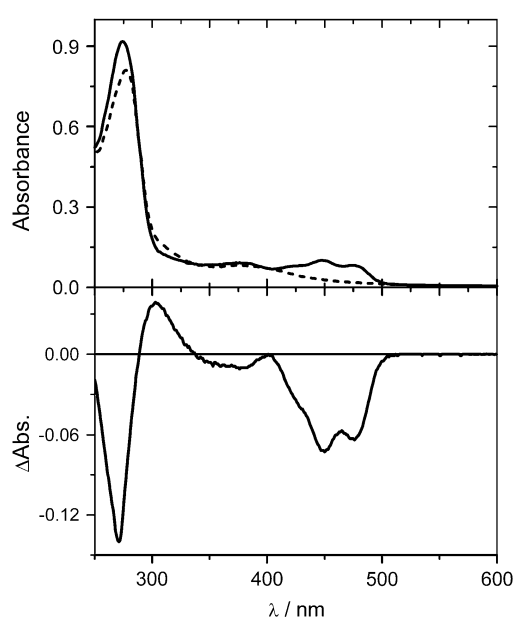


FIGURE 2 (Top) Absorption and (bottom) absorption difference spectra (light-dark) of PST-LOV $_{\Delta\text{RR}}$ before and after blue light irradiation.

6-month-old sample, kept at -40°C and identically prepared, showed a composition of 86:4:10 for FMN/FAD/riboflavin.

The absorption spectrum in the visible region is typical for FMN-binding LOV proteins, showing the three vibrational bands of the $S_0 \rightarrow S_1$ transition (29,30). In the ultraviolet-A (UVA) range ($S_0 \rightarrow S_2$ transition), the absorption maximum is red shifted (381 nm) with respect to YtvA (376 nm) and to Cr-phot-LOV1 and PpSB2-LOV (both showing a broad band centered at ~ 360 nm). In riboflavin derivatives this band is the most sensitive to the polarity of the microenvironment (31), and it is characteristically different between phot-LOV1 and LOV2 (shifted more to the red in LOV2) (28). The light-dark difference spectrum resembles the formation of the covalent adduct in LOV domains, generating the characteristic bleaching of the $S_0 \rightarrow S_1$ transition (Fig. 2).

In the dark, the photoadduct slowly reverts to the dark state, as can be followed by recording the recovery of absorbance at 447 nm, the full-length PST-LOV being slightly faster than the truncated protein (Fig. 3). The kinetic trace can best be fitted with a double exponential decay function, yielding an average life time of 5650 s for the full-length protein and 6210 s for the truncated protein. We can, however, not exclude that the biexponential behavior is an artifact due to a slight change in the scattering during the long-lasting measurements.

The average lifetime for the dark recovery reaction, $\langle\tau_{\text{rec}}\rangle$, is extremely long for both constructs (Table 1), even when compared to other bacterial LOV proteins ($\tau_{\text{rec}} = 3200$ s for YtvA, at 20°C) (19).

Fluorescence of the conserved W111

Phot-LOV domains and the vast majority of bacterial LOV domains carry a single, conserved tryptophan residue localized on the H β strand (8). The specific function of this residue is unknown; in YtvA (W103), it is involved in intraprotein interactions (32), most probably via contacts with the N-terminal cap (A. Losi and V. Buttani, unpublished) and/or with the

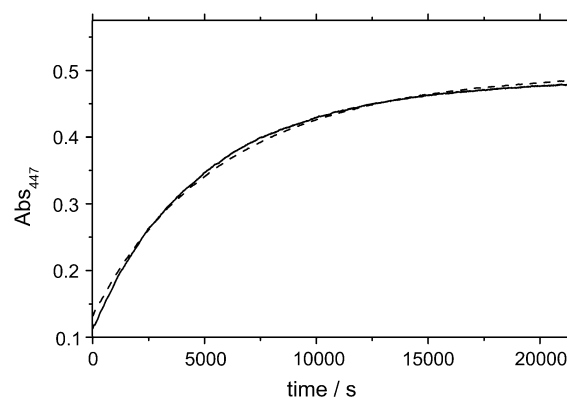


FIGURE 3 Dark-recovery time course (20°C) for full-length PST-LOV (solid line) and for the truncated protein PST-LOV $_{\Delta\text{RR}}$ (dashed line), obtained by measuring the absorbance at 447 nm. Experimental data were fitted by a two-exponential decay function.

TABLE 1 Kinetic and spectroscopic data of recombinant proteins PST-LOV and PST-LOV_{ΔRR} from *P. syringae* pv. *tomato*

20°C	LOV+kinase	Full-length protein
A1	27% ± 1%	65% ± 2.5%
τ ₁ /s	3505 ± 33	3950 ± 55
A2	73% ± 1%	35% ± 2.5%
τ ₂ /s	7210 ± 24	8820 ± 36
⟨τ⟩/s*	6210	5650

*⟨τ_{rec}⟩ = ΣA_iτ_i/100.

linker region C-terminal to the LOV core (29). The fluorescence of W103 in full-length YtvA is blue shifted with respect to the isolated YtvA-LOV (32), but no major changes are observed upon formation of the photoadduct. Conversely, in phot1-LOV2 W491 undergoes conformational changes upon formation of the photoadduct due to the unfolding of the linker region (33,34). In PpSB2-LOV the fluorescence of W97 slightly increases in the photoadduct with a concomitant broadening of the band, reverting to the original value after dark conversion of the protein (35).

In PST-LOV_{ΔRR} and PST-LOV, the fluorescence maximum of W111 (again the only tryptophan in the whole protein) is localized at ~332 nm, slightly blue shifted with respect to YtvA (335 nm) (32). Only very small changes are detectable by selective excitation of the Trp residue with 295 nm light (not shown). Excitation at 280 nm, however, caused a reversible change for the full-length protein, namely a slight increase of the fluorescence intensity and a spectral broadening. This reversible, light-induced change is much smaller in the truncated PST-LOV_{ΔRR} (Fig. 4).

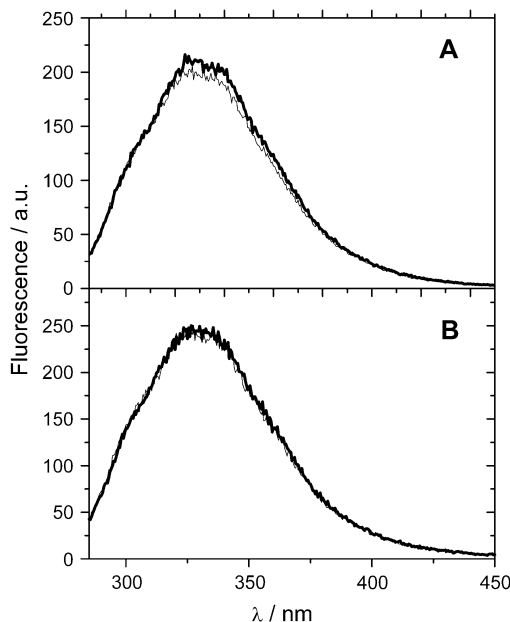


FIGURE 4 UVA fluorescence of (A) PST-LOV and (B) PST-LOV_{ΔRR} after 280 nm excitation in the dark- (thin line) and light- (thick line) adapted states.

The fluorescence change observed for PST-LOV may originate from conformational changes involving tyrosine(s) that increase energy transfer to W111 in the light state as suggested for YtvA (32), since these aromatic residues also are excited at 280 nm. This idea is supported by the fact that the change is not detected upon selective excitation of W111 at 295 nm. The important observation here is the difference between the truncated protein, PST-LOV_{ΔRR}, and the full-length protein, PST-LOV, the former one showing practically no change of the fluorescence in the dark or lit state, whereas the full-length protein exhibits an increase of fluorescence upon illumination. These data demonstrate an interaction between the LOV-HK and the RR domains that changes upon illumination. Most probably this involves one or more amino acids on the LOV core that change their conformation or environment upon formation of the photo-product. A mutation of the tryptophan111 to identify its role in this process failed and produced only (misfolded) apoprotein void of any chromophore.

LIOAS measurements

The LIOAS signals at $T_{B=0} = 3.70^\circ\text{C}$ are similar to those recorded for other LOV proteins (19,30,35,36) with a transient species formed within 20 ns (time resolution of the measurement) showing a small contraction ($\Delta V_1 = -0.8$ ml/einstein), assigned to the FMN triplet state (PST-LOV_T). The triplet decays with a lifetime of $\tau_2 = \sim 1.5 \mu\text{s}$ into a long-lived species, assigned to the covalent, blue-shifted photoadduct (PST-LOV₃₉₀). Different from the LOV proteins previously analyzed, the formation of the adduct does not correspond to a further, larger contraction but to a very small expansion, $\Delta V_2 < 0.5$ ml/einstein (Table 2).

With the knowledge that the FMN triplet state, both in solution and in LOV proteins, lies at ~ 200 kJ/mol (30,36,37), it is possible to calculate the triplet formation quantum yield, Φ_T , from Eq. 3:

$$\Phi_T \frac{E_T}{E_\lambda} = 1 - \alpha_1 - \Phi_F \frac{E_F}{E_\lambda}, \quad (3)$$

where E_F is the average energy for the fluorescence emission (232 kJ/mol, 515 nm).

$\Phi_F = 0.25$ is the flavin fluorescence quantum yield, and $E_\lambda = 265.8$ kJ/mol is the photon energy at 450 nm. The triplet quantum yield and also the yield of adduct formation is on the order of 0.45–0.5, typical for LOV proteins. The energy level of the adduct was calculated by means of Eq. 4 and requires the measure of Φ_{390} . This was done relative to YtvA, as previously reported (19).

$$\alpha_2 = \Phi_T \frac{E_T}{E_\lambda} - \Phi_{390} \frac{E_{390}}{E_\lambda}. \quad (4)$$

Finally, the molecular volume changes are evaluated by means of Eqs. 5a and 5b:

TABLE 2 LIOAS data for the PST-LOV proteins

	α_1 ($\tau_1 < 20$ ns)	ΔV_1 (mL/mol)	$\alpha_2(\tau_2/\mu\text{s}^*)$	ΔV_2 (mL/mol)
PSPTO2896 Δ RR	0.34 ± 0.03	-1.57 ± 0.34	0.16 ± 0.02 (1.6 ± 0.27)	$+0.22 \pm 0.12$
PSPTO2896	0.44 ± 0.03	-1.49 ± 0.15	0.13 ± 0.03 (1.4 ± 0.2)	$+0.31 \pm 0.18$

The statistical error originates from an averaging of eight values for each temperature.

*Average value at 3.70°C and 10°C.

$$\Delta V_T = \frac{\Delta V_1}{\Phi_T} \quad (5a)$$

$$\Delta V_{390} = \Delta V_T + \frac{\Delta V_2}{\Phi_{390}}. \quad (5b)$$

The results are reported in Table 3 and compared with other LOV proteins.

The values of Φ_T and Φ_{390} are, within experimental error ($\sim 20\%$), very similar for all the proteins analyzed, as well as the high energy level for the adduct that stores $\sim 50\%$ of the excitation energy. The latter aspect points to a strained conformation and small conformational changes with respect to the unphotolyzed state, a peculiar characteristic of LOV domains (19,35,36). The μs decay kinetics of the triplet state into the adduct indicates that the photocycle is similar to other LOV proteins (30,38,39). A notable difference is that the total structural volume change corresponding to the formation of the adduct, ΔV_{390} , is very small and almost entirely derives from the formation of the triplet state (Table 3, Eqs. 5a and 5b). Actually, the formation of the adduct corresponds to a small expansion (ΔV_2 in Table 2) instead of being a quite large contraction as in other LOV proteins (19,35,36). This does not necessarily imply that, as a whole, the protein conformational changes are smaller. In photoreceptors the light-induced ΔV s recorded by means of the LIOAS technique may receive different contributions, e.g., changes in the protein secondary structure, in hydrogen bonds (HBs) around the chromophore, or solvation/electro-

striction effects (40). In LOV domains the negative ΔV_2 originates mainly from a rearrangement of the HB network around the flavin chromophore, which results in an overall contraction as shown by means of mutagenesis studies on Cr-phot-LOV1 (36). In the relatively large PST-LOV and PST-LOV Δ RR constructs, other conformational changes of opposite sign might compensate for this HB rearrangement, resulting in an overall small expansion. This hypothesis is supported by a comparison of the results obtained with full-length YtvA and the isolated YtvA-LOV in that the value of ΔV_2 is more negative in the latter system (19).

Phosphorylation assay

Systems like the PST-LOV protein presented here—composed of input domains ready to detect a broad variety of incoming stimuli, thereby activating its HK domain, which in turn activates a signal-transducing RR protein (or protein domain)—are well known and precisely characterized in many other prokaryotic organisms (9). Whereas two-component signal transduction systems are furnished with highly variable input domains and also induce quite different physiological responses, the central building blocks, i.e., the HK activity and the RR (domain), show a remarkable sequential and structural conservation. The central reaction step is the transfer of a phosphate group, initially bound upon activation to a fully conserved histidine of the receptor, to an aspartate residue of the RR.

An analysis of this reaction with PST-LOV by addition of ATP would result in a phosphorylated full-length protein with no insight into the different steps. An attempt to dissect this reaction would be possible by separating both protein domains. This approach yielded the truncated LOV-HK protein (46 kDa) and the RR domain (16 kDa) as independently expressed proteins, as described above. For functional studies, the full-length protein as also a C-terminally truncated construct consisting only of the LOV domain and the HK motif was subjected to light-dependent phosphorylation assays. The separately expressed RR protein, added later in the course of the experiment, would allow us to identify the essential phosphate transfer from HK to RR in a separate experiment. In both full-length and C-terminally truncated PST-LOV, radioactive phosphate is incorporated, but in a much higher yield upon blue light irradiation than under dark conditions (Fig. 5).

It should be taken into account that the very slow recovery rate of the dark state impedes the reaction such that any

TABLE 3 Photophysical and energetic parameters of PST-LOV proteins

	Φ_T	$E_{390}/\text{kJ/mol}$	Φ_{390}	$\Delta V_T/\text{mL/mol}$	$\Delta V_{390}/\text{mL/mol}$
PST-LOV Δ RR	0.58	144	0.51	-2.5	-2.0
PST-LOV	0.47	149	0.41	-2.9	-2.1
*PpSB2-LOV	0.46	133	0.42	-1.74	-16.0
[†] YtvA	0.62	136	0.49	-0.71	-12.5
[†] YtvA-LOV	0.69	113	0.55	-0.67	-17.2
[‡] Cr-phot-LOV1	0.63	171	0.6	-1.15	-8.0

The values of E_{390} , ΔV_T , and ΔV_{390} are affected by the measurement error ($<10\%$, see Table 2) and by the quantum yield determination, whose error depends on a variety of factors (e.g., absorption coefficients, reference standard values, and energy level of the triplet state). Repeated measurements (four) for Φ_{390} gave an experimental variation within 8%.

*Full-length SB2 LOV protein from *Pseudomonas putida* (35).

[†]Full-length YtvA from *Bacillus subtilis* and its isolated LOV domain, YtvA-LOV (19).

[‡]Isolated LOV1 domain of phototropin from *Chlamydomonas reinhardtii* (36).

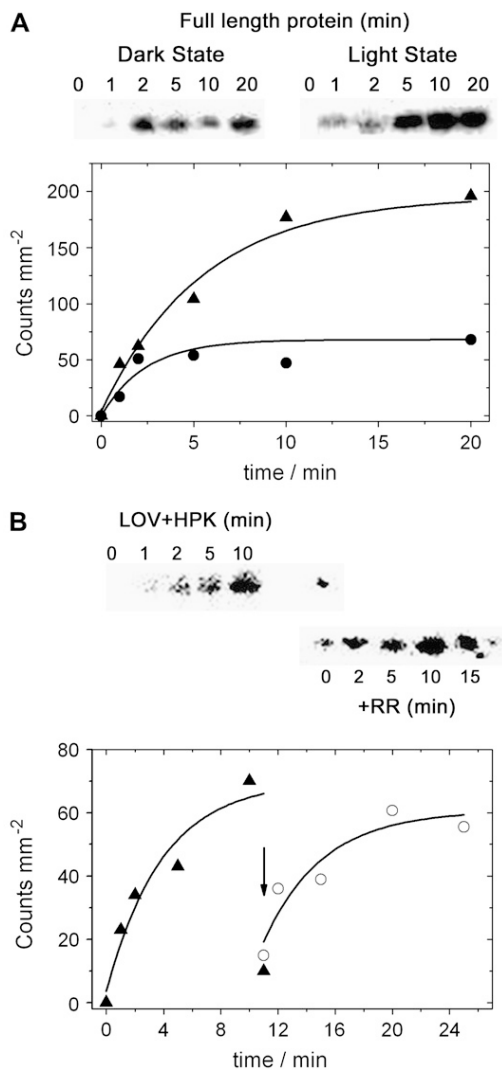


FIGURE 5 Assay of phosphorylation activity of PST-LOV. Full-length and C-terminally truncated protein were incubated with ^{32}P - γ -ATP (see Materials and Methods), either in the dark or upon blue light irradiation. Aliquots were withdrawn at indicated time points and were separated on an SDS-PAGE electrophoresis gel. The gels were then covered with foil and the incorporated radioactivity was determined. (A) Full-length protein. From left to right: time course (0–20 min) of ^{32}P -phosphate incorporation under blue light irradiation and in the dark. The time course of radioactivity incorporation is shown below. The slight downward deviation of the data point at 10 min might be due to an experimental (pipetting) error. (B) C-terminally truncated fragment containing solely the LOV and the HK domains. This autoradiogram also shows phosphate transfer to the RR after being added to the reaction mixture. Addition is indicated by an arrow. The time course of phosphate incorporation (and phosphate transfer) is shown below. Note that the final data point for the HK domain drops instantaneously upon RR addition (solid triangle at 10 min).

scattering light accumulates in the lit state and thus mimics apparent activity of the dark state. The reaction reaches a plateau for both constructs within ~ 10 min, indicating that i), apparently the residual amount of illuminated sample is fully phosphorylated and ii), the removal of the RR domain does

not impede the phosphorylation of the histidine residue in the HK domain. Addition of the RR to the fully phosphorylated LOV-HK fragment (Fig. 5 B, arrow) resulted in a practically instantaneous phosphate transfer to the RR. The apparently lower radioactivity in the samples of RR taken after very early time points (2 and 5 min) is due to the experimental conditions such that a large excess of the RR was added. The ongoing incorporation of radioactivity into the RR, even after the HK domain does not show any radioactivity, is due to ^{32}P - γ -ATP, which is still present in the reaction mixture that is rapidly attached to the RR by the very active HK domain.

Implications from the *P. syringae* LOV protein for the transduction mechanism of LOV proteins

The experiments demonstrate a blue light-driven, flavin-bearing HK activity in prokaryotes, which thereby adds blue light to the large number of stimuli that are recorded by this bacterial two-component signal transduction system (41). A similarly built sensory protein, carrying a photoactive yellow protein (PYP)-domain has recently been described (42). The different chromophore structure in both types of proteins becomes immediately clear from an inspection of the absorption spectra: broad and unstructured in the PYP-case and fine structured for the flavin-protein.

A very similar reactivity was recently demonstrated for red light activated bacterial phytochromes, also furnished with an HK domain and a separate RR (26,43). These findings show the modular setup for many bacterial systems, where a broad variety of input signals induce an ensemble of output responses, mediated by a highly conserved signal processing mechanism.

The observation that W111 or a neighboring tyrosine (e.g., Y103) is probably in close vicinity to the RR domain implies the direct interaction of RR with the light-responsive LOV core. This agrees with the low resolution structure (4.2 Å) of ThKA from *Thermotoga maritima*, a PAS-HK kinase in complex with its RR, i.e., a similar architecture to PST-LOV (44) (the LOV domain is a PAS fold (45)). In this complex the RR is in direct contact with both the HK and the PAS domain, and it was suggested that RR not only acts as an efficient phosphoryl carrier but also exerts a regulative role on the PAS-sensing domain (e.g., by a feedback regulation of sensing) (44). It is also conceivable that the LOV core directly interacts with the HK domain, given the enhancement of the self-phosphorylation activity upon light-activation, again in agreement with the structure of ThKA. The highly conserved W111 and Y103 correspond to W103 and Y95 in YtvA (32) and are localized on strand H β and G β , respectively, neighboring K105 in the G β -H β loop. K105 in turn is involved in a salt bridge with E64, a feature of LOV domains suggested to be important in light-to-signal transduction (7). Molecular dynamics simulations suggest that light-induced modifications of the E-K salt bridge are typical for LOV1

activation and are triggered by a change in HBs between FMN and N99 (corresponding to N110 in PST-LOV). Note that this asparagine is directly adjacent to the conserved Trp (46). Conversely, LOV2 activation could be mostly related to conformational changes in the H β -I β loop (46). This preferential activation for LOV1 and LOV2 via distinct pathways might be related to their specific role within phototropins, with LOV being necessary and sufficient to elicit the majority of light-elicited phot responses and LOV1 probably playing a regulatory role (47,48). In bacterial LOV proteins, the LOV domain has intermediate characteristics between LOV1 and LOV2 (8), in agreement with the data presented here that point both to a light triggered activation of the kinase activity and to regulation via interactions with RR; this intermittent function probably even indicates its ancestry to the LOV proteins of eukaryotes.

Beyond the biochemical characterization presented here, a question on the biological role of this protein remains. Such an approach probably requires the generation of knockout mutants and investigations on modified pathogenicity of such constructs. A search of the locus of this gene (PSPTO_2896) revealed several ORFs encoding signaling or DNA-regulating proteins which could be involved in signal transduction: ORF 2901, DNA-binding protein; ORFs 2903, 2906, transcriptional regulators; and ORF 2907, GGDEF domain/EAL domain protein. However, no detailed investigation has yet been performed.

CONCLUSION

The results presented here add blue light as a stimulus to the large family of bacterial two-component signal transduction systems. The data demonstrate a functional system, showing light-regulated communication between the various domains of this protein. The aspect of blue light regulation, employing receptor structures in *P. syringae* very similar to those used by plants, points to a putative role of the bacterial photoreceptors in light-regulated host pathogen interactions, a research field with a strong scientific and potentially economic impact. Yet, only a few reports on that topic are available, clearly demanding much stronger research activity.

Note added in proof: During the time this manuscript was being processed, an exciting report from T. Swartz and co-workers showed that an LOV-kinase regulates infectivity in the animal pathogen *Brucella abortus*. In the same work they have characterized the kinase activity of a few other bacterial LOV proteins (49).

We kindly acknowledge the help of Dr. K. Ernst, University of Düsseldorf, during the radioactivity work, and the technical help of N. Dickmann (Max-Planck-Institut Mülheim) for the MALDI-TOF measurements, and the expert support of Ms. Astrid Wirtz, FZ Jülich, during the HPLC analysis of chromophore content. Robin Buell (The Institute for Genomic Research, 9712 Medical Center Drive, Rockville, MD 20850) kindly provided a cell culture of *P. syringae* pv. *tomato* DC3000.

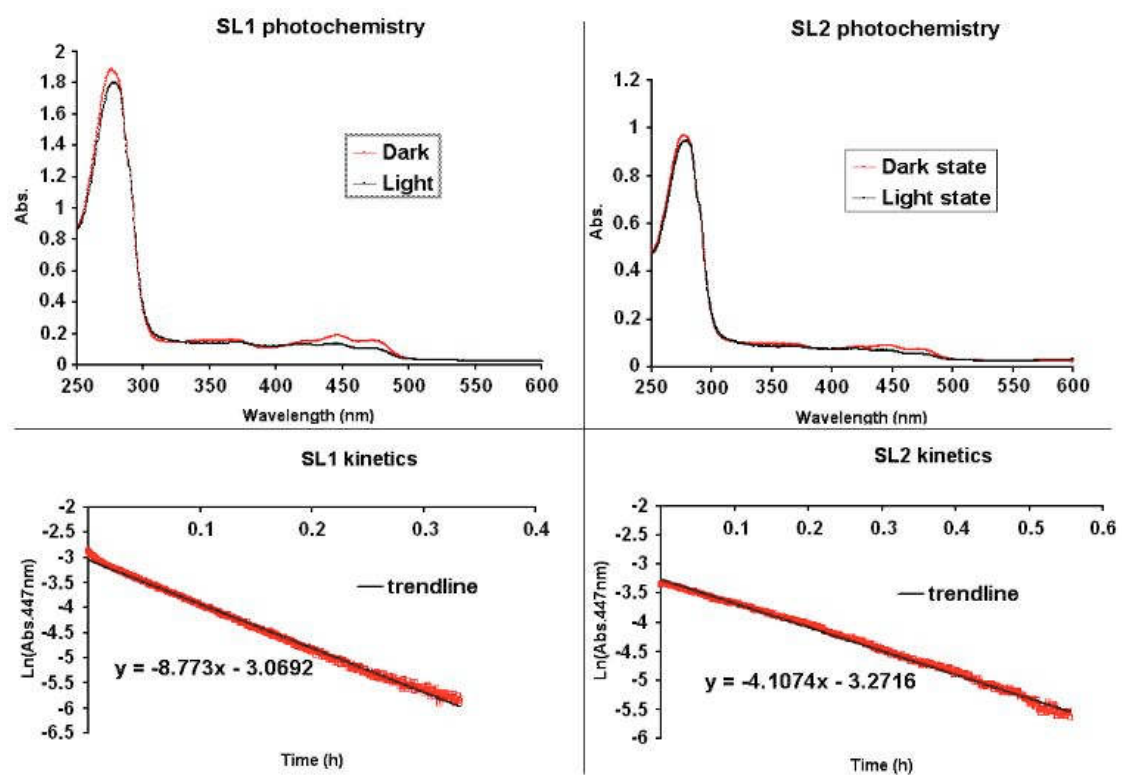
This work was financially supported by the Deutsche Forschungsgemeinschaft (FOR526, project A1).

REFERENCES

- Pattison, D. I., and M. J. Davies. 2006. Actions of ultraviolet light on cellular structures. In *Cancer: Cell Structures, Carcinogens and Genomic Instability*. Birkhäuser, Basel, Switzerland. 131–157.
- Spikes, J. D. 1989. Photosensitization. In *The Science of Photobiology*. K. C. Smith, editor. Plenum Press, New York and London. 79–110.
- Miranda, M. A. 2001. Photosensitization by drugs. *Pure Appl. Chem.* 73:481–486.
- Weber, S. 2005. Light-driven enzymatic catalysis of DNA repair: a review of recent biophysical studies on photolyase. *Biochim. Biophys. Acta.* 1707:1–23.
- Armitage, J. P., and K. Hellingwerf. 2003. Light-induced behavioral responses ('phototaxis') in prokaryotes. *Photosynth. Res.* 76: 145–155.
- Losi, A. 2006. Flavin-based photoreceptors in bacteria. In *Flavin Photochemistry and Photobiology*. Elsevier, Amsterdam, The Netherlands. 223–276.
- Crosson, S., S. Rajagopal, and K. Moffat. 2003. The LOV domain family: photoreponsive signaling modules coupled to diverse output domains. *Biochemistry.* 42:2–10.
- Losi, A. 2004. The bacterial counterparts of plants phototropins. *Photochem. Photobiol. Sci.* 3:566–574.
- West, A. H., and A. M. Stock. 2001. Histidine kinases and response regulator proteins in two-component signaling systems. *Trends Biochem. Sci.* 26:369–376.
- Grebe, T. W., and J. B. Stock. 1999. The histidine protein kinase superfamily. *Adv. Microb. Physiol.* 41:139–227.
- Genoud, T., A. J. Buchala, N. H. Chua, and J. P. Metraux. 2002. Phytochrome signalling modulates the SA-perceptive pathway in Arabidopsis. *Plant J.* 31:87–95.
- Zeier, J., M. Delledonne, T. Mishina, E. Severi, M. Sonoda, and C. Lamb. 2004. Genetic elucidation of nitric oxide signaling in incompatible plant-pathogen interactions. *Plant Physiol.* 136:2875–2886.
- Delledonne, M. 2005. NO news is good news for plants. *Curr. Opin. Plant Biol.* 8:390–396.
- Buell, C. R., V. Joardar, M. Lindeberg, J. Selengut, I. T. Paulsen, M. L. Gwinn, R. J. Dodson, R. T. Deboy, A. S. Durkin, and J. F. Kolonay, R. Madupu, S. Daugherty, L. Brinkac, M. J. Beanan, D. H. Haft, W. C. Nelson, T. Davidsen, N. Zafar, L. Zhou, J. Liu, Q. Yuan, H. Khouri, N. Fedorova, B. Tran, D. Russell, K. Berry, T. Utterback, S. E. Van Aken, T. V. Feldblyum, M. D'Ascenzo, W. L. Deng, A. R. Ramos, J. R. Alfano, S. Cartinhour, A. K. Chatterjee, T. P. Delaney, S. G. Lazarowitz, G. B. Martin, D. J. Schneider, X. Tang, C. L. Bender, O. White, C. M. Fraser, and A. Collmer. 2003. The complete genome sequence of the Arabidopsis and tomato pathogen *Pseudomonas syringae* pv. *tomato* DC3000. *Proc. Natl. Acad. Sci. USA.* 100:10181–10186.
- Hirano, S. S., and C. D. Upper. 2000. Bacteria in the leaf ecosystem with emphasis on *Pseudomonas syringae*—a pathogen, ice nucleus, and epiphyte. *Microbiol. Mol. Biol. Rev.* 64:624–653.
- Joardar, V., M. Lindeberg, R. W. Jackson, J. Selengut, R. Dodson, L. M. Brinkac, S. C. Daugherty, R. DeBoy, A. S. Durkin, M. G. Giglio, R. Madupu, W. C. Nelson, M. J. Rosovitz, S. Sullivan, J. Crabtree, T. Creasy, T. Davidsen, D. H. Haft, N. Zafar, L. W. Zhou, R. Halpin, T. Holley, H. Khouri, T. Feldblyum, O. White, C. M. Fraser, A. K. Chatterjee, S. Cartinhour, D. J. Schneider, J. Mansfield, A. Collmer, and C. R. Buell. 2005. Whole-genome sequence analysis of *Pseudomonas syringae* pv. *phaseolicola* 1448A reveals divergence among pathogens in genes involved in virulence and transposition. *J. Bacteriol.* 187:6488–6498.
- Feil, H., W. S. Feil, P. Chain, F. Larimer, G. DiBartolo, A. Copeland, A. Lykidis, S. Trong, M. Nolan, and E. Goltsman, J. Thiel, S. Malfatti, J. E. Loper, A. Lapidus, J. C. Detter, M. Land, P. M. Richardson, N. C. Kyrpides, N. Ivanova, and S. E. Lindow. 2005. Comparison of the complete genome sequences of *Pseudomonas syringae* pv. *syringae* B728a and pv. *tomato* DC3000. *Proc. Natl. Acad. Sci. USA.* 102: 11064–11069.

18. van den Berg, P. W., J. Widengren, M. A. Hink, R. Rigler, and A. G. Visser. 2001. Fluorescence correlation spectroscopy of flavins and flavoenzymes: photochemical and photophysical aspects. *Spectrochim. Acta [A]*. 57:2135–2144.
19. Losi, A., B. Quest, and W. Gärtner. 2003. Listening to the blue: the time-resolved thermodynamics of the bacterial blue-light receptor YtvA and its isolated LOV domain. *Photochem. Photobiol. Sci.* 2:759–766.
20. Rudzki, J. E., J. L. Goodman, and K. S. Peters. 1985. Simultaneous determination of photoreaction dynamics and energetics using pulsed, time resolved photoacoustic calorimetry. *J. Am. Chem. Soc.* 107:7849–7854.
21. Abbruzzetti, S., C. Viappiani, D. H. Murgida, R. Erra-Balsells, and G. M. Bilmes. 1999. Non-toxic, water-soluble photocalorimetric reference compounds for UV and visible excitation. *Chem. Phys. Lett.* 304:167–172.
22. Small, J. R., L. J. Libertini, and E. W. Small. 1992. Analysis of photoacoustic waveforms using the nonlinear least squares method. *Biophys. Chem.* 42:24–48.
23. Rudzki-Small, J., L. J. Libertini, and E. W. Small. 1992. Analysis of photoacoustic waveforms using the nonlinear least square method. *Biophys. Chem.* 41:29–48.
24. Malkin, S., M. S. Churio, S. Shochat, and S. E. Braslavsky. 1994. Photochemical energy storage and volume changes in the microsecond time range in bacterial photosynthesis—a laser induced optoacoustic study. *J. Photochem. Photobiol. B.* 23:79–85.
25. Buttani, V., A. Losi, T. Eggert, U. Krauss, K.-E. Jaeger, Z. Cao, and W. Gärtner. 2007. Conformational analysis of the blue-light sensing protein YtvA reveals a competitive interface for LOV-LOV dimerization and interdomain interactions. *Photochem. Photobiol. Sci.* 6:41–49.
26. Hübschmann, T., H. J. M. M. Jorissen, T. Börner, W. Gärtner, and N. T. deMarsac. 2001. Phosphorylation of proteins in the light-dependent signalling pathway of a filamentous cyanobacterium. *Eur. J. Biochem.* 268:3383–3389.
27. Briggs, W. R., T. S. Tseng, H. Y. Cho, T. E. Swartz, S. Sullivan, R. A. Bogomolni, E. Kaiserli, and J. M. Christie. 2007. Phototropins and their LOV domains: versatile plant blue-light receptors. *J. Integr. Plant Biol.* 49:4–10.
28. Kasahara, M., T. E. Swartz, M. A. Olney, A. Onodera, N. Mochizuki, H. Fukuzawa, E. Asamizu, S. Tabata, H. Kanegae, M. Takano, J. M. Christie, A. Nagatani, and W. R. Briggs. 2002. Photochemical properties of the flavin mononucleotide-binding domains of the phototropins from Arabidopsis, rice, and *Chlamydomonas reinhardtii*. *Plant Physiol.* 129:762–773.
29. Losi, A., E. Ghiraldelli, S. Jansen, and W. Gärtner. 2005. Mutational effects on protein structural changes and interdomain interactions in the blue-light sensing LOV protein YtvA. *Photochem. Photobiol.* 81:1145–1152.
30. Losi, A., E. Polverini, B. Quest, and W. Gärtner. 2002. First evidence for phototropin-related blue-light receptors in prokaryotes. *Biophys. J.* 82:2627–2634.
31. Johansson, L. B., A. Davidsson, G. Lindblom, and K. R. Naqvi. 1979. Electronic transitions in the isoalloxazine ring and orientation of flavins in model membranes studied by polarized light spectroscopy. *Biochemistry.* 18:4249–4253.
32. Losi, A., E. Ternelli, and W. Gärtner. 2004. Tryptophan fluorescence in the *Bacillus subtilis* phototropin-related protein YtvA as a marker of interdomain interaction. *Photochem. Photobiol.* 80:150–153.
33. Harper, S. M., L. C. Neil, and K. H. Gardner. 2003. Structural basis of a phototropin light switch. *Science.* 301:1541–1544.
34. Harper, S. M., L. C. Neil, I. J. Day, P. J. Hore, and K. H. Gardner. 2004. Conformational changes in a photosensory LOV domain monitored by time-resolved NMR spectroscopy. *J. Am. Chem. Soc.* 126:3390–3391.
35. Krauss, U., A. Losi, W. Gärtner, K.-E. Jaeger, and T. Eggert. 2005. Initial characterization of a blue-light sensing, phototropin-related protein from *Pseudomonas putida*: a paradigm for an extended LOV construct. *Phys. Chem. Chem. Phys.* 7:2229–2236.
36. Losi, A., T. Kottke, and P. Hegemann. 2004. Recording of blue light-induced energy and volume changes within the wild-type and mutated phot-LOV1 domain from *Chlamydomonas reinhardtii*. *Biophys. J.* 86:1051–1060.
37. Gauden, M., S. Crosson, I. H. M. van Stokkum, R. van Grondelle, K. Moffat, and J. T. M. Kennis. 2004. Low-temperature and time-resolved spectroscopic characterization of the LOV2 domain of *Avena sativa* phototropin. In *Femtosecond Laser Applications in Biology*. S. Avrielleir and J. M. Tualle, editors. SPIE, Bellingham, WA. 97–104.
38. Swartz, T. E., S. B. Corchnoy, J. M. Christie, J. W. Lewis, I. Szundi, W. R. Briggs, and R. A. Bogomolni. 2001. The photocycle of a flavin-binding domain of the blue light photoreceptor phototropin. *J. Biol. Chem.* 276:36493–36500.
39. Kottke, T., J. Heberle, D. Hehn, B. Dick, and P. Hegemann. 2003. Phot-LOV1: photocycle of a blue-light receptor domain from the green alga *Chlamydomonas reinhardtii*. *Biophys. J.* 84:1192–1201.
40. Losi, A., and S. E. Braslavsky. 2003. The time-resolved thermodynamics of the chromophore-protein interactions in biological photosensors. Learning from photothermal measurements. *Phys. Chem. Chem. Phys.* 5:2739–2750.
41. Alm, E., K. Huang, and A. Arkin. 2006. The evolution of two-component systems in bacteria reveals different strategies for niche adaptation. *PLoS Comput. Biol.* 2:e143.
42. Jiang, Z. Y., L. R. Swem, B. G. Rushing, S. Devanathan, G. Tollin, and C. E. Bauer. 1999. Bacterial photoreceptor with similarity to photoactive yellow protein and plant phytochromes. *Science.* 285:406–409.
43. Yeh, K. C., S. H. Wu, J. T. Murphy, and J. C. Lagarias. 1997. A cyanobacterial phytochrome two-component light sensory system. *Science.* 277:1505–1508.
44. Yamada, S., S. Akiyama, H. Sugimoto, H. Kumita, K. Ito, T. Fujisawa, H. Nakamura, and Y. Shiro. 2006. The signaling pathway in histidine kinase and the response regulator complex revealed by x-ray crystallography and solution scattering. *J. Mol. Biol.* 362:123–139.
45. Crosson, S., and K. Moffat. 2001. Structure of a flavin-binding plant photoreceptor domain: insights into light-mediated signal transduction. *Proc. Natl. Acad. Sci. USA.* 98:2995–3000.
46. Freddolino, P. L., M. Dittrich, and K. Schulten. 2006. Dynamic switching mechanisms in LOV1 and LOV2 domains of plant phototropins. *Biophys. J.* 91:3630–3639.
47. Christie, J. M., T. E. Swartz, R. A. Bogomolni, and W. R. Briggs. 2002. Phototropin LOV domains exhibit distinct roles in regulating photoreceptor function. *Plant J.* 32:205–219.
48. Cho, H. Y., T. S. Tseng, E. Kaiserli, S. Sullivan, J. M. Christie, and W. R. Briggs. 2007. Physiological roles of the light, oxygen, or voltage domains of phototropin 1 and phototropin 2 in arabidopsis. *Plant Physiol.* 143:517–529.
49. Swartz, T. E., T. S. Tseng, M. A. Frederickson, G. Paris, D. J. Comerci, G. Rajashekara, J. G. Kim, M. B. Mudgett, G. A. Splitter, R. A. Ugalde, F. A. Goldbaum, W. R. Briggs, and R. A. Bogomolni. 2007. Blue-light-activated histidine kinases: two-component sensors in bacteria. *Science.* 317:1090–1093.

IV. Light-regulated GGDEF-EAL proteins



A Blue Light-inducible Phosphodiesterase Activity in the Cyanobacterium *Synechococcus elongatus*

Zhen Cao¹, Elsa Livoti², Aba Losi² and Wolfgang Gärtner^{*1}

¹Max-Planck-Institute for Bioinorganic Chemistry, Mülheim, Germany

²Department of Physics, University of Parma, Parma, Italy

Received 20 August 2009, accepted 28 January 2010, DOI: 10.1111/j.1751-1097.2010.00724.x

ABSTRACT

A blue light-inducible phosphodiesterase (PDE) activity, specific for the hydrolysis of cyclic di-GMP (c-di-GMP), has been identified in a recombinant protein from *Synechococcus elongatus*. Blue light (BL) activation is accomplished by a light, oxygen, voltage (LOV) domain, found in plant phototropins and bacterial BL photoreceptors. The genome of *S. elongatus* contains two genes coding for proteins with LOV domains fused to EAL domains (SL1 and SL2). In both cases, a GGDEF motif is placed in between the LOV and the EAL motifs. Such arrangement is frequently found with diguanylate-cyclase (DGC) functions that form c-di-GMP. Cyclic di-GMP acts as a second messenger molecule regulating biofilm formation in many microbial species. Both enzyme activities modulate the intracellular level of this second messenger, although in most proteins only one of the two enzyme functions is active. Both *S. elongatus* LOV-GGDEF-EAL proteins were expressed in full length or as truncated proteins. Only the SL2 protein, expressed as a LOV-GGDEF-EAL construct, showed an increase of PDE activity upon BL irradiation, demonstrating this activity for the first time in a LOV-domain protein. Addition of GTP or c-di-GMP did not affect the observed enzymatic activity. In none of the full-length or truncated proteins was a DGC activity detected.

INTRODUCTION

Microbes have developed a remarkable capability to adapt to a broad variety of environmental stimuli based on a relatively simple program of physiological activities. The most prominent responses that microbes have at hand are escape reaction from harmful or toward advantageous environment (in case they are motile), regulation of gene expression causing an increase or decrease of enzymatic activity (e.g. expression of photolyases or production of shielding pigments) (1,2) or the generation of a biofilm (3). This latter activity is often found as a response to environmental conditions. The extracellular carbohydrate matrix, into which microbes are incorporated, offers a number of advantageous conditions: a limited diffusion facilitates exchange of nutrients and genetic material, and

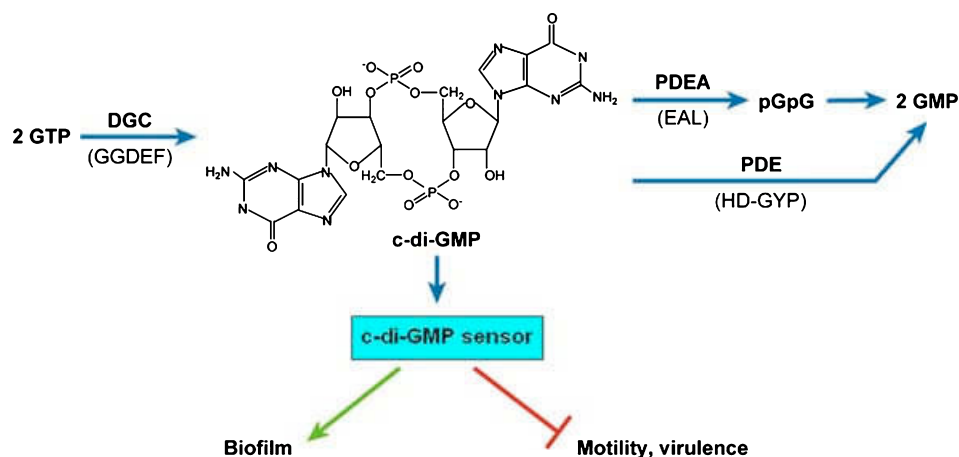
the extracellular matrix might provide protection against predators compared with living unsheltered (3).

A major challenge in adjusting metabolic functions is the detection of the external light conditions with respect to the spectral range, intensity and duration. In particular, the quality and quantity of light from the ultraviolet (UV) and blue light (BL) region is most important to detect. Intense UV light causes damage of many biological compounds, and efficient DNA-repair systems (photolyases) have evolved (4). Also BL (around 440 nm) represents a threat to living organisms. This light quality generates triplet states of ubiquitous porphyrins when present in their metal-free form. In turn, porphyrin triplets can form the singlet state of oxygen with a high quantum yield (Φ of $^1\text{O}_2$ usually >0.5) and other reactive oxygen species (5). Detection of BL is chiefly accomplished by flavin-containing BL sensitive photoreceptors (6). The most abundant class of these receptors in the microbial world are the LOV-domain proteins (7). These photoreceptors carry a modified PAS domain called LOV domain (light, oxygen, voltage [LOV]) that holds—in its inactivated state—a noncovalently bound flavin mononucleotide (FMN) chromophore (8). Upon absorption of light (λ_{max} of LOV domains = 445–450 nm), the flavin chromophore becomes transiently covalently bound to the protein through the side chain of a cysteine residue, forming a thio-ether bond to position 4a of the flavin molecule. This state is considered as the signaling state and is detected by a shift of the absorption maximum to ca. 390 nm, a loss of vibrational bands in the absorption spectrum, and a loss of fluorescence. The covalent bond reopens to generate the parent state of the photoreceptor within minutes or, in some proteins, after hours at room temperatures (9).

LOV-domain proteins are present in many microbial genomes (ca. 12% of fully sequenced bacteria) (8). They show a broad variety of fused signaling domains (7). The dominant signaling motif is the histidine kinase domain ($>40\%$ of all LOV-domain proteins), making this subclass of LOV proteins members of the well-characterized two component system (10). Nearly one quarter (23%) of LOV proteins carry a GGDEF signaling module, in the majority of cases associated with an EAL domain (GGDEF and EAL refer to guanylate cyclase and phosphodiesterase [PDE] activities, respectively, and indicate conserved, functionally essential sequence motifs). These enzyme functions have been assigned to formation (GGDEF) and degradation (EAL) of cyclic di-GMP (c-di-GMP), an important second messenger molecule involved in the formation

*Corresponding author email: gaertner@mpi-muelheim.mpg.de (Wolfgang Gärtner)

© 2010 The Authors. Journal Compilation. The American Society of Photobiology 0031-8655/10



Scheme 1. Enzymatic regulation of c-di-GMP concentration in a bacteria cell.

of biofilms and other responsive microbial functions (Scheme 1) (11–13). GGDEF domains form c-di-GMP from two molecules of GTP via an intermolecular cyclization, whereas EAL domains hydrolyze this molecule. An EAL subclass (phosphodiesterase A, PDEA) generates a linear G–G dinucleotide, whereas another group of phosphodiesterases directly cleaves c-di-GMP into two GMP molecules.

A GGDEF-EAL signaling domain had recently been reported for a red light-sensing photoreceptor protein from the photosynthetic bacterium *Rhodobacter sphaeroides* (BphG1) (14). Interestingly, the GGDEF domain of this protein showed no enzymatic activity, whereas the EAL domain was active already in the dark. Light regulation of the GGDEF activity in BphG1 could only be demonstrated after the EAL domain had been cleaved off.

“Genome mining” revealed several ORFs encoding LOV-GGDEF-EAL domain proteins (7), although many of the putative gene products are multi-domain proteins, rendering a straightforward functional analysis difficult. The simplest combination of domains, LOV-GGDEF-EAL, was identified for the gene product of ORF 0188 from *Synechococcus elongatus* PCC 7942. This organism contains a second ORF, 1355, encoding a protein also exhibiting LOV-GGDEF-EAL domains, yet in a more complex domain organization. We here present the heterologous expression and functional (photochemical and biochemical) characterization of both gene products upon light activation.

MATERIALS AND METHODS

Cloning, heterologous expression and purification of recombinant proteins. Cyanobacterial cells of *S. elongatus* PCC 7942 were grown in BG11 medium for 1 week at ambient temperature (~20°C). From these cultures, genomic DNA was isolated using the mi-Bacterial Genomic DNA Kit (Metabion, Martinsried, Germany); this material was used for cloning. For a schematic presentation of the various proteins and protein fragments that were generated, see Fig. 1.

- 1 Full-length proteins.** The ORFs Synpcc7942_0188 (Syn-LOV1) and Synpcc7942_1355 (Syn-LOV2) were amplified by PCR from the genomic DNA, using the primers (for Syn-LOV1): 5'-CAG-GGACCCGGTATGATTGCCCGTCCTATGGTGC (0188-forward), 5'-GGCACCAGAGCGTTCCAGCGGGAGCTTGCGG-GCGAT (0188-reverse); and (for Syn-LOV2): 5'-CAGGGAC-CCGGTATGACCTATAGCGAAGTTCACTGGCGG (1355-

forward), 5'-GGCACCAGAGCGTTTGGAAGTTCGCGCGC-AGCTTCATCCA (1355-reverse). PCR conditions: 95°C 2 min, 30-times (95°C 30 s, 59°C 45 s, 72°C 3 min), 72°C 10 min, 4°C hold. All primers contained sequences (shown in bold) for direct insertion of the PCR product into the plasmid pET52 3C/LIC (Novagen-Merck, Darmstadt, Germany), which is furnished at its 3'-end with a His₈-tag. Heterologous expression in *Escherichia coli* BL21-AI™ One Shot® (Invitrogen GmbH, Karlsruhe, Germany) cells was carried out in TB medium (yeast extract was purchased from MP Biomedicals, Heidelberg, Germany); the culture was induced by L-arabinose (final concentration of 0.2%) and isopropyl β-D-thiogalactopyranoside (IPTG; final concentration of 1 mM) at 25°C for 8 h. Syn-LOV2 could not be isolated in soluble form, whereas Syn-LOV1 was directly isolated from the lysed *E. coli* cells (lysis in all cases was performed using an Ultra-Turrax, IKA Staufen, Germany, in liquid nitrogen) by passage of the crude lysate (separated from the cell debris by ultracentrifugation, 368 000 g, 1 h, 4°C) over a Ni²⁺-resin affinity chromatography column (Prochem, USA). Such obtained Syn-LOV1 protein was practically pure and was used for further studies without additional purifications.

- 2 Truncated proteins.** For generation of a protein fragment LOV-GGDEF from Syn-LOV1 (aa 1–310), this part was amplified by PCR from the full-length encoding DNA, using the primers: 0188-forward and 5'-GGCACCAGAGCGTTTCGAGACTGAGGT-GACCTTGTTGCTGCG (0188-GGDEF-reverse); The two fragments LOV-GGDEF-EAL (aa 368–929) and LOV-GGDEF (aa 368–660) from Syn-LOV2 were amplified by PCR from the full-length DNA, using the following primers separately: 5'-CAG-GGACCCGGTATGATTGCCCGTCCTATGGTGC (1355-LOV-forward), 1355-reverse; and 1355-LOV-forward, 5'-GGCACCAGAG-CGTTGGTATACCACTGATAATTATTCGAC (1355-GGDEF-reverse). Again, the conserved sequences used for direct cloning into pET52 3C/LIC are shown in bold. All the truncated proteins are furnished with a C-terminal His₈-tag. Further procedures, e.g. cell growth, L-arabinose/IPTG induction, cell harvest and protein purification were performed in the same way as described for the full-length protein (see above).

Cloning was verified by full-length sequencing of the final constructs. MALDI spectra of purified proteins were measured with an ABI Voyager DE Pro MALDI-TOF, using Sina and DHB as matrix.

Photochemistry and thermally driven reactions. The various LOV-domain-containing recombinant proteins were BL-irradiated as described (15). Temperature-controlled (20°C) thermal recovery kinetics was followed using a Shimadzu UV-2401PC UV-Vis recording spectrophotometer.

Enzyme activity assay. Cyclic di-GMP was purchased from Biolog (Bremen, Germany); other nucleotides (GTP, GMP and NAD⁺) were obtained from Sigma-Aldrich (Munich, Germany). Enzymatic assays were performed at 25°C in a water bath. The standard buffers for both PDE and diguanylate cyclase (DGC) were as follows: 50 mM Tris-HCl (pH 7.5, 8.0 and 8.5 separately for different assays), 0.5 mM EDTA, 50 mM NaCl, 5 mM MgCl₂, 5 mM MnCl₂ and the appropriate

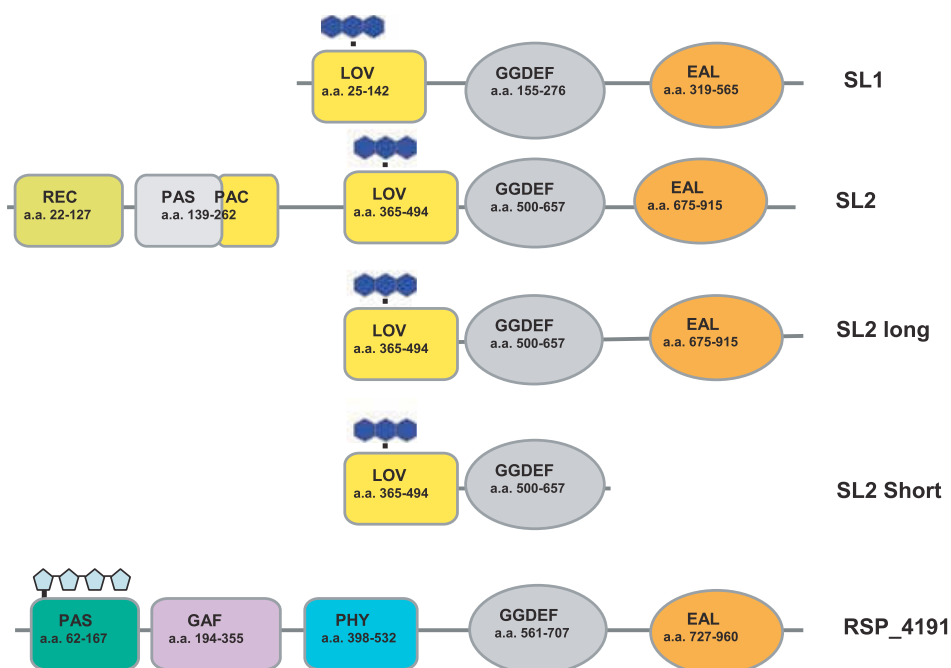


Figure 1. Domain architecture of various constructs of the light-regulated LOV-GGDEF-EAL proteins from *S. elongatus*. The bottom line (RSP_4191) refers to the red light-regulated GGDEF-EAL protein described by Tarutina *et al.* (14).

nucleotide substrate at a concentration of 150 μM . A potential dependence from the metal cation concentration of the enzymatic activities of the fragments with both GGDEF and EAL motifs were controlled in the same buffer without MgCl_2 or MnCl_2 . In some cases, a double-concentrated standard buffer was used instead. The proteins were kept in the dark overnight before the enzymatic reaction was investigated, and the portion used for the light state activity was irradiated for 5 min in BL or white light before beginning the assays. The light was kept on during the whole process. The reactions were started by the addition of enzymes (different protein constructs with final concentration of 10 μM) into two samples (one in the dark and one under BL irradiation). Both samples contained the same amounts of substrates and buffer. After a certain time period (0, 30, 60 min), 100 μL aliquots were withdrawn from the appropriate reaction. For the PDE assays, 5 μL CaCl_2 (200 mM) was added to each aliquot to stop the reaction and the aliquots were placed in boiling water for 3 min. After centrifugation at 18 600 g for 10 min, the supernatants were filtered through a Microcon YM3 centrifugal concentrator (13 000 rpm, 1 h; Millipore, Billerica, MA, USA; MWCO 3000 Da), and the nucleotides were directly analyzed by reversed-phase HPLC (16).

Binding assays. Binding of GTP to SL2 and binding of c-di-GMP to SL1 were tested in a microcalorimetry device (VP-ITC; MicroCal Northampton, MA). Concentrated solutions of GTP and c-di-GMP were titrated into the reservoir containing either SL2 or SL1. The principal set-up for isothermal titrations has been described recently (17).

HPLC conditions. An identical amount of NAD^+ (300 μM , 10 μL to each aliquots) was added as a reference. Ten μL of each sample was injected into a HPLC system (Shimadzu). Separation was performed with a reverse phase column (Phenomenex Luna 5 μC 18 column, 125 \times 4.6 mm) at a flow rate of 0.8 mL min^{-1} employing a gradient program described previously (18). For quantification, a Shimadzu SPD 10AV detector was employed.

RESULTS

The proteins

The genome of *S. elongatus* PCC 7942 contains two open reading frames encoding potential BL-regulated GGDEF-EAL

enzyme activities (Synpcc7942_0188 and Synpcc7942_1355). Synpcc7942_0188 codes for a protein (SL1) of 578 amino acids that shows a short N-terminal extension (aa 1–24), followed by a typical LOV domain (aa 25–139), a GGDEF (aa 155–276) and an EAL (aa 319–565) domain. The LOV domain (as that of SL2, *vide infra*) exhibits all salient features of these BL-sensing FMN-binding photoreceptors, including the adduct-forming cysteine (position 73), directly followed by one of two arginines (position 74) that establish electrostatic interaction with the phosphate group of the FMN chromophore (Fig. 1). As mentioned in the Introduction, in at least one case (BphG1 from *R. sphaeroides*) truncated constructs had to be prepared to demonstrate light-regulated enzyme activity. Similar constructs were also made for the proteins investigated here: SL1 was generated as truncated protein, consisting only of the LOV-GGDEF domains (aa 1–314).

The domain structure of SL2 turned out to be more complex. Synpcc7942_1355 encodes a protein of 929 amino acids, consisting of a CheY-type response regulator (10) (aa 10–124), followed by two PAS domains (aa 137–360), before the above mentioned motif LOV-GGDEF-EAL is found. The full-length protein could not be expressed in soluble form, even if expression systems were changed and the expression parameters were varied. For that reason, two truncated constructs were generated, SL2-L (LOV-GGDEF-EAL, aa 368–929) and SL2-S (LOV-GGDEF, aa 368–660).

A comparison of the GGDEF and EAL domains of both proteins revealed for the two domains of SL1 deviations from the conserved sequence and a lack of amino acids essential for the enzymatic activity. In this protein, the GGDEF motif is strongly altered (HLNHHQF). In contrast, inspection of the SL2 sequence confirms its classification, showing a high degree of conservation for the essential amino acids (RIGGDEF at positions 575–581). A more detailed view on the EAL domains



Figure 2. Sequence alignment of EAL domains from *S. elongatus* (this work) to the EAL domain from PdeA1 of *Gluconacetobacter xylinus*. PdeA1 has an enzymatically active EAL domain. The multiple alignment was generated using Clustal W 2 (EMBL-EBI). Residues identical in more than 80% of active EAL domains are marked in yellow; residues conserved in all active EAL domains are marked with red asterisks in the consensus line. Positions with similar residues in all active EAL domains are marked in gray (16).

yields similar results, such that variations to the conserved sequence motifs are found for SL1, whereas for SL2 all amino acids essential for phosphodiesterase activity can be identified (Fig. 2).

Photochemistry and thermal recovery kinetics of the LOV domains

All three proteins, SL1, SL2L and SL2S (L,S, long, short constructs, respectively; see Fig. 1) showed a chromophore-to-protein ratio of close to one, the typical three peaked absorption spectrum ($\lambda_{\max} = 447$ nm) of a LOV-domain protein and the known photochemistry (Fig. 3): BL irradiation generated a hypsochromically shifted intermediate that

reconverted thermally into the parent state. However, the recovery kinetics varied by more than a factor of 2. Whereas SL1 showed a fast dark recovery ($\tau_{\text{rec}} \sim 284$ s), the SL2S and the SL2L proteins returned slower to the dark state, irrespective of the extent of truncation: $\tau_{\text{rec}} = 608$ s and $\tau_{\text{rec}} = 686$ s, respectively. All measurements were performed at 293 K.

Enzymatic activity

In all cases, where soluble proteins could be obtained, enzyme activity assays were performed. However, even these soluble proteins showed only limited stability and in some cases started to aggregate within 1 h at room temperature.

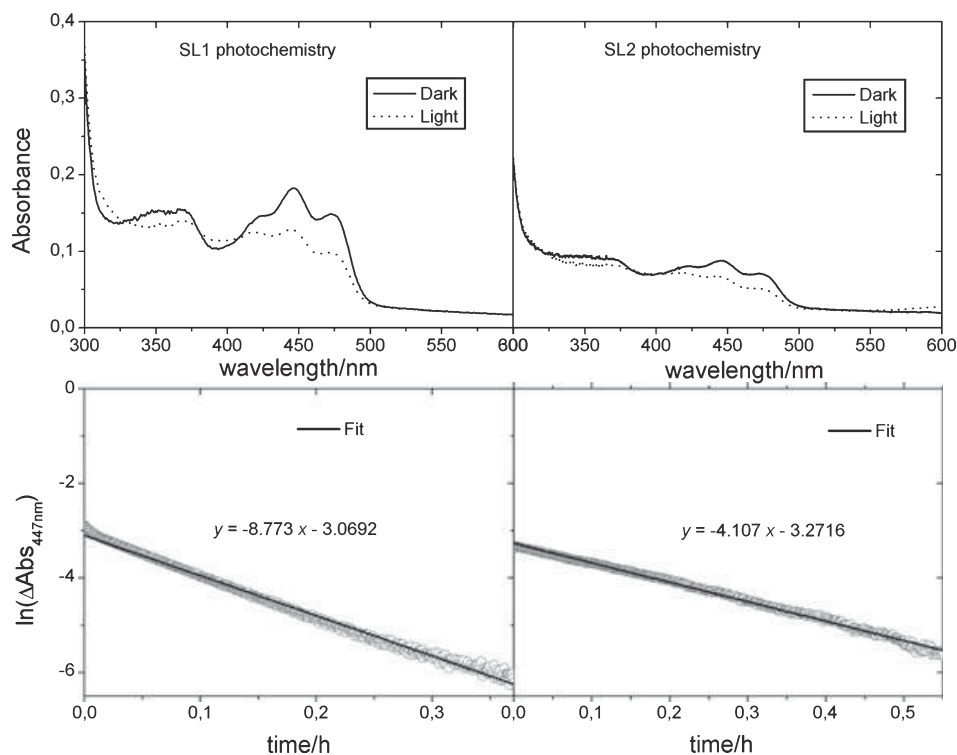


Figure 3. Photochemistry of SL1 and SL2.

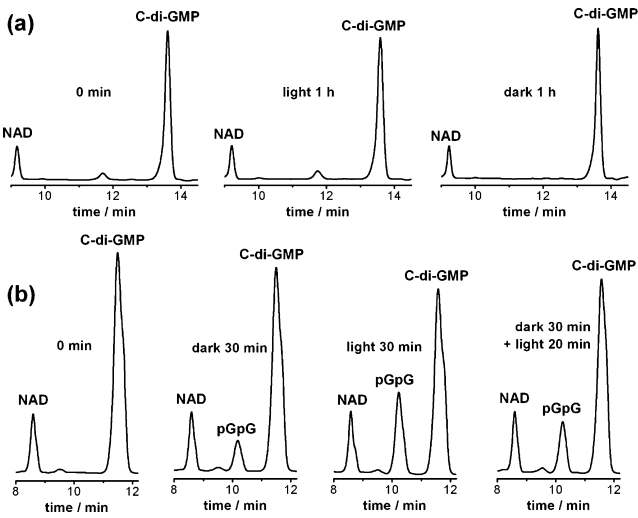


Figure 4. High-pressure liquid chromatograms showing the progression of c-di-GMP hydrolysis for (a) SL1, demonstrating the lack of activity, and for (b) SL2L. For more details, see Table 1.

GGDEF assays were performed under various conditions following published protocols (see Materials and Methods). Assays were always performed at two different pH values, 7.5 and 8.5, respectively, and were repeated several times. In some cases, a double concentrated buffer was used that seemed to improve the stability of the protein in this experiment. However, even after changing the assay conditions, no c-di-GMP formation could be observed (see HPLC analyses and comparison to references compounds, Fig. 4).

No phosphodiesterase activity could be detected for the full-length protein SL1, even when several experimental parameters were changed. When the SL2L construct was investigated, no enzymatic activity was observed at pH 7.5 (even with the presence of Mg^{2+} and Mn^{2+} ions, as was reported for other proteins of this type). However, when the pH-value was adjusted to 8.5 in the presence of Mg^{2+} and Mn^{2+} ions, c-di-GMP hydrolysis could be determined, and this activity could be increased by BL (Fig. 4 and Table 1).

For several enzymes showing these sequence motifs, an effect of GTP- or c-di-GMP addition has been reported. We investigated a potential binding of these two compounds (GTP to SL2 and c-di-GMP to SL1) by microcalorimetry titrations (see Materials and Methods section), but did not find significant binding.

DISCUSSION

Cyclic-di-GMP is an important prokaryotic second messenger involved in the regulation of cellular functions, such as biofilm formation, motility and virulence. Up to now, this signaling molecule is only known to be present in bacteria but not in eukaryotes or archaea (12,13).

Our data presented here link a LOV-domain-mediated, BL-sensing to the intracellular regulation of this bacterial second messenger. The LOV domains of both proteins exhibit fairly rapid dark recovery processes in comparison with most other prokaryotic LOV domains which probably explains the relatively low increase in enzyme activity upon irradiation: even though an overall conversion into the light state of more than 50% can be achieved for all molecules in a given experiment, each single molecule has a relatively limited time to remain in the lit state before it is converted back into the dark state (and will be photo-activated again). Accordingly, one might assume a higher enzymatic activity in a hypothetical pure (100%) light state.

It should also be noticed that SL2 shows a c-di-GMP hydrolysis activity already in the dark that is doubled upon illumination. This allows assuming contributions of additional regulatory factors, similar as for the GGDEF domains, which could not be activated by illumination. This finding is in line with literature reports that demonstrate the presence of an inactive GGDEF domain being essential for an EAL domain to achieve its enzymatic activity (19). The full-length SL2 protein carries at its N-terminal end a CheY type response regulator and another PAS domain, although no obvious cofactor-binding motif is found for the latter. Receptors for the detection of environmental stimuli are often organized in signaling complexes (*e.g.* the “stressosome” of *Bacillus subtilis* [20]). One might thus propose that these two proteins interact with other receptors via their GGDEF domains. In addition, one should keep in mind that PAS domains quite frequently are found as dimerization/oligomerization motifs in multimeric complexes, allowing a cross-talk between various receptors and an integration of various external stimuli (21).

The SL1 protein might have different functions rather than directly controlling the concentration of c-di-GMP. There are indeed many GGDEF/EAL proteins that show other functions, as, *e.g.* LapD and YcgF (22,23). LapD from *Pseudomonas fluorescens* has a degenerate EAL domain, which is not active in PDEA function, but can bind c-di-GMP and trigger

Table 1. HPLC analyses and contents’ comparison for different compounds

	0 min (mV·min)	Dark 30 min	Light 30 min	D30 min + L20 min
NAD ⁺	0.371	0.392	0.365	0.389
C-di-GMP	2.464	2.287	1.857	2.199
C-di-GMP conc. normalized to NAD ⁺ standard (Dark)	2.603	2.287	1.994	2.216
pGpG	0	0.280	0.673	0.455
pGpG conc. normalized to NAD ⁺ standard (Dark)	0	0.28	0.723	0.460

Given are the peak integrals (mV·min). The amount of NAD⁺ was used as a reference to compare other compounds in different samples. 0 min is the starting point of the assay. Two different assays were performed in parallel, one in dark and the other under blue light (BL). After 30 min, the sample under BL and half of the sample in dark were withdrawn from the reaction and stopped. The other half of the sample from dark incubation was then given BL for another 20 min.

an inside-out signaling pathway to regulate the function of LapD at its periplasmic part. This periplasmic part is a HAMP domain that has been demonstrated to modulate biofilm formation (23). A similarly interesting protein is YcgF from *E. coli*: this protein has an N-terminal photochemically active, BL-sensing BLUF domain and a C-terminal EAL domain, which shows no PDEA activity. It has been proven that YcgF can interact under BL with the MerR-like repressor YcgE and can release YcgE from its operator DNA. This in turn activates a regulon responsible for biofilm formation under cold or starvation conditions (22). Whereas YcgF does not show PDEA activity, but is involved in the regulation of DNA transcription (24), its ortholog from *Klebsiella pneumoniae* (BlrP1) exhibited a light-induced increase of its enzymatic activity (25).

Some more cases reported in the literature for partial or complete loss of function for either of the GGDEF or EAL domains should be presented here to emphasize the functional variability to similar proteins. GGDEF and EAL domains are often present together in one protein, and normally only one activity (DGC or PDEA) prevails; however, the inactive domain is essential for the activity of the active domain (19). A well-studied case is the GGDEF-EAL composite protein CC3396 from *Caulobacter crescentus* that has both domains in tandem; however, the second glycine in its GG(D/E)EF motif has been replaced by a glutamic acid. Thus, CC3396 cannot perform the DGC function, but its GGDEF domain has conserved its GTP-binding capacity, thus activating the EAL domain through lowering the K_m of c-di-GMP (11,25,26). A similarly unexpected function shows BphG1 from *R. sphaeroides* with both a GGDEF and an EAL domain (see above). This protein also possesses an N-terminal light-sensing phytochrome domain, and together with its GGDEF and EAL domains, it joins detection of red light to the regulation of c-di-GMP concentration. BphG1 as full-length protein showed a light-independent PDEA activity, but light-dependent regulation of the DGC function could only be demonstrated after the EAL domain was removed (14).

GGDEF/EAL domain(s) often team up with other sensory or regulatory domains, such as GAF, PAS, HAMP, HTH (helix turn helix) motifs or the receiver domain from a response regulator. This indicates that the cellular c-di-GMP level may be regulated by many input signals, such as light, oxygen, redox potentials and phosphorylation of particular proteins (11).

Acknowledgements—This work was supported by the Deutsche Forschungsgemeinschaft (FOR526, to Z.C. and A.L.) and by the Erasmus student exchange program of the European Community (to E.L.). The financial support of the Max-Planck-Society is also gratefully acknowledged.

REFERENCES

- Bailey, S. and A. Grossman (2008) Photoprotection in cyanobacteria: Regulation of light harvesting. *Photochem. Photobiol.* **84**, 1410–1420.
- Goosen, N. and G. F. Moolenaar (2008) Repair of UV damage in bacteria. *DNA Repair* **7**, 353–379.
- Jefferson, K. K. (2004) What drives bacteria to produce a biofilm? *FEMS Microbiol. Lett.* **236**, 163–173.
- Friedberg, E. C. (2002) The intersection between the birth of molecular biology and the discovery of DNA repair. *DNA Repair* **1**, 855–867.
- Redmond, R. W. and J. N. Gamlin (1999) A compilation of singlet oxygen yields from biologically relevant molecules. *Photochem. Photobiol.* **70**, 391–475.
- Losi, A. (2007) Flavins-based blue-light photosensors: A photobiophysics update. *Photochem. Photobiol.* **83**, 1283–1300.
- Losi, A. and W. Gärtner (2008) Bacterial bilin- and flavin-binding photoreceptors. *Photochem. Photobiol. Sci.* **7**, 1168–1178.
- Losi, A. (2004) The bacterial counterparts of plant phototropins. *Photochem. Photobiol. Sci.* **3**, 566–574.
- Christie, J. M. (2007) Phototropin blue-light receptors. *Annu. Rev. Plant Biol.* **58**, 21–45.
- Stock, A. M., V. L. Robinson and P. N. Goudreau (2000) Two-component signal transduction. *Annu. Rev. Biochem.* **69**, 183–215.
- Tamayo, R., J. T. Pratt and A. Camilli (2007) Roles of cyclic diguanylate in the regulation of bacterial pathogenesis. *Annu. Rev. Microbiol.* **61**, 131–148.
- Hengge, R. (2009) Principles of c-di-GMP signalling in bacteria. *Nat. Rev.* **7**, 263–273.
- Römling, U. and D. Amikam (2006) Cyclic di-GMP as a second messenger. *Curr. Opin. Microbiol.* **9**, 228.
- Tarutina, M., D. A. Ryjenkov and M. Gomelsky (2006) An unorthodox bacteriophytochrome from *Rhodobacter sphaeroides* involved in turnover of the second messenger c-di-GMP. *J. Biol. Chem.* **281**, 34751–34758.
- Cao, Z., V. Buttani, A. Losi and W. Gärtner (2008) A blue light inducible two-component signal transduction system in the plant pathogen *Pseudomonas syringae* pv. tomato. *Biophys. J.* **94**, 897–905.
- Schmidt, A. J., D. A. Ryjenkov and M. Gomelsky (2005) The ubiquitous protein domain EAL is a cyclic diguanylate-specific phosphodiesterase: Enzymatically active and inactive EAL domains. *J. Bacteriol.* **187**, 1774–1781.
- Sharda, S., M. S. T. Koay, Y.-J. Kim, M. Engelhard and W. Gärtner (2009) A non-hydrolyzable ATP derivative generates a stable complex in a light-inducible two-component system. *J. Biol. Chem.* **284**, 33999–34004.
- Ryjenkov, D. A., M. Tarutina, O. V. Moskvina and M. Gomelsky (2005) Cyclic diguanylate is a ubiquitous signaling molecule in bacteria: Insights into biochemistry of the GGDEF protein domain. *J. Bacteriol.* **187**, 1792–1798.
- Jenal, U. and J. Malone (2006) Mechanisms of cyclic di-GMP signaling in bacteria. *Annu. Rev. Genet.* **40**, 385–407.
- Kim, T. J., T. A. Gaidenko and C. W. Price (2004) A multicomponent protein complex mediates environmental stress signalling in *Bacillus subtilis*. *J. Mol. Biol.* **341**, 135–150.
- Kim, S. K., J. T. Mason, D. B. Knaff, C. E. Bauer and A. T. Setterdahl (2006) Redox properties of the *Rhodobacter sphaeroides* transcriptional regulatory proteins PpsR and AppA. *Photosynth. Res.* **89**, 89–98.
- Tschowri, N., S. Busse and R. Hengge (2009) The BLUF-EAL protein YcgF acts as a direct anti-repressor in a blue-light response of *Escherichia coli*. *Genes Dev.* **23**, 522–534.
- Newell, P. D., R. D. Monds and G. A. O'Toole (2009) LapD is a bis-(3',5')-cyclic dimeric GMP-binding protein that regulates surface attachment by *Pseudomonas fluorescens* Pf0-1. *Proc. Natl Acad. Sci. USA* **106**, 3461–3466.
- Barends, T. R. M., E. Hartmann, J. J. Griese, T. Beitlich, N. V. Kirienko, D. A. Ryjenkov, J. Reinstein, R. L. Shoeman, M. Gomelsky and I. Schlichting (2009) Structure and mechanism of a bacterial light-regulated cyclic nucleotide phosphodiesterase. *Nature* **458**, 1015–1018.
- Christen, M., B. Christen, M. G. Allan, M. Folcher, P. Jenö, S. Grzesiek and U. Jenal (2007) DgrA is a member of a new family of cyclic diguanosine monophosphate receptors and controls flagellar motor function in *Caulobacter crescentus*. *Proc. Natl Acad. Sci. USA* **104**, 4112–4117.
- Christen, M., B. Christen, M. Folcher, A. Schauerte and U. Jenal (2005) Identification and characterization of a cyclic di-GMP-specific phosphodiesterase and its allosteric control by GTP. *J. Biol. Chem.* **280**, 30829–30837.

V. General Discussion

In higher plants, LOV-domain containing proteins act as photoreceptors to regulate many different physiological responses, such as phototropism, chloroplast relocation, leaf opening and stomatal opening^{1,2}. Most of these plant proteins possess a C-terminal serine/threonine kinase domain as the downstream effector partner for the sensory LOV domain³.

Besides plants, the LOV signaling module can also be found widely distributed in green algae, archaea and bacteria (including some non-photosynthetic and/or non-phototactic bacteria)⁴. Unlike the phototropin-like proteins from plants, these prokaryotic LOV-containing proteins possess quite diverse output domains like kinases, phosphodiesterases, regulators of stress-responsive sigma factors (such as the STAS domain in YtvA) and many different transcription factors^{4,5}. They also carry only one LOV domain – in contrast to the plant tandem arrangement of two LOV domains. But up to date, only a few of these blue light sensors have been linked to a cellular function. YtvA from the soil bacterium *Bacillus subtilis* is by far the best characterized bacterial LOV-containing protein, it serves as a positive regulator of the σ_B stress response pathway⁶. The *in vivo* present amount of YtvA (which can be as low as 5-10 copies per cell) can regulate one of the σ_B -controlled promoter activities under blue light or white light, but these effects disappear under red light or in dark⁷.

Among other blue light-regulated physiological functions in prokaryotes, a photo-sensory LOV histidine kinase from the mammalian pathogen *Brucella abortus* has been proven to be necessary for the proliferation in a macrophage infection model, and this effect can be regulated by light exposure too⁸. The LOV kinase (LovK/LovR) two-component system from *Caulobacter crescentus* is involved in the regulation of light-dependent cell attachment⁹. Two short LOV proteins from *Pseudomonas putida* have been demonstrated to up-regulate a blue light

dependent iron-starvation response⁴. Together with downstream-located helix-turn-helix (HTH)-protein encoding genes, these LOV-domain proteins from *P. putida* may represent an interesting light-regulated gene expression system.

Although LOV proteins are important in different light-dependent biological functions, in most cases the molecular mechanisms behind the signal transduction from light sensing to physiological regulation remain uncharacterized. The following paragraphs will elaborate in more detail the biochemical and structural basis of how light signals of similar origin could be coupled to various regulatory functions in several bacterial LOV proteins.

5.1 Domain-domain interactions in YtvA-LOV and YtvA full-length proteins

(The publications discussed in this chapter can be found in Chapters 2.1, 2.2 and 2.3)

Bacillus subtilis, also called grass bacillus, is a Gram-positive bacterium commonly found in soil. Under extreme environmental conditions it can form a protective endospore to tolerate the environmental stress¹⁰. In *B. subtilis*, the expression of the general stress regulon is controlled by the alternative transcription factor σ_B , which can be activated by a serine-threonine kinase RsbT through a stress-signaling pathway. This kinase activity is regulated by a family (RsbR) of paralogous proteins including five negative regulators¹¹ and the positive regulator YtvA (Figure 5-1)⁶.

All the RsbR family proteins bear a similar STAS domain. But in contrast to the other regulators, YtvA-STAS lacks the phosphorylatable serine and the conserved threonines that are critical for the function. YtvA also possesses an N-terminal sensory LOV domain that binds an FMN molecule as chromophore and can form a photo-adduct with the critical residue Cys62 upon blue light illumination. This residue Cys62 in the LOV domain is also necessary for YtvA to exert its positive regulatory role in the absence of other stress signals⁶, which demonstrated that the light signal in fact acts as a stimulus and is integrated into the modulation network in response to the environmental stress.

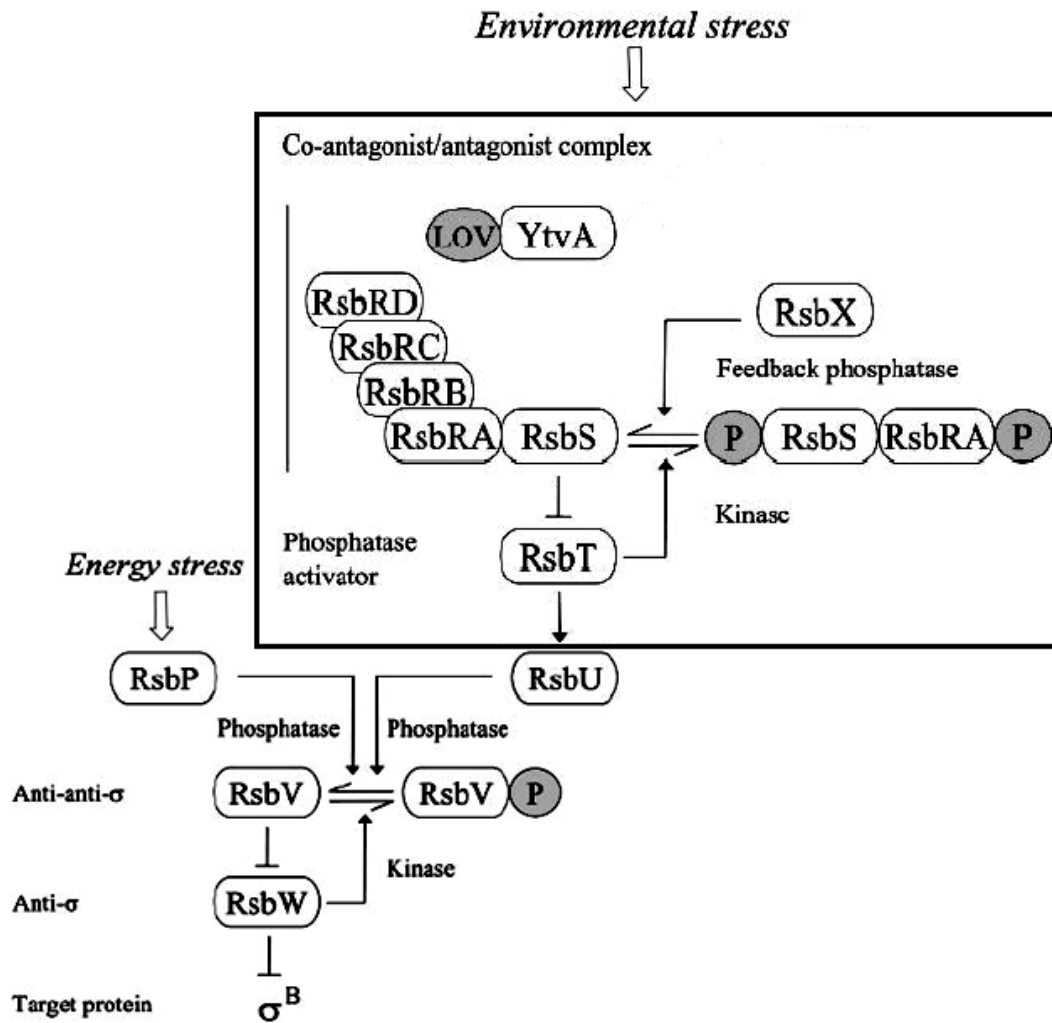


Figure 5-1: Model of the σ_B signal transduction network with two independent signaling pathways that converge on RsbV anti-anti- σ and RsbW anti- σ , the direct regulators of σ_B activity⁶. RsbS and RsbT in the environmental stress box are paralogs of RsbV and RsbW, respectively. RsbRA, RsbRB, RsbRC, and RsbRD can form a large signaling complex with RsbS and inactivate the RsbT phosphatase regulator. YtvA is also part of this signaling complex⁶.

For the STAS domain, another STAS-containing protein SPOIIAA from *Bacillus subtilis* has already been proven to bind GTP and ATP and to have a weak NTPase activity¹². The phosphorylation of a conserved serine in the loop (Figure 5-2 in purple) between D β and E α can abolish the NTPase activity; the high conservation of this particular loop in many different STAS domains suggests

that this domain could be a general NTP binding domain with the β -scaffold to be the possible accommodation space for the NTP molecule¹³.

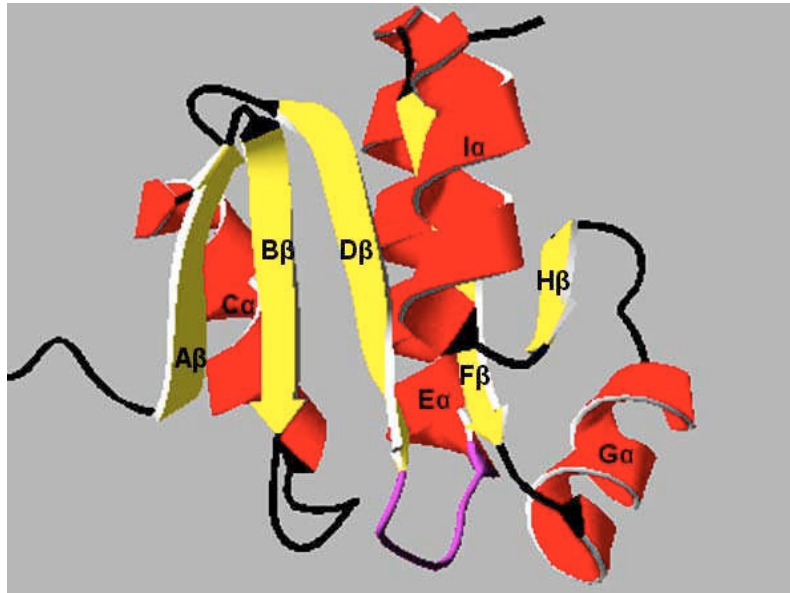


Figure 5-2: 3D-Ribbon structure of the STAS domain Tm1081 from *Thermotoga maritima* (pdb entry: 3F43). The conserved loop that is possibly involved in NTP binding is shown in purple.

Although lacking the phosphorylatable serine, YtvA shows a potential phosphate binding motif (DxxG) in that conserved D β -E α loop (D₁₉₃LSG in YtvA). Recently it has in fact been proven that YtvA possesses an unspecific NTP (GTP and ATP) binding function, and the formation of a photo-adduct in the LOV domain introduces a dark-light reversible change in YtvA's binding activity (Figure 5-3)¹⁴. This suggests that light-induced conformational changes in the LOV core can be transmitted through certain intra-protein interactions to the NTP binding site in STAS domain.

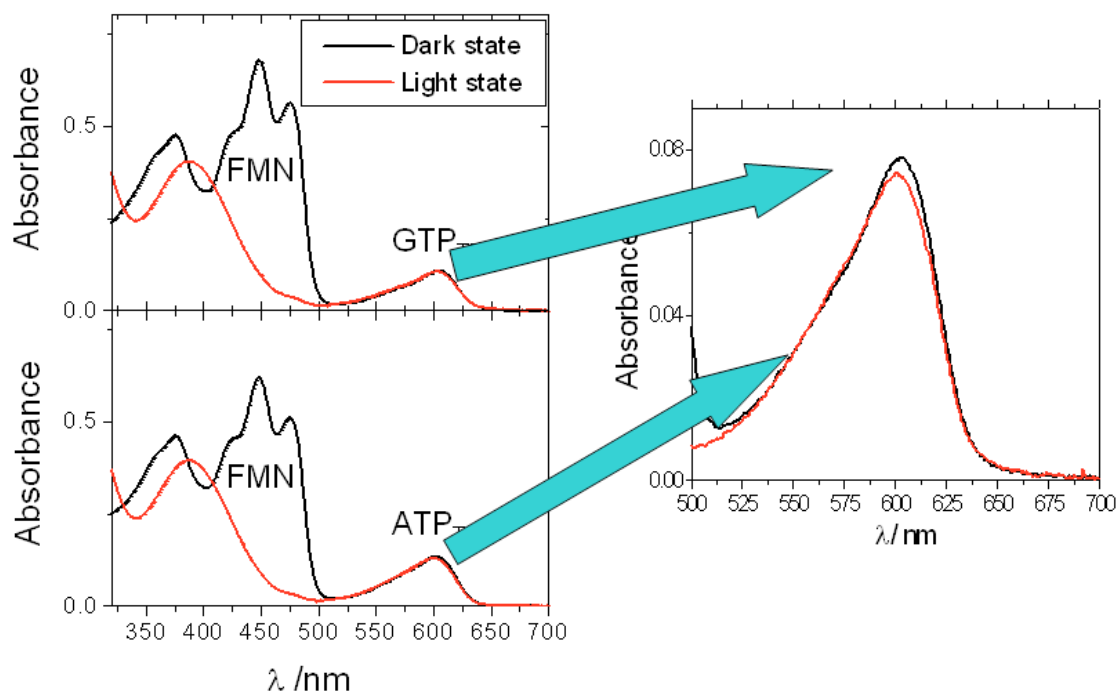


Figure 5-3: YtvA's binding activity of a fluorescent GTP/ATP-analogue; blue light illumination can introduce a dark-reversible blue-shift in the absorption spectrum of GTP/ATP derivatives¹⁴. The modification in the NTP-molecule shows an absorption in the range around 600 nm and a strong further red-shifted fluorescence.

It is now quite clear that YtvA as a blue light sensor can regulate the σ_B activity and intra-protein communication. From the molecular point of view, however, the signal relay pathway from the light sensing core to the STAS domain and then to the downstream partners is still unidentified. Due to the lack of structural information of full-length YtvA, it is necessary to investigate the protein surface involved in domain-domain interactions and STAS activation.

5.1.1 The competitive interface for LOV-LOV dimerization and interdomain interactions

In many sensory proteins with the conserved PAS fold, both, a homo- or hetero-dimerization state and also ligand binding are important processes to affect inter/intra-protein interactions, which, in turn, regulate protein functions¹⁵. Besides the light induced conformational changes in the LOV core, currently the dimerization states of different LOV domains are controversially under debate, especially when we consider those LOV domains in the signal transmission processes that affect their downstream partners.

As described in chapter 2.1, phot1-LOV1 tends to form a dimer, whereas phot1-LOV2 prefers to stay as a monomer¹⁶. Combined with the fact that phot1-LOV2 has a higher quantum yield in its photo-cycle than phot1-LOV1¹⁷, it is then plausible that LOV1 might be responsible for dimerization and LOV2 might act as the predominant light sensing domain, providing a possible explanation for the organization of two tandem LOV domains in phototropin^{16,17}. In contrast with the result mentioned above, the small angle X-ray scattering experiments showed that phot1-LOV2 has a tendency to dimerize, whereas only phot2-LOV2 is monomeric. Recently, with the help of time-resolved techniques such as pulsed thermal grating, a transient dimerization state of phot1-LOV2 (including the N-terminal helical cap and the Ja-linker) with a time constant 300 μ s upon light activation has been detected¹⁸. The authors from the same group suggested that the presence of the Ja-linker inhibited the dimer formation in dark state. A light induced unfolding of the LOV2- Ja-linker helical construct with a time constant of 1 ms has also been observed^{18,19}. A further transient thermal lensing (TrL) experiments demonstrated that this unfolding is caused by a dissociation of the Ja-linker from the LOV core, and the time constant of this dissociation has been determined as 300 μ s²⁰. The similar time constants between the transient dimerization state and the dissociation of Ja-linker might imply that the blue-light induced conformational changes in the LOV core can cause unfolding of the Ja-

linker and affect the possible hydrophobic interactions between J α -linker and the LOV core²¹.

The sequence identity level among different LOV domains is quite high, but there are still some differences at several crucial positions. This may account for their diverse signal transmission mechanisms as well as for the different oligomerization modes. As discussed in Chapter 2.1, the central β -scaffold might be involved in both the LOV-LOV dimerization and the signal transmission from the LOV core to the effector domain. This has partially been confirmed by the crystal structure of a YtvA-LOV dimer, in which YtvA also displayed an extended β -scaffold (H β and I β) with a more hydrophobic patch (Figure 5-4)²¹. On the other hand it was previously noticed that in YtvA the J α -helix has more polar residues than other LOV domains and that this helix is connected to the LOV core by a shorter loop²¹⁻²³. It is therefore conceivable that the J α -helix can not readily cover the central β -scaffold and the hydrophobic residues on the outer β -sheets are exposed for the inter/intra-protein interactions.

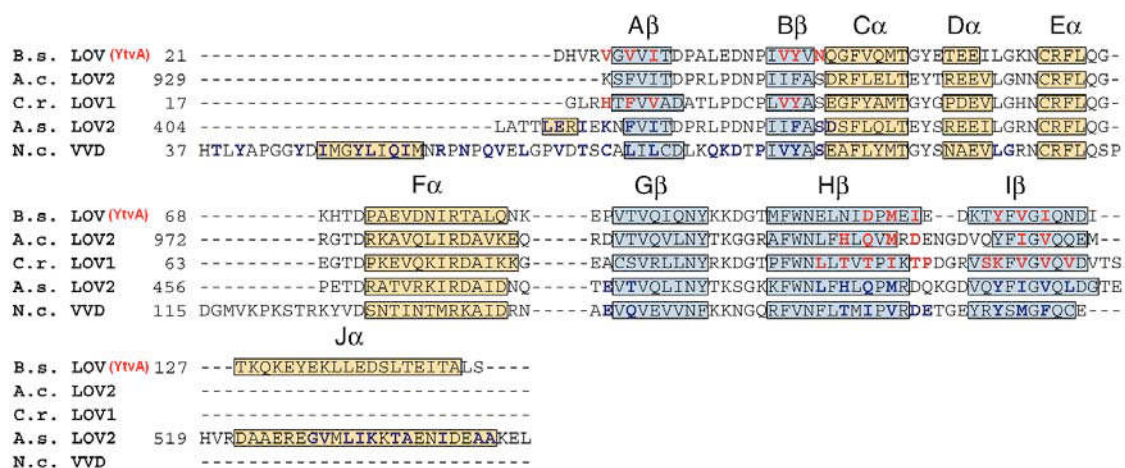


Figure 5-4: Sequence alignment of YtvA-LOV domain and other LOV domains with known 3-D structure. The sequence of α -helices is highlighted in yellow boxes and β -strands in blue boxes. Residues in bold red are involved in homodimeric contacts in the crystal structure; residues in bold blue are involved in intra-protein interactions between the LOV core and C-terminal or N-terminal extensions²⁴⁻²⁸. Abbreviations: *B. subtilis* (B. s.), *Avena sativa* (A. s., oat), *Adiantum capillus-veneris* (A. c., fern), *Chlamydomonas reinhardtii* (C. r.), *Neurospora crassa* (N. c.)²¹.

In the full length YtvA protein, as shown in Chapter 2.1, the protein prefers to stay as a monomer at least *in vitro*. A possible interpretation might be that the J α -linker together with the C-terminal STAS domain acts as a competitor for the LOV-LOV dimerization by blocking the exposed β -sheets. Thus, the dissociation or unfolding of the J α -helix, caused by conformational changes in the LOV core, might make the central β -scaffold accessible for the interactions with the STAS domain. However, unfolding of the J α -helix could not be observed through the CD experiments as shown in Chapter 2.1. In the crystal structure²¹ the J α -helix points to an opposite direction rather than being packed underneath the LOV-core, and also the loss of helical content could not be clearly revealed either when applying circular dichroism measurements²¹.

In summary, the available data from diverse experiments suggest different mechanisms for the signal transmission from the FMN-binding pocket to effector domains, as discussed in Chapter 1.5.2. On the other hand, the central β -scaffold is probably the common interface for different signal transduction processes. In YtvA from *B. subtilis*, the J α -helical linker may also play an important role to regulate the possible interaction between the central β -scaffold of the LOV domain and the STAS domain. Thus, a further mutational study concerning several key positions in both the central β -scaffold and the J α -linker will provide more experimental evidences for the assumption mentioned above. This is discussed in Chapter 2.3 and Chapter 5.1.3. Before the mutational study is presented, a crystal structure of a similar YtvA-LOV domain from *Bacillus amyloliquefaciens* FZB42 will be discussed in following chapter.

5.1.2 The LOV-domain crystal structure of YtvA from *Bacillus amyloliquefaciens* FZB42

For proteins with a conserved PAS domain, not only the dimerization states are controversially under debate, the interfaces involved in dimerization are also quite different. The PAS domains from LOV1-like proteins form the dimer through the canonical PAS central β -scaffold. This mode of dimerization can also be found in other PAS proteins, such as the aryl hydrocarbon receptor nuclear translocator (ARNT)²⁹, hypoxia inducible factor (HIF)³⁰, and KinA histidine kinases^{31,32}.

As discussed in Chapter 2.1 and 5.1.1, YtvA from *B. subtilis* employs the central β -scaffold as the dimer interface too, although the J α helix may also play an important role to regulate potential interactions. In the *B. subtilis* YtvA LOV constructs with an N-terminal cap, this helical cap is also expected to participate in dimerization, but due to the lack of information on the orientation of this cap, this type of dimer could not be modeled in the work from Chapter 2.1.

As described in Chapter 2.2, we could resolve the crystal structure of another YtvA-LOV domain from *Bacillus amyloliquefaciens* FZB42; this protein has 77% identity (201 out of 261 a.a.) with YtvA from *B. subtilis*. In the crystal structure, one finds two molecules in the asymmetric unit as a dimer, and the N-cap α -helix from one monomer has close interactions with both the N-cap helix and the central β scaffold of the other monomer (Figure 5-5).

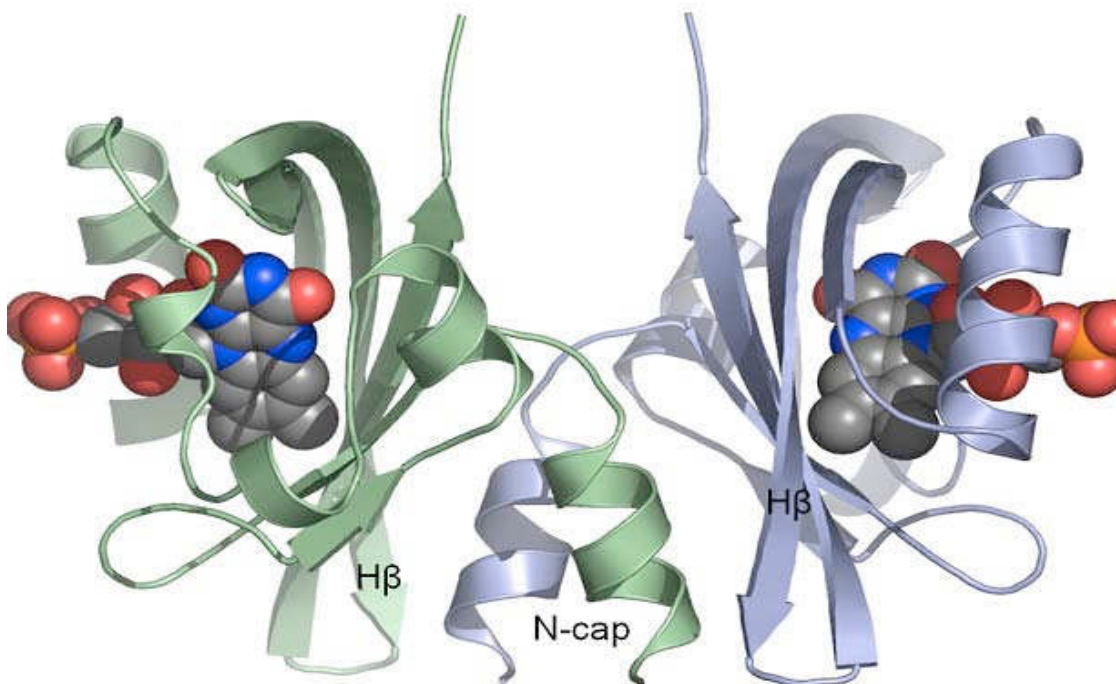


Figure 5-5: 3D-Ribbon structure of the dimer complex of YtvA-LOV from *Bacillus amyloliquefaciens* FZB42. FMN molecules are shown in VDW mode (picture from Dr. Hideaki Ogata).

This N-cap is a conserved amphipathic helix spanning residues 13-22 immediately N-terminal to the LOV core. The alignment in Figure 5-6 demonstrates the similarity between two YtvA-LOV domains with AvNifLf, another PAS protein that forms a dimer through N-cap interactions³³.

		N-cap α-helix	Aβ	Bβ	Cα	Dα	Eα
FZB YtvA LOV	10	-EQLELIKALDHARI	GVVITDPSLEDNPI	IYTNQGFMDMTGYS	SEEILGKNCRFL	QSKE	
YtvA LOV	10	-GQLEVIKKALDHVRV	GVVITDPALEDNPI	IVYVNOGFVQMTGY	ETEELGKNCRFL	QGKH	
AvNifLF	21	ELLPEIFRQTVEHAPI	AIISITDLKAN---	ILYANRAFRITITGY	SSEVLGKNESIL	SNGT	
		*:::*****	:::***	:*::*::*	:***	:*****	:*
		Fα	Gβ	Hβ	Iβ		
FZB YtvA LOV		TDRQQVAKIRKSLTQKE	KITVRLKNVKKDGT	PFWNELNIDPLYVED	---	KLYFVGFKDIT	
YtvA LOV		TDPAEVDNIRTALQNKEP	VTVQIQNYKKDGT	TMFWNELNIDPMEIED	---	KTYFVGIQNDIT	
AvNifLF		TPRLVYQALWGRLAQKKP	WSGVLVNRKDK	TLYLAEELTVAPVLNE	AGETIYYLGMHRDTS		
		*:::***	:*::*	:*::*	:*::*	:*::*	:*::*

Figure 5-6: Sequence alignment of the LOV domains of YtvA-LOV from *B. amyloliquefaciens* FZB42 (FZB YtvA LOV) and *B. subtilis* (YtvA LOV) with the PAS domain of *A. vinelandii* NifL (AvNifLF)³³. Secondary structures are shown in different colors, α-helices in red and β-sheets in blue.

In the complex, the amphipathic N-cap helices interact with each other to form a dimer through a leucine zipper like motif³⁴ being composed of Leu13, Leu15, Ile16, Ala19 and Leu20. In addition, the helix is also packed against the hydrophobic surface of the β -sheets from the opposing monomer³³. These interactions then form a hydrophobic core that can tightly pack the two monomers together. A helical wheel diagram of this FZB YtvA-LOV N-cap helix in comparison with AvNifL³³ demonstrates the similarity between both proteins (Figure 5-7).

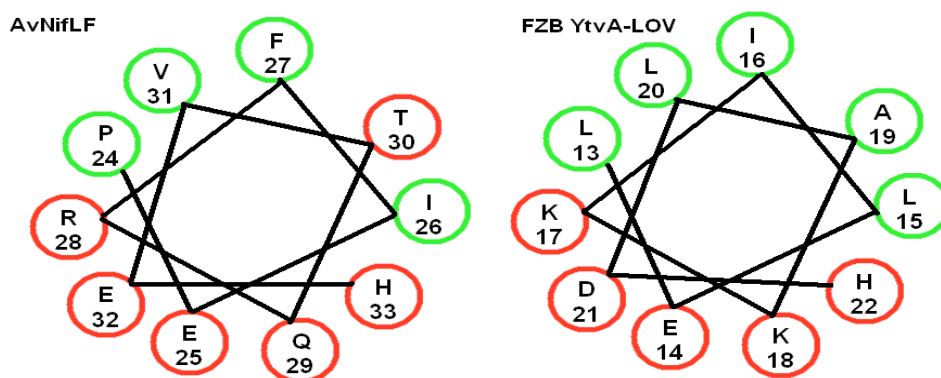


Figure 5-7: Helical wheel diagrams of the N-cap helices from *A. vinelandii* (left) and *B. amyloliquefaciens* (right). Hydrophobic residues are shown in green, hydrophilic ones in red³³.

Besides the FMN-based YtvA-LOV and FAD-based NifL, many other PAS domains also employ the amphipathic N-terminal helix for their dimerization. Such as the oxygen sensor FixL that uses heme as co-factor³⁴ and the heme based phosphodiesterase EcDOS^{31,35}. It has been suggested that the N-cap helix is a common structural dimerization motif of PAS sensors, although the relevance of this motif to the function of these proteins represent still open questions in most cases³¹. For example in AvNifL, structural changes caused by the redox state can be transmitted to the dimerization interface. The binding affinity between monomers can then be altered and the C-terminal domains of NifL can ultimately be regulated by this binding affinity³³.

As discussed in Chapter 2.1, the full length YtvA protein is a monomer in solution under both light and dark state. An final explanation whether the LOV domains can form dimers whereas the full proteins stay as monomer can currently not be given, although the given argument of a competition in case the linker and the STAS domain are present appears plausible. Nevertheless, a more detailed delineation of the inter-domain interactions may still provide important information to our understanding of the relationship between YtvA's structure and its functions. This will be further discussed in next chapter.

5.1.3 The signal transmission pathway between YtvA-LOV domain and YtvA-STAS domain

As mentioned in Chapter 2.1 and 5.1.1, the central β -scaffold of YtvA is probably the common interface for both dimerization and intra-protein interactions; the $\text{J}\alpha$ -helical linker may also play an important role to regulate the possible interaction between the central β -scaffold of LOV domain and the STAS domain. In the crystal structure of both YtvA LOV domains (PDB entry 2PR6 for *B. subtilis* and Chapter 2.2 for *B. amyloliquefaciens*), the $\text{J}\alpha$ -helix is pointing outwards the central β -scaffold²¹, whereas in the structure of *Avena sativa* phot1 LOV2 domain (PDB entry: 2V1B), this $\text{J}\alpha$ -helix is packed on top of the β -sheet³⁶. Up to now, there are no 3-D structure available for full length YtvA, thus we can not say that this $\text{J}\alpha$ -helix is indeed pointing in that direction *in vivo*. This discussion can still provide some indication for our understanding of the signal transmission mechanism in YtvA, which might be different to plant phototropins with respect to the interactions between the central β -scaffold and its partners, either the $\text{J}\alpha$ -helix from the same molecule or the β -scaffold from another monomer.

5.1.3.1 The H β -sheet in the LOV core

A glutamic acid residue (E105) in H β of YtvA-LOV domain acid is conserved only in some bacterial LOV proteins that contain a STAS domain. In other phototropins, this position is usually occupied by a hydrophobic residue⁵. In YtvA,

however, this glutamic acid in YtvA has been proven to play a key role in the signal transmission pathway, as the mutation of this residue to a leucine abolishes the light-induced changes in the absorption spectrum of a non-covalently bound GTP derivative³⁷. *In vivo* experiments have also shown that the same mutant protein (E105L) was locked in a constantly active state and increases the σ B activity³⁸.

A second acidic residue in the same β -sheet, aspartic acid 109, has also been linked to the regulation of both *in vitro* and *in vivo* function of YtvA. This residue is unique in YtvA-like proteins from the bacterial phylum *Firmicutes*. As mentioned in Chapter 2.3, the YtvA D109L mutant has a higher ability to bind GTP, but this binding affinity can not be affected by the illumination, very similar to the situation in the E105L mutant. One has to keep in mind that the purified protein D109L has a lower capability to bind FMN in its LOV core, and consequently, a higher portion of apo-protein is present (it has formerly been shown that the apo-protein of wild type YtvA has a higher affinity to GTP than FMN-loaded YtvA, i.e. GTP can also be bound into the LOV core). *In vivo* experiments showed that the D109L mutant, opposite to E105L, can be locked at a constantly inactive state with respect to the regulation of the σ B activity³⁸. This might be related to the lack of chromophore in this mutant protein; alternatively, it can also be due to the key role of this aspartic acid, which has been suggested to form a hydrogen bond with tyrosine 41 from the other monomer in the YtvA dimeric crystal²¹.

Both E105 and D109 are opposite to the FMN binding pocket and are exposed to the interface between the LOV core and its possible partner domains (either STAS or another LOV). In the crystal structure, E105, together with the whole H β -sheet, propagates the light induced conformational changes to the J α -linker and causes it to bend away from the dimerization interface²¹.

It can be proposed that D109 plays a more direct role in the dimerization; the mutation of this aspartic acid to leucine may break the intermolecular hydrogen

bond between its side chain and the tyrosine 41 from the other monomer^{21,38}. This may suggest that the dimerization of YtvA could indeed be an important step for its proper function. Previous work on STAS domain-containing proteins (RsbS, RsbR paralogs, like YtvA) from *B. subtilis* has proposed that these proteins can form an architecture called “stressosome”, where the STAS domains arrange as dimers to form the core of this stressosome, and the N-terminal domains are connected to these STAS domains through a helical linker region³⁹. Although full length YtvA dimer has not yet been structurally characterized neither *in vitro* nor *in vivo*, the existence of possible dimerization sites in YtvA-LOV domain is still an important information for the signal transmission in the full protein, as discussed in Chapter 5.1.1 and 5.1.2. In a recently constructed 3-D model of YtvA (Figure 5-8)³⁸, the two acidic residues in H β -sheet are both exposed to the dimerization interface.

Leucine 106 in the H β -sheet is conserved in many LOV domain-containing proteins, including all bacterial LOV proteins and plant LOV1 proteins. LOV2 is an exception as it presents a phenylalanine in this position⁵. It has been reported that this leucine undergoes a close interaction with the FMN molecule and thus plays an important role during the photocycle⁴⁰. As mentioned in Chapter 2.3, this leucine, together with the reactive cysteine, holds the FMN molecule in a sandwich-like structure. The mutation of this residue to phenylalanine can also impair the signal transmission from the LOV core to the STAS domain. Although the reason why bacterial LOV proteins “chose” a LOV1-like leucine rather than LOV2 like phenylalanine is not clear, given the fact that L106 locates in H β and has close interactions with both FMN and the other two important residues in H β . This position is no doubt a key position for the signal transmission from the LOV core to the downstream part of the protein.

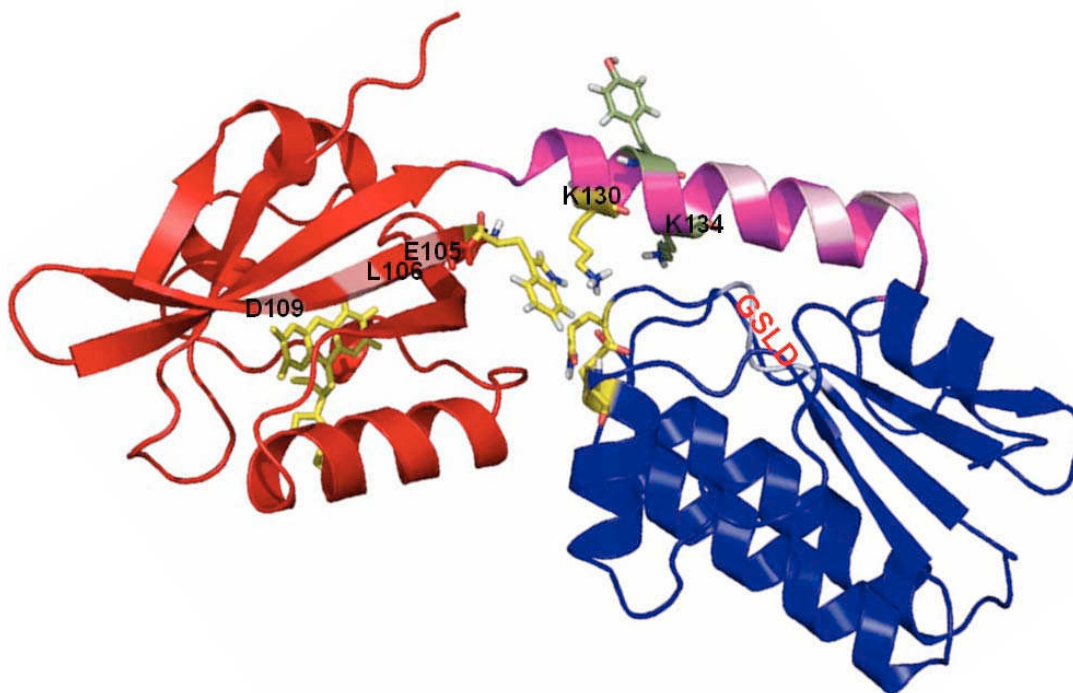


Figure 5-8: Ribbon representation of the 3-D model for YtvA full protein. The LOV domain is in red, STAS domain is in blue and the linker is in purple. The key positions have been labeled³⁸, as also the putative GTP binding site in the STAS domain (DLSG).

5.1.3.2 The J α -Linker region

As mentioned in Chapter 2.3, the J α -Linker region has many polar and charged amino acids, among which two positively charged residues K130 and K134 have been proven to be involved in the signal transmission from the LOV core to the STAS domain. A plausible mechanism are the interactions of these two lysines with E105 and/or D109 in the H β strand. However, given the fact that K134 is not conserved in other LOV proteins, it is less likely for K134 to be directly involved in possible interactions.

If YtvA indeed functions as a monomer *in vivo*, it is very improbable that the linker region will point outwards the LOV core as shown in the crystal structure²¹, because this would be very difficult to connect E105 and D109 with their possible

partners in the linker region or in the STAS domain. In this case the competition between the other monomer and the linker region in the dimeric crystal might be the reason why the linker region is not closely packed against the central β -scaffold.

On the other hand, if YtvA requires a dimer formation for a proper function, residue D109 will most probably play its role in dimerization, and the domain organization showed in Figure 5-8 may be a possible way to map the signal transmission pathway within YtvA. In this model, the linker region is indeed pointing outwards the LOV core; K130 and K134 are pointing towards the STAS domain instead towards the LOV core. The possible interactions between these two residues and the NTP binding loop might be the reason why also the K130A and K134A mutants can interrupt the signal transmission to the NTP binding site³⁸.

Based on the current experimental results, it is still not possible to document which of the two possibilities mentioned above is closer to the reality. This still remains an open question to be confirmed by further investigations.

5.1.3.3 The NTP binding site in the STAS domain

Proteins that can bind and/or hydrolyze nucleoside triphosphates (NTPs) are widely distributed in almost all kingdoms of life; these proteins (NTPases) normally possess structurally conserved NTP binding folds, among which the “P-loop” (phosphate-binding loop) is by far the most popular one. P-loop containing NTPases normally exhibit a conserved α/β sandwich-like fold with an anti-parallel central β -scaffold surrounded by α -helices on both sides⁴¹. Typically, P-loop NTPases bind the β and γ phosphate group of NTP molecule and sometimes can hydrolyze the β - γ phosphate bond of this bound NTP; two highly conserved sequence motifs are responsible for the binding activity: the Walker A motif is a glycine-rich loop between an N-terminal β -sheet and a C-terminal α -helix, the typical sequence of this motif is GxxxxGK(S/T). The Walker B motif is C-terminal

to the Walker A motif. It contains a conserved sequence DxxG and is also preceded by a β -sheet; these two motifs can bind the β and γ phosphate group of the NTP molecule, respectively. In addition, a Mg^{2+} ion is also involved in the binding activity⁴².

The YtvA-STAS domain possesses a DLSG sequence (a.a. 193-196) which has a partial topological and sequence similarity to the Walker B motif, but the Walker A motif is missing in this protein. Besides the DLSG sequence, another GTP-specific binding sequence (N/T)KxD (NKLD, a.a. 226-229 in YtvA) can be found in YtvA, but this sequence is following an α -helix rather than a β -sheet. Thus it is quite reasonable that the DLSG sequence is the key binding site for both GTP and ATP, although this time the binding of NTP could follow another mechanism: the DLSG might be responsible for the binding of the γ phosphate group, whereas the space between the β -scaffold and the two N-terminal α -helices might accommodate the remaining of the NTP molecule¹³.

The result from Chapter 2.3 has shown experimental evidences that the DLSG sequence is indeed quite important for the GTP binding activity. The mutations of D193 and S195 clearly impair the binding ability of YtvA, whereas D193 and G196 are important for the signal transmission from the light sensing LOV core. This result has also partially been confirmed *in vivo*: the mutations of D193 and S195 clearly decrease the σ B activity³⁸.

N201 is another residue that is involved in the light-switched conformational change within GTP binding cavity (as shown by mutagenesis). On the one hand, this residue locates at the end of the conserved NTP-binding loop, it can easily affect the proper fold of the loop. On the other hand, as the model from Figure 5-8 demonstrates, the backbone of N201 can form an intra-molecular hydrogen bond with the side chain of T204, which might stabilize the proper folding of the binding site. *In vivo* experiments have shown that the mutation of T204

destabilizes the protein, and the light-induced responses are also abolished³⁸. In order to confirm this hypothesis, further mutants of YtvA should be produced.

Different to other GTP-binding STAS domains from *B. subtilis*, YtvA-STAS domain does not contain the conserved phosphorylatable serine or threonine, and so far the experimental result has shown that YtvA can not be phosphorylated. Whereas the RsbS and RsbR paralogs need to be phosphorylated by RsbT before they can perform their functions⁶, YtvA has only shown a blue light regulated NTP-binding activity. Therefore it has been proposed that YtvA may serve as a light dependent NTP recruiter for the kinase RsbT, which can then phosphorylate RsbS and other RsbR paralogs³⁸.

Although YtvA with its STAS domain is by far the best characterized bacterial LOV domain-containing protein, it is still not the most popular LOV protein in the prokaryotic world. A histidine kinase with or without the downstream response regulator is the most widely distributed bacterial paradigm that is coupled with diverse sensor domains. A LOV-domain containing histidine kinase from the plant pathogen *P. syringae* pv. *tomato* DC3000 will be discussed in next chapter.

5.2 A blue light inducible two component signal transduction system in bacterial LOV proteins

(The publication discussed in this chapter can be found in Chapter 3)

5.2.1 Two-component signal transduction systems

For an organism, the key to adapt itself to the surrounding environment is to efficiently recognize the changing stimuli and to rapidly regulate gene expression of the cell to fit the new situations. Both, stimuli sensing and gene expression regulation are normally achieved by the cellular signal transduction networks that is composed of many different proteins. In both prokaryotic and eukaryotic cellular signal transduction systems, reversible protein phosphorylation is one of the most important mechanisms to control the proper functions of different proteins, especially for those related in signal transductions⁴³.

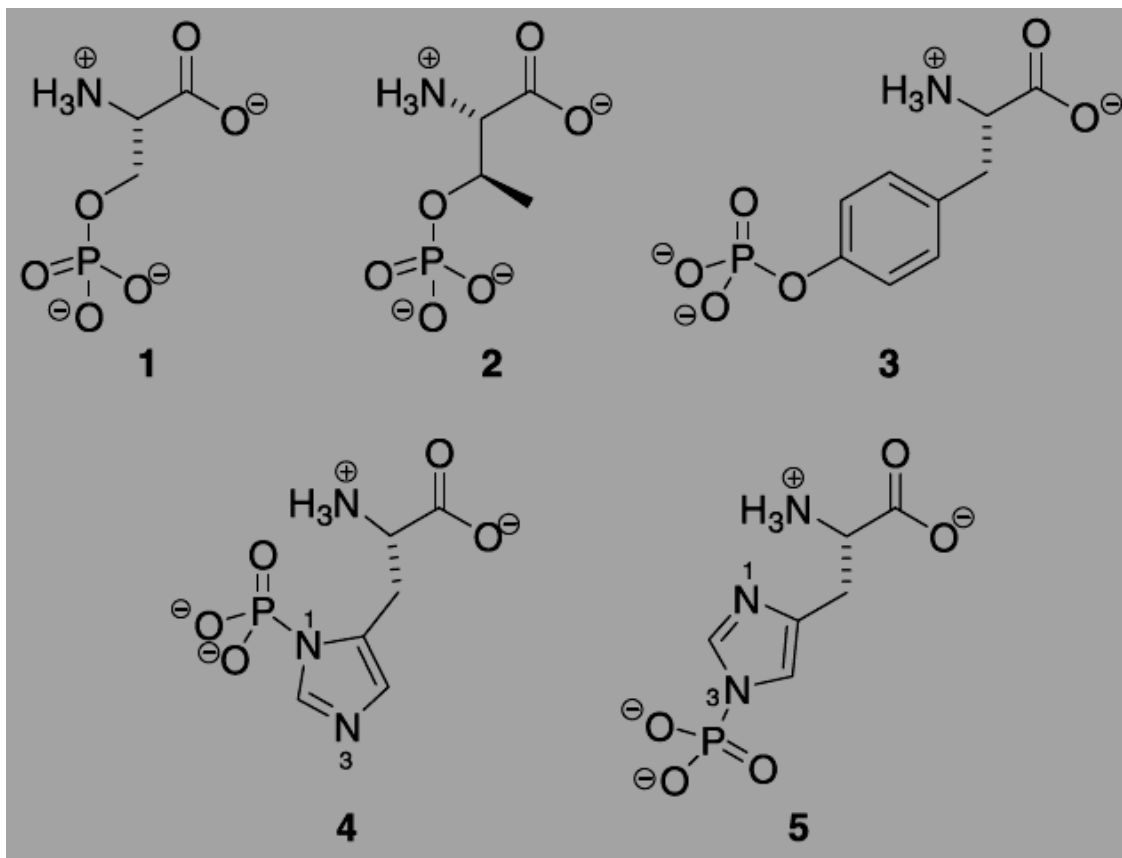


Figure 5-9: Common phosphorylated amino acids. 1, phospho-serine; 2, phospho-threonine; 3, phospho-tyrosine; 4, 5, N1- and N3-phospho-histidines⁴⁴.

Protein phosphorylation is a biochemical process to add a phosphate group (PO_4^{3-}) to a particular amino acid in a target protein, which can then be regulated with respect to a correct cellular location, or a proper enzymatic activity or sometimes an interaction with other molecules. Enzymes involved in the reversible protein phosphorylation are protein kinases (phosphorylation) and protein phosphatases (dephosphorylation), respectively. The kinase can remove the γ -phosphate group from an ATP molecule and covalently attach it to the target amino acid. In eukaryotic cells the predominant and best-characterized kinases are serine/threonine/tyrosine kinases, which can catalyze the phosphorylation of these three amino acids at their hydroxyl side chain (Figure 5-9). Chemically, the phosphate group forms a phosphoester bond with the oxygen

of the amino acid hydroxyl group^{43,45,46}. Opposite to kinases, protein phosphatases can remove the phosphate group from the substrate⁴⁷.

In bacteria, another kind of kinases is predominant in the signal transduction network; these enzymes catalyze the phosphorylation of one of the nitrogen atoms of the imidazole side chain of a histidine residue (Figure 5-9)⁴⁴. This phosphoramidate bond in phospho-histidine has a greater negative free energy than a phosphoester bond and is unstable under acidic conditions, thus it can facilitate the transfer of the phosphoryl group to a partner protein (e.g., a response regulator) in the well-organized bacterial two-component signal transduction system^{44,46}.

Two component signal transduction systems comprise two kinds of conserved proteins as key elements, a histidine kinase and a response regulator. The histidine kinase normally possesses a sensory domain in its N-terminal end that can be regulated by a variety of stimuli, either from inside the cell or outside the cell. The conformational changes in the sensory domain can result in an ATP-dependent autophosphorylation in the histidine kinase. Phosphorylation normally occurs based on kinase dimer, and the ATPase from one monomer catalyzes the phosphorylation of the histidine in the dimerization domain of the other monomer. The phosphoryl group is then transferred from the histidine to a conserved aspartic acid in the cognate response regulator. The phosphorylation of the aspartic acid produces a high energy acyl phosphate, which can drive conformational changes in the response regulator⁴⁸.

Response regulators are not just the acceptor of the phosphoryl group from the histidine, they actually act as an enzyme to catalyze an ongoing of the phosphotransfer, while sometimes the histidine kinases can act also as phosphatases to dephosphorylate their cognate response regulators⁴⁹.

Two-component histidine kinases have been found in bacteria, fungi, and plants; although in mammalian cells there are also histidine kinases, their biological functions are still unclear in most cases⁴⁶. Some two-component signal systems are normally quite simple in phosphotransfer, especially those from prokaryotic cells. These response regulators directly act as transcription factors after phosphorylation of their aspartic acids (Figure 5-10a). In some other two-component systems, however, especially such from eukaryotic cells, a more complex scheme with several steps of a phosphorelay is predominant (Figure 5-10b). These more complex systems often help to transmit signals from the cytoplasm to the nucleus, where the regulation of gene expression takes place⁴⁸.

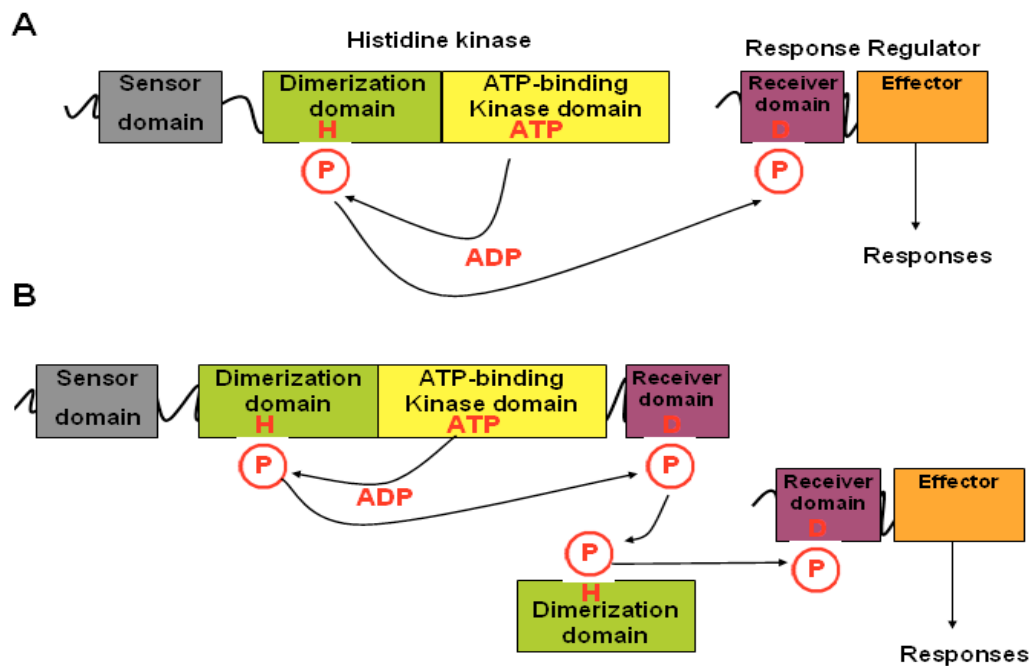


Figure 5-10: Two-component phosphotransfer schemes: a) a typical simple two component phosphotransfer system with one histidine kinase and its cognate response regulator; b) a multi-component phosphorelay system that has multiple histidine phosphotransfer proteins (HPt) as intermediate phosphorelay elements⁴⁹

The complex phosphorelay systems are also very important in bacteria. The multiple steps of phosphotransfer can integrate both negative and positive signals into the network, thus allowing regulation of some complex cellular

functions like cell cycle control and cell development for bacteria to adapt themselves to the changing environment⁵⁰

5.2.2 The plant pathogen *Pseudomonas syringae* pv. *tomato* DC3000

Pseudomonas syringae are a group of gram-negative, rod shaped bacteria. Most of its variants are plant pathogenic and are responsible for a wide range of plant diseases⁵¹. *Pseudomonas syringae* pv. *tomato* was once a pathovar from *Pseudomonas syringae*, but later according to the DNA-relatedness studies, it has been recognized as a different species and some other pathovars from *Pseudomonas syringae* group have also been incorporated into this new species with the (inofficial) name *Pseudomonas tomato*⁵².

Pseudomonas syringae pv. *tomato* DC3000 is a model strain for plant pathogen researches, it can attack tomato and other plants, e.g., *Arabidopsis*. It was shown that the phytotoxin coronatine is required for its effective virulence⁵³. Coronatine is a kind of polyketide and is composed of coronafacic acid plus coronamic acid (a leucine-related moiety). It induces light-dependent effects on tomato seedlings' photosynthetic machinery, and necrotic cell death during the tomato speck disease is caused by *P. syringae* pv. *tomato* DC3000⁵⁴.

5.2.3 The two-component systems in bacterial pathogenicity

Virulence and pathogenicity of potential pathogenetic bacteria require the regulation of certain genes that are responsible for effective invasion and growth in the host cells. The widely distributed bacterial two-component systems coupled with diverse sensor domains are thus good candidates for the integration of environmental information into the pathogenetic regulation pathways⁵⁰.

The intra- and extracellular stimuli can result in conformational changes in the sensory domains, which in turn can regulate the kinase and/or phosphatase

functions of the histidine kinase domains to control the phosphorylation level of the downstream response regulator proteins/domains. Thus the DNA-binding response regulators can properly tune the gene expression for the cell to effectively fit to the input stimuli⁵⁵.

The two-component systems can be divided into two different types according to their sensor domains: the cytoplasmic systems and the transmembrane periplasmic systems. Most of the cytoplasmic sensory elements present some conserved folds: the PAS (PER, ARNT, SIM); GAF (c-GMP specific phosphodiesterase, Adenylate cyclase, FhlA) and HAMP (histidine kinase, adenylyl cyclase, methyl-accepting protein, other prokaryotic signaling protein). Among these sensory domains the PAS and GAF proteins are already well-characterized⁵⁵, and the LOV domain is one of the most “popular” PAS sensing elements to integrate blue light as the environmental information.

For the two-component periplasmic sensory domains, most of their structures intriguingly possess a special part that presents a fold similar to the PAS proteins⁵⁵, which may suggest that these two-component systems share similar mechanisms for intra-molecular signal transductions.

As discussed at the beginning of this chapter, several LOV domain-containing histidine kinases have been related to certain cellular functions. Among these proteins, the photo-sensory LOV histidine kinase from the mammalian pathogen *Brucella abortus* has been proven to be essential for the proliferation of the bacterium in a macrophage infection model system. In fact, this effect can be regulated by light exposure⁸. Recently, the LOV histidine kinase (PSPTO-LOV) from *P. syringae* pv. *tomato* DC3000 has also been related to a blue light regulated cellular effect, in a PSPTO-LOV knock-out mutant strain, the cells moved towards the light source (Blue light, 447 nm); whereas the wild type strain as a control still stays close to where they were inoculated (Figure 5-11, personal communication Rashmi Shah).

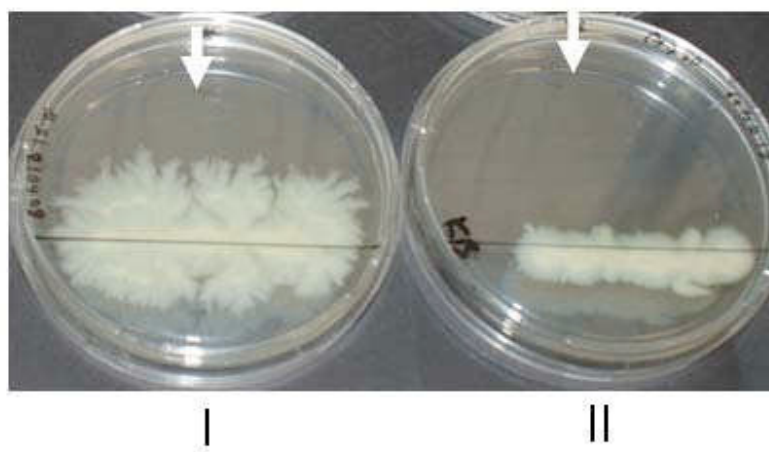


Figure 5-11: *P.syringae* grown in blue-light (447 nm), direction of light source shown by white arrows: (I) PSPTOΔLOV-mutant, (II) wild type (Control).

Up to now, however, the molecular basis of the intra-molecular signal transmission in these LOV-containing histidine kinases is still far from being resolved. In Chapter 3, a LOV domain-containing two component protein from *Pseudomonas syringae* pv. *tomato* DC3000 was biochemically and biophysically characterized. Irradiation with blue light has been proven to up-regulate the phosphorylation in the two-component system (histidine kinase and/or response regulator). It was also shown that the phosphotransfer takes place between the kinase domain and the response regulator domain, in experiments when the originally fused HK- and the RR-domains have been separated. Biophysical measurement also proved the interaction between these domains. But still, the detailed interaction mechanism remains an open question.

Recently, the histidine kinase of a heme-based oxygen sensor FixL (*Bradyrhizobium japonicum*) has been redesigned to combine with an N-terminal LOV domain from YtvA. This fusion protein can function as a blue light regulated kinase both *in vitro* and *in vivo*⁵⁶, with the “old” oxygen sensing domain and the “new” light sensing domain, both present as a conserved PAS fold. Based on the results of the well characterized LOV domain, these authors have proposed that light can act as a rotating switch to change the conformation of the LOV core,

then the α -helical coiled-coil linker would undergo a rotational movement of 40°-60° to affect the connected histidine kinase⁵⁶.

Compared to YtvA, LOV-containing histidine kinases are still poorly characterized, both structurally and functionally. Interestingly, however, the histidine kinase containing LOV proteins are much more widely distributed in the bacterial world than STAS domain-containing LOV proteins. Another important aspect of histidine kinase proteins is their significantly different functions and distribution patterns in bacterial and mammalian organism, making them potential drug targets of antibiotics. Thus, a better understanding of the functional mechanisms of different histidine kinases is very promising for further investigation.

Following histidine kinases, the GGDEF-EAL motifs are the second most widely distributed bacterial LOV proteins⁵⁷. In chapter 5.3, LOV domain-containing GGDEF-EAL proteins will be discussed.

5.3 Light-regulated GGDEF-EAL proteins

(The publication discussed in this chapter can be found in Chapter 4)

5.3.1 The regulation of the bacterial second messenger c-di-GMP

The bis-(3', 5')-cyclic dimeric guanosine monophosphate (c-di-GMP) was first described as an allosteric activator of the *Gluconacetobacter xylinus* cellulose synthase⁵⁸. Later, it has been proven that c-di-GMP is a novel prokaryotic second messenger involved in the regulation of cellular functions, such as biofilm formation, motility and virulence. Up-to-now, this signaling molecule is only known to be present in bacteria but not in eukaryotes or archaea⁵⁹.

C-di-GMP is a cyclic dimer of guanosine monophosphate, in which the two GMP molecules are linked by two ester bonds between the ribose units and the phosphates groups (Figure 5-12).

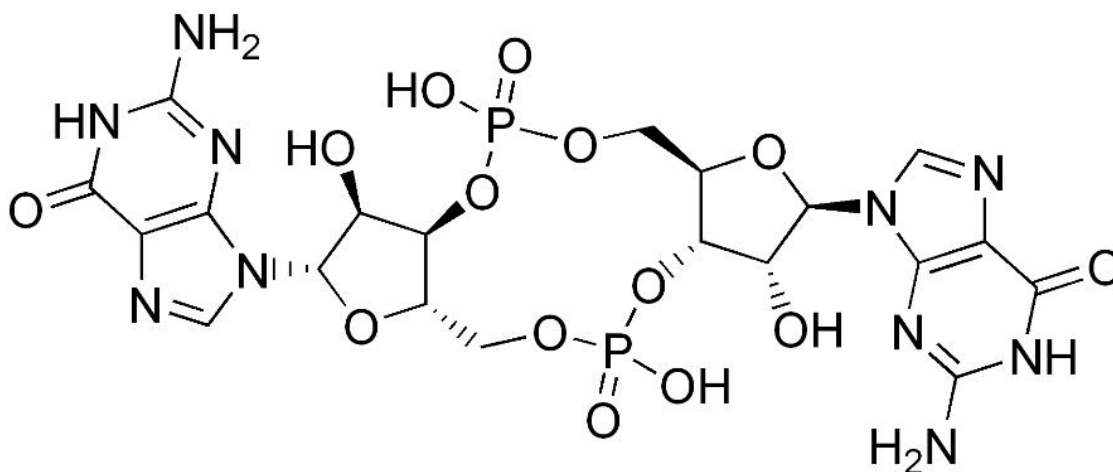


Figure 5-12: Structure of c-di-GMP. The phosphate groups from each monomer form ester bonds with the 3' hydroxyl group from the ribose from the other unit.

The biosynthesis and hydrolysis of c-di-GMP are controlled by two enzymes, diguanylate cyclase (DGC) and phosphodiesterase (PDE). These two kinds of enzymes were first identified in *Gluconacetobacter xylinus*. Both possess two

conserved domains, which were termed GGDEF domain and EAL domain based on their highly conserved sequences⁶⁰. These two domains are widely distributed in bacteria, latterly it was proven that GGDEF domains are responsible for the diguanylate cyclase activity and can use two GTP molecules to synthesize c-di-GMP. The EAL domain, in contrast, hydrolyzes c-di-GMP into a linear dimeric GMP molecule 5'-pGpG. Accordingly, this enzyme activity is termed phosphodiesterase A (PDEA) which requires Mg^{2+} or Mn^{2+} but can be inhibited by Ca^{2+} (Figure 5-13)⁶¹.

Recently, another kind of PDE proteins has been identified⁶². These proteins have a HD-GYP domain, which contains a GYP motif and belongs to a conserved metal-dependent phosphohydrolase HD superfamily⁶³. HD-GYP domains can directly cleave c-di-GMP into two GMP molecules (Figure 5-13)^{61,62}.

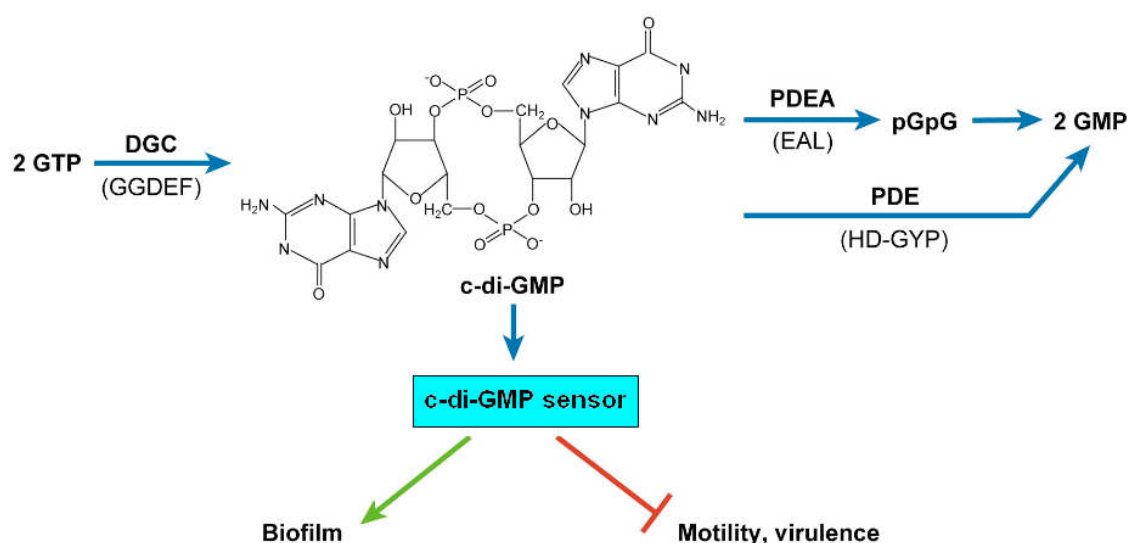


Figure 5-13: Biosynthesis and degradation of c-di-GMP. DGCs (GGDEF) can catalyze the biosynthesis of c-di-GMP from two GTP molecules; PDEAs (EAL) can cleave c-di-GMP into linear dimeric GMP 5'-pGpG, which can then be further hydrolyzed into two GMPs by other PDEs; HD-GYP domain-containing proteins can completely cleave c-di-GMP into two GMPs. The cellular amount of c-di-GMP is sensed by special sensor domains, e.g. PilZ from *P. aeruginosa*. The sensor proteins can then regulate the lifestyle of the bacterial cells⁶¹.

The cellular concentration of c-di-GMP is similar like another second messenger, cAMP, and about 100-fold lower than GTP. Most of the cellular c-di-GMP is bound by different proteins with only a small amount diffusing freely in the cell. It is thus not surprising that the regulation of c-di-GMP is strictly controlled by different enzymes, which are also regulated by many other factors^{64,65}. The GG(D/E)EF motif in GGDEF domains is the active site for the DGC activity. Any mutation of the first four residues in this motif abolishes the DGC activity^{66,67}. Immediately before the N-terminal of GG(D/E)EF motif, most active GGDEF domains also contain an RxxD motif, which can bind c-di-GMP and then inhibit the DGC activity⁶⁸. This organization of two antagonistic motifs in DGCs can help to limit the c-di-GMP concentration in a reasonable range and thus prevent an excessive consumption of GTP⁶¹. The active site in EAL domains has by far not been confirmed, although the glutamic acid in the EAL motif is believed to be important for the cation (Mg^{2+} or Mn^{2+}) dependence⁶¹. Several conserved sequences in EAL domains have been proposed to be the candidate active sites for the PDEA activity⁶⁹. This will be further discussed later in chapter 5.3.3 (see also Figure 5-14).

Besides the important sequence motifs in GGDEF and EAL domains, the domain organization of these proteins is also quite important in the regulation of c-di-GMP. GGDEF and EAL domains are often present together in one protein, and normally only one activity (DGC or PDEA) prevails, the inactive domain might assist the activity of the active domain⁷¹. For example, a GGDEF-EAL composite protein CC3396 from *Caulobacter crescentus* has both domains in tandem, the second glycine in its GG(D/E)EF motif has been replaced by a glutamic acid and thus CC2296 can not perform the DGC function; but its GGDEF domain can still bind GTP and activate the EAL domain through lowering the K_m of c-di-GMP^{61,70,71}. Interestingly, an unorthodox protein BphG1 with both GGDEF domain and EAL domain was recently found in *Rhodobacter sphaeroides*, this protein also possesses an N-terminal photo-sensing phytochrome domain. The

full-length protein showed a PDEA activity, whereas the truncated protein without the EAL domain could also perform the DGC function⁷².

GGDEF/EAL domain(s) often couple with some other sensory or regulatory domains, such as GAF, PAS, HAMP (for the meaning of these three domains, see Chapter 5.2), REC (receiver domain from response regulator), and HTH (helix turn helix) domains. This indicates that the cellular c-di-GMP level can be regulated by many input signals such as light, oxygen, redox potentials and phosphorylation of particular domains⁶¹.

Recently, some GGDEF/EAL proteins with no experimental evidence for DGC or PDEA activities have been linked to some other cellular functions, e.g., LapD from *P. fluorescens*. This protein has a degenerate EAL domain, which is not active in PDEA function. However, this cytoplasmic EAL domain can bind c-di-GMP, and the binding can trigger an inside-out signaling pathway to regulate the function of LapD at its of the periplasmic part. This periplasmic part is a HAMP domain that can modulate biofilm formation⁷³. YcgF from *E. coli* is another interesting example: this protein has an N-terminal blue light-sensing BLUF domain and a C-terminal EAL domain, which shows no PDEA activity. It has been proven that YcgF can interact under blue light irradiation with the MerR-like repressor YcgE and can release YcgE from its operator DNA. This in turn activates a regulon responsible for biofilm formation under cold or starvation conditions⁷⁴.

5.3.2 The photosynthetic cyanobacterium *Synechococcus elongatus*

Synechococcus elongatus is a rod-shaped, Gram-negative cyanobacteria that preferentially grows in freshwater with low nutrients at moderate temperatures⁷⁵. *S. elongatus* is photoautotrophic and can perform photosynthesis using carbon dioxide, water and the energy from sunlight. For this function, *S. elongatus* has to find appropriate growth conditions with respect to depths in the water column and

sufficient light illumination for photosynthesis^{75,76}. It is thus not surprising that this organism possesses many light sensing molecules to integrate the detected light quality into its cellular regulation networks.

The genomes of two strains of *S. elongatus* have been sequenced: *Synechococcus elongatus* PCC 6301 and *Synechococcus elongatus* PCC 7942. Both contain one circular chromosome and two plasmids, and a sequence comparison reveals their close phylogenetic relation^{77,78}.

5.3.3 The two LOV-containing GGDEF-EAL proteins from *Synechococcus elongatus* PCC 7942

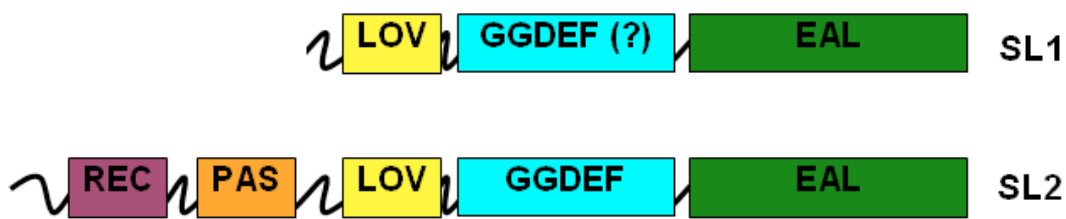


Figure 5-14: Domain architecture of the two LOV-containing proteins from *S. elongatus*

As discussed in Chapter 4, the two strains of *Synechococcus elongatus* both have two LOV domain-containing GGDEF-EAL proteins. Interestingly, the GGDEF and EAL domains from one of these two LOV proteins (SL2) are quite conserved to other DGC/PDEA proteins, whereas the other one (SL1) is degenerate in both domains. The shorter (Figure 5-14) LOV-containing GGDEF-EAL protein from *S. elongatus* PCC 7942 has an N-terminal LOV domain followed by a possible “GGDEF”-EAL motif. The active site (GG(D/E)EF) for the “GGDEF” domain is almost entirely missing in SL1 (showing an N₂₁₅HHQF motif in the supposed position for GGDEF), thus this domain has been excluded from the GGDEF family in some online prediction databanks (SMART from EMBL-Heidelberg). On the contrary, the longer LOV-containing GGDEF-EAL protein (Figure 5-14) from *Synechococcus elongatus* PCC 7942 possesses a much more conserved GGDEF domain with the complete DGC active site (G₅₇₇GGDEF).

PdeA1 <i>G. xylinus</i>	DRLVLGSALRDSLAQGMLQLHYQPQVRTHLTLELSGVFEALSRWHHPHLGNIFPSRFTAVAE	60
SL2 EAL	ERVHLRNELQKATETEAFELYFQPKIEGCSGQVIGLEALLRWQHPQMGFTSPATFVPIAE	60
SL1 EAL	EQYSRDRDWQQAIAAGELTLALQBPQMGLRNRQLRGFEVQLRWQHPQQGTLLASQLMEHLE	60
	* * * *	
PdeA1 <i>G. xylinus</i>	ETGQIEATGRWSLEACRQIVKWDRDGVHVPTVAVNLSAVHFRNRALPEHTAALLKDHNL	120
SL2 EAL	DTGQIIPLSQWVLETACRQLRDLLQQGIAAPSVAVNISTVQFRINFVKSVQSAIQKYQL	120
SL1 EAL	QSQHRETVGRWFLDQAGQLLSQWRNSAQFSGLFALSLLPQQWKSPFSFIHDLRSLETYQI	120
	*	
PdeA1 <i>G. xylinus</i>	KPARLTVEITESVM...LQSRNIGCGLSMDDFGTGYSSLSRLTRLPLTEIKIDRSFIND	187
SL2 EAL	KSEHLEITEITENVL...LQRLKELGVNISTDDFGTGFSSLSYKELPIDTVKIDRSFVQE	187
SL1 EAL	PPEQLELDLPAQSL...VYAVRDLGIGIGLADFGSRSIGLYDLRNPLPLTTKLERRFVVG	187
	* * * * * *	
PdeA1 <i>G. xylinus</i>	FEYDTNAQAVTMAVIGIGSRLGMTVVTEGVETEQQRDLLLEKLNCDVMQGYLFAKPLAPQD	247
SL2 EAL	INTDSRDAAITQGTISMHHRLRLNVVAEGVETEQQKFLLQSNCDQYQGYFAKPMPFEEA	247
SL1 EAL	LPDDANDRAIVRGVAMSQALKVRIVARGVDTVDQAKFLARAECDAHQGLAYSAPLTIEE	247
	* * * *	

Figure 5-15: Sequence alignment of EAL domains. PdeA1 from *G. xylinus* has an enzymatically active EAL domain. The multiple alignment was generated using Clustal W 2 (EMBL-EBI). Residues identical in more than 80% of active EAL domains are marked in yellow (only PdeA1 from *G. xylinus* together with SL1 and SL2 are shown); residues conserved in all active EAL domains are marked with red asterisks in the consensus line; Positions with similar residues in all active EAL domains are marked in grey⁶⁹.

The EAL domain from SL1 also seems to lack most of the predicted active sites from other proved PDEAs, whereas the EAL domain from SL2 again contains most of the possible active sites (Figure 5-15)⁶⁹. Thus it is not surprising that SL1 is neither active as a DGC nor active as a PDEA, whereas SL2 can hydrolyze c-di-GMP. Although in the work of Chapter 4, the DGC activity of SL2 can not be testified *in vitro*, the GGDEF domain of this protein is nevertheless conserved in most of the possible active sites.

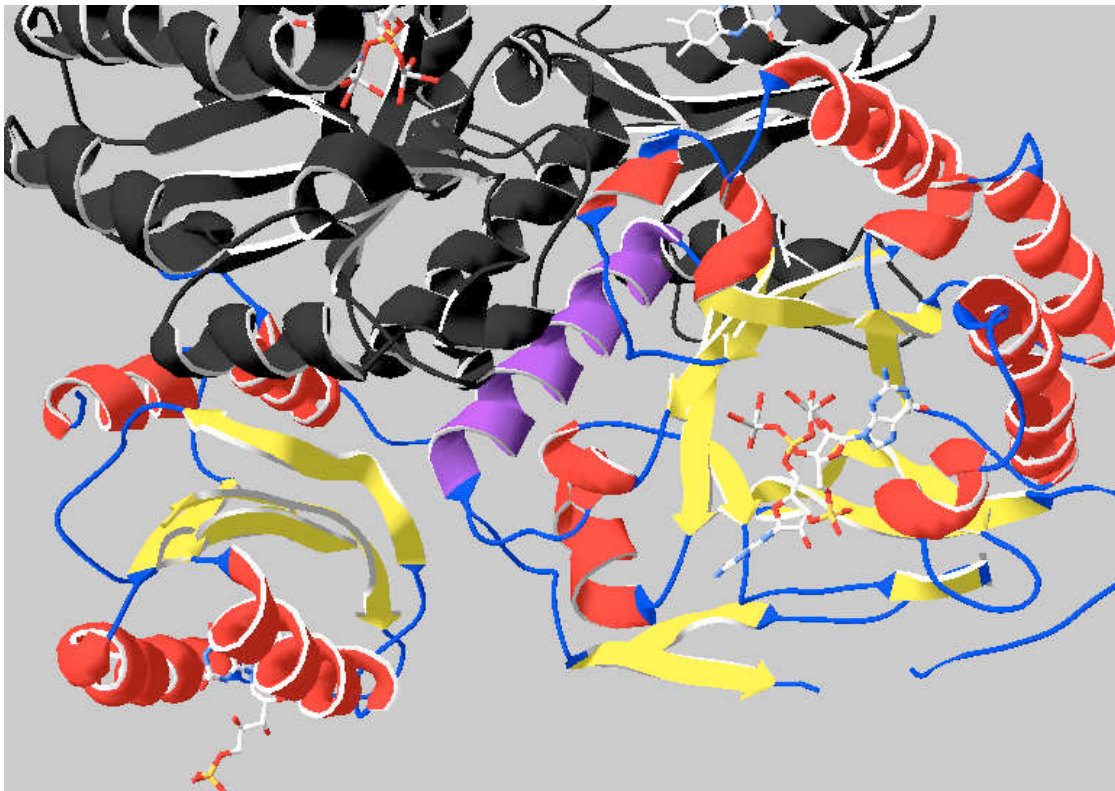


Figure 5-16: 3D-Ribbon structure of BlrP1 dimer (PDB: 3GG0) from *Klebsiella pneumoniae*. The monomer in the upper side is shown in black. The BLUF domain with FAD from the second monomer is on the left side. On the right side is the barrel-like EAL domain that holds the c-di-GMP in the barrel formed by β -strands. The conserved helices $\alpha 6$ of the two EAL domains are involved in dimerization (for one monomer shown in purple)⁷⁹.

An active PDEA BlrP1 (also called KPN_01598) from *Klebsiella pneumoniae* has recently been crystallized, the structure of the protein together with its substrate c-di-GMP and the position of the key metal cations have provided a clue for the elucidation of the reaction mechanism (Figure 5-16). In an enzymatically highly active conformation, BlrP1 binds its substrate c-di-GMP with the help of two metal cations and one bridging water molecule (Figures 5-17 and 5-18)⁷⁹

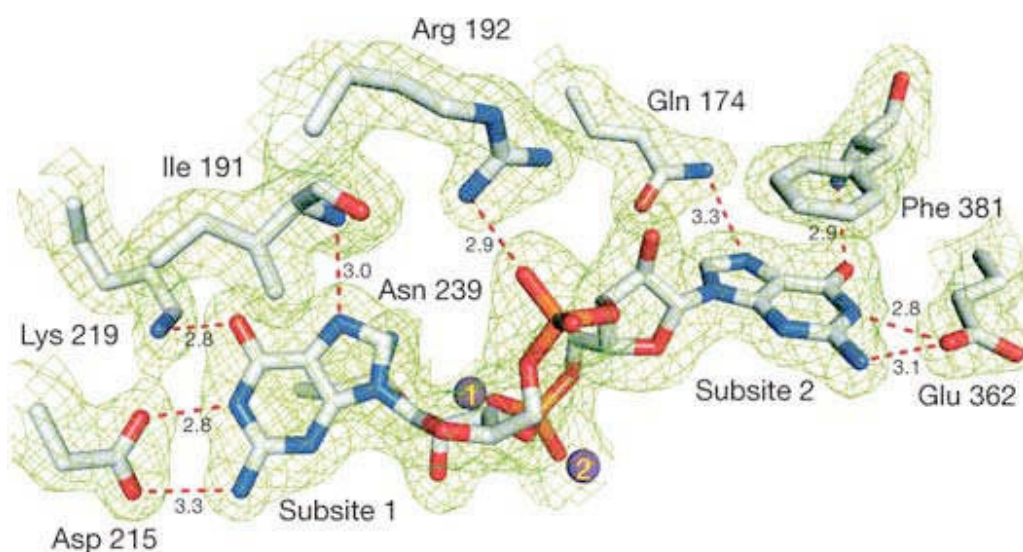


Figure 5-17: Binding site of c-di-GMP in BlrP1 EAL domain. The two purple balls (numbered 1 and 2) are manganese cations; the electron density is in green color; possible interactions between different residues and the c-di-GMP are shown in red dashed lines⁷⁹.

The binding of c-di-GMP in BlrP1 (Figure 5-17⁷⁹) indicates those residues that might be responsible for the c-di-GMP binding including Q174, I191, R192, D215, K219, N239, E362 and F381. Comparing with the marked sequences shown in Figure 5-15, it is clear that only Q174 (Q691 in SL2), R192 (R709 in SL2), N239 (N764 in SL2) and E362 (E886 in SL2) are necessarily conserved in those active PDEAs^{69,79}.

Figure 5-18 gives a more detailed view of the active sites of the BlrP1 EAL domain. It can be seen that the first manganese cation M1 is coordinated into an octahedron together with E188, N239, E272, one oxygen atom of the phosphate from c-di-GMP, a bridging water molecule W1 and the metal binding residue D302. The second manganese cation M2 is coordinated into a distorted bipyramid together with W1, D302, another oxygen atom of the phosphate from c-di-GMP, D303, E359 and another water molecule W2⁷⁹.

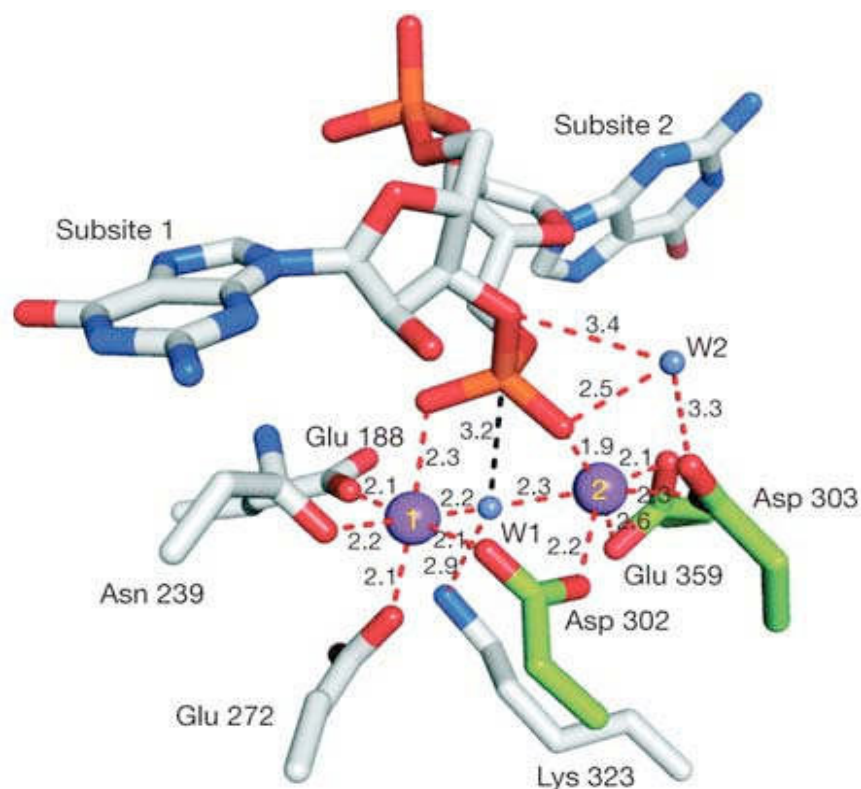


Figure 5-18: Detailed structure of the active site of BlrP1 EAL domain. Again, the two manganese cations are shown as purple balls; water molecules (W1 and W2) are shown as blue balls. Possible interactions between residues and substrates are shown as red dashed lines⁷⁹.

Proteins	Residues for M1 coordination with phosphate oxygen and the bridging water			
BlrP1	E188	N239	E272	D302
SL2	E705	N764	E796	D826
SL1	E355	S414	D446	A476
	Residues for M2 coordination with phosphate oxygen and the bridging water			
BlrP1	D302	D303	E359	
SL2	D826	D827	E883	
SL1	A476	D477	R533	

Table 5-1: Comparison of the conserved residues that are responsible for metal cations binding in the EAL domains from BlrP1, SL2 and SL1^{69,79}.

Comparing with the marked sequences shown in figure 5-15, it is not surprising that these key residues are quite conserved in SL2 and almost all the other

active PDEAs, but in SL1, most of these residues have been replaced by some quite different residues (Table 5-1)^{69,79}.

From the comparison of different residues that might be responsible for c-di-GMP binding and metal cation binding, respectively, it is plausible to propose that the metal binding cavity in EAL domains need to be strictly conserved in order to perform a PDEA activity, whereas the binding of c-di-GMP is relatively flexible.

It should also be noticed that SL2 can hydrolyze c-di-GMP in both light state and dark state, yet with a clearly higher activity upon blue light irradiation. One possible explanation is that the LOV domain in this protein has a fast kinetics property, i.e., it can undergo the dark recovery in a very fast mode, thus this protein actually has no absolute light state. This situation is also true for SL1, although no PDE activity could be detected so far for this protein.

Besides the fast kinetics of the LOV domain, there are still two other possible regulatory domains in SL2: one finds an N-terminal REC domain and another PAS domain between the REC domain and the LOV domain. These two domains could also integrate other input signals into the regulation of the downstream GGDEF-EAL domains, such signals may include oxygen, redox potential and a phosphoryl transfer from other proteins; another possibility is that the upstream PAS domain might act as a dimerization site, since the activity of EAL domains depend on dimerization. In this case, the receiver domain then can act as a regulator for the dimerization process. However, these proposals still need further investigations.

For SL1, this protein might have some other functions rather than directly controlling the concentration of c-di-GMP. There are indeed many GGDEF/EAL proteins that show other functions, e.g., LapD and YcgF as discussed in Chapter 5.3.1. One should keep in mind that the GGDEF and EAL motifs can be found in many different proteins, the presence of some conserved primary sequences

does not necessarily indicate that these proteins will possess similar functions. The detailed mechanisms for the regulation of c-di-GMP are still open questions and thus it is quite possible that we can further divide proteins with GGDEF/EAL motifs into different subgroups based on their functions.

Conclusion

This work has shown that blue light-sensing LOV domains are quite versatile in activating several functionally fairly different “output domains”. Although still at its infancy, the blue light regulation of metabolic processes has clearly been proven, and the role of blue light as a regulating factor in microbial communities has definitely been demonstrated. Our knowledge about the molecular basis of signal transmission within several bacterial LOV domain-containing proteins have been broadened. The connection between the structure of one of the best characterized bacterial LOV protein (YtvA) and the functions of some of them have also been part of this work.

5.4 References for chapter 5

1. Christie, J. M., T.E.Swartz, R.A.Bogomolni & W.R.Briggs Phototropin LOV domains exhibit distinct roles in regulating photoreceptor function. *Plant J.* **32**, 205-219 (2002).
2. Christie, J. M. Phototropin blue-light receptors. *Annu. Rev. Plant Biol.* **58**, 21-45 (2007).
3. Huala, E. *et al.* *Arabidopsis* NPH1: a protein kinase with a putative redox-sensing domain. *Science* **278**, 2120-2123 (1997).
4. Krauss, U. Bacterial blue-light photoreceptors of the LOV family. Ph. D. thesis, University of Düsseldorf, 2007.
5. Losi, A. The bacterial counterparts of plant phototropins. *Photochem. Photobiol. Sci.* **3**, 566-574 (2004).
6. Gaidenko, T. A., T.J.Kim, A.L.Weigel, M.S.Brody & C.W.Price The blue-light receptor YtvA acts in the environmental stress signaling pathway of *Bacillus subtilis*. *J. Bacteriol.* **188**, 6387-6395 (2006).
7. Avila-Pérez, M., K.J.Hellingwerf & R.Kort Blue light activates the sigmaB-dependent stress response of *Bacillus subtilis* via YtvA. *J. Bacteriol.* **188**, 6411-6414 (2006).
8. Swartz, T. E. *et al.* Blue-light-activated histidine kinases: two-component sensors in bacteria. *Science* **317**, 1090-1093 (2007).
9. Purcell, E. B., D.Siegal-Gaskins, D.C.Rawling, A.Fiebig & S.Crosson A photosensory two-component system regulates bacterial cell attachment. *Proc. Natl. Acad. Sci. USA* **104**, 18241-18246 (2007).
10. Kunst, F. *et al.* The complete genome sequence of the gram-positive bacterium *Bacillus subtilis*. *Nature* **390**, 249-256 (1997).
11. Akbar, S. *et al.* New family of regulators in the environmental signaling pathway which activates the general stress transcription factor sigma(B) of *Bacillus subtilis*. *J. Bacteriol.* **183**, 1329-1338 (2001).
12. Najafi, S. M., D.A.Harris & M.D.Yudkin The SpoIIAA protein of *Bacillus subtilis* has GTP-binding properties. *J. Bacteriol.* **178**, 6632-6634 (1996).
13. Aravind, L. & E.V.Koonin The STAS domain - a link between anion transporters and antisigma-factor antagonists. *Curr Biol.* **10**, R53-R55 (2000).
14. Buttani, V., A.Losi, E.Polverini & W.Gärtner Blue news: NTP binding properties of the blue-light sensitive YtvA protein from *Bacillus subtilis*. *FEBS Lett.* **580**, 3818-3822 (2006).
15. Hefti, M. H., K.J.Francoijs, S.C.de Vries, R.Dixon & J.Vervoort The PAS fold. A redefinition of the PAS domain based upon structural prediction. *Eur. J. Biochem.* **271**, 1198-1208 (2004).
16. Salomon, M., U.Lempert & W.Rüdiger Dimerization of the plant photoreceptor phototropin is probably mediated by the LOV1 domain. *FEBS Lett.* **572**, 8-10 (2004).

17. Kasahara, M. *et al.* Photochemical properties of the flavin mononucleotide-binding domains of the phototropins from *Arabidopsis*, rice, and *Chlamydomonas reinhardtii*. *Plant Physiol.* **129**, 762-773 (2002).
18. Nakasone, Y., T.Eitoku, D.Matsuoka, S.Tokutomi & M.Terazima Kinetic measurement of transient dimerization and dissociation reactions of *Arabidopsis* phototropin 1 LOV2 domain. *Biophys. J.* **91**, 653 (2006).
19. Nakasone, Y., T.Eitoku, D.Matsuoka, S.Tokutomi & M.Terazima Dynamics of conformational changes of *Arabidopsis* phototropin 1 LOV2 with the linker domain. *J. Mol. Biol.* **367**, 432-442 (2007).
20. Eitoku, T. *et al.* Photochemical intermediates of *Arabidopsis* phototropin 2 LOV domains associated with conformational changes. *J. Mol. Biol.* **371**, 1290-1203 (2007).
21. Möglich, A. & K.Moffat Structural basis for light-dependent signaling in the dimeric LOV domain of the photosensor YtvA. *J. Mol. Biol.* **373**, 112-126 (2007).
22. Losi, A., E.Ghiraldelli, S.Jansen & W.Gärtner Mutational effects on protein structural changes and interdomain interactions in the blue-light sensing LOV protein YtvA. *Photochem. Photobiol.* **81**, 1145-1152 (2005).
23. Losi, A., E.Ternelli & W.Gärtner Tryptophan fluorescence in the *Bacillus subtilis* phototropin-related protein YtvA as a marker of interdomain interaction. *Photochem. Photobiol.* **80**, 150-153 (2004).
24. Zoltowski, B. D. *et al.* Conformational switching in the fungal light sensor Vivid. *Science* **316**, 1057 (2007).
25. Fedorov, R. *et al.* Crystal structures and molecular mechanism of a light-induced signaling switch: The Phot-LOV1 domain from *Chlamydomonas reinhardtii*. *Biophys. J.* **2003**, -2474 (2003).
26. Harper, S. M., L.C.Neil & K.H.Gardner Structural basis of a phototropin light switch. *Science* **301**, 1541-1544 (2003).
27. Crosson, S. & K.Moffat Photoexcited structure of a plant photoreceptor domain reveals a light-driven molecular switch. *Plant Cell* **14**, 1067-1075 (2002).
28. Crosson, S. & K.Moffat Structure of a flavin-binding plant photoreceptor domain: insights into light-mediated signal transduction. *Proc. Natl. Acad. Sci. USA* **98**, 2995-3000 (2001).
29. Card, P. B., P.J.Erbel & K.H.Gardner Structural basis of ARNT PAS-B dimerization: use of a common beta-sheet interface for hetero- and homodimerization. *J. Mol. Biol.* **353**, 664-667 (2005).
30. Erbel, P. J., P.B.Card, O.Karakuzu, R.K.Bruick & K.H.Gardner Structural basis for PAS domain heterodimerization in the basic helix--loop--helix-PAS transcription factor hypoxia-inducible factor. *Proc. Natl. Acad. Sci. USA* **100**, 15504-15509 (2003).
31. Zoltowski, B. D. & B.R.Crane Light activation of the LOV protein vivid generates a rapidly exchanging dimer. *J. Mol. Biol.* **47**, 7012-7019 (2008).
32. Lee, J. *et al.* Changes at the KinA PAS-A Dimerization Interface Influence Histidine Kinase Function. *Biochemistry* **47**, 4051-4064 (2008).

33. Key, J., M.Hefti, E.B.Purcell & K.Moffat Structure of the redox sensor domain of *Azotobacter vinelandii* NifL at atomic resolution: signaling, dimerization, and mechanism. *Biochemistry* **46**, 3614-3623 (2007).
34. Miyatake, H. *et al.* Sensory mechanism of oxygen sensor FixL from *Rhizobium meliloti*: crystallographic, mutagenesis and resonance Raman spectroscopic studies. *J. Mol. Biol.* **301**, 415-431 (2000).
35. Kurokawa, H. *et al.* A redox-controlled molecular switch revealed by the crystal structure of a bacterial heme PAS sensor. *J. Biol. Chem.* **279**, 20186-20193 (2004).
36. Halavaty, A. S. & K.Moffat N- and C-terminal flanking regions modulate light-induced signal transduction in the LOV2 domain of the blue light sensor phototropin 1 from *Avena sativa*. *Biochemistry* **46**, 14001-14009 (2007).
37. Buttani, V., W.Gärtner & A.Losi NTP-binding properties of the blue-light receptor YtvA and effects of the E105L mutation. *Eur Biophys J.* **36**, 831-839 (2007).
38. Avila-Pérez, M. *et al.* *In vivo* mutational analysis of the *Bacillus subtilis* LOV-domain containing protein YtvA: mechanism of light-activation of the general stress response. *J. Biol. Chem.* **284**, 24958-24964 (2010).
39. Marles-Wright, J. *et al.* Molecular architecture of the "stressosome," a signal integration and transduction hub. *Science* **322**, 92-96 (2008).
40. Yamamoto, A., T.Iwata, S.Tokutomi & H.Kandori Role of Phe1010 in light-induced structural changes of the neo1-LOV2 domain of *Adiantum*. *Biochemistry* **47**, 922-928 (2008).
41. Leipe, D. D., Y.I.Wolf, E.V.Koonin & L.Aravind Classification and evolution of P-loop GTPases and related ATPases. *J. Mol. Biol.* **317**, 41-72 (2002).
42. Leipe, D. D., E.V.Koonin & L.Aravind Evolution and classification of P-loop kinases and related proteins. *J. Mol. Biol.* **333**, 781-815 (2003).
43. Cozzzone, A. J. Protein phosphorylation in prokaryotes. *Annu. Rev. Microbiol.* **42**, 97-125 (1988).
44. Attwood, P. V., M.J.Piggott, X.L.Zu & P.G.Besant Focus on phosphohistidine. *Amino Acids* **32**, 145-156 (2007).
45. Burnett, G. & E.P.Kennedy The enzymatic phosphorylation of proteins. *J. Biol. Chem.* **211**, 969-980 (1954).
46. Besant, P. G. & P.V.Attwood Mammalian histidine kinases. *Biochim. Biophys. Acta.* **1754**, 281-290 (2005).
47. Barford, D., A.K.Das & M.P.Egloff The structure and mechanism of protein phosphatases: insights into catalysis and regulation. *Annu. Rev. Biophys. Biomol. Struct.* **27**, 133-164 (1998).
48. Stock, A. M., V.L.Robinson & P.N.Goudreau Two-component signal transduction. *Annu. Rev. Biochem.* **69**, 183-215 (2000).

49. West, A. H. & A.M.Stock Histidine kinases and response regulator proteins in two-component signaling systems. *Trends Biochem. Sci.* **26**, 369-376 (2001).
50. Hoch, J. A. Two-component and phosphorelay signal transduction. *Curr. Opin. Microbiol.* **3**, 165-170 (2000).
51. Anzai, Y., H.Kim, J.Y.Park, H.Wakabayashi & H.Oyaizu Phylogenetic affiliation of the pseudomonads based on 16S rRNA sequence. *Int. J. Syst. Evol. Microbiol.* **50**, 1563-1589 (2000).
52. Gardan, L. *et al.* DNA relatedness among the pathovars of *Pseudomonas syringae* and description of *Pseudomonas tremiae* sp. nov. and *Pseudomonas cannabina* sp. nov. (ex Suty and Dowson 1959). *Int. J. Syst. Bacteriol.* **49**, 469-478 (1999).
53. Sreedharan, A., A.Penalosa-Vazquez, B.N.Kunkel & C.L.Bender CorR regulates multiple components of virulence in *Pseudomonas syringae* pv. *tomato* DC3000. *Mol. Plant Microbe Interact.* **19**, 768-779 (2006).
54. Uppalapati, S. R. *et al.* Pathogenicity of *Pseudomonas syringae* pv. *tomato* on tomato seedlings: phenotypic and gene expression analyses of the virulence function of coronatine. *Mol Plant Microbe Interact.* **21**, 383-395 (2008).
55. Szurmant, H., R.A.White & J.A.Hoch Sensor complexes regulating two-component signal transduction. *Curr. Opin. Struct. Biol.* **17**, 706-715 (2007).
56. Möglich, A., R.A.Ayers & K.Moffat Design and signaling mechanism of light-regulated histidine kinase. *J. Mol. Biol.* **385**, 1433-1444 (2009).
57. Losi, A. & W.Gärtner Bacterial bilin- and flavin-binding photoreceptors. *Photochem. Photobiol. Sci.* **7**, 1168-1178 (2008).
58. Ross, P. *et al.* Regulation of cellulose synthesis in *Acetobacter xylinum* by cyclic diguanylic acid. *Nature* **325**, 279-281 (1987).
59. Cotter, P. A. & S.Stibitz C-di-GMP-mediated regulation of virulence and biofilm formation. *Curr. Opin. Microbiol.* **10**, 1-7 (2007).
60. Jenal, U. & J.Malone Mechanisms of cyclic-di-GMP signaling in bacteria. *Annu. Rev. Genet.* **40**, 385-407 (2006).
61. Tamayo, R., J.T.Pratt & A.Camilli Roles of cyclic diguanylate in the regulation of bacterial pathogenesis. *Annu. Rev. Microbiol.* **61**, 131-148 (2007).
62. Ryan, R. P. *et al.* Cell-cell signaling in *Xanthomonas campestris* involves an HD-GYP domain protein that functions in cyclic di-GMP turnover. *Proc. Natl. Acad. Sci. USA* **103**, 6712-6717 (2006).
63. Dow, J. M., Y.Fouhy, J.F.Lucey & R.P.Ryan The HD-GYP domain, cyclic di-GMP signaling, and bacterial virulence to plants. *Mol. Plant. Microbe Interact.* **19**, 1378-1384 (2006).
64. Römling, U., M.Gomelsky & M.Y.Galperin C-di-GMP: the dawning of a novel bacterial signalling system. *Mol. Microbiol.* **57**, 629-639 (2005).

65. Römmling, U. & D. Amikam Cyclic di-GMP as a second messenger. *Curr. Opin. Microbiol.* **9**, 228 (2006).
66. Ryjenkov, D. A., M. Tarutina, O. V. Moskvina & M. Gomelsky Cyclic diguanylate is a ubiquitous signaling molecule in bacteria: insights into biochemistry of the GGDEF protein domain. *J. Bacteriol.* **187**, 1792-1798 (2005).
67. Chan, C. *et al.* Structural basis of activity and allosteric control of diguanylate cyclase. *Proc. Natl. Acad. Sci. USA* **101**, 17084-17089 (2004).
68. Christen, B. *et al.* Allosteric control of cyclic di-GMP signaling. *J. Biol. Chem.* **281**, 32015-32024 (2006).
69. Schmidt, A. J., D. A. Ryjenkov & M. Gomelsky The ubiquitous protein domain EAL is a cyclic diguanylate-specific phosphodiesterase: enzymatically active and inactive EAL domains. *J. Bacteriol.* **187**, 4774-4781 (2005).
70. Christen, M. *et al.* DgrA is a member of a new family of cyclic diguanosine monophosphate receptors and controls flagellar motor function in *Caulobacter crescentus*. *Proc. Natl. Acad. Sci. USA* **104**, 4112-4117 (2007).
71. Christen, M., B. Christen, M. Folcher, A. Schauerte & U. Jenal Identification and characterization of a cyclic di-GMP-specific phosphodiesterase and its allosteric control by GTP. *J. Biol. Chem.* **280**, 30829-30837 (2005).
72. Tarutina, M., D. A. Ryjenkov & M. Gomelsky An unorthodox bacteriophytochrome from *Rhodobacter sphaeroides* involved in turnover of the second messenger c-di-GMP. *J. Biol. Chem.* **281**, 34751-34758 (2006).
73. Newell, P. D., R. D. Monds & G. A. O'Toole LapD is a bis-(3',5')-cyclic dimeric GMP-binding protein that regulates surface attachment by *Pseudomonas fluorescens* Pf0-1. *Proc. Natl. Acad. Sci. USA* **106**, 3461-3466 (2009).
74. Tschowri, N., S. Busse & R. Hengge The BLUF-EAL protein YcgF acts as a direct anti-repressor in a blue-light response of *Escherichia coli*. *Genes Dev.* **23**, 522-534 (2009).
75. Perkins, F. O., L. W. Haas, D. E. Phillips & K. L. Webb Ultrastructure of a marine *Synechococcus* possessing spinae. *Can. J. Microbiol.* **27**, 318-329 (1981).
76. Olson, R. J., S. W. Chrischolm, E. R. Zettler & E. V. Armbrust Pigment size and distribution of *Synechococcus* in the North Atlantic and Pacific oceans. *Limnol. Oceanogr.* **35**, 45-58 (1990).
77. Copeland, A. *et al.* Complete sequence of chromosome 1 of *Synechococcus elongatus* PCC 7942. 2005.
Ref Type: Unpublished Work
78. Sugita, C. *et al.* Complete nucleotide sequence of the freshwater unicellular cyanobacterium *Synechococcus elongatus* PCC 6301 chromosome: gene content and organization. *Photosynth. Res.* **93**, 55-67 (2007).
79. Barends, T. R. M. *et al.* Structure and mechanism of a bacterial light-regulated cyclic nucleotide phosphodiesterase. *Nature* **459**, 1015-1018 (2009).

Die hier vorgelegte Dissertation habe ich eigenständig und ohne unerlaubte Hilfe angefertigt. Die Dissertation wurde in der vorgelegten oder in ähnlicher Form noch bei keiner anderen Institution eingereicht. Ich habe bisher keine erfolglosen Promotionsversuche unternommen.

Unterschrift..... Düsseldorf, den/...../20....